

TECHNISCHE UNIVERSITÄT MÜNCHEN

Fachgebiet für Hydrologie und Flussgebietsmanagement

Preferential Flow in a cultivated lower meso-scale catchment:
observation, modelling and implications for solute transport

Julian Klaus

Vollständiger Abdruck der von der Fakultät für Bauingenieur- und Vermessungswesen der Technischen Universität München zur Erlangung des akademischen Grades eines

Doktors der Naturwissenschaften

genehmigten Dissertation.

Vorsitzender: Univ.-Prof. Dr. Harald Horn

Prüfer der Dissertation:

1. Univ.-Prof. Dr. Erwin Zehe
Karlsruher Institut für Technologie
2. Univ.-Prof. Dr. Rainer Meckenstock
3. Univ.-Prof. Dr. Markus Weiler
Albert-Ludwigs-Universität Freiburg

Die Dissertation wurde am 01.03.2011 bei der Technischen Universität München eingereicht und durch die Fakultät für Bauingenieur- und Vermessungswesen am 08.07.2011 angenommen.

Contents

CONTENTS	I
FIGURES	III
TABLES	V
TABLE OF SYMBOLS	VI
ABSTRACT	VIII
KURZFASSUNG	X
ACKNOWLEDGMENT	XIII
1 INTRODUCTION	1
1.1 TYPES OF PREFERENTIAL FLOW	2
1.2 OBSERVING PREFERENTIAL FLOW	7
1.3 MODELLING OF PREFERENTIAL FLOW	13
1.4 OPEN RESEARCH QUESTIONS AND THESIS OBJECTIVES	17
1.5 THESIS OUTLINE	19
2 THE WEIHERBACH CATCHMENT	21
2.1 CATCHMENT DESCRIPTION	21
2.2 PREVIOUS RESEARCH IN THE WEIHERBACH CATCHMENT	26
2.3 THE BIPORE PROJECT	29
2.4 ADDITIONAL MEASUREMENT NEEDS	29
3 MODELLING RAPID FLOW RESPONSE OF A TILE DRAINED FIELD SITE USING A 2-DIMENSIONAL-PHYSICALLY BASED MODEL: ASSESSMENT OF “EQUIFINAL” MODEL SETUPS*	31
3.1 INTRODUCTION	32
3.2 METHODOLOGY	34
3.3 RESULTS	42
3.4 DISCUSSION AND CONCLUSIONS	48
4 A NOVEL EXPLICIT APPROACH TO MODEL BROMIDE AND PESTICIDE TRANSPORT IN CONNECTED SOIL STRUCTURES*	53
4.1 INTRODUCTION	54
4.2 METHODOLOGY	56
4.3 RESULTS	58
4.4 DISCUSSION AND CONCLUSION	64

<u>5 LINKING THE OLD WATER WITH THE NEW WATER PARADIGM: MACROPORE – SOIL MATRIX INTERACTION DURING A SERIES OF IRRIGATION EXPERIMENTS AT A TILE DRAINED HILLSLOPE*</u>	73
5.1 INTRODUCTION	74
5.2 STUDY SITE AND METHODS	76
5.3 RESULTS	83
5.4 DISCUSSION	93
5.5 CONCLUSIONS	97
<u>6 ON THE CONTROLLING FACTORS OF PESTICIDE LEACHING WITHIN A SERIES OF THREE IRRIGATION EXPERIMENTS – THE ROLE OF PREFERENTIAL FLOW STRUCTURES AND THRESHOLD BEHAVIOUR*</u>	99
6.1 INTRODUCTION	100
6.2 STUDY AREA AND EXPERIMENTAL METHODS	102
6.3 RESULTS	107
6.4 DISCUSSION	121
6.5 CONCLUSION	124
<u>7 LINKING MACROPOROSITY WITH THE POPULATION OF <i>LUMBRICUS TERRESTRIS</i> L. - A FIRST ATTEMPT TO OBTAIN OBSERVABLE STRUCTURE INFORMATION FOR MODEL PARAMETERISATION</u>	127
7.1 INTRODUCTION	128
7.2 METHODOLOGY	129
7.3 RESULTS	130
7.4 DISCUSSION	134
7.5 CONCLUSION	138
<u>8 A FIRST GLIMPSE TO ANOTHER CATCHMENT: DIFFERENT PHYSICAL CATCHMENT PROPERTIES – DIFFERENT PREFERENTIAL FLOW PATTERN</u>	139
8.1 INTRODUCTION	139
8.2 CATCHMENT DESCRIPTION	139
8.3 FIRST OBSERVATIONS	141
8.4 FURTHER RESEARCH STEPS	143
<u>9 SYNTHESIS</u>	145
9.1 SUMMARY OF ACHIEVEMENTS	145
9.2 DISCUSSION AND OUTLOOK	148
9.3 CONCLUSION	153
<u>REFERENCES</u>	155

Figures

Figure 1-1: Funnelling of a uniform infiltration front	3
Figure 1-2: Different reasons for preferential flow	5
Figure 1-3: Exemplified development of infiltration front instability	7
Figure 1-4: Evidence of preferential flow measured with a FDR	10
Figure 1-5: Hood infiltrometer on a macroporous soil	10
Figure 2-1: Weiherbach catchment	21
Figure 2-2: Soil map of the upper part of the Weiherbach catchment	23
Figure 2-3: Characteristic catena of a loess hillslopes	23
Figure 2-4: View at the Weiherbach catchment	24
Figure 2-5: Observation devices	29
Figure 3-1: Tile drain irrigation experiment of Zehe and Flüßler (2001a)	35
Figure 3-2: Shape of Macropores: observed and generated	38
Figure 3-3: Sensitivity of Nash-Sutcliffe value to time shift	42
Figure 3-4: Ten best model runs	43
Figure 3-5: Hydrographs of the ten best models depending on hillslope width	44
Figure 3-6: Nash-Sutcliffe efficiency versus peak time error	45
Figure 3-7: Pair-wise scatter plots of parameters for runs with Nash-Sutcliffe efficiency (NS) ≥ 0.75	45
Figure 3-8: NS plotted against marginal parameter distribution	46
Figure 3-9: Number of model runs with NS ≥ 0.75 versus marginal distributions of parameters	46
Figure 3-10: NS versus the width of drained cross-section	47
Figure 3-11: Simulated soil moisture pattern	48
Figure 4-1: Discharge, bromide concentrations, cumulated bromide transport (1)	60
Figure 4-2: Discharge, bromide concentrations, cumulated bromide transport (2)	61
Figure 4-3: Discharge, bromide concentrations, cumulated bromide transport (3)	62
Figure 4-4: Simulated bromide concentrations in the hillslope	65
Figure 4-5: Cumulated IPU loss plotted against simulation time (1)	66
Figure 4-6: Cumulated IPU loss plotted against simulation time (2)	67
Figure 4-7: Cumulated IPU loss plotted against simulation time (3)	68
Figure 4-8: Quality of solute transport versus quality of water transport modelling	71
Figure 5-1: Perceptual flow models of macropore flow	82
Figure 5-2: Tile drain data of the three irrigation experiments	86
Figure 5-3: Moisture dynamic during the second irrigation experiment	88
Figure 5-4: Hydrograph separation of the first and second experiment	90
Figure 5-5: Measured isotopic composition of soil water	91
Figure 5-6: Results from the backward hydrograph separation	93
Figure 5-7: Correlation between hydrograph phases and isotopic composition of tile drain water	96
Figure 6-1: Normalised concentration profiles of each soil profile	109
Figure 6-2: Bromide concentration profiles	110
Figure 6-3: Isoproturon concentration profiles	111
Figure 6-4: Flufenacet concentration profiles	112
Figure 6-5: Average of the transport parameters	114
Figure 6-6: Solute breakthrough, first experiment	115
Figure 6-7: Solute breakthrough, second experiment	117
Figure 6-8: Solute breakthrough, third experiment	119
Figure 6-9: Temporal development of the retardation coefficient of FLU	120
Figure 7-1: Sampling locations of the macropore mapping	130

Figure 7-2: Number of macropores versus the number of earthworm, April	132
Figure 7-3: Number of macropores versus the earthworm biomass, April	133
Figure 7-4: Number of macropores versus the number of earthworm, October	134
Figure 7-5: Number of macropores versus the earthworm biomass, October	135
Figure 7-6: Cumulative density function of the macropore lengths, April	136
Figure 7-7: Cumulative density function of the macropore lengths, October	137
Figure 8-1: The Göberlein catchment	139
Figure 8-2: Extend of soil cracks on 50 cm × 50 cm field plots in the catchment.	140
Figure 8-3: Precipitation and discharge in the Göberlein catchment	142
Figure 8-4: Different infiltration patterns in the Göberlein catchment	143

Tables

Table 2-1: Land use in the Weiherbach catchment	25
Table 2-2: Flood events in at the gauge Menzingen	25
Table 3-1: Soil hydraulic parameters of the modelling field site	37
Table 3-2: Values of six key parameter that were combined in a Cartesian product	39
Table 3-3: Parameter and results for the ten best model runs	43
Table 3-4: Parameter combinations that never yield an acceptable model run	47
Table 4-1: Parameters and goodness of fit criteria to characterise the 13 model setups used for bromide modelling	57
Table 4-2: The 13 model runs used for bromide modelling	63
Table 5-1: Pre-experiment conditions before the irrigation experiments	83
Table 5-2: Number of macropores at the field site of the irrigation experiments	83
Table 5-3: Precipitation duration, amount, and intensity during the experiments	84
Table 5-4: Results of the compartmental mixing modelling	92
Table 6-1: Transport parameters and recovery for the five soil profiles	107
Table 6-2: Transport parameters and recovery for the five soil profiles, based on the 60 cm sampling depth	108
Table 6-3: Retardation coefficients of the pesticides over depth	113
Table 6-4: Characteristics of the BTCs of the three experiments	116
Table 7-1: Number of macropores/worm burrows with a diameter ≥ 4 mm	131
Table 7-2: R^2 for April (number of worm burrows and the number/biomass of <i>Lumbricus terrestris</i> L.)	131
Table 7-3: R^2 for October (number of worm burrows and the number/biomass of <i>Lumbricus terrestris</i> L.)	133
Table 7-4: R^2 for macropore diameters ≥ 4mm (number of worm burrows and the number/biomass of <i>Lumbricus terrestris</i> L.)	134

Table of Symbols

Symbol	Unit	Description	Equation
C	(g/l)	solute concentration in the water phase	Equation 4-1
C_a	(g/g)	solute concentration in the adsorbed phase	Equation 4-1
C_D	(‰)	deuterium signature	Equation 5-6 Equation 5-8
C_O	(‰)	oxygen-18 signature	Equation 5-7 Equation 5-8
C_p	(g/l)	tracer concentration of pre-event water	Equation 5-4
C_s	(kg/m ³)	average concentration at the soil depth z_i	Equation 6-1
$C(t)$	(g/l)	tracer concentration in the tile drain discharge at time t	Equation 5-4
D	(m ² /s)	dispersion coefficient	Equation 6-3
$h(z_i)$	(m ⁻³)	relative frequency of concentration depth distribution	Equation 6-1
k_f	(l ^{β} /g g ^{1-β})	Freundlich coefficient	Equation 4-1
$M_{in}(t)$	(g)	tracer mass applied until time t	Equation 5-2
$M_{out}(t)$	(g)	tracer mass that left the tile drain until time t	Equation 5-2
m_t	(kg)	total tracer mass in the soil profile	Equation 6-1
$P(t)$	(l)	total irrigation amount until time t	Equation 5-2
$Q(t)$	(l)	tile drain discharge at time t	Equation 5-3
$Q_e(t)$	(l)	amount of irrigation water in the discharge at time t	Equation 5-3
$Q_p(t)$	(l)	amount of pre-event water in the discharge at time t	Equation 5-3
R	(-)	retardation coefficient	Equation 6-5
R_{Sample}	(‰)	measured ² H/ ¹ H or ¹⁸ O/ ¹⁶ O	Equation 5-1
R_{St}	(‰)	Vienna-Standard Mean Ocean Water	Equation 5-1
t	(s, min)	time	Equation 5-2, 5-3, 5-4, 6-3
V	(m ³)	soil volume	Equation 6-2
v_c	(m/s)	transport velocity of the conservative solute	Equation 6-5
v_s	(m/s)	transport velocity of the reactive solute	Equation 6-5
x_1	(-)	fraction of irrigation water	Equation 5-5, 5-6, 5-7, 5-8
x_2	(-)	fraction of upper compartment water	Equation 5-5, 5-6, 5-7, 5-8
x_3	(-)	fraction of pre-event soil water	Equation 5-5, 5-6, 5-7, 5-8

Symbol	Unit	Description	Equation
\bar{z}	(m)	average transport distance	Equation 6-2
z_i	(m)	depth at soil level i	Equation 6-1, 6-2, 6-3
β	(-)	Freundlich exponent	Equation 4-1

Units. g: gram, kg: kilogram, l: liters, m: meters, s: seconds, min: minutes.

Abstract

Preferential flow is of central importance in hydrology, since it contradicts the classical theories of water flow and solute transport. The rapid flow in connected preferential flow paths has several implications on hydrological processes, such as runoff generation and solute transport. Especially reactive solutes like agrochemicals can be rapidly transported in surface water or groundwater possibly harming the eco-system. Direct observation of the hydrological processes related to preferential flow is challenging and moreover, the representation of preferential flow in hydrological models often remains poor. The models show deficiencies in reproducing both, water and solute transport. To address the limitations of hydrological modelling and to enhance the understanding of processes associated with preferential flow I follow an approach that combines modelling and hydrological experiments.

Earthworms are one important factor in generating preferential flow paths. The study site of this work is the cultivated lower meso-scale Weiherbach catchment, where vertical orientated preferential flow paths are an important landscape element controlling hydrological behaviour. How can these structures be parameterised in a hydrological model? And what are the detailed hydrological processes that generate discharge in the macropores soils of the Weiherbach catchment?

I suggest that a better representation of such preferential flow structures leads to a better representation of hydrological processes and will thus allow better hydrological modelling. I used a spatially explicit approach to represent worm burrows as connected structures of realistic geometry, high conductivity and low retention capacity in a two-dimensional physically based model (CATFLOW). The network of preferential flow was generated based on observable parameters. I used this approach and successfully modelled tile drain event discharge of an irrigation experiment at a tile drained field site. However, I found a considerable equifinality in the spatial setup of the model when key parameters such as the area density of worm burrows, the maximum volumetric water flows inside these macropores and the conductivity of the tile drain were varied within the ranges of either the available measurements or measurements reported in the literature. In total, I found that 67 out of 432 model runs were acceptable (Nash–Sutcliffe (NS) ≥ 0.75). Among these, the 13 best yielded a NS coefficient of more than 0.9. Also, the flow volumes were in good accordance and timing errors were less than or equal to 20 min.

Solute modelling supplies an independent data source in addition to discharge. The probability that a model represents the underlying hydrological processes in a right way is increased, if it can reproduce discharge and solute transport. Thus I performed solute transport modelling, without further model calibration, to: a) test the feasibility of the spatially explicit representation of macropores to reproduce observed bromide transport, b) to reduce the model equifinality, and c) to model the leaching behaviour of a reactive solute. The solute modelling was performed based on the model runs that performed best

in reproducing tile drain discharge ($NS \geq 0.9$). I could reduce the equifinality by the use of solute transport as independent data source, since only four of the 432 model setups could reproduce both, discharge and solute transport. Transport modelling of a reactive solute performed best, when no retardation was parameterised within the preferential flow structures. The modelling study revealed that a better representation of important structures allows successful modelling of water and solute transport. Thus the explicit representation together with the second order information (solute transport) allows reducing model equifinality.

The modelling study showed the importance of process representation and the value of data sources additional to discharge. To gain knowledge about the detailed preferential flow processes at a tile drained field site a series of three irrigation experiments was performed. I employed a multi tracer approach, accompanied by isotope concentrations, soil moisture and discharge observation. Bromide and two pesticides were applied on the field plot. Isotopic composition was measured in the irrigation water, in the soil water, and in the tile drain discharge. I showed that the proportion of irrigation water in the tile drain hydrograph never exceeded 20%, although the discharge increased threefold. Based on a mixing cell modelling approach I showed that significant mixing of irrigation water with pre-event soil water took place in the soil matrix and changed the soil isotopic composition towards the irrigation water. The discharge and solute transport were controlled by a capacity threshold at the field plot. Below the threshold water infiltrated from the preferential flow paths into the matrix. When the moisture threshold was exceeded the soil water entered preferential flow paths, enabled connectivity of the macropore network to the tile drain, and contributed large amounts of water to the hydrograph. The pesticide transport is highly controlled by this mechanism. After the reversal of the macropore-matrix interaction, the solutes could not reach adsorption places and were transported without retardation. This process increases the risk of contaminant remobilisation and groundwater contamination at cultivated field sites.

In summary, I could show that a more realistic process description in a hydrological model and a parameterisation based on observables led to a successful modelling of water and solute transport at a tile drained field site. This means that we should explicitly account for preferential flow processes in hydrological models. In addition, I showed the crucial role of preferential flow in supplying pre-event soil water during event discharge and the importance of these flow paths in the fast transport of pesticides without retardation, controlled by the macropore-matrix interaction. The macropore-matrix interaction is thus of crucial importance in runoff generation and solute transport at hillslope scale, and could explain the high proportion of pre-event water in the hydrograph and the rapid pesticide transport.

Kurzfassung

Präferentieller Fluss hat eine zentrale Bedeutung in der Hydrologie, da er der klassischen Theorie zu Wasser- und Stoffflüssen widerspricht. Der schnelle Fluss in konnektiven präferentiellen Fliesswegen hat weit reichende Konsequenzen auf verschiedene hydrologische Prozesse, wie zum Beispiel auf die Abflussbildung und den Stofftransport. Vor allem stellt der schnelle Transport von eigentlich adsorbierbaren Stoffen wie Pflanzenschutzmittel in Oberflächengewässer oder das Grundwasser eine Gefahr für das Ökosystem dar. Das Messen von hydrologischen Prozessen, die in Verbindung mit präferentiellem Fliessen auftreten, ist schwierig und dazu ist die Darstellung von präferentiellem Fliessen in hydrologischen Modellen häufig limitiert. Modelle haben häufig Probleme damit sowohl den Wasserfluss als auch den Stofftransport zu modellieren. Im Folgenden werden die Limitierungen in der hydrologischen Modellierung angegangen und Untersuchungen durchgeführt um hydrologische Prozesse in Verbindung mit präferentiellem Fliessen besser zu verstehen. Dazu arbeite ich mit einem Ansatz der hydrologische Modellierung mit Feldexperimenten kombiniert.

Präferentielle Fliesswege werden häufig durch die Aktivität von Regenwürmern erzeugt. Die Untersuchungen dieser Arbeit wurden im Weiherbach-Einzugsgebiet durchgeführt, welches ein landwirtschaftlich genutztes Gebiet der unteren Mesoskala ist. Dort spielen vertikal orientierte präferentielle Fliesswege eine herausragende Rolle in Bezug auf das hydrologische Geschehen. Wie lassen sich solche Strukturen in einem hydrologischen Modell parametrisieren? Und wie funktionieren die hydrologischen Prozesse, welche Abfluss in den makroporösen Boden im Einzugsgebiet des Weiherbachs erzeugen, im Detail?

Ich postuliere, dass eine genauere Repräsentation solche präferentieller Fliessstrukturen zu einer besseren Darstellung hydrologischer Prozesse führt und damit verbesserte hydrologische Modellierungen ermöglicht. Ich verwende einen räumlich expliziten Ansatz, der die Wurmgänge als konnektive Strukturen in realistischer Geometrie, mit hoher Leitfähigkeit und geringen Retentionseigenschaften in einem 2-dimensionalen physikalisch basierten Modell (CATFLOW) darstellt. Ein Netzwerk aus präferentiellen Fliesswegen wurde mit Hilfe von messbaren Parametern und einem stochastischen Modell generiert. Mit Hilfe dieses Ansatzes konnte ich den Hydrographen eines drainierten Standortes während eines Beregnungsversuchs erfolgreich modellieren. Durch das Variieren verschiedener Parameter im Rahmen von Messwerten oder Werten aus der Literatur, wie der Oberflächendichte der Wurmgänge, der maximalen Leitfähigkeit der Makroporen und der Leitfähigkeit der Drainage, konnte gezeigt werden, dass eine deutliche Equifinalität im räumlichen Aufbau des Modells vorhanden war. Insgesamt konnten 67 der 432 Modellläufe den Abfluss gut reproduzieren (Nash-Sutcliffe (NS) ≥ 0.75), von diesen wiederum zeigten 13 einen $NS \geq 0.9$. Dazu waren die Abflussvolumina gut modelliert und auch die zeitliche Übereinstimmung der modellierten und gemessenen Abflussspitzen sehr gut (innerhalb von 20 min).

Das Modellieren des Stofftransportes liefert eine zusätzliche vom Abfluss unabhängige Information. Falls ein Modell sowohl den Wasserfluss als auch den Stofftransport richtig reproduzieren kann, erhöht dies die Wahrscheinlichkeit, dass die zugrunde liegenden hydrologischen Prozesse in richtiger Weise dargestellt sind. Daher habe ich die Stofftransportmodellierung ohne weiteres Kalibrieren durchgeführt, um: a) zu testen in wie weit der Ansatz geeignet ist, um den im gleichen Experiment beobachteten Bromidtransport zu modellieren, b) um die Equifinalität zu reduzieren und c) um den Stofftransport eines Pestizides zu simulieren. Dazu habe ich die 13 Modellläufe verwendet, die einen $NS \geq 0.9$ erreichten. Es war dadurch möglich die Equifinalität zu reduzieren, da nur vier dieser Läufe den Stofftransport reproduzieren konnten. Damit waren nur vier der insgesamt 432 Modellläufe in der Lage, sowohl den Wasserfluss als auch den Stofftransport im Rahmen akzeptierter Abweichungen zu modellieren. Die Pestizidmodellierung erzielte die besten Ergebnisse wenn keine Retardation in den präferentiellen Fließpfaden parametrisiert wurde. Durch die Modellierung konnte gezeigt werden, dass eine bessere Repräsentation relevanter Strukturen wichtig für ein erfolgreiches Modellieren von Wasserflüssen und Stofftransport ist. Die explizite Darstellung relevanter Strukturen führt zusammen mit einer Information zweiter Ordnung (Stofftransport) zu einer Reduzierung der Modellequifinalität.

Um ein verbessertes Verständnis über die detaillierten präferentiellen Fließprozesse auf einem drainierten Standort zu erhalten wurde eine Reihe aus drei Beregnungsversuchen am selben Standort durchgeführt. Dafür verwendete ich einen Ansatz mit mehreren Tracern (inkl. Wasserisotopen), Bodenfeuchtemessungen und Abflussmessungen der Drainage. Bromide und zwei Pestizide wurden vor/während der Experimente appliziert. Die Isotopenkonzentrationen wurden im Beregnungswasser, dem Bodenwasser und dem Drainagenabfluss gemessen. Ich konnte zeigen, dass der Anteil des Beregnungswassers nie die Marke von 20% in der Drainage überschritt, obwohl sich der Abfluss mehr als verdreifachte. Mit Hilfe eines Mischungszellenansatzes wurde gezeigt, dass sich das Beregnungswasser stark mit dem vor dem Experiment vorhanden Bodenwasser in der Bodenmatrix vermischt. Der Wasser- und Stofftransport am Untersuchungsstandort wurde von einem Schwellenwertprozess kontrolliert. Unterhalb dieser Schwelle infiltriert das Wasser aus den Makroporen in die Bodenmatrix, wird der Schwellenwert überschritten kehrt sich die Richtung dieser Interaktion um und Bodenwasser trägt zu einem großen Anteil zur Erhöhung des Abflusses bei. Auch der Transport der Pestizide ist durch diesen Mechanismus kontrolliert. Sobald sich die Richtung der Makroporen-Matrix-Interaktion ändert, können diese die Adsorptionsplätze der Bodenmatrix nur noch limitiert erreichen, was zu einem Transport ohne Retardation führt. Daher führen die identifizierten Prozesse zu einer möglichen Remobilisierung von im Boden vorhandenen Pestiziden und zu einem erhöhten Risiko einer Grundwasserkontamination.

Zusammenfassend konnte ich zeigen, dass eine realistische Prozessbeschreibung in einem hydrologischen Modell zu einer erfolgreichen Modellierung von Wasser- und

Stofftransport führen kann. Außerdem konnte ich die wichtige Rolle der präferentiellen Fließwege auf die Mobilisierung von „altem“ Wasser, welches vor dem Versuch im Boden gespeichert war, und den Transport von Pestiziden zeigen. Beides wurde durch einen Schwellenwert kontrolliert, bei dessen Überschreitung sich die Interaktionsrichtung der Makroporen und der Bodenmatrix änderte. Die Interaktion zwischen Makroporen und Bodenmatrix ist daher von entscheidender Bedeutung in der Abflussbildung und dem Stofftransport auf der Hangskala und kann sowohl den Anteil von „altem“ Wasser während Abflussereignissen erklären als auch den schnellen Transport von Pestiziden.

Acknowledgment

I want to thank my advisor Erwin Zehe that he gave me the chance to join his group, for his advice and support, and for the many valuable discussions during my PhD-studies. I want to thank my referees Rainer Meckenstock and Markus Weiler that they took the time to read and review my thesis. Further I want to thank my colleagues at the Department of Hydrology: Conrad for the various creative discussions over the last years, Jan and Thomas for their help whenever I needed some, Simon for having a great time together in the office, Ulli for her various help in Matlab and GIS issues, Uwe that he was always supportive no matter where the problem was, and finally Markus, with whom I spent weeks in the field.

I am grateful that I was able to perform pesticide and isotope analysis at the group of Martin Elsner and I want to thank Sibylle Steinbeiss for her continuing support in the lab. I thank Christoph Külls that he helped me out with the soil water isotope analysis and Dorothee Schneider who helped my out with pesticide analysis in the soils. Moreover, I am thankful to Harald Horn that I could work frequently in the lab of die Institute of Water Quality Control, to Brigitte, Martina, and Steffi for their support. I also enjoyed the time with all the people in the lab. Thanks to the colleagues of the Hydraulic engineering chair and from Oberrach, especially Peter Schwarz for his various support. Thanks to the many students and Hiwis that worked related to my work: Elham, Florian, Francois, Max, Shams, Tobi, and especially Steve for spending so many days in the field. I am glad that Doug, Julien, and Mike helped me out with the english proof, it was a great support.

I want to thank the BIOPORE project members from Potsdam University: Juliane, Loess, and Boris for their great support, the discussions, and the enjoyable field trips. A special thank to the farmers of both research catchments without them the project could have never been carried out. In particular I want to thank Udo Eichinger for his support during the field experiment on his property and Werner Schneider that he was extremely supportive and that he helped out several times.

Last but not least I want to thank my fiends for listening during desperate hours and that I always can have a great time with them. For all their encouragement and love I want to thank my familiy Jutta, Gerhard, Julika, Janis, and Joris.

This study was funded as a part of the BIOPORE project by the DFG (Deutsche Forschungsgemeinschaft). This is gratefully acknowledged.

1 Introduction

Preferential flow includes all process "...where water and solutes move along certain pathways, while bypassing a fraction of the porous matrix" (Hendrickx and Flury, 2001). The importance of macropore flow has been recognized since 1882. Back then, Lawes et al. (1882) noted that "...in a heavy soil, channel drainage will in most cases precede general drainage, a portion of the water escaping by the open channels before the body of the soil has become saturated; this will especially be the case if the rain fell rapidly, and water accumulates on the surface" (in Jarvis, 2007). Lawes et al. (1882) also distinguished between matrix and macropore flow, while recognising the effect of soil type and rainfall intensity on both processes. Years later Moore (1898, in Clothier et al., 2008) recognised the effects of soil cracking on flow, and that this leads to water quality issues, as "...the effluent water is not purified as intended". Preferential flow paths can develop due to soil structure, so preferential flow and transport is common in all soils, thus large parts of the soil matrix are bypassed reducing the filter function of the soil during rainfall. This leads to significant consequences for the water quality of receiving water bodies (Jarvis, 2007). For a long time studies of sub-surface water transport ignored the findings of Lawes et al. (1882) and Moore (1898) and instead focused on convection-dispersion transport in matrix flow which assumes perfect lateral mixing processes and is rapid compared to vertical convective transport (Jury and Flühler, 1992). The actual rate of contaminant transport in groundwater in some cases contradicted the theory of convection-dispersion and thus brought preferential flow back to the fore-front of water science. Since the late 1970s the number of publications on preferential flow has increased dramatically (Jarvis, 2007).

While convection-dispersion theory assumes well mixed conditions and uniform fluxes, this is often not valid in the unsaturated zone, since the vertical transport distances are too small. Water flow in soils including preferential flow is non-uniform and leads to irregular wetting fronts within soil (Gerke, 2006); within this non-uniform flow water can move faster and in higher volumes at certain locations. Physical non-equilibrium induced by preferential flow occurs in unsaturated soils resulting in different water pressures and/or solute concentrations during vertical flow and transport. Preferential flow can be initiated at the soil surface during ponding conditions, under unsaturated conditions flow converges within a distribution layer and is drained by preferential flow paths (Ritsema and Dekker, 1995). The assumption that pores fill and start to participate in water flow depending on their size does not apply in many cases. Thus applying the Richards equation for heterogeneous flow in a homogenous way is not adequate for modelling water flow in unsaturated soils (van Schaik, 2010). Several studies have shown that the occurrence of preferential flow is strongly driven by a threshold behaviour (e.g. Zehe et al., 2005; Zehe and Sivapalan, 2009).

Preferential flow has a broad impact on the hydrological cycle, it influences soil water dynamics, groundwater recharge, contaminant transport, runoff generation, residence

times, and even helps to shape the earth's surface through erosion processes. Preferential flow, therefore, plays a major role in hydrology and adjacent fields of research. What follows is a literature review of different types of preferential flow and where they occur, preferential flow observation techniques, and methods for modelling preferential flow. Finally I present open research questions, define the thesis objectives and present the outline of this thesis.

1.1 Types of preferential flow

Preferential flow can be separated into different types based on characteristic flow patterns within soils or hillslopes. Many researchers have identified various flow types, here I will use a classification based on three flow types following Jury and Horton (2004):

- Funnel Flow
- Macropore Flow
- Unstable Flow

Preferential flow can occur laterally as well as vertically (see McDonnell, 1990; Jones, 1997; Sidle et al., 2001). For example Allaire et al. (2009) classified lateral flow as a separate flow process, while, within this thesis, lateral preferential flow will be summarised within the three preferential flow types mentioned above, because the underlying physical processes are similar to vertical preferential flow processes. Each type of preferential flow has unique characteristics such as occurrence, physical processes, and initiation.

1.1.1 Funnel flow

Funnel flow occurs when flow is redirected on an inclined geological layer (Kung, 1990b), but water still flows in the soil matrix. Kung (1990a) performed a field experiment by uniformly applying a dye tracer solution on a field site consisting of sandy soil. Water flowing through the root zone was funnelled into concentrated flow paths that occupied only a small portion of the soil matrix in the vadose zone yet accounted for most of the transport. Figure 1-1 presents the redirection of soil water and its concentration into preferential flow pathways. In the study of Kung (1990a) small lenses with coarse sand were embedded in the fine sand. Thus, there was a funnel effect caused by a capillary barrier between the two layers. Under unsaturated flow conditions, greater pressure is required to force moisture into a larger pore from a smaller pore (Kung, 1990b). Therefore, moisture tends to flow over the layer rather than through it. With higher flow rates funnel flow is less pronounced because the higher flow rates can create enough pressure so that water flows through the coarse layer rather than over it. Kung (1990b) found a strong effect of the slope of the embedded layer on the funnelling.

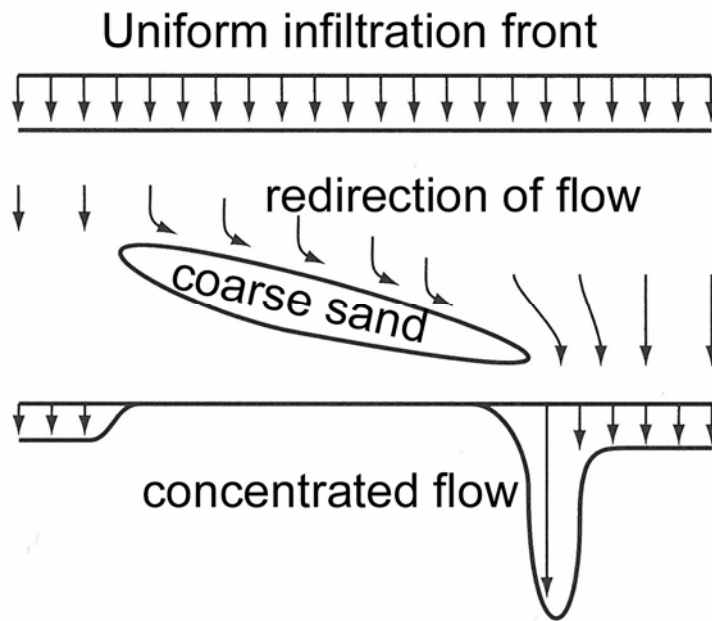


Figure 1-1: Funnelling of a uniform infiltration front on an inclined layer of coarse sand (after Kung, 1990b).

Funnelling has a strong effect on groundwater contamination, as downward movement of contaminants can be greatly enhanced (Kung, 1990b). In a numerical modelling study Ju and Kung (1997) showed that in simulations that included funnel flow the contaminant breakthrough time was four times faster than simulations assuming homogeneous soil layering. They also found that the ratio of the total mass leached from simulations with funnel flow to that of matrix flow increased exponentially as the water application rate decreased. Zhao et al. (2010) observed funnel flow in their study area located in the loess plateau of China. After precipitation the wetting front was unstable due to the slopping layered soil. They concluded that funnel flow can cause additional risk for groundwater contamination.

1.1.2 Macropore flow

Macropores have been described as soil pores that are large enough so that water is not held in them by capillary forces, within these larger pores flow resistance is small compared to matrix flow. Such structures favour preferential flow within soils with locally up to 100-1000 times faster water fluxes than compared to matrix flow (Germann and Beven, 1985; Germann, 1990). Infiltration in soils is strongly influenced by macropore structures typically resulting in higher infiltration rates. Yet, there is no set definition of a macropore. It is assumed that flow within macropores is dominated by gravity while the flow in the soil matrix is affected by different suction heads. The water flow within a macropore will start when the water pressure at the interface of macropore and matrix soil exceeds the water entry pressure (Jarvis, 2007) or if surface water is available that can enter the macropore at the soil surface (e.g. overland flow, surface ponding). A variety of

diameter limits is given within literature to distinguish between macropores and non-macropores (Beven and Germann, 1982; Jarvis et al., 1999; Jarvis, 2007). Common within all definitions is that macropore diameter is an order of magnitude larger than soil matrix texture pores (Greco, 2002). Nevertheless, Jarvis (2007) summarised that most macropore studies consistently show an increase in hydraulic conductivity up to three orders of magnitude starting around a pressure potential of -10 cm to -6 cm. Thus precipitation intensities of ca. 1 mm/h, which corresponds to the unsaturated hydraulic conductivity of arable soils at suction head of -10 cm (Jarvis et al., 2002), has been shown to initiate macropore flow in field studies (Beven and Germann, 1982; Gish et al., 2004). Macropores can originate from different processes:

- Abiotic factors, e.g. soil cracking and subsurface erosion
- Biotic factors, e.g. animal (worm burrows, mice holes) and plant activities (root channels)
- Human factors, mainly to agricultural practice, influencing soil structure

Soil cracking is caused by swelling and shrinking in soils containing a significant amount of smectites and vermiculites clay minerals, this amount has been estimated to be ca. 15% to 20% (Horn et al., 1994, in Jarvis, 2007). The shrinkage characteristic curve represents the volume change of soils in relation to soil moisture (McGarry and Malafant, 1987). Four zones of volume change are usually distinguished: zero, residual, normal, and structural shrinkage (Braudeau et al., 1999). The “normal” shrinkage zone is generally the most important one in terms of the volume change in soils (Peng and Horn, 2005), as volume loss is approximately proportional to the water loss. In this zone, a deformation of pores occurs instead of a penetration or displacement of air in the pores (Bronswijk, 1988; Chertkov, 2000). Thus the volume change of the pores can influence the hydraulic characteristics of the soil matrix (Kim et al., 1999; Chertkov, 2004; Peng and Horn, 2005). These processes lead to soil cracks, which can act as preferential flow paths in soils (Bronswijk, 1988; Wells et al., 2003).

The amount of biological induced macropores can be extraordinary high. Edwards et al. (1988) found 14,000 pores larger than 0.4 mm on 1 m² in an untilled sandy loam cropped with maize. Weiler (2001) and Zehe and Flüßler (2001a) found several hundreds of worm burrows on 1 m². Those burrows showed significantly larger diameters than those of plant roots. Shipitalo and Butt (1999) reported a tortuosity of worm burrows of the anecic (deep-burrowing) worm *Lumbricus terrestris* L. of 1.1-1.2. In contrast, endogeic earthworms formed a random network in the topsoil with less impact on water and solute transport (Jarvis, 2007). Figure 1-2 shows two types of preferential flow patterns, visualised with a dye tracer (brilliant blue) application.

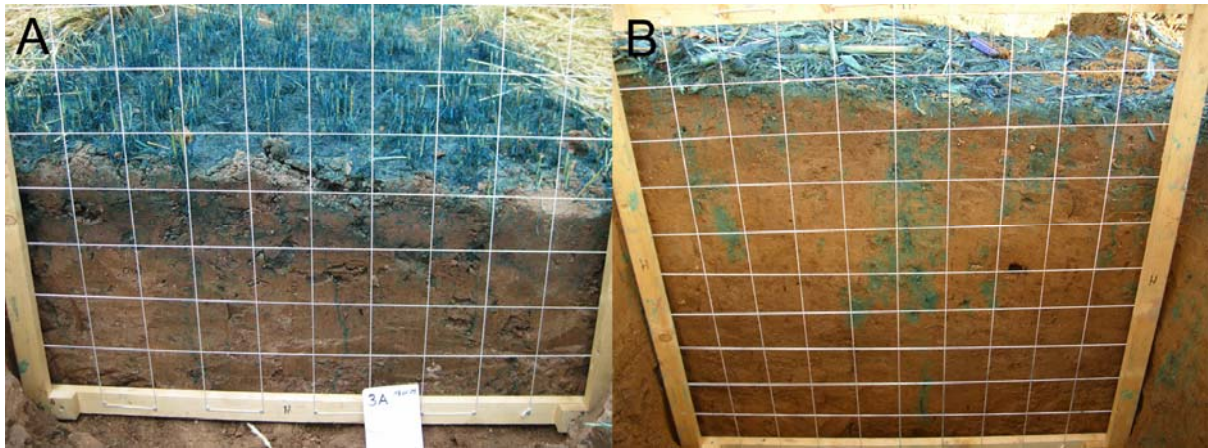


Figure 1-2: Different reasons for preferential flow, visualised with brilliant blue. A) Preferential flow in soil cracks, in the Göberlein catchment, Germany, leading down to the bedrock at 40 cm depth. B) Preferential flow in earthworm burrows, Weiherbach, Germany. Grid size is 10 cm on 10 cm.

Water flow in macropores is driven by interplay of gravity, viscosity, and capillary forces, with the capillary forces playing a minor role. Beven and Germann (1982) showed that not all macropores are active in the soil. Water flow in macropores takes places as film flow at low saturations (e.g. Bouma and Dekker, 1978) and changes to intermittent flow when saturation increases (e.g. Germann, 1987). This intermittent flow starts when capillary bridging across the pore occurs. Reported Reynolds numbers show that water flow in pores can be near turbulent or near full turbulent flow under ponded conditions (Allaire et al., 2009). Mori et al. (1999, in Allaire et al., 2009) reported Reynolds numbers of 50-80, which suggested that the flow regime was transitional to turbulent, while Logsdon (1995) reported Reynolds numbers larger than 1000 in partially saturated artificial macropores of 6 mm diameter, corresponding to near fully turbulent flow conditions. This means that friction is not longer negligible, an assumption which is implicit in the derivation of Darcy's law and the Richards equation. When the flow regime changes to turbulent flow, the relation between flow velocity and hydraulic gradient becomes non-linear and Darcy's law overestimate the effective flow velocity (Bear, 1972). Hence these flow formulations may be inappropriate to model macropore flow.

As mentioned previously, macropore flow can be initiated when water pressure in the soil matrix exceeds a value of -10 cm to -6 cm, so initial soil moisture has a significant influence on when macropore flow initiates (Jarvis, 2007). Other factors influencing the initiation of macropore flow are the rainfall intensity and the total precipitation (e.g. Trojan and Linden, 1992; Gish et al., 2004), micro-relief as it conducts water to macropores openings (Trojan and Linden, 1992), the surface area drained by a macropore (Trojan and Linden, 1992; Weiler and Naef, 2003a), number of pores per unit area (Weiler and Naef, 2003b), slope of the soil surface (Weiler and Naef, 2003b), and the water repellency of the soil (Doerr et al., 2006).

Macropore flow has a significant impact in environmental science. Macropore flow governs infiltration on the plot scale (Weiler and Naef, 2003a) and runoff generation at the

hillslope (van Schaik et al., 2008) and catchment scale (Blöschl and Zehe, 2005). Macropore flow can also affect solute transport. The transport of pesticides and phosphorus to deeper soil depths or surface water and shallow groundwater is widely documented (Flury, 1996; Stamm et al., 1998). Zehe and Flühler (2001a) observed fast transport of bromide caused by macropore flow.

In summary, flow in soil cracks (Blake et al., 1973) and worm burrows (Zehe and Flühler, 2001a) leads to a rapid bypassing of the soil matrix, and therefore can have a significant impact on environmental systems. Macropores are mainly vertical structures that can be interconnected and form a network over a wider scale (e.g. hillslope). Those networks can induce lateral preferential flow that has been observed in several hillslope studies (Sidle et al., 2001; van Schaik et al., 2008). This observed lateral flow frequently occurs in soil pipes (Uchida et al., 2001; Jones, 2010).

1.1.3 Unstable flow

Various conditions can lead to unstable wetting fronts in the infiltration process in unsaturated soils: vertical flow from a fine-textured layer into a coarser layer (Hill and Parlange, 1972), infiltration into a water-repellent soil (Hendrickx et al., 1993), if the infiltration rate is less than saturated hydraulic conductivity in a homogeneous soil (Selker et al., 1992), increasing soil hydraulic conductivity with depth (de Rooij, 2000), and redistribution of soil water after the infiltration process (Wang et al., 2003). Wetting front instability leads to a finger like preferential flow pattern within the soil profile. Or (2008) suggests that fingers starts to form when the Bond number, which relates gravity, capillary forces, and viscous forces, becomes smaller than 0.2. Based on the work of Raats (1973) and Philip (1975) Jury and Horton (2004) summarised that an unstable wetting front is a result of decreasing water pressure from the wetting front towards the soil surface. Figure 1-3 summarises the process of instability of the wetting front and generation of finger flow. The h_{we} , is the water pressure, that allows water to enter the dry soil. The infiltration front is at h_{we} . If a perturbation is formed, the water pressure above this perturbation decreases, and then regions of the surrounding matrix supply the zone above the finger by lateral flow. So the water pressure at the wetting front drops below h_{we} . Then the profile drainage is driven by water flow in the formed finger, while the water flow elsewhere is stopped. A major condition for finger growth is a pronounced threshold water-entry pressure between wet and dry regions in the soil profile, so that water percolation in the matrix adjacent to the finger becomes insignificant when the matrix supplies water to the finger and pressure is lowered above the infiltration front (description follows Jury and Horton, 2004). This condition is often most pronounced in coarse-textured sands. Finally, the formed fingers only propagate further in the soil profile if they do not rapidly vanish through lateral flow to the surrounding dry soil matrix (Jury and Horton, 2004). Preferential flow by unstable flow can enhance the streamflow response of precipitation inputs, the total streamflow, and strongly effect the soil moisture distribution within soils (van Schaik, 2010).

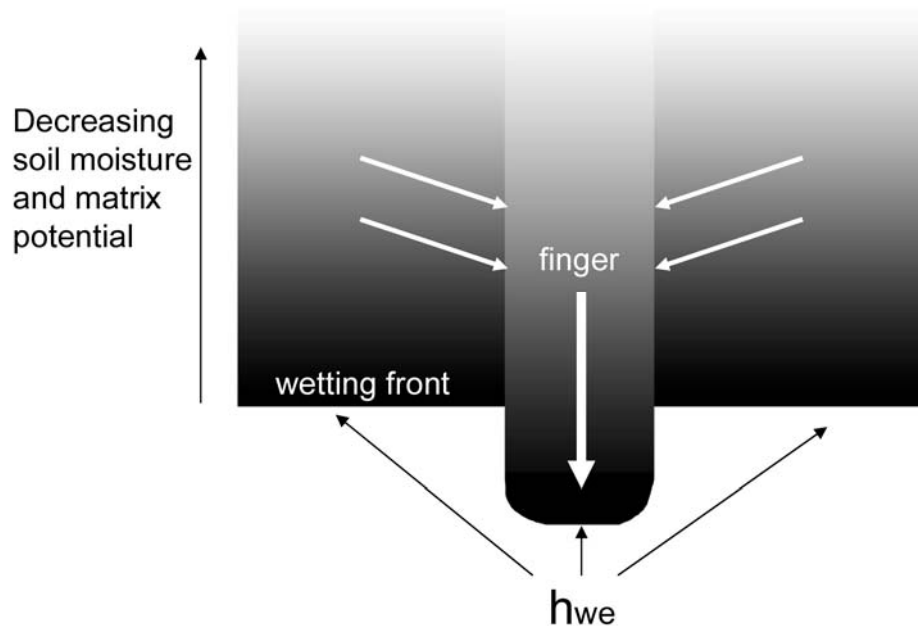


Figure 1-3: Exemplified development of infiltration front instability during moisture redistribution, when the pressure distribution decreases toward the soil surface. If the infiltration front moves deeper into the soil at one location, the pressure distribution above it shifts downward. This leads to a lateral flow gradient from the surrounding soil to the finger (white arrows). Wetter soil parts are indicated by dark shade, dry soil parts by bright shade (Figure after Jury and Horton, 2004).

1.1.4 Summary of preferential flow types

The different types of preferential flow processes have distinct driving factors and occur in specific soil types under different initial conditions. The impact of funnel flow and unstable flow at the catchment scale has to be evaluated together with other processes in the catchment to determine their impact on catchment hydrology (e.g. the connectivity with shallow groundwater). Nevertheless these types of preferential flow can enhance infiltration or change the soil moisture distribution within a catchment. Funnel flow has been shown to enhance solute transport, increasing the probability of ground- and surface water contamination. Macropore flow has been shown to have a substantial effect on catchment-scale hydrology through formation of lateral flow networks and increased water transport velocity. Macropores also have a significant impact on solute transport, particularly the delivery of agrochemicals to surface waters and shallow groundwaters.

1.2 Observing preferential flow

The methods for observing preferential flow processes in soils depend on the spatial and temporal scales under study. Legout et al. (2009) noted the strong scale dependence of preferential flow processes, both on temporal and spatial scale. Of course, the approach for studying the long term impact of preferential flow on groundwater contamination differs from the approach for studying the short term effects of preferential flow during a precipitation event (Allaire et al., 2009). Thus, different methods of measurement are

needed depending on the temporal and spatial scales being investigated. In addition, investigation of preferential flow processes usually requires a larger elementary volume and more samples than standard soil studies (Allaire et al., 2009). In the following I will give a summary of different techniques to observe preferential flow. Three main groups of observation approaches exist: structure observation, measurement of water flow, and tracer methods.

1.2.1 Observation of structures favouring preferential flow

In recent years scanning techniques have been developed that provide a 3-dimensional pattern of soil and pore structure. The big drawback of these approaches is that they are limited to soil cores typically less than 10 cm in diameter, they have to be performed in the lab, and they are very expensive. Nevertheless, they give valuable insights in the pore structure of soils. Hopmans et al. (1994, in Allaire et al., 2009) and Wildenschild et al. (2007) used X-ray tomography to identify the pore system of soil samples between 1.5 mm and 76 mm in diameter and were able to determine the phase distribution in a scanned soil core and the pore structure. Votrubova et al. (2003) used magnetic resonance imaging (MRI) to identify water distribution in soil cores. Deurer and Clothier (2005, in Allaire et al., 2009) used MRI to identify flow velocity in pores. Perret et al. (2000) used single photon emission computed tomography in combination with a radioactive tracer to detect tracer flow in soil pores. Different mathematical concepts are then used to determine the exact pore network based on the scanning (Perret et al., 2003). Usually those scanning techniques are suitable to derive soil structure, while preferential flow is studied by tracer movement in the soil core.

Because these scanning techniques are only applicable to soil cores, other approaches exist to observe structure favouring preferential flow on larger scales. At the plot scale horizontal soil profiles are excavated to count the number of pores, and to measure their diameter and depth (Munyankusi et al., 1994; Zehe and Flüher, 2001a). Image analysis was performed on excavated soil profiles to discriminate between macropores and matrix pores and different preferential flow types (Grevers and de Jong, 1990; Perillo et al., 1999). Also on plot scale Shipitalo and Butt (1999) determined the structure of different macropores by injecting resin in the burrow opening and excavating them after drying. The advantage of this method is the direct measurement of length, depth, and tortuosity at plot scale and the direct determination in the field. On a larger scale, ground penetrating radar can be used to determine soil structures or a 3-dimensional soil moisture pattern, that can provide evidence for preferential flow processes (Kung and Donohue, 1991), but the spatial resolution is limited and the observed pattern is usually rather coarse. Gish et al. (2002, in Allaire et al., 2009) were able to identify soil structures favouring funnel flow at a 7.5 ha study site. Nevertheless, all these methods give more of an idea of the network of preferential flow or the number and type of preferential flow paths and rather than real measurements of the actual preferential flow occurring under field conditions.

1.2.2 Observation of water flow to determine preferential flow

It is possible to measure the flow rate within an unsaturated soil volume in the lab. When measuring the unsaturated flow rate $k(\psi)$ with a tension infiltrometer (Jarvis et al., 1987), a difference in flow rate induced by a slight change in tension, indicates preferential flow when working near saturation (Allaire et al., 2009). This device can be used to compare intact soil cores with repacked cores from the same soil to determine the importance of preferential flow. In addition to the need to compare with repacked soils, problems with dead end pores and air entrapment limit the applicability of these measurements. Although the tension methods provide a good measure of the relevance of preferential flow in soil cores, the prediction of actual preferential flow in the field remains difficult.

Measurements of soil water distribution and dynamics has been used to infer preferential flow processes in soils, both in the lab and the field. Allaire et al. (2009) suggested the use of different kinds of soil moisture measurement equipment. If several probes are installed with a small distance between them covering different depths, it is possible to detect a spatio-temporal pattern of soil moisture change. This pattern has been attributed to preferential flow (Ritsma and Dekker, 1996; Germann and di Pietro, 1999; Cey and Rudolph, 2009). Most frequent is the use of TDR (time domain reflectometry) technologies (Topp et al., 1980), but the possible detection of preferential flow paths depends on integration volume, temporal resolution, and precision of the measurement. Germann et al. (2007) measured preferential flow within macropores with TDR sensors distributed over different depths. Blume et al. (2009) observed preferential flow, by measuring the soil moisture at six soil depth up to one meter with a profile probe (Delta-T Devices, Burwell, UK) with a temporal resolution of 10 min. Figure 1-4 presents the short term variation of water content measured with an FDR (frequency domain reflectometry) system, in this case a Theta Probe (Delta-T Devices, Burwell, UK), at 10 cm depth. The data were collected during a plot scale irrigation experiment. The fast response was achieved by an intermittent irrigation above the measurement devices. A second sensor (20 cm distance) shows a more constant increase, with no preferential flow. One big advantage of these techniques is the long time span preferential flow can be observed and that soil disturbance only occurs during instrument installation (Allaire et al., 2009). The major problem with these measurements is the need for high spatial resolution, if the distance between the measurement devices is too far, the preferential flow pattern may be missed. The observation of soil moisture to infer preferential flow processes in soils can cover different scales. The advantage of these approaches is that they can be applied at the column scale in the lab, but also at the plot scale or even at larger scales in the field as long as the distance between the measurement devices is small enough.

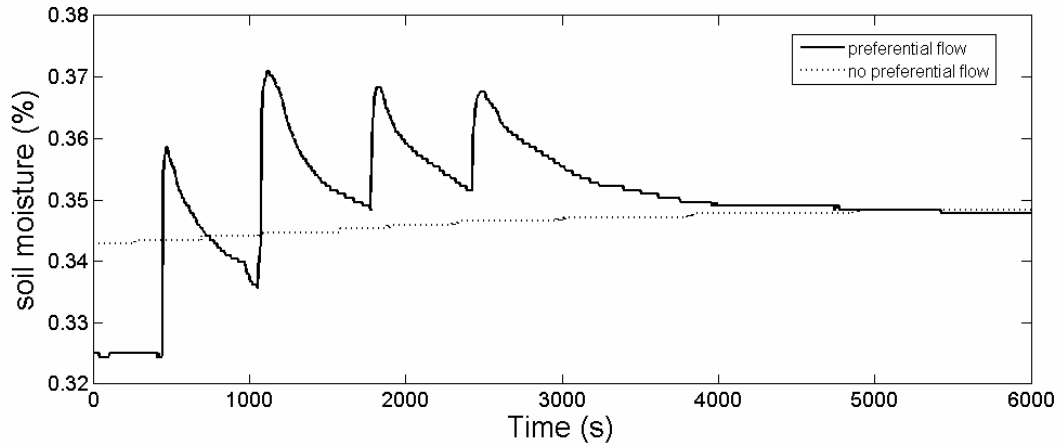


Figure 1-4: Evidence of preferential flow measured with a FDR soil moisture system. Two sensors located within 20 cm distance in 10 cm depth. The solid line show strong preferential flow, while the dotted line is not affected by preferential flow, measured in the Göberlein catchment, Germany (Klaus, unpublished data).



Figure 1-5: Hood infiltrometer on a macroporous soil in the Weiherbach catchment. Soil hydraulic conductivity was measured for different water tensions, and macropores were mapped.

Edwards et al. (1989) and Shipitalo and Butt (1999) measured the conductivity of macropores directly in the field. While the first installed samplers intercepting macropores in a specified depth, the latter constructed an infiltrometer to measure flow rate directly.

Those methods only indicate the effectiveness of specific macropores (Allaire et al., 2009) and are therefore more a measurement of maximum potential preferential flow because neither the full volume of each pore conducts water (Cey and Rudolph, 2009) nor do all pores conduct water (Beven and Germann, 1982). This approach covers single macropores, but with information on the occurrence of those pores the results might be transferred to larger scales.

Schwärzel and Punzel (2007) developed a hood infiltrometer to determine the soil hydraulic conductivity at various suction heads in the field. The advantage of this approach is that it is a direct measurement at the soil surface, however, the lower limit of the applied suction head is fixed by the air entry point. Thus the relevant tension where macropores become active might not be reached. Extensions for tensions below the air entry point are now available. Thus this approach may be a valuable alternative to the use of tension infiltrometers, since it is applicable outside the lab and can measure the hydraulic conductivity of undisturbed soils. Figure 1-5 presents a measurement of soil hydraulic conductivity on a macroporous field soil in the Weiherbach catchment, Germany, with a hood infiltrometer.

1.2.3 Tracer methods to observe preferential flow

Unlike the structure observation and the observation of water flow to determine preferential flow processes, different tracer methods are usually suited for both lab and field observations, and are not necessarily limited to a defined scale. Two different types of tracer based preferential flow observation are available, visualisation of the flow paths with a dye tracer or determination of the tracer breakthrough curve (BTC) at a fixed location.

The choice of the dye tracer for visualisation is strongly dependent on the tracer's chemical properties. The dye tracer used should provide a good contrast with the soil background and permit image analysis (Allaire et al., 2009). Typical dye tracers used are brilliant blue (Flury et al., 1994), methylene blue (Bouma et al., 1977), and rhodamine WT (Zhu and Lin, 2009). Nevertheless, those tracers have some limitations. Kasteel et al. (2002) showed that retardation of brilliant blue is non-linear concentration dependent, and increases with the ionic strength of the tracer solution. Additional sorption depends on the flow velocity (Perillo et al., 1998). It is difficult to compare different dye tracer studies because of differences in the tracer application (Allaire et al., 2009). To process data from dye tracing experiments soil profiles are excavated and photographed (e.g. Zehe and Flüher, 2001a; Weiler and Naef, 2003a). Weiler and Flüher (2004) distinguished different preferential flow types, and the interaction with the soil matrix depended on the dye tracer pattern. While most studies using dye tracer focussed on the plot scale, Anderson et al. (2009) stained a lateral preferential flow network at hillslope scale.

Tracer breakthrough curves are often used to measure the net effect of preferential flow on the integral response. This method involves applying a tracer to the soil and measuring its concentration through time at a certain depth or outlet. Again different tracers can be used

for this purpose: fluorescence tracers (Wienhöfer et al., 2009), ions (e.g. bromide, Zehe and Flüher, 2001a), isotopic tracers (deuterium (D) and oxygen-18 (^{18}O), Stumpp and Maloszewski, 2010) and particle tracers (Pryce, 2010). Allaire et al. (2009) suggested comparing tracers with different retardation coefficients to determine the strength of preferential flow. If the two tracers show a similar arrival time, preferential flow is dominating within the system. This can also be determined by the use of the Peclet number (Wienhöfer et al., 2009).

Several tracer sampling approaches exist to determine the BTC. Jardine et al. (1990) isolated a large undisturbed soil pedon (4 m² surface and 3 m depth) and equipped the pedon with fritted glass samplers applying suction to them to extract soil water and tracer. Using suction cups can create problems, for example Weihermüller et al. (2005) suggested there might be preferential flow towards those cups and good contact with the soil matrix might be difficult to achieve (Grossmann and Udluft, 1991, in Allaire et al. 2009). It is problematic to use suction cups, because it is highly uncertain if water is extracted from stagnant water or high velocity preferential flow paths (Köhne, 2005). Alternatively to suction cups, suction plates can be used (e.g. Kasteel et al., 2007), providing a larger contact area with the soil, compared to suction cups, and thus are more capable of detecting preferential flow. Nevertheless, both methods disturb the flow field. Pan samplers or wick samplers can be used to account for the spatial variability of solute transport and the BTC (de Rooij and Stagnitti, 2000) in field soils or lysimeters. Pan and wick samplers allow continuous sampling of the solute transport in the soil (Boll et al., 1992). Both are installed perpendicular to the direction of water flow under undisturbed soil. The samplers are directly attached to the soil, while the flow into pan samplers is driven by gravity, continuous suction is applied to the wick samplers. Due to the lack of capillary connection between the pan samplers and the soil, problems during dry soil conditions occur, although they work well near saturation (Allaire et al., 2009). These samplers give a good estimate of total preferential flow, but can not distinguish between different types of flow. It is also possible to measure the BTC at the system outlet. McIntosh et al. (1999) extracted soil cores from the field and investigated tracer BTCs within a lab study to estimate preferential flow. Bergström and Jarvis (1993) and Stumpp and Maloszewski (2010) used large undisturbed lysimeters to investigate BTC and sampled the tracer at the lower system boundary. Determination of the BTC on a larger scale is more challenging. Some researchers have sampled tile drains in fields to gain insight of preferential flow over larger areas. Stone and Wilson (2006) sampled a tile drain outlet during naturally occurring rainfall to determine preferential flow using chloride as a natural tracer. Everts et al. (1989) and Zehe and Flüher (2001a) used tile drain sampling to investigate flow processes on the field scale. At hillslopes, researchers have used trenching to determine the BTC and investigate preferential flow at hillslope scales (Leaney et al., 1993; Uchida et al., 2005; Anderson et al., 2009) or used natural springs to determine the BTC (Wienhöfer et al., 2009).

1.2.4 Summary on observation techniques

There are several approaches to observe preferential flow at small scales (core, plot), some of those approaches provide information on the amount of preferential flow but do not provide information on the type of preferential flow, while other approaches help to visualise and quantify the type of preferential flow occurring. On larger scales the methods in use are limited due to difficulties in sampling and little information can be obtained about preferential flow processes. It is necessary to use a combination of the methods described above to gain the best understanding of the type and amount of preferential flow occurring in a given soil. Most of the methods are applicable to smaller scales (plot, hillslope) while catchment scale approaches to determine preferential flow are yet not at hand.

1.3 Modelling of preferential flow

Given that preferential flow is common in soils, there is a need to include concepts that account for preferential flow in hydrological models. Using mathematical models to simulate preferential flow helps us to interpret field observations and allows us an improved modelling of solute transport and thus a better risk assessment of contaminant leaching. In chapter 1.1 the factors influencing the generation of preferential flow are summarised. Those influences have to be considered when preferential flow is modelled. Various approaches have been developed over the last several years, to include non-equilibrium flow in models. They range from approaches to deal with preferential flow at the scale of soil physics to catchment scale applications. In the following I will introduce several theoretical concepts of modelling preferential flow, and show examples of the conceptualisation of preferential flow in different models.

1.3.1 Model concepts

Process-based models are mainly based on the Richards equation (Jury and Horton, 2004) for variability saturated water flow. The Richards equation is invariably accompanied by a set of constitutive relations characterising the unsaturated soil hydraulic properties. The most common way is a conceptualisation with the Mualem-van Genuchten parameters (Mualem, 1976; van Genuchten, 1980). Yet, the exclusive application of the Richards equation does not allow for modelling preferential flow in soils. Thus other approaches have been developed.

The composite function approach

Composite function models provide a simple approach to account for preferential flow and transport in soils by dividing the soil (i.e. a porous media) into different overlapping regions. The Mualem-van Genuchten equation (Mualem, 1976; van Genuchten, 1980) is used to describe the soil hydraulic properties. Linear superposition of the functions for each region gives the function for the entire multi-modal pore systems (e.g. Durner 1994; Mohanty et al., 1997; Durner et al., 1999, in Gerke, 2006). Although these types of models can simulate a significant increase in the hydraulic conductivity near saturation they do not

actually simulate preferential flow, given that they still simulate flow as a uniform wetting front (Šimůnek et al., 2003).

The single porosity approach

A single porosity model for non-equilibrium flow was developed by Ross and Smettem (2000). They used the Richards equation to describe flow, and decoupled pressure heads and water content, conditions that are frequently observed during preferential flow conditions. As such, only one additional parameter, called equilibrium time constant, is needed to describe preferential flow. With this approach Ross and Smettem (2000) were able to describe flow in undisturbed soil columns, while Šimůnek et al. (2001) modelled upward infiltration with this approach.

The dual porosity approach

Dual porosity models assume that the soil consists of two distinguishable interacting pore regions. One region can be attributed to the soil matrix (micropores) and the other to the macropore system. The water flow within the soil matrix domain is assumed to be stagnant, so the soil matrix can exchange, retain, and store water but can not transport it (Šimůnek et al., 2003). The water flow within the macropore domain is usually solved by the Richards equation (Šimůnek et al., 2003; Gerke, 2006) although Germann and Beven (1985) suggested a kinematic wave approach. The soil matrix is described using a mass balance approach (Šimůnek et al., 2003). The conceptualisation of the interaction between the two domains is challenging. Most of the approaches in use are driven by differences in water content or hydraulic head between the two domains. Most often those differences are used in a first order process with parameters based on geometrical assumptions, or structural properties, or just calibrated based on experimental data (Šimůnek et al., 2003; Gerke, 2006), thus the parameters of the exchange term are often not observable. Solute transport is calculated based on convection-dispersion and the mass exchange between the two domains can be calculated on an assumed diffusive exchange. To solve the interaction between the matrix and the macropore domain a diagnostic approach is applied, e.g based on the differences in the hydraulic head. Finally, dual porosity models can explain non-equilibrium between pressure heads and water contents of the two domains (Šimůnek et al., 2003).

The dual permeability approach

In a manner similar to dual porosity models, dual permeability models assume that the soil can be divided into two overlapping flow domains. Again, the domains are separated to account for soil matrix and soil macropores. Unlike dual porosity models, in dual permeability models water is assumed to be mobile in both domains (Šimůnek et al., 2003). Models using the dual permeability concept mainly differ in the description of flow in the macropore domain and the transfer term between the macropore domain and the soil matrix domain (Gerke, 2006). Water flow in the matrix domain is calculated by the Richards equation, while there are different concepts for the macropore domain. Similar to the dual porosity approach water transport in the macropore domain can be modelled based

on Richards equation as in the model DUAL (Gerke and van Genuchten, 1993), a kinematic wave approach as in the model MACRO (Jarvis, 1994), or the law of Hagen-Poiseuille as in the model RZWQM (Ahuja and Hebron, 1992, in Gerke, 2006). While flow in the matrix domain is also described by the Richards equation, the interaction between the two domains has several conceptualisations in dual permeability approaches. The transfer can be determined using first order processes such as pressure head and water saturation leading to a set of coupled partial differential equations. Also it is possible to determine the transfer based on the Green and Ampt equation, or the Philip infiltration model (Šimůnek et al., 2003). The parameterisation of the interaction is a crucial point for a successful modelling, but not directly observable. Preferential solute transport can be modelled with a convection-dispersion approach (Gerke and van Genuchten, 1993) or piston displacement of solutes (Jarvis, 1994). One drawback of dual permeability models is the large number of parameters they require, some of which are derived based on assumptions. If the Richards equation is used to model both domains, determination of the Mualem-van Genuchten parameters is needed for both domains and the matrix-macropore interaction has to be parameterised. Most dual permeability approaches are 1-dimensional (Gerke, 2006), in a 2-dimensional domain Vogel et al. (2000) reported the spatial variability of hydraulic properties were highly sensitive with respect to preferential flow.

The multi porosity/permeability approach

The number of domains within these models can be extended leading to multi porosity/permeability models. They are similar to a model with only two domains, but are more flexible, while more parameters are needed and their identifiability is difficult (Gerke, 2006). Šimůnek et al. (2003) noted that the parameters in multi porosity/permeability models might be “physically poorly defined”. In other words, the over parameterisation results in a model that contains parameters that have no physical meaning, are not observable in the field, and are thus uncertain.

Explicit approaches

These approaches account for an explicit flow network within a soil. Vogel et al. (2006) used a generic model for a 3-dimensional macropore structure and solved the water flow in the matrix and macropore domain based on the Richards equation.

Functional approaches

Functional, in this context, are approaches that are parsimonious and try to capture the preferential flow in a simple way. These approaches are mainly employed to capture the integral system response (e.g. discharge), internal processes cannot be determined. For example CATFLOW (Zehe et al., 2001) accounts for an increase in hydraulic conductivity when a specified saturation threshold is exceeded. McGuire et al. (2007) extended the model Hill-vi (Weiler and McDonnell, 2004) with a bypass term, depending on saturation, as they found too much tracer was retained in the unsaturated zone during their model study. This can be seen as a vertical preferential flow path.

Preferential flow modelling in swelling and shrinking soils

Combining preferential flow and the processes of swelling and shrinking in a model is challenging, as it requires a coupled hydraulic and mechanical model (Gerke, 2006). The water content has to be taken into account to determine the extent of soil cracks. Models accounting for soil cracking typically assume that water and solutes can move instantaneously to a specified soil depth, and are driven by threshold processes that lead to initiation of preferential flow (Šimůnek et al., 2003). The same approaches used in dual permeability models are used to account for the interaction between macropores and soil matrix.

1.3.2 Examples of models accounting for preferential flow

In the following selected examples of preferential flow models are summarised. The focus will be on models accounting for macropore flow, as this thesis is focused on macropore flow. Different studies have dealt with modelling finger flow induced by an unstable wetting front (e.g. Selker et al., 1996; de Rooij, 2000) or funnel flow (Ju and Kung, 1997).

Several different models have been proposed to model preferential flow on small scale (soil core to plot scale). Gerke and Köhne (2004) used the dual permeability model DUAL to account for preferential flow and solute transport on a tile drained field site and were able to capture the dynamics of the tile drain. The model MACRO was successfully extended to account for shallow groundwater and tile drains (Ludwig et al., 1999), for pesticide transport (Jarvis et al., 1997) and for particle transport (Jarvis et al., 1999). The HYDRUS model allows preferential flow to be simulated in more than one way, e.g. dual porosity or dual permeability approaches can be parameterised (Šimůnek et al., 2003; Šimůnek and van Genuchten, 2008). HYDRUS-3D has also been used at the hillslope scale (e.g. Hopp and McDonnell, 2009).

On hillslope and catchment scales many model approaches exist. Hill-vi (Weiler and McDonnell, 2004) was extended to account for lateral pipe flow (Weiler and McDonnell, 2007) on hillslope scale. McGuire et al. (2007) extended the model with a vertical bypass term to account for transport through the unsaturated zone. Bronstert and Plate (1997) developed the model HILLFLOW-3D that accounts for lateral and vertical preferential flow on the hillslope scale. Vertical preferential flow is initiated when the precipitation intensity exceeds the matrix infiltration capacity. Lateral preferential flow is dependent on the water amount delivered by the vertical preferential flow. Jones and Connelly (2002) also modelled lateral preferential flow in soil pipes at the hillslope scale. Tsutsumi et al. (2005) used a 3-dimensional hillslope model, and included a preferential flow network. Flow was modelled using the Richards equation and Manning's equation.

Zhang et al. (2006) extended the REWASH model to account for macropores at the catchment scale (200 km²). The conceptualisation was based on a dual porosity approach, no exchange between soil matrix and macropores was allowed. The results in modelling catchment discharge were significantly improved (Zhang et al., 2006). Mulungu et al.

(2005) used a simple modification of soil hydraulic conductivity to model preferential flow for a forested catchment. In the 3-dimensional catchment model MODHMS Panday and Huyakorn (2004) introduced preferential flow by a bypass routing, depending on rainfall rate and an empirical bypass parameter. Zehe and Blöschl (2004) used a simple modification of soil hydraulic conductivity to simulate the effect of preferential flow on overland flow using the CATFLOW model at catchment scale. Christiansen et al. (2004) coupled a macropore routine based on MACRO (Jarvis, 1994) with the MIKE SHE model, to account for catchment scale preferential flow.

1.3.3 Summary on Preferential Flow models

There are several modelling approaches to account for preferential flow and these approaches have shown promising results for modelling the effects of preferential flow at various scales for solute transport and runoff generation. However, obtaining values for all of the parameters required for preferential flow models (e.g. dual permeability models), especially in two dimensions, remains challenging. The necessary parameters are often physically poorly defined (Šimůnek et al., 2003). In a series of papers (Köhne and Gerke, 2005; Haws et al., 2005; Köhne et al., 2006; Gerke et al., 2007) one- and two-dimensional single and double domain approaches were tested to determine whether they could predict water flows and tracer transport at field/hillslope scale. These studies revealed that even the double permeability approach had deficiencies in reproducing both the water flows and the corresponding tracer BTC at the same time. This shows that we still struggle to use tracer data to improve the overall predictive capability of process models, we are often limited to fit either the water flow or the tracer breakthrough. As a result the models give us the wrong relationship between the transit time of the water and the transit time of solutes (Vaché and McDonnell, 2006). Various assumptions must be made for each model, e.g. distribution of the soil pipe network, catchment scale distribution of macropores, or strength of the macropore-matrix interaction, leading to parameter uncertainty. Thus we need to link the model parameterisation and the model results more closely to experimental data, and most importantly to observable structures.

1.4 Open research questions and thesis objectives

1.4.1 Open research questions - the role of structure in hydrology

I have introduced different approaches for observing and modelling preferential flow and have discussed the limitations in modelling and identification of processes. The role of macropores on hydrological processes was outlined. The research site of this work was the Weiherbach catchment in south-west Germany. Vertical preferential flow paths are the most important characteristic landscape element influencing the hydrologic behaviour of the study site in the Weiherbach catchment (see chapter 2), thus the focus will be on those structures. These bio-geomorphic structures determine the topology and connectivity of the surface connected vertical preferential flow paths (Zehe and Flüßler, 2001a; Weiler and Naef, 2003a) with lateral subsurface preferential flow paths (Buttle and McDonald, 2002; Weiler and McDonnell, 2007). They have a significant effect on solute transport and can

strongly influence the storage and mobilisation of water and solutes. The characteristics of preferential flow paths are of crucial importance for applied hydrology (e.g. contaminant transport) and fundamental research questions such as the “old water paradox” (Kirchner, 2003) and transit time distributions (McDonnell et al., 2010). Various studies have pointed out that structures play a key role in organising hydrological processes (e.g. Schulz et al., 2006; McDonnell et al., 2007). Neglecting the characteristics of such structures, with their fast flow and transport processes reaching several meters into the soil, will lead to several limitations and uncertainties in models, especially in respect to equifinality (Beven, 2006).

1.4.2 Thesis objectives

Modelling preferential flow mainly follows functional approaches, especially at scales larger than soil cores. Structures controlling preferential flow are (mostly) not included in an explicit way. The representation of the location and spatial distribution of preferential flow paths in vadose zone models often remains poor. The role of the preferential flow paths and their spatial distribution is significant in hydrologic models. Without the representation of preferential flow paths we can easily predict the integral system response, while the internal processes and solute transport are poorly represented. I suggest a modelling approach that links the representation of preferential flow in more explicitly to experimental data and to observable structures to address these structure issues. Such an approach allows simulations of preferential flow to be physically based and can account for structures that enable fast vertical and lateral flow processes to be defined in an explicit way. This approach should provide an accurate estimate of internal processes like soil moisture dynamics and solute concentrations, as well as solute BTCs in natural systems. Finally this approach should be able to reproduce both, the transit times of water and the transit times of solute accurately, as indicated by earlier studies (e.g. McGuire et al., 2007) and thus allow model parameters to be physically based. However, it is unclear how those structures should be represented in a hydrological model, how can we represent the relevant structure, how do the processes driven by these structure operate, and what details do we need to include within the hydrological models?

My goal is to shed light on the importance of vertical preferential pathways in the cultivated lower meso-scale Weiherbach catchment by including preferential flowpaths as crucial element of hydrological models and as a driving factor of hydrological processes. I used a combination of field experiments and modelling studies to provide a better understanding of the role of various structures in different hydrological processes and a better representation of structures in hydrological models to enhance our understanding of solute transport and runoff generation at various scales. My goal was to improve preferential flow modelling with respect to parameter identifiability and the differences in solute and water transit times by the integration of observable structures into a hydrological model. For the field experiments I paid particular attention to the nature of the preferential flow paths, their role in the transport of water and solutes, and their importance on connectivity and mobilisation of stored water and solutes. I then related these results to their importance for the transport of agrochemicals in this cultivated catchment. Overall

this thesis addresses the following objectives which are discussed in more detail in subsequent chapters:

- Develop an approach to include bio-geomorphic structures caused by earthworms in a hydrological hillslope model. Data concerning earthworm abundance and the corresponding macropore patterns are key information.
- Test the applicability of an approach to model water and solute transport on hillslope scale
- Conduct field experiments to provide a better understanding of solute transport in soils containing significant population of macropores at hillslope/field scale, the role of water exchange between the macropores and the soil matrix on transit times and pesticide transport, and determine the link between pesticide transport and water drainage to tile drain systems or shallow groundwater.

The Weiherbach catchment is an intensely studied research catchment with an extensive data set that supplied the fundamental data for the modelling study. Based on these data I developed an approach that accounts for preferential flow structures – in this case vertical orientated worm burrows – in an explicit way, and tested its applicability to model water and solute transport at the hillslope scale. Next, I performed a series of irrigation/sprinkling experiment to investigate the role of these preferential flow structures in runoff generation and their relevance to contaminant transport. Hillslopes and catchments can store water for a long time, and release it suddenly within a single event, leading to significant proportions of “old” water in event discharge (Kirchner, 2003). Preferential flow paths also allow pesticides to be transported into tile drains with little (or no) retardation compared to conservative solutes (Kung et al., 2000; Zehe et al., 2001a). The irrigation experiments were conducted to provide an understanding of the role of preferential flow in these processes. Such an insight in the role of structures will, together with the gained data set of flow and solute transport of several experiments, enable a further improvement of hydrological models.

1.5 Thesis outline

After the literature overview, the discussion of open research questions, and the formulation of the general thesis objectives in the introduction (chapter 1), the Weiherbach catchment is introduced in chapter 2. The physical properties, climate, and hydrology are described and previous studies relevant to this thesis are summarised. In the subsequent chapters the outlined objectives are addressed. Within each chapter an introduction supplies an overview of additional literature and presents detailed objectives that are linked to the general objectives.

In chapter 3 I used an agent based approach to generate a network of spatially explicit vertical preferential flow paths at hillslope scale within the CATFLOW model. The simulation of these preferential flow structures was based on observations such as surface density of macropores, depth distribution, and potential water flow within macropores. I

tested the feasibility of this approach against field data collected during an irrigation experiment (Zehe and Flüßler, 2001a) at a tile drained field site in the Weiherbach catchment. Since the initial conditions and the data describing the parameters of the macropore network are uncertain I used different parameter sets to describe the hillslope, and tested the parameter identifiability and the related model equifinality.

Chapter 4 is focussed on solute transport modelling. I tested, whether the approach suggested in chapter 3 allows modelling of solute transport at the hillslope scale. The parameter sets that performed best in chapter 3 were used to model the transport of bromide without additional calibration. The additional information provided by the solute modelling was used to determine if such an additional data source can reduce equifinality and increase the identifiability of model parameters. Finally I used the model setup that performed best in respect to discharge and solute modelling to model the transport of the strongly reactive pesticide Isoproturon.

In the chapters 5 and 6 that deal with the experimental work I focus on the investigation of the rapid transport of water and solute, even strongly adsorbing solutes, to a tile drain. With a series of irrigation experiments at a tile drained field site the role of the preferential flow structures was investigated with a multi tracer approach supported by discharge and soil moisture measurements. In chapter 5 I used the multi tracer approach to investigate the hydrological processes at the tile drained field site. Bromide was applied with the irrigation water while the water isotopes deuterium and oxygen-18 were measured in the precipitation water, in the soil water, and in the tile drain discharge. The effect of rapid mobilisation of old water is addressed and a conceptual flow model is developed.

In chapter 6 I use my conceptual flow model to enhance the understanding of rapid pesticide transport in preferential flow paths. My conceptual model was developed based on the understanding of hydrological processes I gained from my field experiments. Two pesticides were applied in the irrigation experiments. I describe the breakthrough of the pesticides and the particle bound transport. Further I investigate the transport of both pesticides in relation to the onset of the tile discharge, the sources of the discharging water, the role of particle bound transport, and the role of event and pre-event water. In addition, I investigated the value of soil profiles to determine the pesticide transport.

In chapter 7 I investigate the amount and pattern of preferential flow structures based on biological information, i.e. worm abundance, and if they can be linked. Then a glimpse to a second cultivated catchment is given (chapter 8), that is dominated by different preferential flow paths than the Weiherbach. The thesis closes with a final summary of the achievements in chapter 9, a discussion of their limitations and advantages, and a look to further research needs. I will close the thesis by overall conclusions referring to the objectives in this introduction chapter.

2 The Weiherbach catchment

2.1 Catchment description

The Weiherbach valley is located in south-west Germany in the Kraichgau-region, approx. 30 km from the cities Heidelberg and Karlsruhe, and 50 km from Stuttgart (Figure 2-1). The entire Weiherbach catchment has an area of 6.3 km², including the more intensive studied northern sub-catchment which has an area of 3.6 km² (further on referred as upper catchment) and is gauged at the outlet by the gauge “Menzingen”. The highest point is 243 m.a.s.l. and the lowest 142 m.a.s.l. It was a research catchment for a long term BMBF (Federal Ministry of Education and Research, Germany) funded research project led by the University of Karlsruhe during the 1990’s, thus a comprehensive data base is available (Plate and Zehe, 2008).

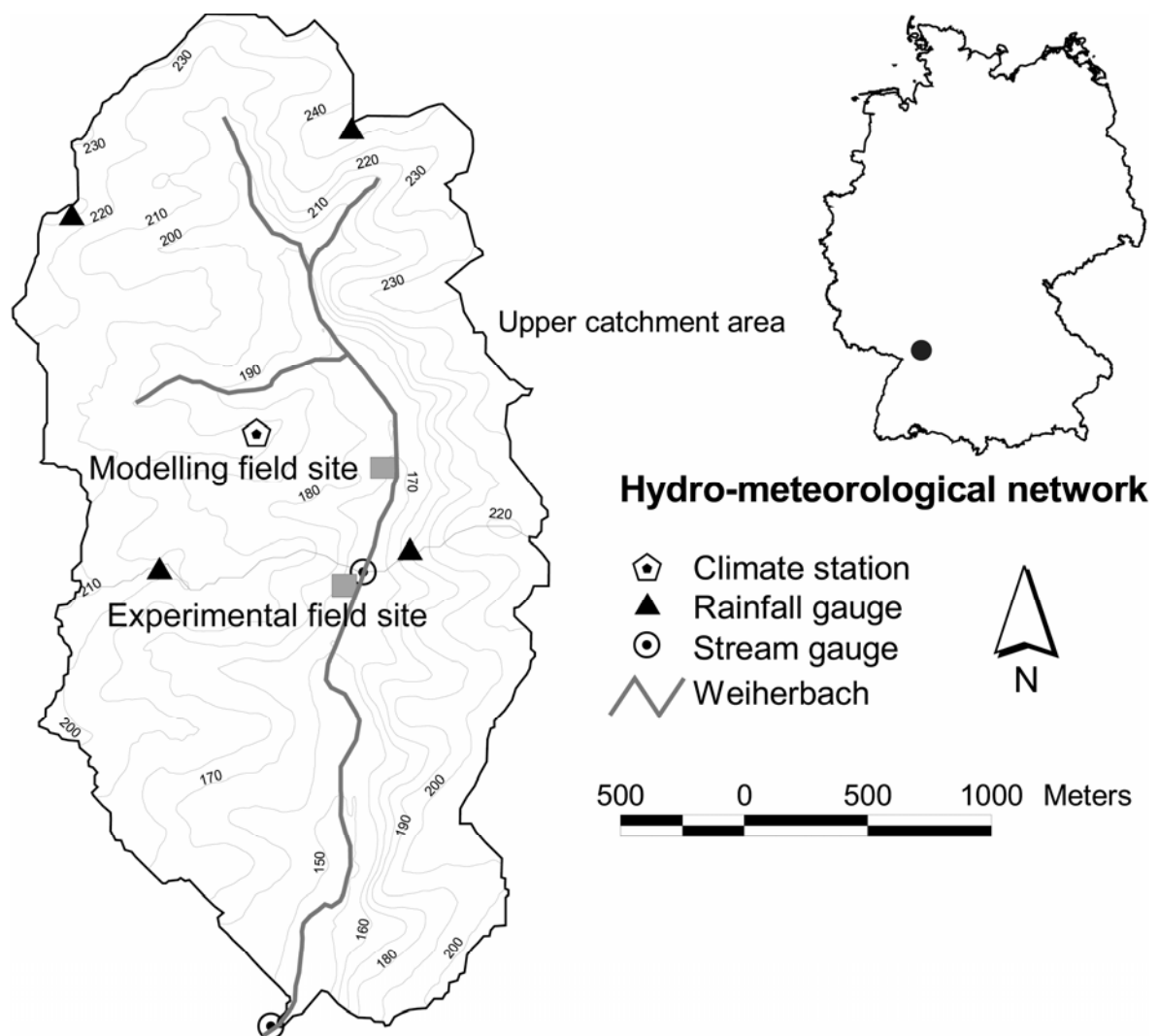


Figure 2-1: Weiherbach catchment with contour lines, stream, the hydro-meteorological network, and the study site of the modelling and the experiments (grey).

2.1.1 Geology and geomorphology

The geology consists of Keuper sandstone, marl and mudstone (lower and middle Triassic) covered with a quaternary loess layer up to 15 m thickness. This loess cover was accumulated in the last glacial period within two phases leading to loamy layer of about 1 m thickness separating both (Eitel, 1989). The loess was transported from the Rhine valley by west wind, and the layers are thicker at the western slopes than at the eastern ones. Erosion in the loess cover of the hilly landscape formed a characteristic erosion catena, and exposed some rocks from the Keuper (Lindenmaier et al., 2008). The Loess in the Weiherbach catchment is enriched in chalk with 25-30%, the content of coarse silt is 50-55%, while its porosity is 0.45-0.50% (Gerold et al., 1992).

The Weiherbach valley has an asymmetric shape with steep hillslopes in the east and gentle slopes in the west (Figure 2-1). This geomorphologic pattern is typical for the Kraichgau region (Lindenmaier et al., 2008). There have been two explanations offered for this asymmetric geomorphology. Eitel (1989) suggested that the layering of the underlying geology led to a stream direction from north to south of the main stream. The sediment load of western tributaries was distinctly higher than the load of eastern tributaries, produced by the inclination of the geological layers. The accumulation of sediment of the western tributaries forced the main stream to move eastwards eroding the eastern hillslopes, creating a steep slope there (Eitel, 1989). Schwarzbach (1988) instead suggested that the valley shape was created through the different impact of thawing and freezing effects on the eastern and western slopes induced by differences in slope exposure. Thus, weathering was more pronounced on eastern slopes, enhancing the movement of the stream eastwards.

2.1.2 Catchment Soils

As the catchment was covered with loess during the glacial periods loess dominates pedogenesis. Nevertheless the soils show differences in their spatial distribution (Figure 2-2). Anthropogenic activities such as forest clearing and cultivation have altered natural soil development within the catchment (Lindenmaier et al., 2008). Soil distribution in the Weiherbach catchment is governed by the dominating landscape element – the loess hillslope. Figure 2-3 presents a characteristic soil distribution at a loess hillslope of the Weiherbach catchment: Luvisols located at the hilltop, calcareous Regosols located at midslopes and Colluvisols located at the hillfoot, accumulated by continuous erosion processes. At the valley bottom the Colluvisols frequently exceed 2 m in thickness, these soils show the highest clay content among the apparent soils in the catchment. The high clay content and groundwater influence in the valley bottom lead to gleyic soils (Lindenmaier et al., 2008). However, significant biological activity was found in these soils, with worm burrows exceeding 1.5 m in depth (Zehe and Flühler, 2001a; 2001b).

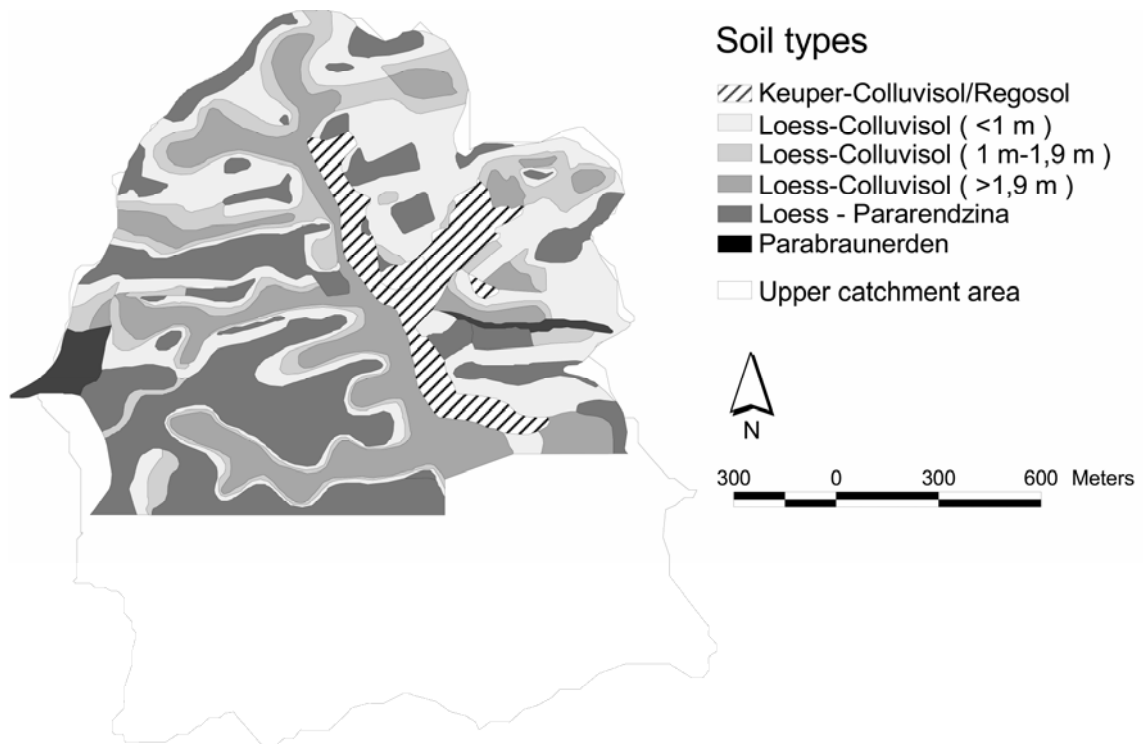


Figure 2-2: Soil map of the upper part of the Weiherbach catchment. The spatial distribution follows the hillslope catena.

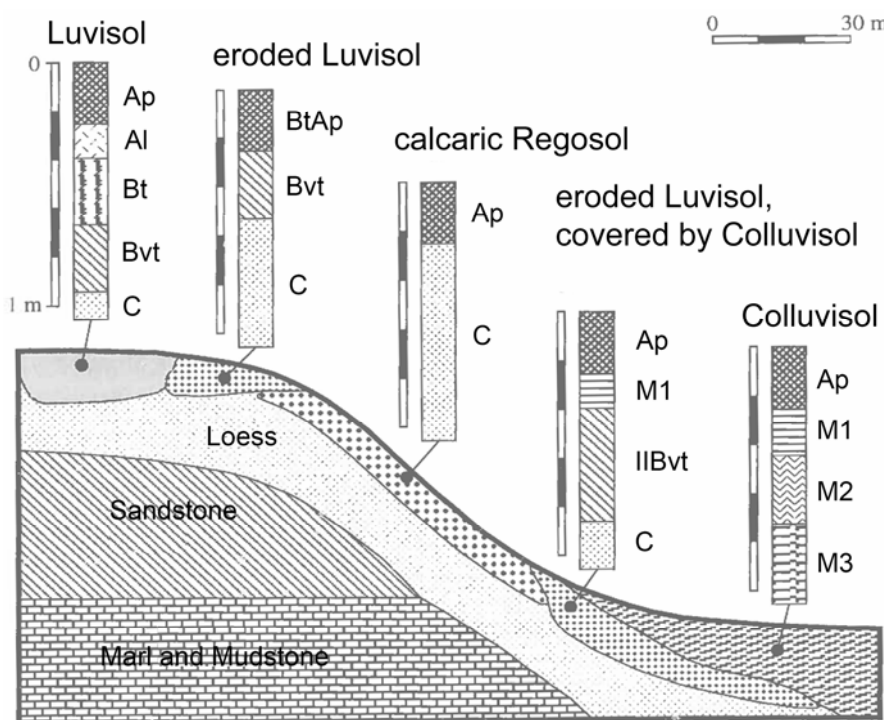


Figure 2-3: Characteristic catena of the loess hillslopes in the Kraichgau-region, representative for the Weiherbach catchment (after Lorenz, 1992).

2.1.3 Land use

The Weiherbach valley is dominated by cultivation. During the 1960's rural replotting led to larger field sizes. Beudert (1997) summarised the land use in the catchment (Table 2-1).

The land use in the upper catchment is slightly different, with a higher percentage of cultivation. There, about 95% of the catchment area is used for agricultural purposes, 4% is forested and 1% is paved. Ploughing is usually to a depth of 25 cm in early spring or early autumn, but has been mainly replaced in recent years by reduced soil surface treatment (5-10 cm depth). Typical main crops are barley (*Hordeum vulgare*), wheat (*Triticum* L.), maize (*Zea mays*), sugar beet (*Beta vulgaris* L.), peas (*Pisum sativum*), and rapeseed (*Brassica napus*); typical intermediate crops are mustard (*Brassica juncea* L.) or clover (*Trifolium* spec.). Figure 2-4 gives an overview of the intensity of land use and the catchment structure.



Figure 2-4: View from the eastern catchment boundary, to the west. The intensive cultivation is apparent.

Table 2-1: Land use in the Weiherbach catchment following Beudert (1997)

Land use	Coverage (%)
Agriculture	69.1
Grassland	1.2
Orchard	4.2
Fallow land	15.8
Forest	7.0
Farm buildings	<1.0
Roads	1.5

2.1.4 Climate and Hydrology

The average annual temperature in the Weiherbach catchment is 9°C. The average annual precipitation between 1979 and 1992 was ca. 830 mm. The average annual catchment discharge for the 6.3 km² catchment is 192 mm. High intensity precipitation events of 75 mm/day are frequently reported (Lindenmaier et al., 2008). More frequent and additional measurements (e.g. soil moisture, energy balance, erosion, solute dynamic) were taken during the period 1991-1996 for a project conducted by the University of Karlsruhe. The average annual precipitation for this period was 789 mm. Precipitation occurred at 49.5% of the days. The daily maximum was 79.4 mm and the highest hourly intensity was 60.2 mm/h (Kolle and Fiedler, 2008). The discharge in the upper catchment was 150 mm for the intensive observation period (Zehe et al., 2001).

Table 2-2: Flood events in at the gauge Menzingen in the observation period between 1991 and 1996 (after Maurer, 1997)

Date	Precipitation amount (mm)	Precipitation duration (h)	Peak discharge (l/s)	Runoff coefficient (%)
21.07.1992	26.9	1.5	788	2.5
20.12.1993	56.2	30.0	143	3.6
25.04.1994	8.3	1.5	447	3.4
27.06.1994	83.1	3.0	7920	11
12.08.1994	34.8	1.5	997	2.9
13.08.1994	7.0	0.5	264	2.7
18.03.1995	30.4	18.0	259	2.4
22.07.1995	32.1	1.0	627	1.9
07.08.1995	33.2	1.5	400	1.4
13.08.1995	67.1	2.0	3165	8.1

The Weiherbach brook passes through the catchment in north-south direction. In the upper catchment the brook flows in an artificial stream bed. The runoff is mainly dominated by

groundwater entering the stream by springs and drains. During high-intensity rainfalls surface discharge contributes strongly to catchment runoff, while other runoff components are less relevant. This is consistent with catchment scale modelling studies (e.g. Zehe et al., 2005). The tributaries are only active during high intensity rainfall events, but many have springs at their outlet to the main stream (Lindenmaier et al., 2008). The runoff coefficients are usually low. At the gauge Menzingen (upper catchment) the event with highest discharge showed a runoff coefficient of 11 %. Table 2-2 summarises the significant runoff events for the intensive measurement period between 1991 and 1996.

The groundwater system in the catchment shows some complex behaviour. There are two main systems one shallow system in the loess layers and one deep fissure groundwater system in the Keuper rocks. Since the rural replanting most springs in the catchment are connected to tile drains (Ackermann, 1998; Lindenmaier et al., 2008) and now directly drain to the main stream.

2.2 Previous research in the Weiherbach catchment

The Weiherbach catchment was a study site for various research. In the following I give a summary on previous research related to the objectives of this thesis. Thus mainly the research about soil water characteristics and soil structures, solute transport (i.e. tracer and pesticides), runoff generation processes, and the long term hydrological observations are reported.

2.2.1 Soil water characteristics and preferential flow paths

Schäfer measured the soil hydraulic properties within the catchment (Schäfer, 1999; Schäfer and Montenegro, 2008). By using suction-water content experiments and an inverse modelling approach they were able to determine the Mualem-van Genuchten parameters for characteristic soils in the catchment and found that those parameters are homogenous within the C-horizon of all soil types throughout the catchment. Dellbrück (1997) also measured the soil hydraulic parameters (direct and inverse) on one intensively studied hillslope on the western slopes in the upper catchment. Zehe and Flühler (2001a; 2001b) investigated the role of soil macropores in the catchment. With plot scale irrigation experiments using the tracer brilliant blue they showed the significance of deep burrowing earthworms for vertical preferential flow. They investigated the conductivity of different macropores depending on their diameter with a constant head method, and mapped the surface density and depth distribution of earthworm burrows. At the soil surface more than 200 macropores per square meter were found, while up to 50 burrows reached a soil depth of 90 cm, and a few even 150 cm (Zehe and Flühler, 2001a). The spatial distribution of the preferential flow patterns were studied by Zehe and Flühler (2001b). They studied the susceptibility of the soils for preferential flow based on the hillslope catena and showed that the soils at the hill foot, especially near the brook, had a higher susceptibility for preferential flow, than those located at the hill top.

2.2.2 Tracer experiments to determine solute transport and hillslope water dynamics

Zehe and Flüher (2001a) performed a field scale irrigation experiment, to investigate tracer and contaminant transport via preferential flow paths into a tile drain. They found fast transport of the pesticide IPU and bromide via the preferential flow paths. Chapter 3.2 summarises this experiment, which provide the field data for the modelling study within this thesis. A hillslope scale tracer experiment was performed between April 1993 and March 1995 at a hillslope along the western slope of the upper watershed. Bromide was applied on a 210 m long and 45 m wide hillslope to study different flow processes. Bromide concentrations, soil moisture, and soil stratification were determined with 600 auger profiles between 1 and 4 meters in depth. The vertical resolution was 10 cm for bromide concentrations and soil moisture. Transpiration and groundwater recharge were estimated at 40-50% each along the hillslope, while other water balance components were of minor relevance. At the end of the investigation period bromide peaks were at depths of 1.9-3.0 m. Lateral flow within the hillslope was only of minor relevance, intermittent, and slow with 96 ± 24 cm/a (Delbrück 1997; Delbrück, 2008). These experiments show the relevance of preferential flow structures on runoff generation in the Weiherbach catchment. Lateral flow processes in the hillslopes play only a minor role. Most of the stream discharge is generated by hortonian overland flow, thus the infiltration driven by macropores is of crucial importance in the runoff generation.

2.2.3 Erosion processes

As stated previously, the soils in the Weiherbach catchment are highly vulnerable to erosion, so there have been several erosion studies within the catchment. Erosion processes must be understood to determine the damage to agricultural production and soil losses from plot to catchment scales, but also important to determine the risk of nutrient and pesticide transport via sediment load in surface runoff (Gerlinger, 2008). Five permanent erosion observation points were monitored and 60 additional local irrigation-erosion experiments were performed in the Weiherbach catchment (1993/1994). The correlation between different soil parameters and the sediment concentration in surface runoff were determined. The experiments showed that soil clay content, organic matter content and soil moisture were the governing parameters of soil erosion in the Weiherbach catchment (Gerlinger, 1997; Gerlinger 2008).

2.2.4 Nutrient and pesticide dynamics

Nutrient and pesticide transport was investigated throughout the catchment in the first half of the 1990ies. Different components were sampled, namely: precipitation, surface runoff of paved (streets and farm yards) and unpaved areas, tile drains, springs, and the stream. Runoff from the farm yards showed high nutrient concentrations. Beudert and Hahn (2008) determined waste water and surface runoff from agricultural fields were main sources of phosphorus to the stream, while nitrogen came mainly from subsurface drains and springs, due to the continuous high fertiliser application rate. The herbicide Isoproturon (IPU) enters the stream mainly by discharge from farm yards or streets. During the pesticide

application period the concentrations in the street runoff were high, up to 329 $\mu\text{g/l}$ (Beudert, 1997; Beudert and Hahn, 2008). The transport via erosion could not be quantified, but the transport via tile drains may be as high as 2% of the applied IPU (Beudert and Hahn, 2008). This point out the relevance of pesticides contamination is an important issue in the Weiherbach catchment. The degradation of IPU in the arable soils of the catchment was investigated by Bolduan and Zehe (2006). They showed that earthworm burrows play a vital role in the degradation process. The degradation is strong in the upper soil layers and was found to be fast (half life of 15 days) at the sampled end of the macropores, while the surrounding soil matrix showed no significant IPU degradation in a 30 day time period.

2.2.5 Hydro-meteorological monitoring

Long term monitoring of climate and soil moisture was performed in the catchment, between 1991 and 1996. All components of the energy balance were measured within this long term measuring campaign (Kolle and Fiedler, 2008). Soil moisture was measured using Time Domain Reflectometry (TDR) (Topp et al., 1980) for the upper catchment at 61 stations with a temporal resolution of 1-2 weeks (Kolle and Fiedler, 2008) and those data were used for the different modelling studies of the catchment (e.g. Zehe et al., 2005).

2.2.6 Model development and modelling studies

Within research in the Weiherbach catchment different hydrological models were developed. Bronstert and Plate (1997) developed the model HILLFLOW. They modelled soil moisture dynamic in the Weiherbach catchment during a 16-day rain period with respect to the importance of the vertical preferential flow paths. Merz and Plate (1997) developed the model SAKE. They used SAKE to investigate the effect of spatial soil moisture variability on runoff generation in the Weiherbach catchment and found that it is especially important for medium size storm events (Merz and Plate, 1997). Merz and Bárdossy (1998) used SAKE to study the effect of different distributed soil hydraulic conductivities (e.g. structured by topographic index, by a semivariogram estimator, random, structured by the hillslope catena, homogenous distribution) in the Weiherbach catchment on the precipitation-runoff relation. Significant differences in the hydrographs occurred by different settings. Maurer (1997) and Zehe (1999) developed the model CATFLOW considering the landscape organisation of the Weiherbach catchment and showed its value on modelling the catchment behaviour. The important role of the earthworm burrows as preferential flow paths on the catchments runoff generation was shown in two modelling studies by Zehe et al. (2001), Zehe and Blöschl (2004), and Zehe et al. (2005). Scherer (2008) extended the model CATFLOW to account for erosion processes. She used sediment data that was sampled during several high flow events (Hahn and Beudert 1997) to validate the modelled catchment scale erosion/deposition for hillslope segments (Scherer, 2008; Scherer and Gerlinger, 2008). Modelling of the performed field experiments was successful. Strong erosion processes at the hillslopes and some deposition at the valley bottom was predicted. Several erosion risk studies were

performed by Scherer (2008), who showed the effect of changing land use, tillage practice, and climate on the erosion rates within the Weiherbach catchment.

2.3 The BIOPORE project

This PhD-thesis was carried out in the frame of the BIOPORE project (“Linking spatial patterns of anecic earthworm populations, preferential flow pathways and agrochemical transport in rural catchments: an ecohydrological model approach”) that has a strong focus on the Weiherbach catchment. The BIOPORE project consists of an ecological project that investigates the spatial and temporal dynamics of *Lumbricus terrestris* L. and aims to develop a model to account for the population dynamics of this earthworm species in a spatiotemporal way. The hydrological project part deals with the relevance of preferential flow structures, vertical orientated macropores in the Weiherbach, to enhance process understanding and modelling, especially with respect to the transport of agrochemicals. Later on, both model approaches should be coupled. It is expected that the model will be applicable for catchment-scale risk assessment that may assist agrochemical registration.

2.4 Additional measurement needs

The only instrumentation present in the catchment at the beginning of this study was the gauge Menzingen (Figure 2-5) therefore a network of meteorological instruments was installed in the upper catchment.



Figure 2-5: The gauge Menzingen (left), and a Davis tipping bucket (right) on the eastern catchment slopes.

One climate station measuring air temperature, air humidity, solar radiation, air pressure, wind velocity and direction, and precipitation was installed. This was accompanied by the installation of four Davies precipitation samplers distributed throughout the upper catchment (Map: Figure 2-1, photo: Figure 2-5). At the same time, an ecological project within BIOPORE was conducting studies of the spatial and temporal variability of earth worm population. For the years 2009/2010 the average annual precipitation was 611.3 mm, underestimating snow precipitation. The total runoff for the years 2009 and 2010 was 155.4 mm (2009: 149.4 mm, 2010: 161.4 mm).

3 Modelling rapid flow response of a tile drained field site using a 2-dimensional-physically based model: assessment of “equifinal” model setups*

This chapter presents a modelling study that deals with the explicit representation of structures – in this case vertical preferential flow paths by earthworms – in the 2-dimensional hillslope module of the model CATFLOW (Zehe et al., 2001). This approach is tested against discharge data of an irrigation experiment by Zehe and Flüßler (2001a). Their experiment supplies comprehensive data about the bio-geomorphic structures, soil parameters, and initial conditions of the field site. The feasibility of the approach developed to reproduce observed tile drain event discharge is tested. A further issue is whether the uncertainty in the observable information about the bio-geomorphic structure leads to “equifinal” model setups. Thus the key parameters of macropore network description such as area density and maximum volumetric flow based on measured data, and the initial conditions are varied. In total 432 different model runs are tested. This chapter deals with the first two objectives outlined in chapter 1.4.2. The chapter starts with an introduction on preferential flow and equifinality in hydrological modelling and detailed objectives of the modelling study. In chapter 3.2 the study site is introduced, a short summary of the irrigation experiment that supplied the data for this modelling study is given, and the uncertainty ranges of key parameters is discussed. Also in chapter 3.2 the model CATFLOW is introduced, the approach to generate connective flow paths was explained and the parameter space covered with 432 different model setups was discussed. Then the main findings are presented, followed by discussion and conclusions.

*based on: Klaus, J. and Zehe, E., 2010. *Hydrological Processes* 24, p.1595-1609.

3.1 Introduction

Rapid water flow along spatially connected - often biologically mediated - flow paths of minimum flow resistance is widely acknowledged to play a key role in the transport of agro-chemicals in cohesive soils (Flury, 1996; Šimůnek et al., 2003) but also runoff generation at the hillslope (Weiler and Naef, 2003a; Weiler and McDonnell, 2007) and small catchment scales (Zehe and Blöschl, 2004; Blöschl and Zehe, 2005; Zehe et al., 2007). Especially in tile drained fields, connected vertical flow structures such as worm burrows, roots or shrinkage cracks act as short cuts allowing water flow to bypass the soil matrix. This may cause a rapid flushing through of tracers (Villholth et al., 1998; Lennartz et al., 1999; Köhne et al., 2006), nitrate (Mohanty et al., 1998) or even of strongly adsorbing phosphorus (Stamm et al., 1998; 2002) or pesticides into surface waters (Kladivko et al., 1991; 2001; Zehe and Flühler, 2001a). Furthermore, discharge from tile drains contributes primarily to the base flow in agricultural sites (Schilling and Helmers, 2008) and thereby controls the potential for long term leaching of nutrients and pesticides into water bodies. Understanding and predicting the mobility of phosphorus, and especially pesticides, from tile drained field sites is thus of major importance both for environmental risk assessment and for registration of novel pesticides. Modelling the event response of tile drains is therefore a precondition for predicting solute breakthrough via tile drains into surface water bodies and, for several reasons, is a rather complicated task. A tile drained field site is a system of intermediate complexity in the sense of that expressed by Dooge (1986) as it is a heterogeneous system with some “degree of organisation”. Key factors that organise vertical flows are the surface area density, and depth distribution of connected flow paths, the geometry of the tile drains and the volume/catchment area drained by a single tile drain tube. Even at well investigated research sites these key parameters are subject to considerable uncertainty. We might assess (statistical) estimates but never their exact values or the exact spatial patterns of preferential pathways. I therefore suggest that the structural setup of a physically based model has to account for this uncertainty in key factors and hypothesise that there might even be several model structural setups that may reproduce the observed tile drain flow response equally well.

Equifinality in hydrological modelling was introduced and followed by Beven (1993; 1996; 2001a; 2001b and 2002) and co-workers (Freer et al., 1996; Schulz et al., 1999; Zak and Beven, 1999; Beven and Freer, 2001) who showed in various studies that there is an almost infinite set of model parameter sets that may reproduce the behaviour of hydrological systems – mainly catchment stream flow response – in an acceptable manner and must therefore be considered to be equally likely. Beven and Freer (2001) and Beven (2006) postulated the equifinality thesis as “working paradigm” in environmental modelling, and recommend consideration of multiple behavioural model setups in assessing predictive uncertainty. While the equifinality thesis is widely acknowledged in the context of stream flow predictions, applications in the context of solute transport modelling are less frequent. Klaus et al. (2008) gave evidence that equifinality causes a huge predictive uncertainty in tracer-based mixing cell modelling of groundwater systems

in Africa, which can however be reduced by means of age dating. Page et al. (2007) included conservative chemical mixing in TOPMODEL to simulate daily chloride concentrations at the Plynlimon catchments. They report that equifinality of model parameters did not allow identification of the most likely ratio of occult mass inputs and chloride mass inputs from the catchment immobile-store. They concluded that only more detailed measurements could reduce the equifinality in their model results. McIntyre and Wheeler (2004) explain predictive uncertainty of their in-river phosphorus model partly by equifinality of model parameter sets. Zhang et al. (2006) showed that their used model CXTFIT gave very good fits to observed pesticide breakthrough curves, resulting in very small parameter uncertainty estimates. With the application of GLUE they showed that a much wider parameter range can provide acceptable fitting curves.

Assessment of equifinality of a physically based model is even more infrequent. Schulz et al. (1999) provided evidence for equifinality in nitrogen leaching simulations within a Monte Carlo analysis using the model DYNAMIT, which is based on the 1-dimensional Richards- and convective-dispersion equations. Binley and Beven (2003) found that a large set of different soil hydraulic parameter sets allowed simulation of subsurface wetness dynamics, assessed by cross bore hole radar, when used within the HYDRUS-1D model. In the context of modelling tile drain flow responses with 2-dimensional or 3-dimensional physically based models, equifinality of the spatial model setup has, to my knowledge, never been investigated. The common credo is to assume there is only one well defined model setup that allows successful reproduction of observed leaching and flow events at tile drained sites, because the model equations are based on “soil physics” and most of the parameters as well as subsurface heterogeneity are in principle observable. Nonetheless, whether a 2-dimensional model is adopted that describes macropore flow in a separate continuum as recommended by Šimůnek et al. (2003), Gerke et al. (2007), and Jarvis (2009) or as in this thesis a single continuum model that represents macropores as connected effective flow paths of high hydraulic conductivity and low retention properties on a very fine grid, we cannot observe exactly all the key parameters that are necessary to parameterise these models, even at well investigated sites. The number of macropores/connective flow paths per unit area, their depth distribution, the maximum volumetric flow rates in these burrows, the hydraulic conductivity of the tile drain, their exact depths and location as well as the hydraulic properties of the soil below the tile drains – all these parameters are subject to considerable uncertainty. Nevertheless, within simulation studies macropore parameters are usually set to default values, even though model predictions are rather sensitive to these parameters (e.g. Larsbo and Jarvis, 2006). When using 2-dimensional instead of 3-dimensional models the “catchment” area drained by a single drain tube is, furthermore, an uncertain quantity. Given this uncertainty in the key factors that organise flow and transport at tile drained sites the main objectives of the present study is to shed light on the following three questions:

- Does a simplified approach that explicitly represents the effect of worm burrows in continuous effective flow paths of small flow resistance and low retention properties allow successful reproduction of event flow response at a tile drained

field site in the Weiherbach catchment with a 2-dimensional physically based model?

- Does the uncertainty in key factors cause equifinality i.e. are there several spatial model setups that reproduce event flow response in an acceptable manner without compromising our physical understanding of the system?
- If so, what are the key factors that have to be known at high accuracy to reduce the equifinality of spatial model structure?

3.2 Methodology

The focus of this study is to simulate an irrigation experiment (Figure 3-1) that was performed in April 1997 by Zehe and Flühler (2001a) on a tile-drained field in the Weiherbach catchment close to the stream channel (see Figure 2-1, chapter 2.1). On the day before irrigation of the 900 m² site the pesticide Isoproturon (IPU) was applied with a tractor and a mounted spray bar and the site was instrumented with 25 TDR-Probes of 30 cm length. Irrigation was performed with 12 evenly distributed sprinklers in three blocks with a sum of 46±5 mm. Ten minutes after onset of the first irrigation block a bromide and brilliant blue pulse was added to the sprinkling water. Water samples were taken at the tile drain outlet, which was located approximately 1.2 m below the field level. Tile drain discharge was measured using a calibrated Venturi tube and a pressure sensor. Zehe and Flühler (2001a) report a first flush of high bromide and IPU concentrations in the early phase (10 and 30 min after onset) via the tile drains into the brook, while the tile discharge showed only a very small reaction. In contrast, later on during the second and third irrigation blocks, peak concentrations and peaks in tile drain discharge were correlated well. Additional dye tracer experiments showed that connected burrows of anecic worms that linked the surface and the gravel layer above the tile drain likely acted as short cuts for water and solutes to bypass the soil matrix during the irrigation experiment.

The prime objective of the present study is to reproduce tile drain flow reaction as a necessary precondition to model solute breakthroughs at this site with the physically based model CATFLOW, based on the available comprehensive data set with its inherent uncertainties (see chapter 3.2.3). The latter includes the initial soil moisture measured in the upper 30 cm at 25 locations, irrigation and discharge data (Zehe and Flühler, 2001a) as well as hydraulic properties of the soil matrix measured from several undisturbed soil cores (Schäfer, 1999; Zehe et al., 2001). Additionally, measurements of the area density of deep earthworm burrows and their depth distribution were made at two horizontal soil profiles of 4 m² size (Zehe and Flühler, 2001a; Zehe and Blöschl, 2004) and data on the maximum water flow in worm burrows were derived from macroporous soil samples (Zehe and Blöschl, 2004).

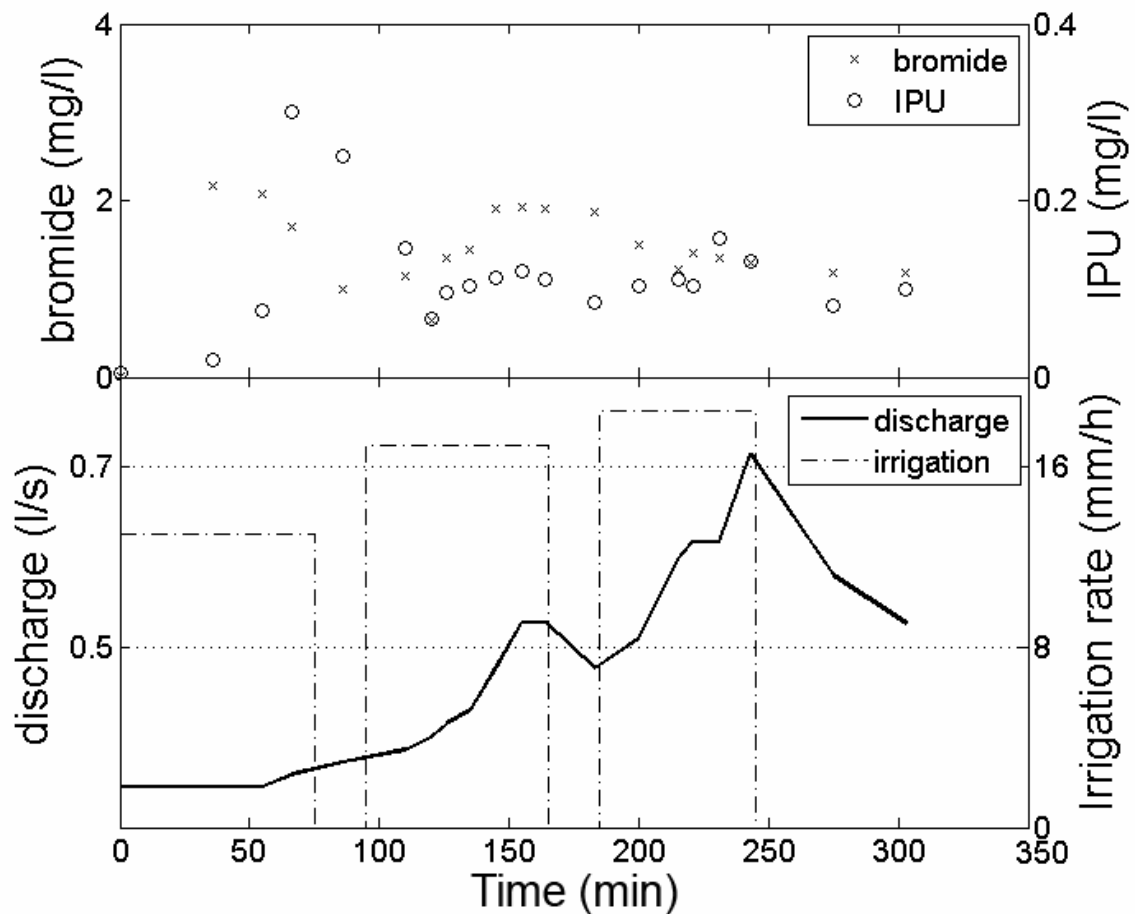


Figure 3-1: The experimental results from the study of Zehe and Flüher (2001a). The upper panel presents the bromide and Isoproturon concentrations, while the lower panel presents the tile drain discharge and the irrigation rate.

3.2.1 The CATFLOW model

CATFLOW is a physically based model for plot, hillslope and catchment scale modelling of water and solute transport (Maurer, 1997; Zehe et al., 2001; Zehe and Blöschl, 2004; Zehe et al., 2005). A catchment is treated as an ensemble of hillslopes that are interconnected via the drainage network. In CATFLOW a hillslope is represented as a 2-dimensional cross section along the steepest descent line that is discretised by 2-dimensional curvilinear orthogonal coordinates. The hillslope is thus assumed to be uniform perpendicular to the slope line. Soil water dynamics are described by the Richards equation in the potential form that is numerically solved by an implicit mass conservative Picard iteration (Celia et al., 1990). The simulation time step is dynamically adjusted to achieve optimal convergence of the iteration scheme and reaches from several seconds during rainfall conditions up to one hour, which is the allowed maximum. Soil hydraulic functions are described after van Genuchten (1980) and Mualem (1976). Evapotranspiration is represented by an advanced Soil Vegetation Atmosphere Transfer (SVAT) approach based on the Penman-Monteith equation. Surface runoff routing down the

hillslopes is based on the diffusion wave approximation to the 1-dimensional Saint-Venant equations. It is numerically solved by an explicit upstream finite difference scheme.

Solute transport in CATFLOW is calculated by a particle tracking scheme based on a Random Walk approach. The deterministic part of a particle step is determined based on the seepage velocities using backward two level Runge Kutta scheme as suggested by Roth and Hammel (1996). The random part of the particle step is determined based on square root of the dispersion/diffusion coefficient multiplied by the time step. A linear sorption isotherm is available in the model, also first order decay (Jury and Horton, 2004).

To account for the complex chemical transport behaviour of pesticides, I included the Freundlich and the Langmuir isotherme in the model, to account for different sorption behaviour (Jury and Horton, 2004). Based on different sorption isothermes the retardation coefficient of the solutes can be calculated for every model time step.

3.2.2 Model domain and flow representation in connected flow paths

Domain setup

Following Vogel et al. (2006) I wanted to represent the dominant structures, in this case worm burrows, as explicit connected effective flow paths of high hydraulic conductivity and low retention properties. Ideally this is done using a very fine grid size in downslope/lateral direction which is of order 2-3 cm, so that each surface element of the 2-dimensional domain contains either a single burrow or not (Zehe et al., 2010a). Such a fine lateral discretisation of the 30 m long hillslope combined with a vertical grid size of 2 cm resulted, however, in computation times of 200 hours for a single model run. As the current purpose was to test multiple spatial model setups I had thus to balance the necessary detail to represent worm burrows as connected structures and yet keep computation time for a single realisation within a few hours. I thus selected 30 cm as lateral (downslope) grid size and a vertical grid size of 2 cm down to 2 m. In a first step I assigned the soil hydraulic parameters listed in Table 3-1 to each model node. The soil was a Colluvisol with three different layers with different hydraulic properties (Table 3-1).

The next step was to represent the effect of connected worm burrows using a statistical approach proposed by Zehe and Blöschl (2004) that was further refined here. To this end I assumed that the 2-dimensional domain is 10 cm wide, each surface element had thus a cross sectional area of 300 cm². For each surface element I simulated the number of worm burrows at the surface assuming they are Poisson distributed as suggested by Beven and Clarke (1986). The Poisson parameter is the average worm burrow density per unit area multiplied with the area of a surface element. Next I simulated the lengths of each macropore located in the surface element (can be more than one) assuming a normal distribution and then extended the worm burrow downwards to its length and allowed for a deviation from the pure vertical direction with a probability of $p_{lat}=0.05$ to allow for

tortuosity. When used with a grid as fine as outlined above this procedure yields a worm burrow system that is consistent with the findings of Zehe et al. (2010a) and those reported by Shipitalo and Butt (1999) (see Figure 3-2). Due to the small cross section of the model elements I assumed a) that vertical water flow in the grid elements with worm burrows is dominated by macropore flow and b) this might be accounted for by assigning an effective medium to these model elements. To this end I multiplied the number of macropores in a grid element by the maximum volumetric water flow in the worm burrow and divided this value by the cross sectional of the grid element to obtain its effective hydraulic conductivity. As the literature reports different volumetric water flows in worm burrows I used values from different experimental studies of Shipitalo and Butt (1999), Weiler (2001) and Zehe and Flühler (2001a) for this purpose. Finally, I assigned an effective porous medium with very low retention properties to the model elements containing macropores to minimise the effect of capillary forces during simulation.

Table 3-1: Soil hydraulic parameters determined by Schäfer (1999). S: specific storage coefficient of the soil (-), ks: saturated hydraulic conductivity (m/s), θ_s : saturated soil moisture (-), θ_r : residual soil moisture (-), α : van Genuchten’s alpha (m^{-1}), n: quantity characterising the pore size distribution (-), $\log_{10} \psi_{min}$: logarithm of minimum suction head (ψ_{min} in m), $\log_{10} \psi_{max}$: logarithm of minimum suction head (ψ_{max} in m), ρ : bulk density (kg/m^3).

Parameter	Colluvisol	ploughed Colluvisol 0-10cm	ploughed Colluvisol 10-35cm	Poremedium
S	5×10^{-3}	5×10^{-3}	5×10^{-3}	1.1×10^{-1}
ks	5×10^{-5}	5×10^{-4}	2.7×10^{-5}	variable
θ_s	0.4	0.46	0.43	0.4
θ_r	0.04	0.1	0.11	0.057
α	1.9	2.4	3.8	11.4
n	1.25	1.22	1.2	2.28
$\log_{10} \psi_{min}$	0.6	-7	-8	-4
$\log_{10} \psi_{max}$	5	4	3	4
ρ	1.50×10^3	1.3×10^3	1.59×10^3	1.6×10^3

Due to the small area of the model elements I think this approach to treat macropore flow and matrix flow in one domain is still feasible. The big drawback of this approach is the high computational cost. The advantage is that it is a spatially explicit effective representation of structure that may be parameterised on field data. Figure 3-2a shows an example setup that was used in Zehe et al. (2010a) to highlight the similarity to the shapes reported by Shipitalo and Butt (1999) shown in Figure 3-2c. While an infiltration pattern as a result of worm burrows is shown in Figure 3-2b. Figure 3-2d presents one of the structural hillslope setups used within the present study. The different soil layers and the effective connected preferential pathways (red) are clearly visible.

The tile drain located at a depth approx. 1.2 m below the soil surface and its embedding gravel layer (starting between 90 and 100 cm depth) were represented by assigning the “worm burrow” medium to a depth of 95-120 cm and with no separation between the tile-drain tube and the surrounding gravel layer. Since the thickness of the gravel layer is not

known exactly, the lateral flow path started at 95 cm depth integrating the drain and the gravel layer.

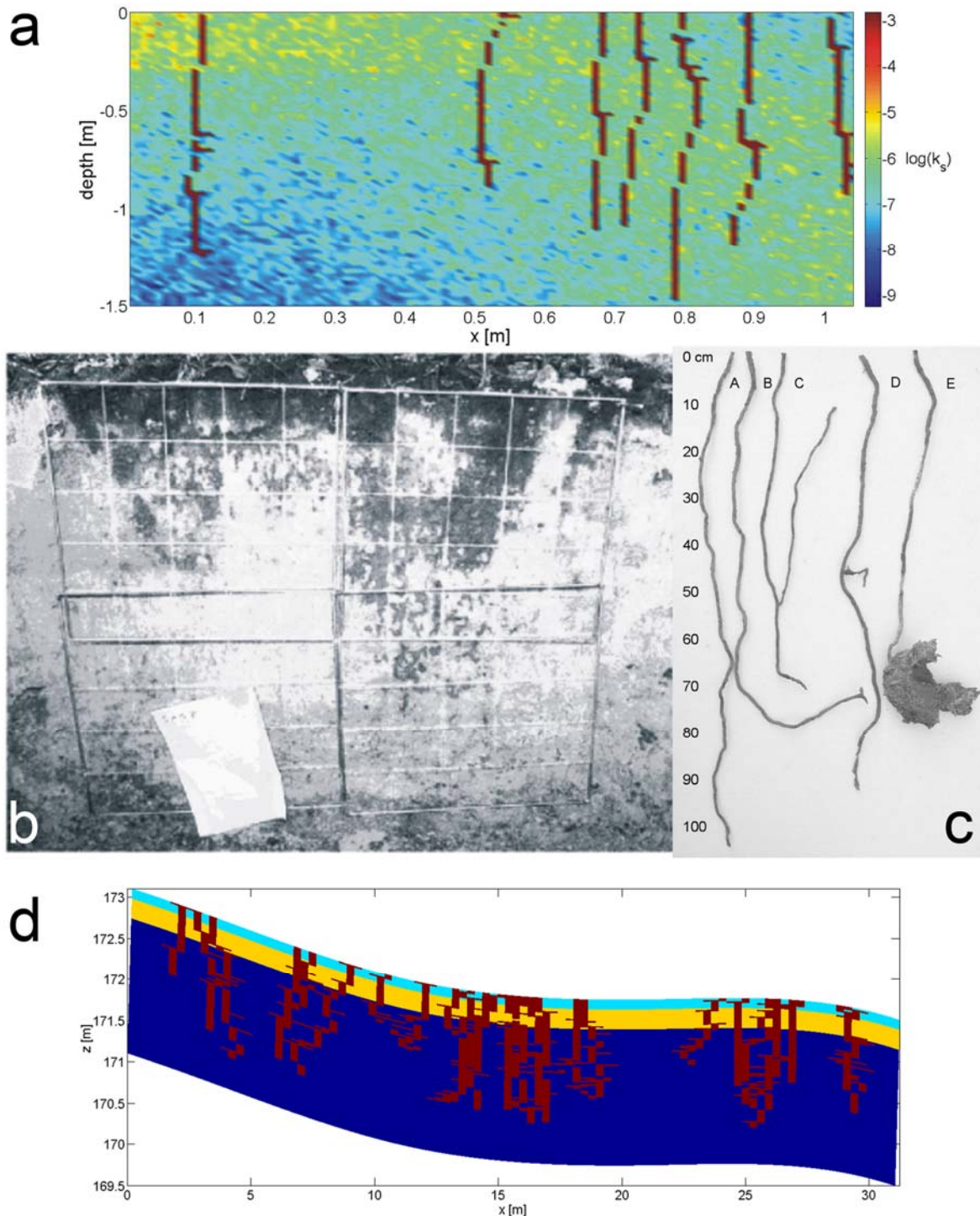


Figure 3-2: Generated pattern of of anecic worm burrows (a) compared to the architecture of worm burrows (c) reported by Shipitalo and Butt (1999), their figure. Dye tracer pattern (b) obtained at the irrigation site after the irrigation experiment. (d) shows one used hillslope setup with different soil layers and the macropores (red).

Infiltration into connected effective structures and boundary conditions

As explained in Zehe et al. (2001) the uppermost model layer is usually very fine (1-5 cm) because of the numerical treatment of overland flow formation using a Cauchy boundary

condition. This means rainfall is treated as flow boundary condition, as long as the uppermost grid cell is unsaturated. In case of saturation, the model switches to a Dirichlet boundary condition using the overland flow depth pressure boundary to drive infiltration. The infiltrating water flux is then calculated using Darcy’s law. This approach works well to capture onset of overland flow as shown for instance in Zehe et al. (2001) or to simulate infiltration at small scales Zehe and Blöschl (2004). Infiltration into the grid cells that contain the effective macropore medium works identical. However, due to the very high conductivity and low retention properties of the medium the upper most elements never get saturated until the “macropores are full”. In case of overland flow effective catchment area of the macropore elements may increase due to runoff from upslope sectors. The boundary conditions at the remaining boundaries were no flow at the left, free flow right and gravity flow at the lower boundary.

3.2.3 Uncertainty of key parameters and simulation variants

My general constraint was to vary uncertain key parameters within a feasible range that is either within the range of available measurements or within a range that does not compromise physical and hydrological understanding. As a single model run takes up to one day on a numeric server it was, however, not possible to sample the feasible parameter space within a Monte Carlo simulation. I thus selected fixed values of key parameters made the Cartesian product to allow for all combinations (Table 3-2), which resulted in 432 simulation runs. Additionally, a series of runs without any vertical preferential flow structures was performed.

Table 3-2: Values of six key parameter that were combined in a Cartesian product within in the 432 simulation runs. P: number of pores (m²), L: maximum volumetric water flow in a macropore (m³/s), IMC: initial moisture conditions, D: tile drain conductivity (cm/s), GW: Groundwater occurrence, IL: occurrence of low permeable layer beneath tile drain.

Parameter	Value 1	Value 2	Value 3	Value 4
P	10	20	30	40
L	2.5x10 ⁻⁶	7.9x10 ⁻⁶	1.33x10 ⁻⁵	-
IMC	dry	intermediate	wet	-
D	0.608	2.03	20.3	-
GW	yes	no	-	-
IL	yes	no	-	-

To account for uncertainty in the number of deep worm burrows that link the surface and the tile drain I varied the number of deep macropores between 10, 20, 30, and 40 burrows per m². This is in accordance with Zehe and Flüßler (2001a) who found up to 50 pores per square meter with a depth greater than 90 cm within two horizontal soil profiles of 2 by 2 m². Average macropore length was in all cases 1.2 m with a standard deviation of 0.25 m. Worm burrow tortuosity was kept constant, because a number of simulation trials indicated

this is to be a less important parameter. Different experimental studies report different values for the maximum volumetric water flow rate in a large macropore. I thus tested three different values, namely 2.5×10^{-6} m³/s, 7.9×10^{-6} and 1.33×10^{-5} m³/s reported by Zehe and Flühler (2001a), Weiler (2001), and Shipitalo and Butt (1999), respectively. Flow velocity in the tile drain is also uncertain as I neither know the exact form of the tubes, nor the porosity and hydraulic conductivity of the gravel embedding of a tile drain tube, nor the exact slope. I thus tested three different hydraulic conductivity values namely 6.08×10^{-3} , 2.03×10^{-2} and 2.03×10^{-1} m/s.

The reason for tile drainage of field sites can either be an impermeable layer beneath the drain or a near surface groundwater system. As I have no measurement evidence whether the former or the latter is the case, I allowed for both options within my simulation variants: either a lower permeability layer with $k_s = 5.1 \times 10^{-9}$ m/s of 6 cm thickness below the tile drain, or no impermeable layer. Finally I allowed for either or non-saturated conditions beneath the drain.

Initial soil moisture was only measured in the upper 30 cm, with an average value of 0.35 m³ m⁻³. In this simulation I compare three different initial states to find out whether soil moisture conditions that differ from the observed average state also yield acceptable model results. The wet case corresponds to a suction head of -50.66 hPa throughout the profile. The intermediate case had a suction head of -303.98 hPa in the upper 40 cm of the profile and -101.33 hPa below this layer. The dry setting corresponds to a head of -405.3 hPa in the upper 40 cm of the profile and -151.99 hPa in the remaining soil profile.

3.2.4 Key assumption of the underlying 2-dimensional approach

Using a 2-dimensional domain to address the problem of preferential flow as outlined above means that we essentially assume symmetry of the flow problem with respect to the main direction of the tile drain. This implies the assumption that the breakthrough times/residence times simulated within this 2-dimensional domain and are representative for what happens in 3-dimensional volume that is drained by a single tile drain tube. To compare simulation and observation I thus have to scale the 2-dimensional domain to the width of this drained control volume. The width of this volume is also uncertain; the upper limit is constrained by the width of the irrigated site (30 m). This scaling has two important implications. The first one is that not all worm burrows in the 3-dimensional reality connect directly to a single drainage tube, but some of them connect to the surrounding gravel embedding. This embedding is a well conducting “buffer” of approximately less than 1 m around the tube. If a less permeable layer is located below the tile drain, one expects fast lateral flow into tube within this gravel layer. This process is, however, deemed to be slower than vertical inflow through worm burrows that connect directly to the tube. In the 2-dimensional medium, however, the preferential structures connect directly to the depth where the tile drain medium is located and directly sustain drainage outflow. This means that in fact I merge direct vertical inflow and combined vertical and

lateral inflow from the gravel buffer into a single fast process. The hydraulic conductivity characterising the tile drain must be therefore seen as an effective combination of the true hydraulic conductivity of the gravel embedding and the water velocity in the tile tube itself.

The second point is the effective preferential pathway in a grid cell extends homogeneously across the assumed width of the cross section. This means that the surface contribution area/catchment area of the effective preferential pathway scales linearly with the width of the domain. In true 3-dimensional reality the width of the area that feeds macropore flow has, however, an upper limit determined by micro topography. In case of overland flow this implies that the entire runoff from upslope is “captured” within this catchment area of the effective preferential pathway, whereas in 3-dimensional reality a part of the runoff should bypass this surface catchment area.

The proposed approach is thus not fully equivalent to a spatially explicit treatment of preferential flow in connected structures in a 3-dimensional domain. In particular, I expect that the above specified structural shortcomings imply that the 2-dimensional approach underestimates the width of the control volume drained by a single drain tube. The approach can be deemed to be unbiased in case of “narrow” hillslopes with smooth micro topography.

3.2.5 Model evaluation

The model evaluation was done in three steps. In a first step I scaled the width of the modelling domain such that observed and simulated peak discharge were identical. The next step was to test whether the simulated hydrograph, after scaling of the peak, allowed a good match of the shape of the observed hydrograph without any further adjustment. To evaluate matching of the shapes, I employed the Nash-Sutcliffe efficiency (Nash and Sutcliffe, 1970). However, it is well known that Nash-Sutcliffe coefficient is very sensitive to timing errors. Figure 3-3 shows as example two identical hydrographs, one shifted in time (regarded as simulation result) as well as the averaged hydrograph. The shifted hydrograph yields, though it matches exactly the shape, a Nash-Sutcliffe efficiency -0.23. To calculate a Nash coefficient that indicates exclusively the error in matching the shape, without being contaminated by the timing error, I corrected for the time shift of simulated and observed peaks before calculating the adjusted Nash. The last step was to select model runs that a) reproduce the hydrograph shape in an acceptable way (Nash-Sutcliffe >0.75), b) had a small timing error less than two output time steps (20 min) and c) where the scaling width to match the peak was less than the upper limit of 30 m. In the following I always refer to this adjusted Nash-Sutcliffe efficiency (NS), additionally I refer to runs with an adjusted Nash-Sutcliffe ≥ 0.9 as very good runs.

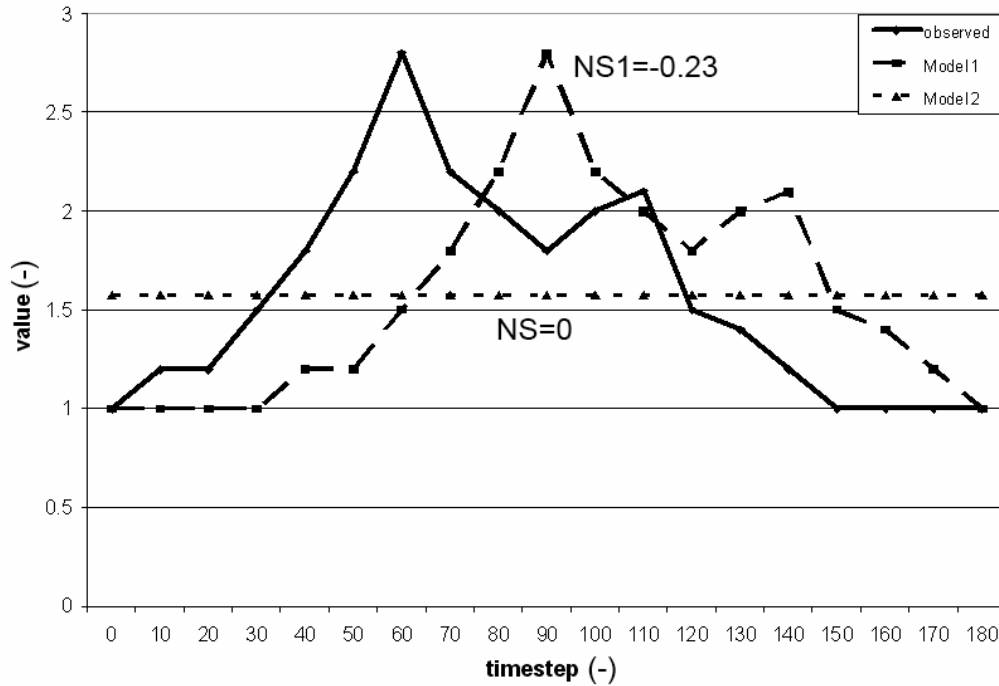


Figure 3-3: Sensitivity of Nash-Sutcliffe value to time shift. The figure shows a timeline of observed values, compared to two assumed model outputs, and their Nash-Sutcliffe value. Model 1, consisting of the same timeseries, but time shifted, shows a distinctly lower NS, then a model assuming the average value for every timestep.

3.3 Results

3.3.1 Modelling rapid flow and tile drain response in a 2-dimensional physically based model

Overall 67 of the 432 setups were acceptable as specified above (compare Table 3-3 for parameters of the ten best). Figure 3-4 shows the ten best among the acceptable model runs and the corresponding NS values. Please remember, that timing errors were only neglected for calculating the NS, the simulated hydrographs shown in Figure 3-4 are not corrected to match timing. The best runs match the temporal pattern and the volume well. Those runs were obtained with 10 or 30 worm burrows per m^2 , eight out of ten had wet initial conditions (consistent with the field observations), and all were simulated with an impermeable layer. Best runs were obtained with the two highest values of the maximum water flow in the macropores and the two highest conductivities of the tile drain. Five of the best runs were obtained with, and five without, groundwater. The width of the cross section was in all cases less than 3 m (Figure 3-5a). Even when assigning a width of 30 m to the cross section, simulations without connected vertical worm burrows did not yield a successful reproduction of the hydrograph (Figure 3-5b). Thus it can be stated that the proposed way of representing the macropores as effective connected vertical structures is feasible for reproducing the observed fast tile drain flow response. This finding is consistent with the study of Vogel et al. (2006), who showed that a realistic representation of structures in a hillslope allows successful modelling of flow and transport even when using an approximate flow law.

Table 3-3: Parameter and results for the ten best model runs. They are ordered by the adjusted NS value. Time in minutes denotes the difference between modelled and simulated peak. P: number of pores (m²), L: maximum volumetric water flow in a macropore (m³/s), IMC: initial moisture conditions, D: tile drain conductivity (cm/s), GW: Groundwater occurrence, IL: occurrence of low permeable layer beneath tile drain, C-Sec: is width of cross-section in meters needed to reproduce the hydrograph.

NS	time	P	L	IMC	GW	IL	D	C-Sec
0.952	7	30	7.90×10^{-06}	wet	yes	yes	20.3	0.83
0.948	7	10	1.33×10^{-05}	wet	yes	yes	2.03	2.11
0.942	7	10	1.33×10^{-05}	wet	no	yes	2.03	2.15
0.941	7	30	7.90×10^{-06}	wet	no	yes	20.3	0.82
0.934	7	30	7.90×10^{-06}	wet	no	yes	2.03	1.59
0.932	7	30	7.90×10^{-06}	wet	yes	yes	2.03	1.59
0.923	7	10	1.33×10^{-05}	intermediate	yes	yes	20.3	1.99
0.917	17	10	1.33×10^{-05}	dry	no	yes	20.3	2.24
0.914	7	10	1.33×10^{-05}	wet	yes	yes	20.3	1.34
0.907	7	10	1.33×10^{-05}	wet	no	yes	20.3	1.33

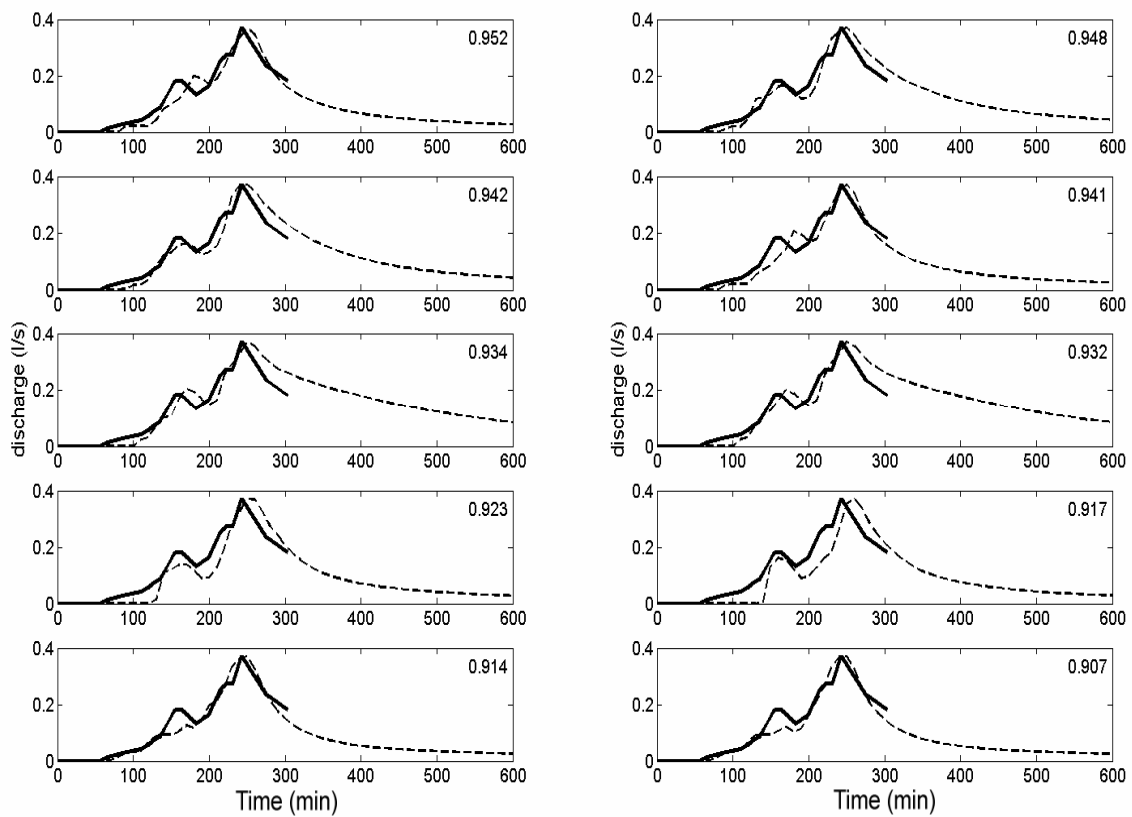


Figure 3-4: Ten best (scaled) model runs (dashed line) and measured tile drain discharge (constant line), Nash-Sutcliffe values are given in the panels.

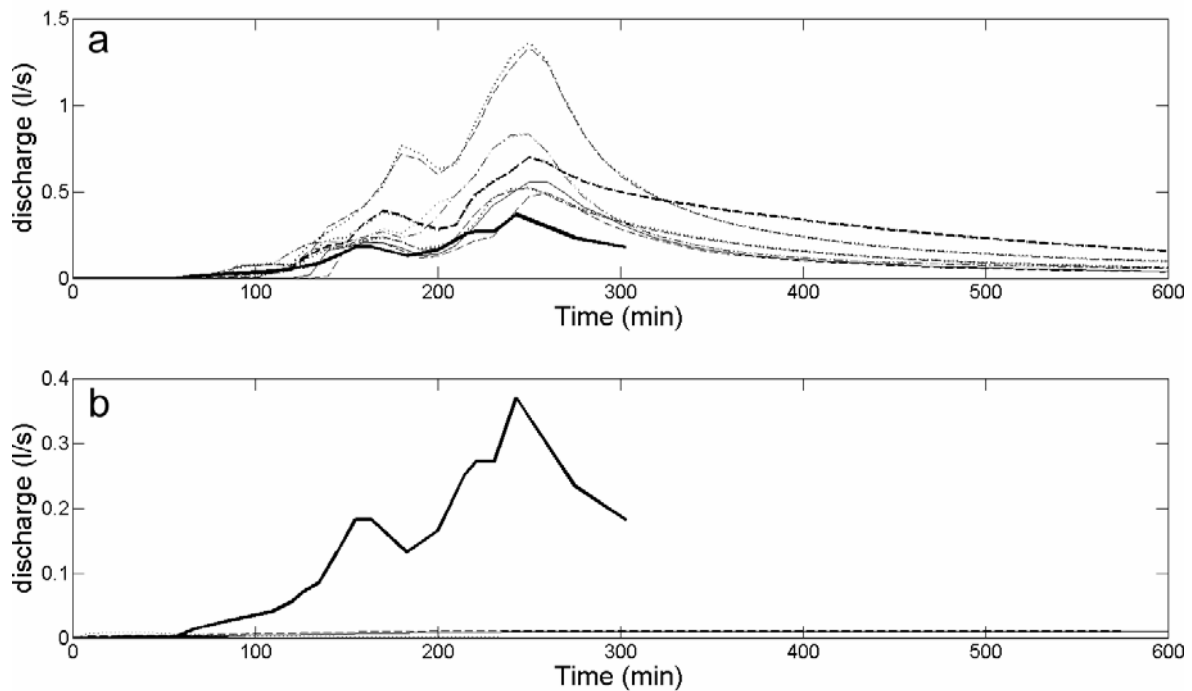


Figure 3-5: a) Hydrographs of the ten best models assuming a width of the drained cross section of 3m. b) Discharge simulated without macropores compared to the measured hydrograph (solid). We assumed that the drained cross section is equal to the entire width of the irrigation site.

3.3.2 Non-uniqueness of acceptable model structures

87% of the 77 model runs with $NS \geq 0.75$ have a timing error of less than or equal 20 minutes (Figure 3-6). Bárdossy (2007) showed for a Nash cascade that part of the equifinality stems from the fact that increasing the number of reservoirs, n , may be compensated by decreasing the average residence time k such that the product, i.e. the residence time in the cascade stays the same. To investigate whether part of the equifinality that was found here stems from similar parameter compensation, bivariate plots of the acceptable model runs were made for all pairs of parameters that were varied in the study. Based on the evaluated runs, there is no obvious sign of parameter compensation for instance a hyperbolic shape of the “point cloud” (see Figure 3-7).

Figure 3-8 shows the NS values of the acceptable runs plotted against the different parameter values. When looking for the best model runs with $NS \geq 0.9$, there is a clear pattern that has already been explained in 3.3.1. It can clearly be seen that worm burrow densities of 10 and 30 pores per m^2 lead to higher efficiencies than densities of 20 and 40 per m^2 . This is especially true for parameter sets with a worm burrow density of 30 per m^2 which show the highest efficiencies. Table 3-4 shows a short summary of parameter combinations that never led to satisfactory model runs. These were runs that combined low volumetric flow rates in macropores with low tile drain conductivity, dry initial moisture conditions and a low number of macropores per m^2 .

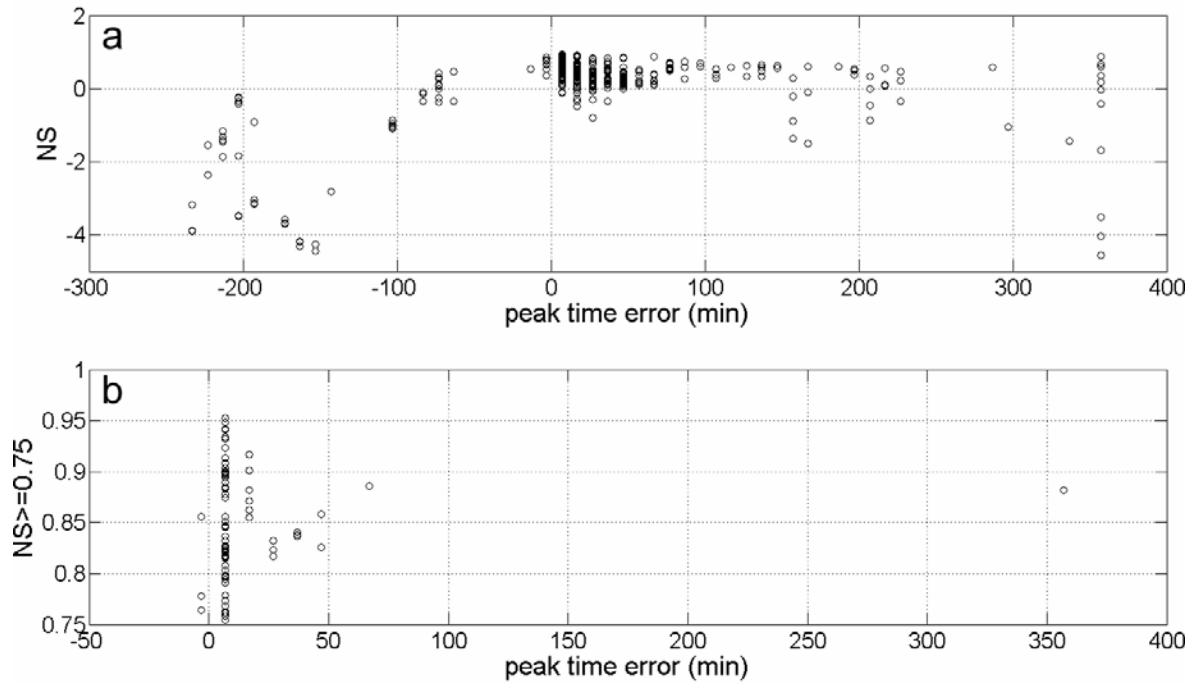


Figure 3-6: a) Nash-Sutcliffe efficiency (NS) plotted against time difference between simulated and observed discharge peak. b) Model runs with $NS \geq 0.75$ plotted against the time difference between measured and observed peak.

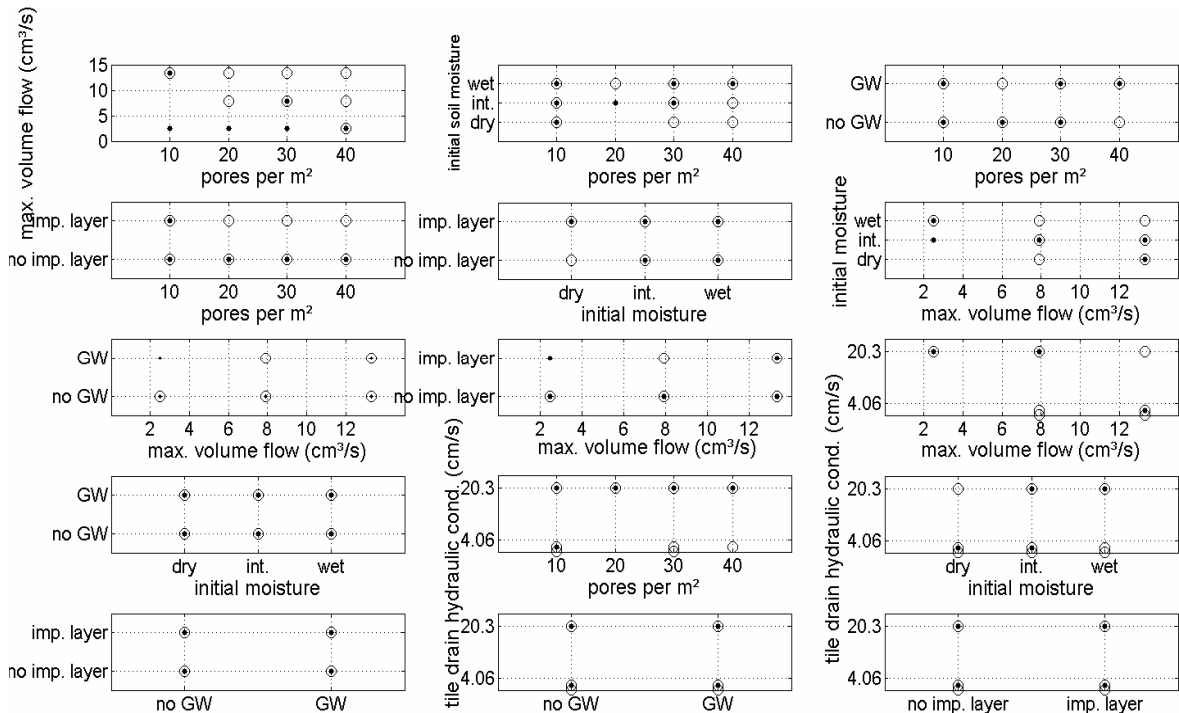


Figure 3-7: Pair-wise scatter plots of parameters for runs with Nash-Sutcliffe efficiency $NS \geq 0.75$. Circles indicate that the time difference between simulated and observed discharge peak is less than or equal to 20 min/two simulation output time steps, points indicate only $NS \geq 0.75$. Max. volume flow denotes the allowed maximum volumetric water flow in a macropore.

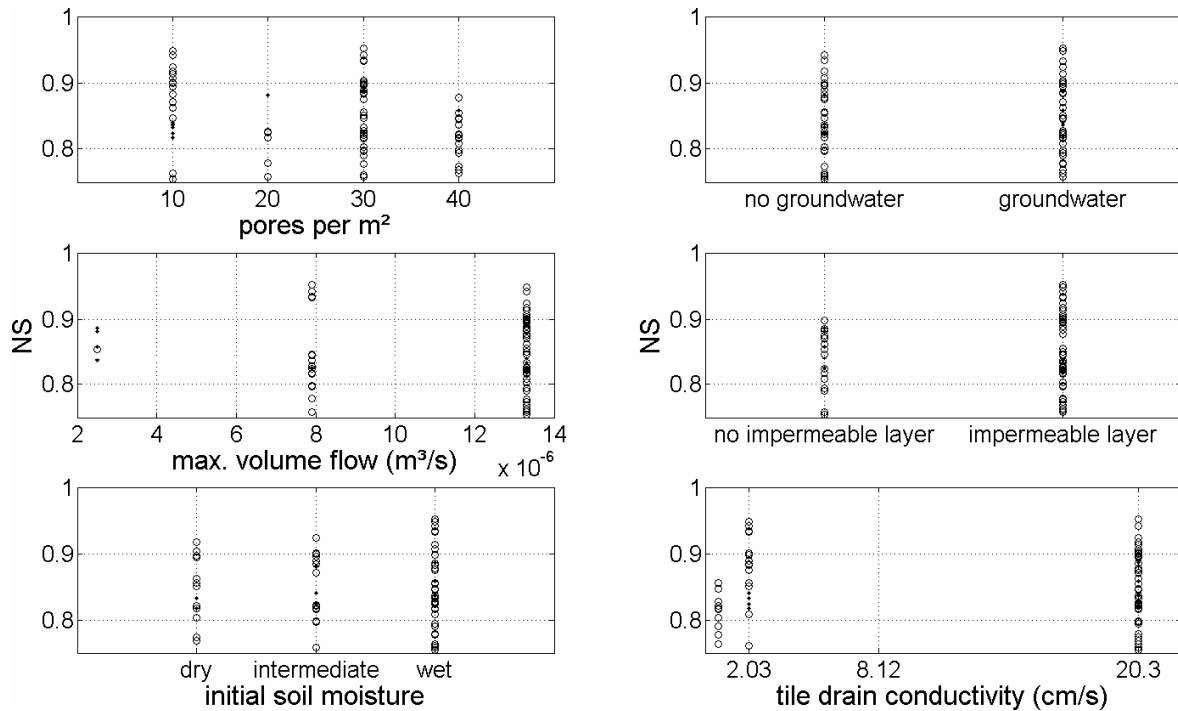


Figure 3-8: Nash-Sutcliffe efficiency $NS \geq 0.75$ plotted against marginal parameter distribution. Circles indicate that the time difference between simulated and observed discharge peak is less or equal than 20 min/two simulation time steps, points indicate only $NS \geq 0.75$. Max. volume flow denotes the allowed maximum volumetric water flow in a macropore.

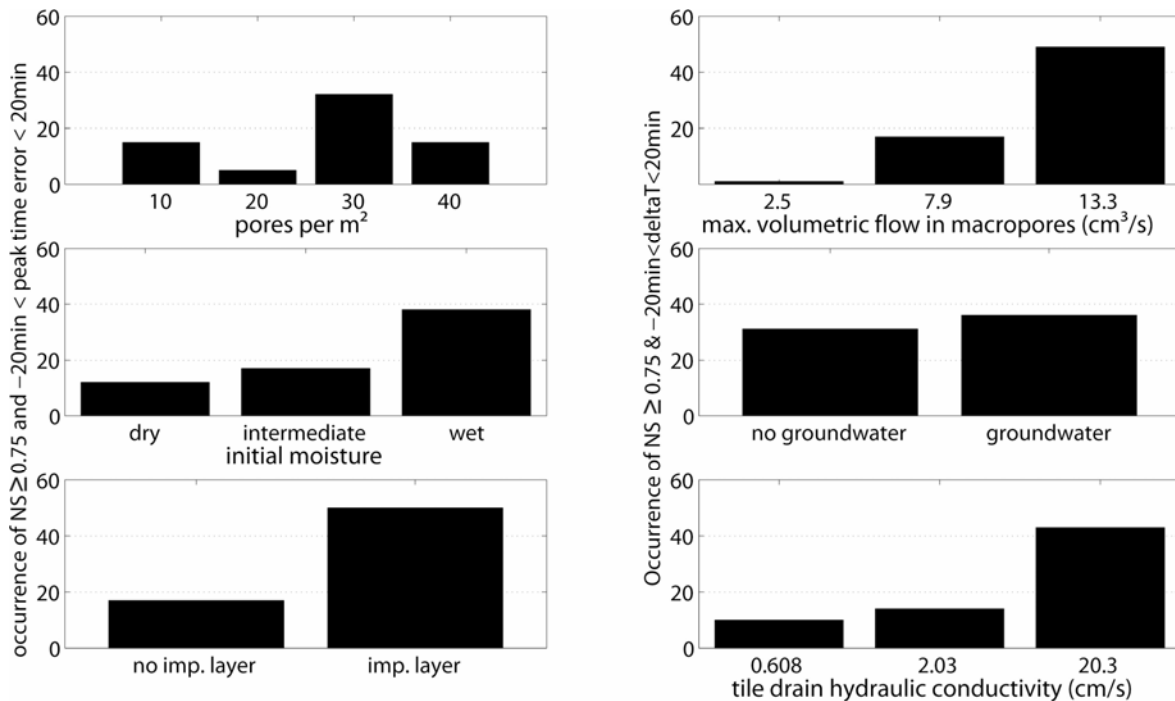


Figure 3-9: Number of model runs with Nash-Sutcliffe efficiency $NS \geq 0.75$ plotted against marginal distributions of parameters (pore density in m^{-2} , maximum volumetric flow in a macropore in cm^3/s , initial conditions, groundwater occurrence, impermeable layer occurrence and D: tile drain velocity).

Figure 3-9 presents the number of acceptable model runs plotted against the different parameter values. The highest number of acceptable model runs is obtained with 30 worm burrows per square meter. A high maximum volumetric water flow of the macropores and high hydraulic conductivity of the tile drain is also favourable for obtaining acceptable

model runs. These high values of maximum volumetric water flow measured by Shipitalo and Butt (1999) and partly by Weiler (2001) seem thus to be more reliable than those suggested by Zehe and Flüßler (2001a). A similar clear picture can be seen for the initial soil moisture conditions. Model runs with the wet initial state, which corresponds to the average value measured by Zehe and Flüßler (2001a), yield more often an acceptable performance than the intermediate and the dry case. Whether or not groundwater was present cannot be inferred from the investigated model runs, both seem equally likely. In contrary I obtain more acceptable runs when including an impermeable layer below the tile drain.

Table 3-4: Parameter combinations that never yield an acceptable model run. P: number of pores (m⁻¹), L: maximum volumetric water flow in a macropore (m³/s), D: tile drain conductivity (cm/s), IMC: initial moisture conditions

Value 1	P = 10	P = 20	P = 20	P = 20	P = 40	L = 2.5 x 10 ⁻⁶	L = 2.5 x 10 ⁻⁶	L = 2.5 x 10 ⁻⁶
Value 2	L = 7.9 x 10 ⁻⁶	IMC = dry	D = 0.608	D = 2.03	D = 0.608	IMC = dry	D = 0.608	D = 2.03

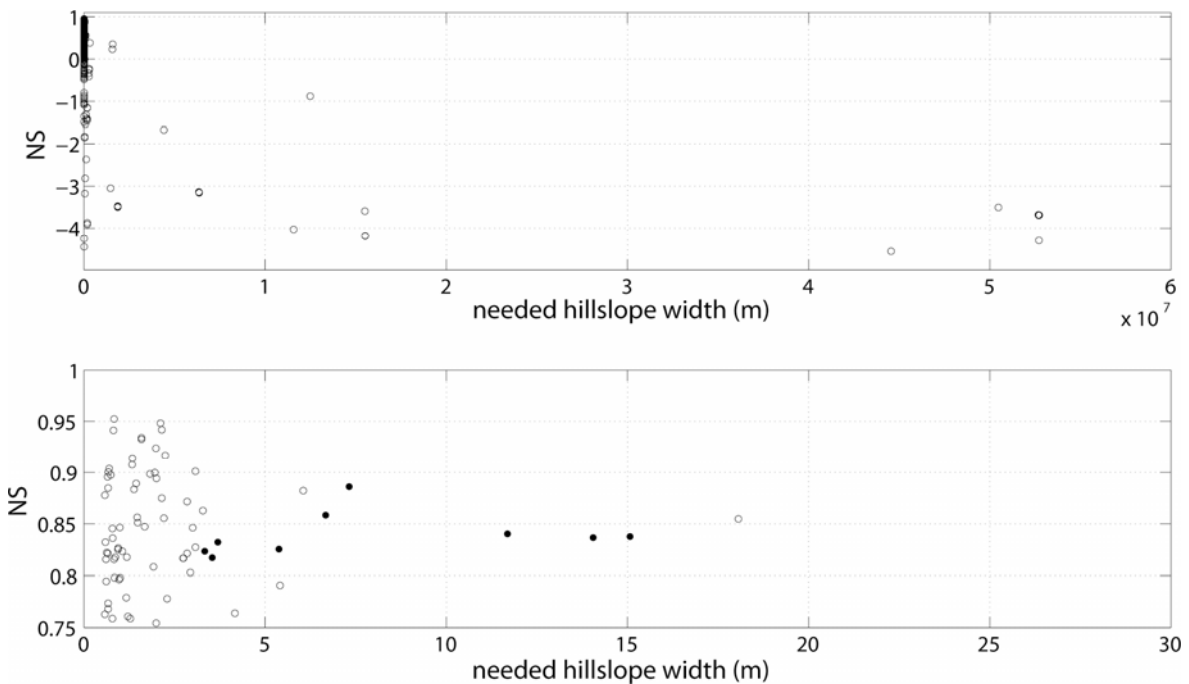


Figure 3-10: a) Nash-Sutcliffe efficiency (NS) versus the width of drained cross-section that is necessary to match the observed peak discharge. b) the lower panel shows all runs with a NS \geq 0.75 (points) and NS \geq 0.75 and the time difference of observed vs. simulated peak within 20 min (circle).

Figure 3-10a and Figure 3-10b shows the model efficiency of all simulation runs plotted against the width of the cross section that was necessary to scale the simulated discharge peak height to the observed one. The upper panel shows all runs, the unacceptable ones required a scaling factor much larger than the width of the irrigated site. The lower panel shows the acceptable runs, i.e. NS \geq 0.75, a time lag smaller or equal than 20 min (circles) plotted against the necessary width of the cross section within the allowed range. The points are model runs with NS \geq 0.75 but with larger timing errors. Twenty-seven of the

acceptable model runs (67) showed a width of cross-section up to 1 meter, 19 a width of 1-2 m, 13 a width of 2-3 m, and 8 a width of up to 18 m.

3.4 Discussion and Conclusions

3.4.1 Worm burrows as explicit connected structures

The suggested way to represent the effect of worm burrows as effective connected structures of realistic geometry, high conductivity and low retention capacity allowed successful reproduction of the observed fast tile drain flow event. This finding is consistent with the study of Vogel et al. (2006). I found a considerable equifinality in the model setup, when key parameters were varied within the ranges of either the measurements if Zehe and Flüher (2001a) or measurements reported in the literature (Shipitalo and Butt, 1999; Weiler, 2001). Sixty-seven model setups yielded an $NS \geq 0.75$. The 13 best among those yielded an NS of more than 0.9, which means that more than 90% of the flow variability is explained by the model. Also the flow volumes were in good agreement and timing errors were less than or equal 20 min (two output time steps).

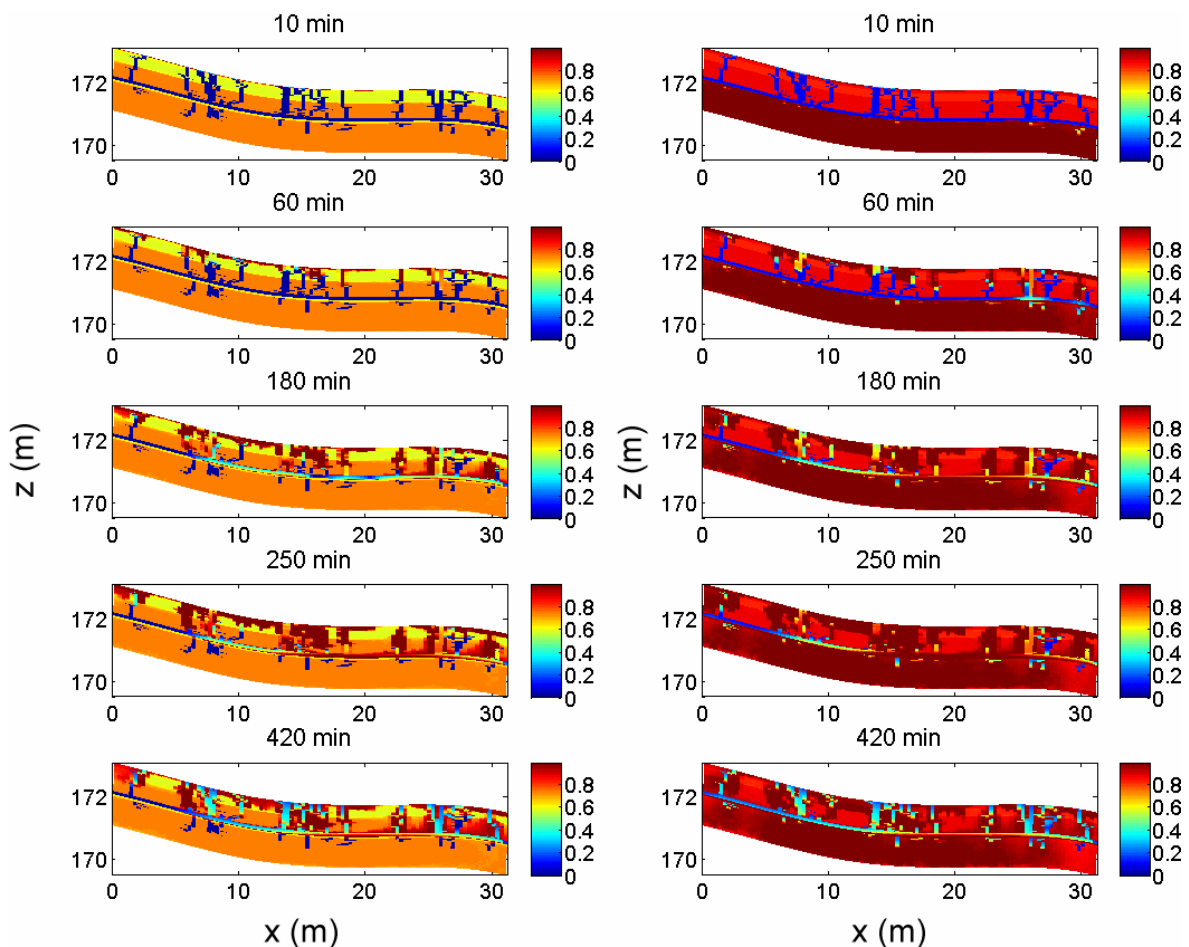


Figure 3-11: Simulated soil moisture pattern during different stages of the experiment taken from two best model runs with Nash-Sutcliffe efficiency >0.9 . The left column was obtained with dry and the right column with wet initial conditions, respectively. The colour bar indicates relative water saturation of the soil.

Figure 3-11 shows as an example the soil moisture patterns during different stages of the simulations for two of the 10 best simulations, one with dry the other with wet initial conditions. Both flow patterns can be deemed as quite realistic, when compared to Figure 3-2b. Simulated soil moisture exhibits high spatial variability, and water does indeed flow along the paths of minimum flow resistance. This is consistent with several observations. Penna et al. (2009), found an increasing variability with decreasing soil moisture at the hillslope scale, and variability over depth. De Lannoy et al. (2006) explained increasing temporal soil moisture variability over depth by preferential flow paths and shallow groundwater. Western and Grayson (1998) and Western et al. (1998) found highly variable soil moisture conditions in the upper 30 cm in the Tarrawarra field site. The included macropore structure is sufficient to reproduce the observed spatial variability and the strong interaction of preferential flow paths and the soil matrix. Additionally, simulated soil moisture patterns exhibit a higher variability when using dry initial soil moisture conditions compared to the wet case.

3.4.2 Equifinality of model structures

As it can be concluded by examination of Figure 3-7, parameter compensation may not explain the equifinality in the spatial setup I found here, at least in the measured range of the parameters. The best 10 model runs are partly based on different parameter setups. Simulations with dry initial soil moisture as well as wet initial conditions do both yield hydrographs which accord very well with the observations. Nevertheless, not all parameter combinations seem equally likely. Starting with the most distinct pattern, it is apparent that I found most of the acceptable and nearly all the best runs when using the highest value for the volumetric water flow in the macropores, based on the measurements of Shipitalo and Butt (1999). This indicates that the hydraulic conductivity of the biopores at the study site was indeed that high. This in turn means that mainly large and deep worm burrows, which have such high conductivities, control the fast flow response, because smaller worm burrows are not as efficient in transporting water (Shipitalo and Butt, 1999). Additional model studies could further elaborate on the role of smaller macropores and variable macropore conductivity. This would, however, mean an even higher spatial model resolution, but could answer the question of how much detail is needed at this scale and show whether more details in this respect would reduce equifinality in the model setup.

A high hydraulic conductivity of the tile drain resulted in a higher number of acceptable model runs. However, this parameter is expected to partly interact with the hydraulic conductivity of the macropores. As I compared only three different values between 6.08 mm/s and 20.3 cm/s, a clear relation between the effect of macropores and the tile drain is not detected. This parameter is, furthermore, difficult to measure as it depends on the gravel embedding, the tube geometry and slope (see chapter 3.2.4).

Although I found acceptable model runs for dry, intermediate and wet initial soil moisture conditions, most of the acceptable model runs cluster within the wet initial state (which is

consistent with the observations in the top 30 cm). I conclude that more detailed information on the initial soil moisture state at greater depths would thus reduce equifinality at least to one-third. This would, however, require more sophisticated observation methods that are currently not at hand.

The dependency of the model performance on the number of macropores per m^2 appears surprising at first sight. Why do 30 pores per square meter yield an acceptable simulation more often than 20 or 40 pores per m^2 ? And then, why are 10 pores better than 20 and 40? This can be explained by the random placement of the macropores along the simulation domain. We know that the “shape” of the catchment and of the river network governs the shape of the hydrograph. In principle we have the same effect here, but on a smaller scale. The arrangement of the preferential pathways along the cross sections corresponds to the arrangement of the river network. A larger amount of macropores that either directly connects the surface to the tile drain or is located near the hillslope foot means a decreasing residence time of the water in the system. More macropores upslope have the opposite effect. This is consistent with the findings of Zehe et al. (2006) who showed that “flipping” of the spatial pattern of worm burrows at the hillslopes in the Weiherbach at a constant average area density had a strong effect on simulated catchment runoff response. Thus it is not sufficient to compare the macropore density per m^2 . Future studies have thus to account for the location along the transect hillslope.

Finally, when referring to Figure 3-10 it can be seen that more detailed data on the width of the control volume that is drained by a single drainage tube would considerably reduce equifinality of the model setup. The small width of the drained control between 1 and 2.5 m that is suggested by most of the acceptable model runs is, due to the 2-dimensional approach likely an underestimation of the true width (compare 3.2.4). Information about the width of the drained control volume could be in principle gained by applying different tracers in stripes parallel to the tile drain direction. However, such measurements are difficult and time-consuming.

The overall conclusion is that the chosen approach is able a) to reproduce the rapid flow response well and b) to produce a realistic pattern of internal dynamics, and is therefore feasible to model vertical preferential flow processes. This underpins that the underlying key assumption like symmetry of the flow problem and homogeneity in the third direction may not be rejected here. This way of modelling rapid flow is, as already discussed, restricted to narrow hillslopes of smooth micro topography or periodic problems and likely underestimates the true width of the drained control volume. The approach is furthermore computationally very demanding. Such a model can, however, be used as a learning tool to get a better quantitative understanding of how the architecture of the burrow system affects rapid flow and transport and how we can mitigate the hazard of rapid flow events. The work presented here suggest, however, that such studies must account for predictive model uncertainty as I found 67 setups with an $\text{NS} \geq 0.75$ and an acceptable timing error and that 13 setups work very well ($\text{NS} \geq 0.9$) without compromising neither field knowledge or the

available data base. This uncertainty/equifinality could surely be reduced considerably when more precise data on initial states and on the drainage area of a single drainage tube were available. However, one has to keep in mind that this is already a very well investigated site; data availability at most sites will certainly be worse and equifinality will be stronger. As the observations at most sites will never be sufficient to characterise the key factors governing preferential flow in an exhaustive manner (Blöschl and Zehe, 2005) we have to keep in mind that predictive uncertainty due to equifinality is an issue when modelling rapid flow with 2-dimensional physically based models.

4 A novel explicit approach to model bromide and pesticide transport in connected soil structures*

This chapter is the follow-up study of chapter 3, where discharge of a tile drain during an irrigation experiment was successfully modelled. This was done by including vertical preferential flow structures in an explicit representation in the hillslope module of CATFLOW. Within the acceptable model results a considerable equifinality was found. After the successful modelling of water transport, the solute transport is modelled with the same approach used in the previous chapter. Tracer data supplies independent information in addition to discharge data. Using these data to validate models can improve parameter identifiability and thus can reduce equifinality (McGuire et al., 2007). Including structures in hydrological models allows a better approximation to the underlying physical process, and may thus reproduce both the transit time distribution of water and solutes in the model domain. Thus it may help to perform better hydrological modelling and it is one major preconditions of successful modelling of the transport of contaminants (e.g. pesticides) with non-conservative transport behaviour. Within this chapter the 13 best model runs ($NS \geq 0.9$) of the previous chapter are employed. The transport of bromide is modelled based on the experimental data of Zehe and Flüher (2001a). One of those model runs is used to model the transport of the pesticide Isoproturon. Thus this chapter contributes to the second of the overall objectives of this thesis (see chapter 1.4.2). After an introduction to the topic the detailed research objectives of this study are presented in chapter 4.1. Then the methodological background and the modelling procedure are introduced in chapter 4.2. Chapter 4.3 presents the results, followed by discussion and conclusion in chapter 4.4.

*based on: Klaus, J. and Zehe, E., 2011. *Hydrology Earth System Sciences* 15, p.2127-2144.

4.1 Introduction

Since the mid-nineties it has become evident that preferential flow is the rule rather than the exception in structured soils (Flury 1996). Preferential flow processes are highly relevant in runoff generation at the hillslope (Lindenmaier et al. 2005; Weiler and McDonnell, 2007; Wienhöfer et al. 2009; Zehe and Sivapalan, 2009) and headwater scales (Zehe and Blöschl, 2004; Zehe et al., 2005; 2006) and consequently are a prime cause for the spatial variability in soil water content at hillslope scale (De Lannoy et al., 2006; Zehe et al., 2010b). Originally, the term “preferential flow” was coined after realising that water flow and transport in soils containing non-capillary structures – often worm burrows, root channels or soil cracks – was much faster than could be expected from classical theory of flow and transport in porous media (Beven and Germann 1982; Zehe and Flühler, 2001a). Rapid flow in morphologically connected preferential flow paths controls transport and residence times of pesticides (e.g. Flury et al., 1995; Elliot et al., 2000; Šimůnek et al., 2003), anions (Flury et al., 1995; Villholth et al., 1998; Lennartz et al., 1999; Köhne et al., 2006; Stone and Wilson, 2006) and of strongly adsorbing phosphorus (Stamm et al., 1998; 2002). Vertical flow distances through the unsaturated zone are in most cases too small for the central limit theorem to apply (Blöschl and Zehe, 2005), thus fully mixed conditions cannot be assumed. Therefore it is not possible to describe the imperfect mixing by a well defined macro dispersion coefficient.

Consequently a variety of approaches has been proposed to effectively represent preferential flow in soil physical or soil hydrological models. Šimůnek et al. (2003), Gerke (2006) and Köhne et al. (2009a) published very nice and helpful reviews of different approaches, like composite hydraulic function models (Zurmühl and Durner, 1996), dual porosity and dual permeability models. Recent studies suggested explicit representation of preferential flow paths as connected structures in the model domain either at the pedon scale (Allaire et al., 2002a,b; Vogel et al., 2006; Sander and Gerke, 2009) or at hillslope scale (Klaus and Zehe, 2010 see chapter 3; Zehe et al., 2010a). These studies showed promising results to reproduce water flow or solute transport. The number of studies dealing with modelling preferential transport of solutes at the hillslope and field scale is so large that an exhaustive overview is beyond the scope of this paper. Hendriks et al. (1999) simulated bromide and nitrate transport in a soil with apparent shrinkage cracks using a modified version of the FLOCR/ANIMO model. Model parameters were estimated by using data of groundwater levels, soil moisture, and concentrations of bromide in both the groundwater body and the soil profile. While the model results for nitrate were poor, bromide concentrations in soil could be adequately reproduced, and predicted bromide concentrations in groundwater matched the mean observed values. Gerke and Köhne (2004) modelled water flow and bromide transport at a tile drain field site using a dual porosity approach (based on the DUAL model of Gerke and van Genuchten (1993)) and a single domain approach. While the single domain approach failed to reproduce observed transport, the DUAL model was able to reproduce the long term dynamics of water and bromide transport well. Nevertheless, the authors report that the DUAL model failed in exactly reproducing observed bromide concentrations. Köhne et al. (2006) used seasonal discharge and bromide data observed at one plot to calibrate different

models and then predicted seasonal transport behaviour at two nearby field plots. They compared a single porosity and a mobile-immobile model where both were set up in one and two dimensions. Calibration and prediction of bromide plateau concentrations were only successful when using the 2-dimensional mobile-immobile model approach. Haws et al. (2005) compared a single-porosity and a dual-porosity approach based on HYDRUS-2D (Šimůnek et al., 1999) to simulate tile drain discharge and the transport of applied chloride and bromide. Although both model approaches were able to reproduce the shape of measured cumulative outflow well, simulated transport deviated considerably from the observations. The authors stated that no approach was able to reproduce rapid transport of solutes to the subsurface tile drain in an acceptable manner and concluded that a well matched hydrograph does not automatically imply that the corresponding model parameters are physical meaningful (see also McGuire et al., 2007). Köhne and Gerke (2005) compared a model based on 2-dimensional Richards equation and 2-dimensional Convection-Dispersion equation (CDE) with a model based on the mobile-immobile approach when simulating tile drain discharge and bromide transport observed at an experimental field site in northern Germany. As only the mobile-immobile approach yielded a good match of the observed bromide peak, the authors concluded that this peak was caused by preferential transport. Gerke et al. (2007) achieved a clearly better match of tracer concentrations observed at the same site when using a 2-dimensional dual-permeability model and injecting the bromide tracer exclusively into the soil matrix domain of the model. Pang et al. (2000) studied bromide and pesticide transport at a tile drained field site in New Zealand using HYDRUS-2D. Simulated soil moisture was in good accordance with observation. The model failed, however, in reproducing observed bromide and pesticide concentrations. Pang et al. (2000) thus concluded that a successful match of preferential transport requires a refinement of the dual-permeability approach.

Leaching and long term fate of non-conservative solutes such as pesticides and pharmaceuticals is even far more difficult to predict as sorption behaviour and degradation processes come into play (Köhne et al., 2009b). Gärdenäs et al. (2006) compared four different approaches to simulate long term soil water flows and pesticide transport at a tile drained field site in southern Sweden. Transport behaviour was observed by taking 13 water samples during a period of 6 weeks. One approach was based on a modification of soil hydraulic conductivity near saturation and the remaining were a mobile-immobile, a dual-porosity and a dual-permeability approach, respectively. The dual-permeability approach performed best, followed by the dual-porosity approach, while the other approaches failed both to reproduce water flows and pesticide transport. Boivin et al. (2006) also used HYDRUS-2D to simulate tile drain discharge and pesticide concentrations observed during a 100-day period for three different soils. Water samples were taken as flow proportional daily mixing samples. Simulated discharge was, after the soil hydraulic functions were modified to account for preferential flow, in good accordance with observations. Boivin et al. (2006) stress that the non-equilibrium mobile-immobile approach allowed acceptable reproduction of the observed pesticide concentrations, while the advection-dispersion approach failed.

The listed studies corroborate that it is most difficult to assess a model parameterisation that allows an acceptable match of both water flows and transport behavior, even when using a dual permeability approach. There is furthermore no straight forward link between parameters that characterise the preferential flow domain in dual permeability models and those parameters that can be measure to characterise the density and depth distribution of a macropore network in natural field soils. Thus I test in this chapter whether an alternative approach, which may be parameterised on field observables, is feasible to simulate transport behavior in structured field soils. The essence is to represent vertical and lateral preferential flow paths explicitly as morphologically connected paths of low flow resistance in the spatially highly resolved model domain. In chapter 3 I gave evidence that this approach allows successful reproduction of tile drain event discharge recorded during an irrigation experiment at a tile drained field site in the Weiherbach catchment (Zehe and Flühler, 2001a). The relevant preferential flow paths - in this case anecic worm burrows – were generated using an agent based model (compare chapter 3.2.2). However, in accordance with studies of Larsbo and Jarvis (2005) and McGuire et al. (2007) a considerable equifinality (Beven, 1993) was found in the setup of chapter 3.4.2. Several “hillslope architectures” that were all consistent with the available extensive data base allowed a good reproduction of tile drain flow response (compare Sect. 3.1). In this follow-up chapter I use the best 13 best hillslope architectures (effective Nash-Sutcliff \geq 0.9) of the previous chapter to address the following questions:

- Does the approach proposed (see chapter 3.2.2) additionally allow reproduction of the bromide and the Isoproturon (IPU) concentrations that have been observed during the irrigation experiment at this site?
- Can the set of the best model setups be reduced by rejecting those that do not match observed bromide transport behaviour?
- Can those behavioural model setups that allowed a good match of both the discharge and bromide loss be employed for simulating transport behaviour of the pesticide at this site?

4.2 Methodology

The experimental data used for the modelling study in this chapter was summarised in the previous chapter (3.2). A rapid breakthrough of bromide and IPU was observed during the irrigation experiment performed by Zehe and Flühler (2001a), see Figure 3-1. Since the modelling is based on the results of the previous chapter I want to refer to chapter 3.2 for the model description and the representation of the preferential flow paths. The detailed description of the generation of the macropore network and their handling in the model are described there. Within this chapter I employ the 13 best spatial model setups, and simulate transport of bromide and compare the results with the corresponding concentrations observed during the field experiment. Table 3-1 characterises the soil profile at the field site and lists the corresponding soil water characteristics and describes the macropore medium. Table 4-1 lists the most important characteristics of the 13 best model runs, the corresponding Nash-

Sutcliffe efficiency and the differences between simulated and observed time to peak (denoted as timing error hereafter).

4.2.1 Scaling factor for length specific output

As CATFLOW is a 2-dimensional model the output is length specific and must be scaled by multiplying simulated length specific outflow by the width of cross section that is drained by the tile drain. Consequently I scaled the output such that simulated peak flows matched the observed peak flows (chapter 3.2.4). The previous chapter revealed that the drained width of the cross section was in most cases around 1 to 3 m (compare Table 4-1). Please note that within the solute modelling these widths were not modified to match bromide concentrations and cumulated bromide loss from the tile drain. This is thus a generic test to find out whether my proposed approach allows a consistent prediction of flow and transport. For further details about the limitations of the scaling approach see chapter 3.2.4.

Table 4-1: Parameters and goodness of fit criteria to characterise the 13 model setups. NS: is the Nash-Sutcliffe efficiency, DT: differences between modelled and simulated time to peak (min), NP: number of macropores per unit area (m^{-2}), MWF: maximum volumetric water flow in a macropore (m^3/s), IMC: initial moisture conditions (the wet case corresponds to a suction head of -50.66 hPa throughout the profile; the intermediate case had a suction head of -303.98 hPa in the upper 40 cm of the profile and -101.33 hPa below this layer; the dry setting corresponds to a head of -405.3 hPa in the upper 40 cm of the profile and -151.99 hPa in the remaining soil profile), k_D : tile drain conductivity (cm/s), GW: Groundwater occurrence, C-Sec: drained width of the cross-section in meters adjusted to match the peak.

run	NS	DT	NP	MWF	IMC	GW	k_D	C-Sec
1	0.952	7	30	7.90×10^{-06}	Wet	yes	20.3	0.83
2	0.948	7	10	1.33×10^{-05}	Wet	yes	2.03	2.11
3	0.942	7	10	1.33×10^{-05}	Wet	no	2.03	2.15
4	0.941	7	30	7.90×10^{-06}	Wet	no	20.3	0.82
5	0.934	7	30	7.90×10^{-06}	Wet	no	2.03	1.59
6	0.932	7	30	7.90×10^{-06}	Wet	yes	2.03	1.59
7	0.923	7	10	1.33×10^{-05}	intermediate	yes	20.3	1.99
8	0.917	17	10	1.33×10^{-05}	Dry	no	20.3	2.24
9	0.914	7	10	1.33×10^{-05}	Wet	yes	20.3	1.34
10	0.907	7	10	1.33×10^{-05}	Wet	no	20.3	1.33
11	0.904	7	30	1.33×10^{-05}	Dry	yes	20.3	0.70
12	0.901	17	10	1.33×10^{-05}	intermediate	yes	2.03	3.09
13	0.9	7	30	1.33×10^{-05}	intermediate	yes	20.3	0.67

4.2.2 Transport parameters and modelling procedure

Bromide transport was simulated for the 13 model setups using the initial soil moisture state listed in Table 4-1. Simulated irrigation occurred during the field experiment in three blocks of uniform intensity with a sum of 46 ± 5 mm. At the beginning of simulation 1500 g of bromide was evenly distributed within the upper layer of the model domain (2 cm). During all simulated cases I used a constant isotropic effective diffusion coefficient of $D = 5 \times 10^{-7} \text{ m}^2/\text{s}$

for bromide (Zehe and Blöschl, 2004) and IPU. This selection is corroborated by observations from nearby tracer profiles that were obtained under a similar irrigation conditions and similar a soil, where I determined a dispersion coefficient D of $5.4 \times 10^{-7} \text{ m}^2/\text{s}$ for a travel time of 24h and a D of $7.5 \times 10^{-8} \text{ m}^2/\text{s}$ after 48h travel time (see chapter 6.3). As I mainly intend to test the feasibility of the explicit representation of preferential flow paths I do not present a sensitivity study of the dispersion coefficient on the simulation results.

IPU transport was simulated for the model setup named “run 1” that yielded the best discharge simulation and an acceptable good match of the time series of cumulated bromide mass flow at the tile drain outlet (see chapter 4.3.2). Due to the high computational cost I restricted the IPU transport modelling exercise solely to this spatial model setup. As initial state 270 g of IPU were spatially homogeneously distributed in the upper 2 cm of the soil corresponding to the amount of IPU that has been applied to the field one day before the experiment. This considers the redistribution of the IPU that was applied on the soil surface the day before irrigation and likely entered the top soil by means of diffusion. I used the same effective diffusion coefficient as for bromide transport. Non-linear adsorption behaviour of IPU was parameterised according to the Freundlich-isotherm:

$$C_a = k_f \times C^\beta \quad \text{Equation 4-1}$$

Where C_a is the concentration in the adsorbed phase (g/g), k_f is the Freundlich coefficient ($\text{l}^\beta/\text{g g}^{1-\beta}$), C is solute concentration in the water phase (g/l) and β is the Freundlich exponent (-).

As Zehe and Flühler (2001a) did not determine the Freundlich parameters for IPU at their irrigation site, I tested different values reported in the Footprint data base (Footprint, 2006). According to the Footprint data base, k_f may range from 0.26 and 27.1 $\text{l}^\beta/\text{g g}^{1-\beta}$ while β is reported as 0.8. During simulation I varied k_f between 0.26 and 20 within 9 steps and allowed β to vary within 0.2, 0.5, 0.8, and 1.0. Since simulated cumulated leaching of IPU did not at all match observed cumulated leaching (see chapter 4.3.3), I further reduced k_f in 8 steps to stepwise reduce the retardation in the preferential flow and the matrix domain (k_f : 0.1, 0.05, 0.01, 1×10^{-3} , 1×10^{-4} , 1×10^{-5} , 1×10^{-6} , and $1 \times 10^{-7} \text{ l}^\beta/\text{g g}^{1-\beta}$).

As a first step I assumed that adsorption was uniform in the entire domain and selected the parameter set that performed best. Next I assigned these parameters exclusively to the macropore medium and characterised adsorption behaviour in the soil matrix by means of average parameters $\beta=0.8$ and $k_f=10 \text{ l}^\beta/\text{g g}^{1-\beta}$.

4.3 Results

4.3.1 Simulated and observed hydrographs

Figure 4-1, Figure 4-2, and Figure 4-3 present simulated discharge plotted against observed tile drain discharge (panels in the left column). Simulated discharge is generally in very good accordance with the observations, except that the first discharge increase comes

systematically too late during simulations. While Nash-Sutcliffe efficiencies are larger than 0.9 (compare Table 4-1 and Table 4-2), some of the simulations (runs 7, 8, 11, and 13) have water mass balance errors (deviation between modeled and observed total discharge volume) that exceed 10%. Peak time errors are in general of the order of 7 or 17 min, corresponding to 1 or 2 model output time steps. Please note that discharge measurements during the irrigation experiment stopped 5 h after irrigation, although tile drain discharge was still approximately two times above the pre-event level. For additional details on the entire Monte Carlo study, especially on the sensitivity of predicted discharge on key parameters such as average density of worm burrows or maximum flow rates in macropores, please refer to chapter 3.

4.3.2 Simulated and observed bromide concentration and mass flows

Figures Figure 4-1, Figure 4-2, and Figure 4-3 present the time series of simulated and observed bromide concentrations (in the middle column) and cumulated bromide loss from the 13 simulations plotted against the corresponding observation (right column). As can be seen from Figure 3-1 or the panels in the middle column of Figure 4-1, Figure 4-2, and Figure 4-3, observed bromide concentration peaked in the very first sample taken 36 min after irrigation onset. This first flush can be attributed to rapid preferential transport as no significant increase in discharge was detectable. Within the second irrigation block, 145 minutes after irrigation onset, bromide concentration levelled out at a concentration of 1.9 mg/l for almost 40 min, and then declined to a pretty constant value of around 1.2 mg/l.

Simulated bromide concentrations are calculated from the cumulated bromide loss within a model output time step, which is 10 min, divided by the accumulated water volume that left the model domain within this time. Simulated bromide concentrations are clearly more “noisy” than the observed ones. Although the simulated bromide concentrations are different among model runs, the temporal pattern is similar for all runs. Simulated concentrations show an early peak in the order of 0.5 to 2 mg/l within the first 30 min, then decrease to zero or near zero values for all runs and re-rise again to values of about 2 mg/l. The observed peak at minute 36 is often reproduced as a double peak by the model. During the second irrigation block some simulations reproduce a concentration peak instead of a plateau concentration, while some runs capture this plateau. Simulated concentrations are in acceptable accordance with the observed ones during the last irrigation block. Overall, it can be stated that simulated concentrations match the magnitude of the observed ones and also roughly the timing of the peaks. Part of the mismatch might be attributed to the fact that rather small errors in simulated discharge (magnitude and timing) propagate to considerable errors in concentrations (magnitude and timing). However, as the model was not tuned to reproduce the observed concentration I did not expect a really good match in absolute concentrations on a time scale of minutes.

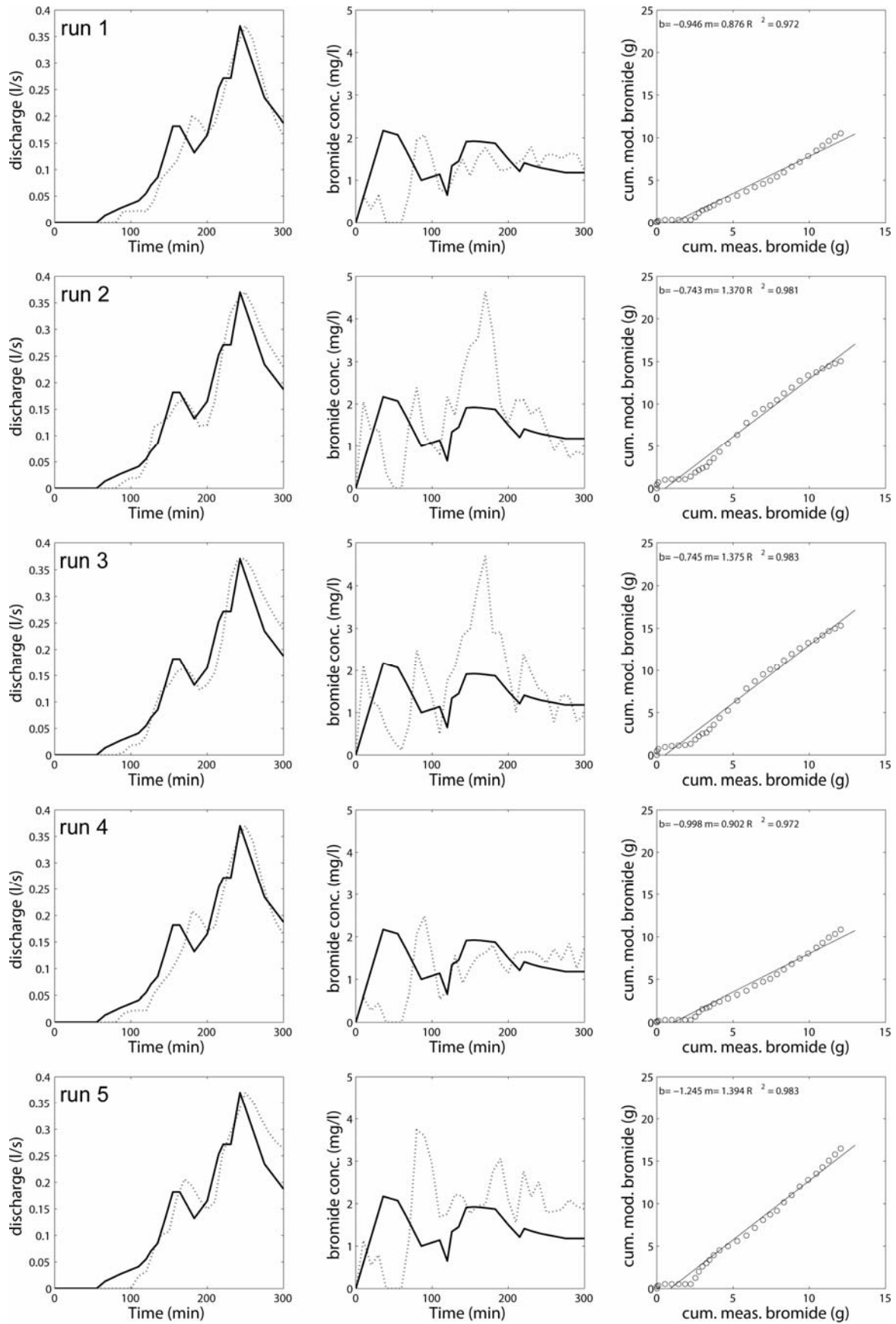


Figure 4-1: The right column presents the observed discharge (solid line) and the modelled discharge (dotted line), the centre column presents the observed (solid line) and modelled (dotted line) bromide concentrations in the tile drain, while the right column presents the cumulated modelled bromide outflow versus the measured one and a linear regression line between them (b denotes the intercept and m the slope of the regression).

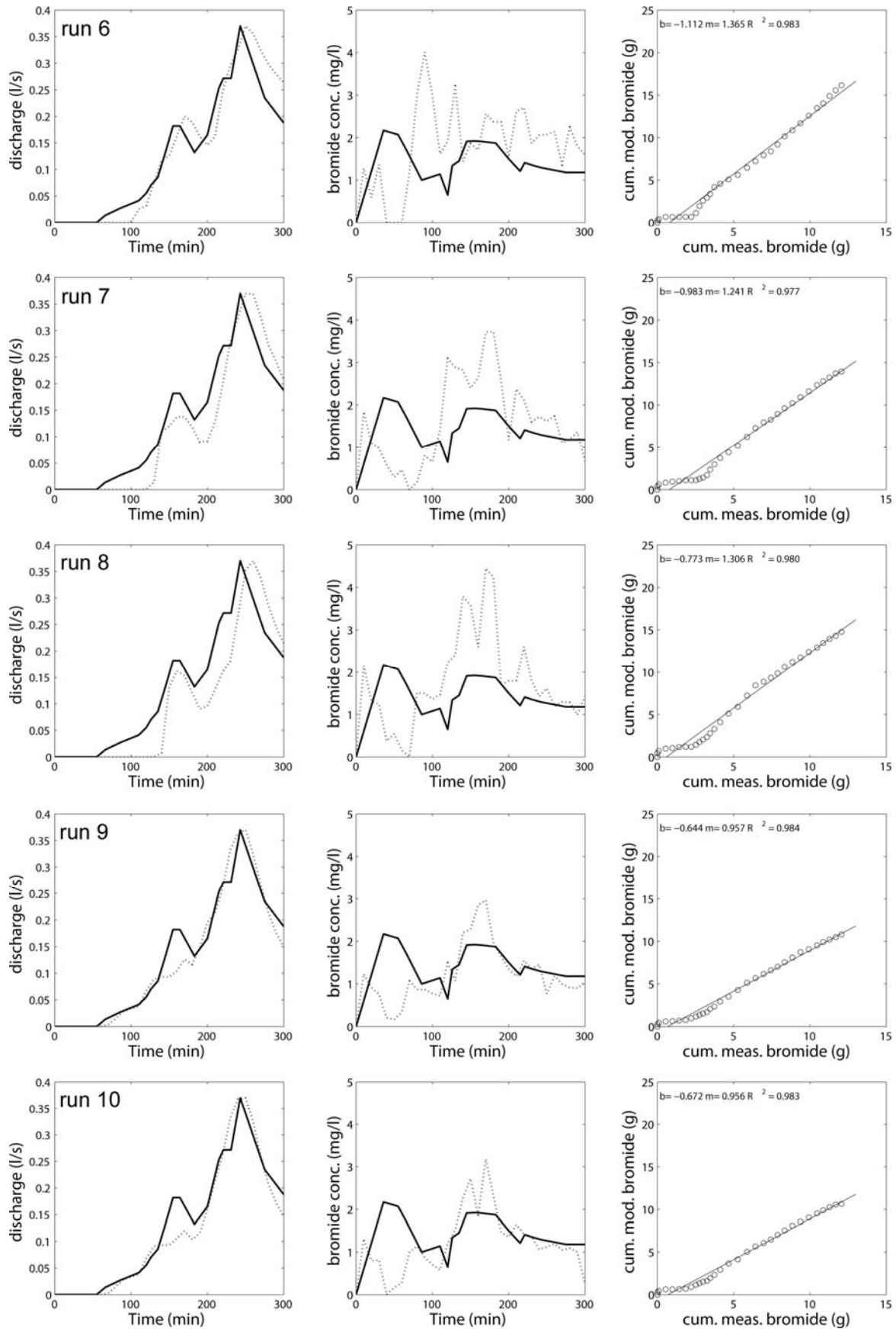


Figure 4-2: The right column presents the observed discharge (solid line) and the modelled discharge (dotted line), the centre column presents the observed (solid line) and modelled (dotted line) bromide concentrations in the tile drain, while the right column presents the cumulated modelled bromide outflow versus the measured one and a linear regression line between them (b denotes the intercept and m the slope of the regression).

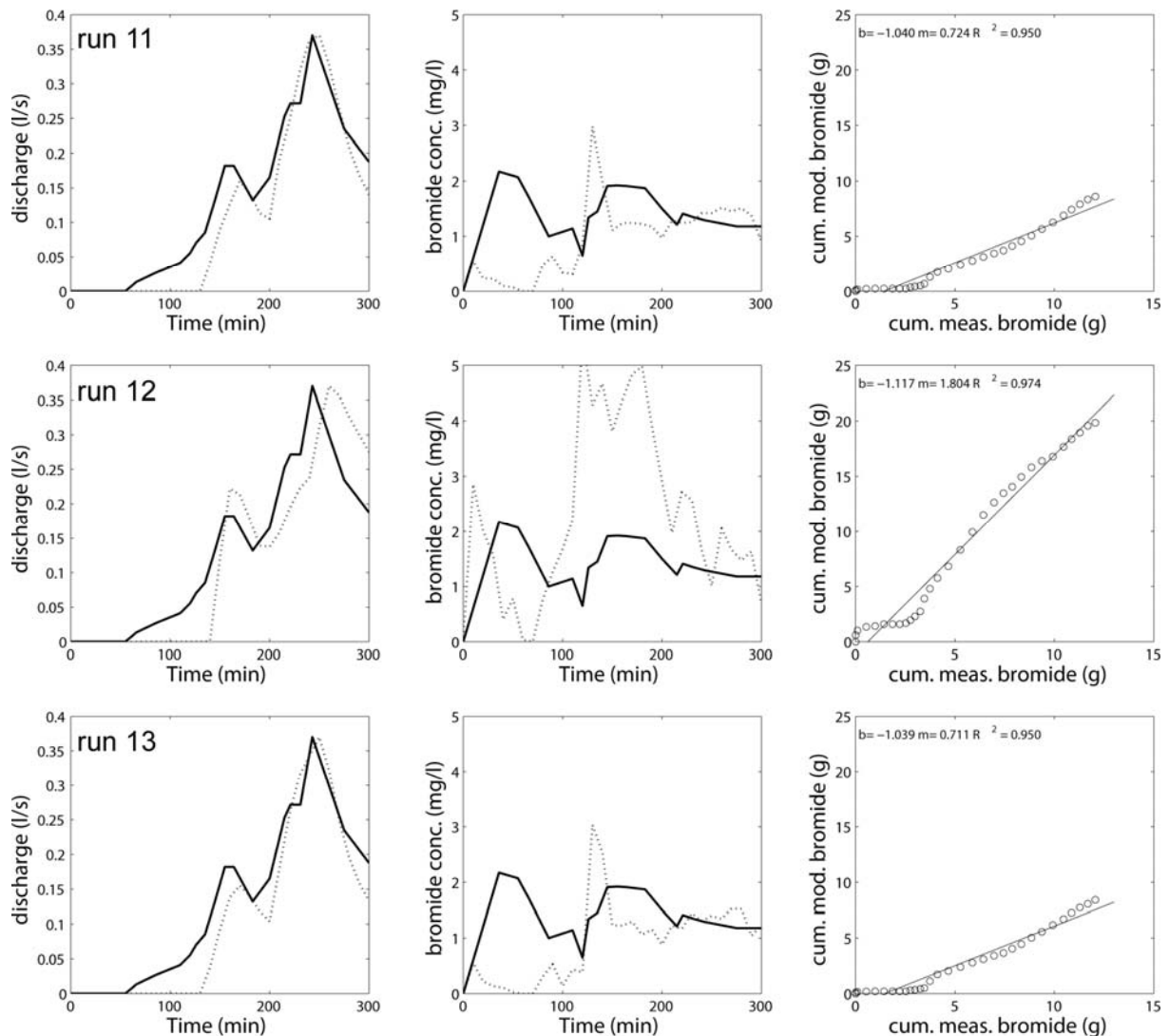


Figure 4-3: The right column presents the observed discharge (solid line) and the modelled discharge (dotted line), the centre column presents the observed (solid line) and modelled (dotted line) bromide concentrations in the tile drain, while the right column presents the cumulated modelled bromide outflow versus the measured one and a linear regression line between them (b denotes the intersect and m the slope of the regression).

There is however a good accordance between the cumulated bromide losses derived from simulation when compared to the observed cumulated bromide loss (Figure 4-1, Figure 4-2, and Figure 4-3, right column). Despite the fact that all simulations underestimate the observed cumulated leaching within the early phase of the irrigation, simulation and observations are in very good linear accordance, as the coefficients of determination (not time corrected), R^2 , are always larger than 0.95. Within the model runs 1, 4, 9, and 10, the simulation matches the observed accumulated bromide loss to the tile drain with a relative error in the order of 5-12%, which is within the error range of the observed data, 10% for discharge and 15% for bromide (compare Table 4-2). Table 4-2 lists furthermore the slope and intersect of a linear regression between observed and simulated cumulative bromide leaching; regression lines of model runs 1, 4, 9, and 10 are close to one. Thus it may be stated that the spatial model setups of 1, 4, 9, and 10 reproduce the observed time series of cumulated bromide loss in an almost unbiased manner. This is remarkable as the model has not been attuned for this purpose. I showed in chapter 3 that the soil moisture dynamics followed a realistic pattern. Figure 4-4

presents the hillslope scale bromide concentrations at five different time points. The simulated bromide concentration pattern is apparently controlled by the macropore system as patches of higher bromide concentration cluster along the border of the preferential flow paths.

Table 4-2: The thirteen model runs used for bromide modelling. Number of model run, Nash-Sutcliffe efficiency (NS) of hydrograph modelling, relative water balance error in % (WB), relative error in bromide mass balance in % (BMB), the slope of the regression line fitted to the compared cumulative transport of measured and modelled values (m), the intercept of the regression line (b) and the corresponding coefficient of determination (R²).

run	NS	WB	BMB	m	b	R ²
1	0.952	-6.5	-13.47	0.876	-0.946	0.972
2	0.948	0.31	23.63	1.37	-0.743	0.981
3	0.942	-0.77	25.74	1.375	-0.745	0.983
4	0.941	-6.86	-10.97	0.902	-0.998	0.972
5	0.934	1.6	35.39	1.394	-1.245	0.983
6	0.932	2.04	32.69	1.365	-1.112	0.983
7	0.923	-13.06	14.55	1.241	-0.983	0.977
8	0.917	-19.03	21.28	1.306	-0.773	0.98
9	0.914	-5.05	-11.34	0.957	-0.644	0.984
10	0.907	-7.5	-12.64	0.956	-0.672	0.983
11	0.904	-16.3	-29.36	0.724	-1.046	0.95
12	0.901	-8.19	63.06	1.804	-1.117	0.974
13	0.9	-17.87	-30.93	0.711	-1.039	0.95

4.3.3 Simulated and observed cumulative leaching of IPU

I selected the model setup one (run 1) for simulating IPU transport as it performed best with respect to discharge and was ranked fourth with respect to reproducing cumulated bromide loss. Simulated and observed cumulated leaching of IPU is shown in Figure 4-5, each panel corresponds to a case where β was fixed at 0.2, 0.5, 0.8 or 1 and k_f was varied between 0.26 and $20 \text{ l}^\beta/\text{g g}^{1-\beta}$. To put it in short, none of the simulations based on these parameterisations came anywhere close to the observed leaching behaviour. Retardation was clearly far too strong. This finding is in accordance with observations during the irrigation experiment (Zehe and Flüher, 2001a) who pointed out that the effective retardation coefficient of IPU against bromide was almost one.

I therefore reduced k_f as explained in chapter 4.2.2 to reduce the retardation coefficient stepwise to one and compared simulated and observed cumulated leaching of IPU (Figure 4-6). The lowest k_f -values of 1×10^{-6} and $1 \times 10^{-7} \text{ l}^\beta/\text{g g}^{1-\beta}$ yield a good match of the early non-linear rise of the cumulative leaching curve regardless which value is used for β . However, in total they lead to a strong overestimation of the total IPU mass that leached into the tile drain. Figure 4-6 also shows that a combination of $\beta=0.2$ and $k_f=1 \times 10^{-5} \text{ l}^\beta/\text{g g}^{1-\beta}$ or $\beta=0.8$ and $k_f=1 \times 10^{-4} \text{ l}^\beta/\text{g g}^{1-\beta}$ allow an acceptable estimate of the total mass of IPU that leached into the

tile drains. This suggests that there are several combinations of β and k_f -values that allow either a good match of cumulated IPU leaching in the early stages or of total IPU mass at the end of the experiment. However there was no parameterisation that yielded a good match of both, the rapid increase at the beginning of the experiment and the total observed transport.

I thus tested whether different adsorption characteristics in the soil matrix and in the macropore medium would improve the model performance. I selected a β -value of 0.8 for the soil matrix and the macropores and varied the k_f -values in the macropores (1×10^{-3} , 1×10^{-4} , 1×10^{-5} , 1×10^{-6} l ^{β} /g g^{1- β}), while the k_f -values in the soil matrix was kept constant (10 l ^{β} /g g^{1- β}). Heterogeneous adsorption caused a slight “damping” of the cumulated leaching curves, but did not improve the shape of the modelled breakthrough curve (Figure 4-7). Thus it may be stated that without any prior knowledge about the retardation behaviour, simulated leaching is way off the observations. When such information is available, as in the present case, the proposed model approach can be attuned to reproduce the overall amount that leached to the tile drain, while the dynamics is hardly reproduced. Including non-equilibrium sorption into simulation could allow a better match of the observed leaching dynamics.

4.4 Discussion and Conclusion

4.4.1 Preferential structures for preferential transport

The proposed approach to represent vertical macropores - in this case anecic earthworm burrow - and the tile drain as morphologically connected structures in a 2-dimensional model domain (Klaus and Zehe, 2010, see chapter 3; Zehe et al., 2010a) is feasible to:

- Setup several spatial hillslope architectures that are consistent with detailed field observations, especially on the density and depth distribution of worm burrows and to reproduce observed tile drain discharge (see chapter 3). This is consistent with findings at even smaller scales i.e. column experiments of Comegna et al. (2001) and Abasi et al. (2003).
- The 13 best hillslope architectures, which achieved a Nash-Sutcliffe efficiency larger than 0.9 in combination with a small peak time error, predicted dynamics of accumulated bromide leaching into the tile drain well ($R^2 > 0.95$) without additional calibration.

Four of those hillslope architectures (run 1, 4, 9, and 10) matched the total accumulated water balance (compare Table 4-2) within the relative error range of 10% according to Zehe and Flüßler (2001a). It is remarkable that the same hillslope architectures also matched the total amount of bromide that leached into the tile drain within the range of the observation errors (please note that due to Gaussian error propagation, the relative error of the bromide mass flow at the tile drain outlet equals the sum of the relative errors in discharge (10%) and bromide concentrations (5%)). Thus it may be stated that only four of the 432 hillslope architectures tested in chapter 3 matched both flow dynamics and bromide leaching very well and in an unbiased manner.

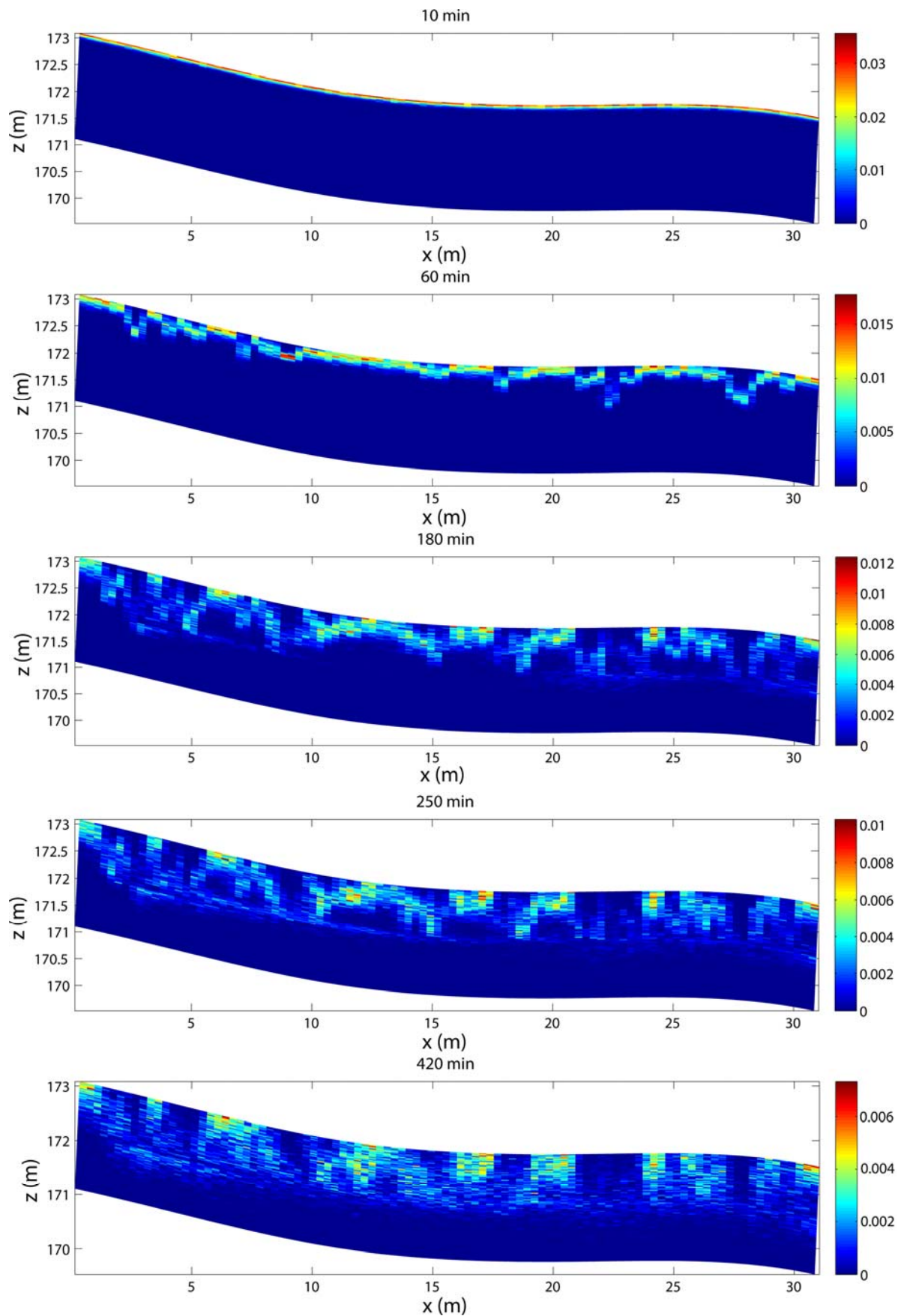


Figure 4-4: Bromide concentrations g per kg dry soil in the model domain, and the development over time. Please note that the concentrations are plotted for a 30 m wide hillslope, and that the colour scale changes over time.

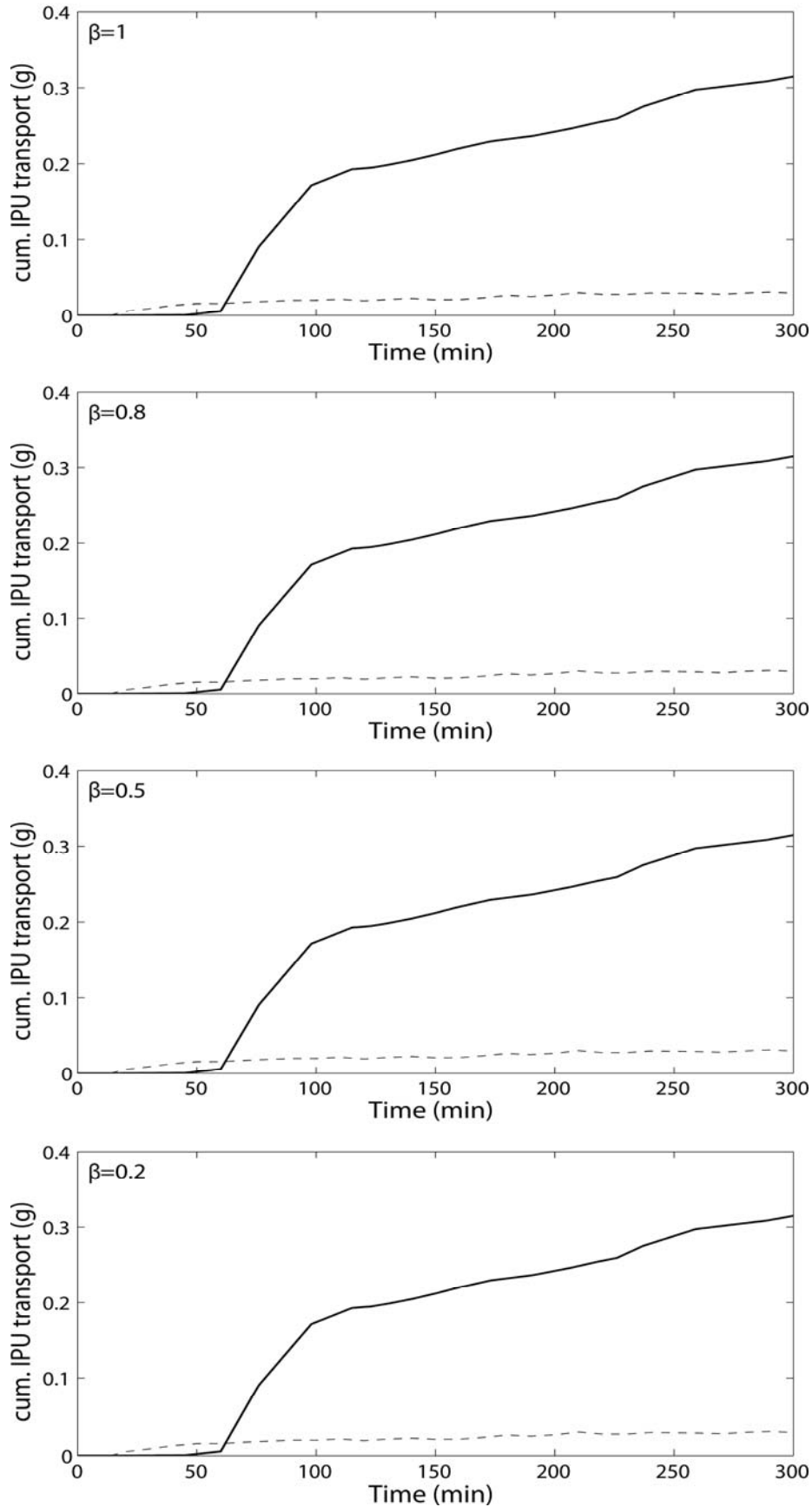


Figure 4-5: Cumulated IPU loss plotted against simulation time for different parameterisations of the Freundlich isotherm. The solid line presents the observed IPU leaching, the dashed lines model runs with different parameterisation of the Freundlich parameters. Every plot includes eight model realisations with a fixed value for the Freundlich exponent β and varied values for the Freundlich coefficient k_f between 0.26 and $20 \text{ l}^\beta/\text{g}^{1-\beta}$ (lowest line) within 9 steps.

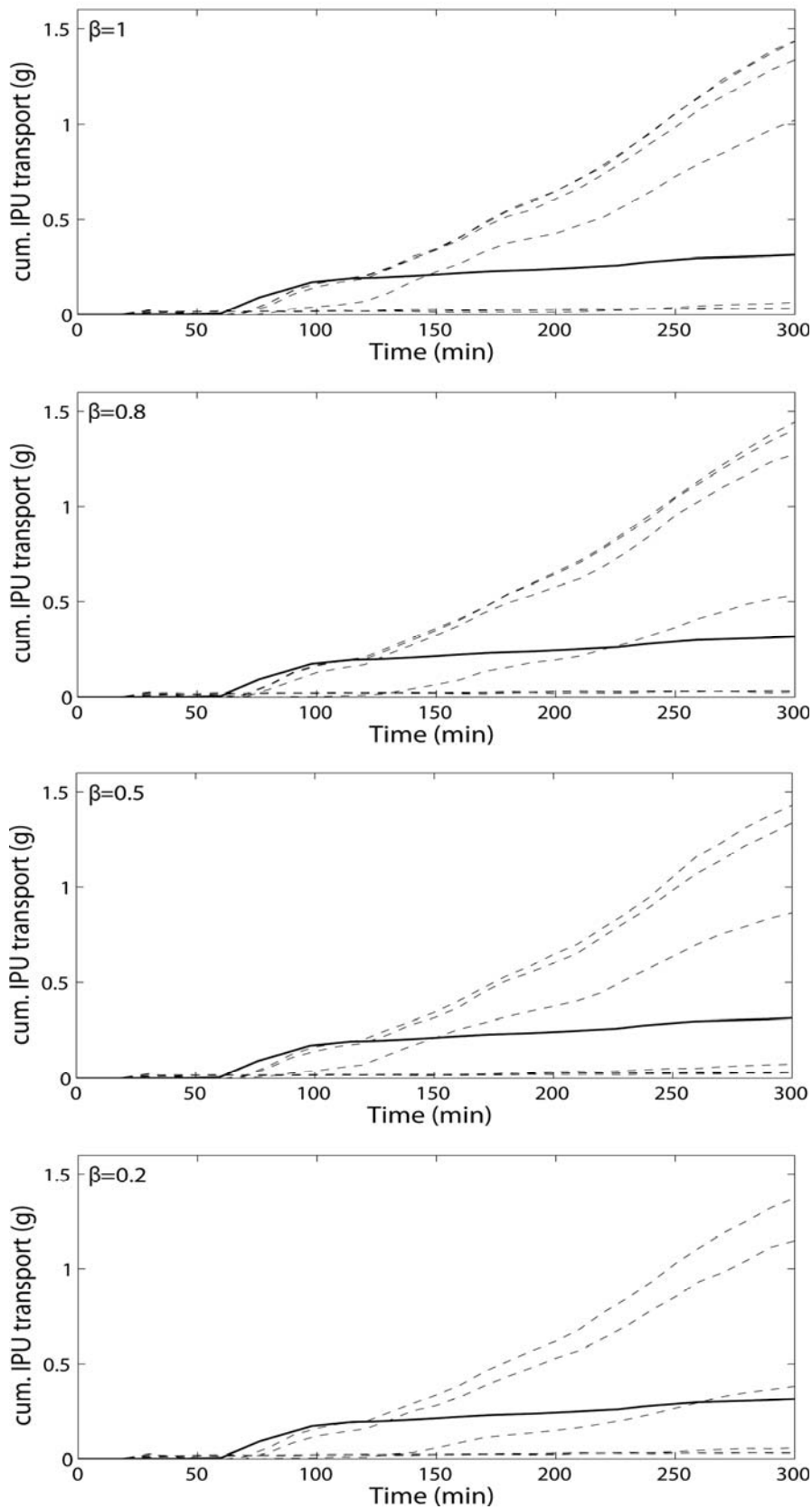


Figure 4-6: Cumulated IPU loss plotted against simulation time for different parameterisations of the Freundlich isotherm. The solid line presents the observed IPU leaching, the dashed lines model runs with different parameterisation of the Freundlich parameters. Every plot includes eight model realisations with a fixed value for the Freundlich exponent β and varied values for the Freundlich coefficient k_f between 0.1 (lowest line) and $1 \times 10^{-7} \text{ l}^\beta/\text{g g}^{1-\beta}$ within 8 steps.

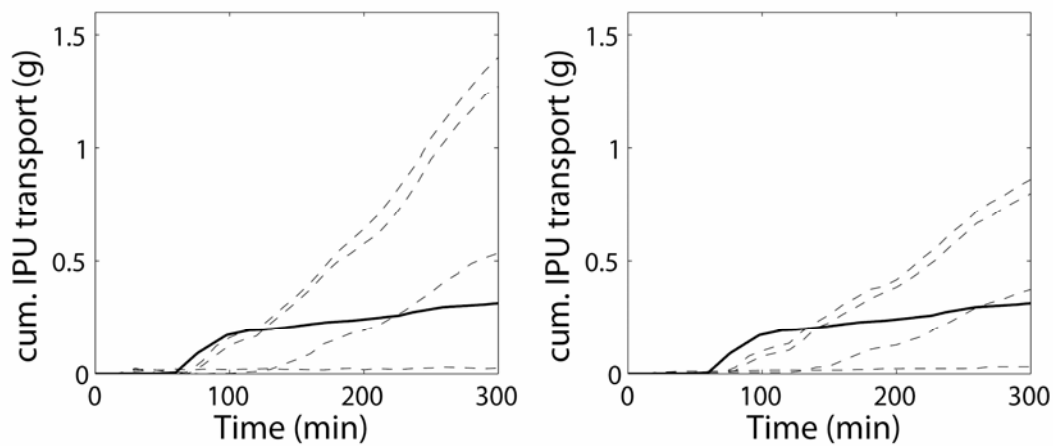


Figure 4-7: Modelling IPU transport with spatial homogenous (left) and spatial heterogeneous (right) sorption parameter. The solid black line denotes the sampled cumulative breakthrough curve, the dashed lines display the modelled breakthrough curves.

However, the proposed model structures are, without additional calibration, unable to reproduce exactly the time series of bromide concentrations, but do capture the order of magnitude of the concentrations. Bromide concentrations and mass flows in the first phase of the irrigation experiment are systematically underestimated. A closer look at model runs 1, 4, 9, and 10 reveals that predicted concentrations match the observations in later stages ($t > 100$ min) in an acceptable manner. Run 4 performs best with respect to the overall bromide mass balance, and run 1 captures even the magnitude of the maximum observed bromide concentration, although the timing is roughly 50 min too late. This is consistent with the fact that first discharge reactions within the model are also systematically 50 min too late (except for run 9 and 10).

Transport velocities and bromide concentration in the model are obviously both too small to match the first flush of bromide into the tile drain. One possible explanation for this is that the proposed approach is too slow to capture the obviously very fast initialisation of macropore flow in the real system. This might be true, but note that simulated first arrivals of bromide are around 10 min (compare Figure 4-1, Figure 4-2, and Figure 4-3), which is deemed to be rather fast. Another explanation for the mismatch of early concentrations is that the proposed approach does not sufficiently account for bromide exchange between the surrounding soil matrix and the connected structures (Weiler and Naef, 2003a; Coppola et al., 2009) – although exchange happens as indicated by Figure 4-4. The proposed approach can certainly neither account for processes like solute exclusion nor for the possibly hydrophobic behavior of the worm burrow coating. An increased model complexity for instance by including mobile-immobile water would certainly add more flexibility to the model to closer reproduce the bromide concentrations. The drawback is however to include additional parameters that are not directly observable in field soils. This would thus also result in increased equifinality.

Furthermore, an explanation for the mismatch of early concentrations is that I simulate a spatially homogeneous irrigation, while Zehe and Flüßler (2001a) reported that their irrigation

scheme was rather heterogeneous shortly after bromide application: a lot of irrigation water with a large amount of bromide concentrated along the middle axis of the 30 by 30 m² large irrigation site (compare their Fig. 12). These locally increased irrigation and mass inputs could, according to Weiler and Naef (2003a), cause fast preferential flow rates and enhance mass transport into the tile drain and result in the observed first flush. This effect cannot be reproduced by simulating (a) a homogeneous irrigation and (b) neglecting the microtopography that determines local scale lateral redistribution of ponded irrigation water. I have neither information about the exact spatial pattern of irrigation rates nor details on microtopography (which would be rather difficult to include into a 2-dimensional model). I thus omit any trial to reproduce this first flush effect within a simulation, as the underlying assumption would be rather speculative.

As CATFLOW is a 2-dimensional model, predicted discharge is length specific and model output has thus to be scaled to 3-dimensional reality by specifying the width of the irrigated site that feeds tile drain discharge. As elaborated in chapter 3 I selected this drained width such that the simulated peak discharge matched the observed peak discharge. As these values, which are in the order of 1-3m (compare Table 4-1), were kept constant in the present study, it can be stated that the same scaling factor allows simulation of flow and transport in a consistent manner. This corroborates that this factor is more than a “quick fix” to reproduce water flows, but is related to the width of the irrigation site that contributed to the tile drain water flow and bromide mass flows and integrates different processes that lead to transport perpendicular to the direction of the tile drain. This does not mean that the scaling factor matches the contributing width of the hillslope in an exact manner.

I thus overall conclude that:

- A realistic representation of dominating structures and their topology enables the prediction of preferential water and mass flows at tile drained hillslopes. This requires detailed knowledge about the density and topology of the preferential flow paths, in our case anecic worm burrows, that are structures that emerge at the hillslope scale. They are a fingerprint of population dynamics and behavior of earthworms as ecosystem engineers and obey ecological rather than physical principles. Thus the necessary realistic representation is needed to describe the structures and no upscaling from microscale physical principles is possible to obtain the necessary information.
- Those hillslope architectures that perform best with respect to the integral discharge response are also suitable for predicting dynamics of accumulated bromide leaching, partly without a bias. This finding is clearly opposite to what has been achieved by Haws et al. (2005) but in accordance with the finding of McGuire et al. (2007).

The first point implies that I had to be very open to learn from soil ecologists. The major outcome of this learning process is that the generated structures match geometry, tortuosity and topology of worm burrows well when used at a finer grid resolution (Zehe et al., 2010a). The necessary data for generation of these burrow systems furthermore can be directly observed in the field and on the long term hopefully inferred from species distributions models from soil ecology.

4.4.2 Clear deficiencies to reproduce observed pesticides leaching

Even if the model structure has been shown to reproduce both discharge and bromide transport behaviour, the reproduction of the observed accumulated leaching for IPU was rather challenging. A parameterisation of the Freundlich isotherm based on values reported in the Footprint data base (Footprint, 2006) did not reveal any meaningful result. Based on the finding of Zehe and Flühler (2001a) at this site, who report an effective retardation coefficient of one at the end to the experiment and similar findings of Kung et al. (2000) who found similar behaviour for bromide and the sorbing tracer rhodamin WT, I reduced the k_f -values and thus the retardation coefficient stepwise to one. With this, the proposed model approach could be attuned to reproduce the overall IPU mass that leached to the tile drain. Temporal dynamics of cumulated leaching was hardly reproduced.

The strongly reduced retardation of reactive solutes is likely caused by the differences in the chemical and physical properties of the organic coating of the macropore walls compared to bulk soil matrix. While adsorption capacity of macropore walls can be stronger than in bulk soil material, the overall retardation may still be less, due to the smaller surface area per volume in macropores or rate limited adsorption (e.g. Jarvis, 2007). As travel times in macropores are likely small compared to the time scale of lateral diffusive mixing equilibrium approaches are deemed to be too simple to describe adsorption behavior. A more complex kinetic approach may lead to an improvement match of the temporal dynamics. A heterogeneous parameterisation of adsorption parameter between the soil matrix and the connected flow paths (e.g. as suggested by Ray et al., 2004) did not lead to a clear improvement. The retardation characteristics of the soil at the study site are probably more heterogeneous, both in the soil matrix and the soil macropores, when considering effects like macropore coating (e.g. Gerke, 2006).

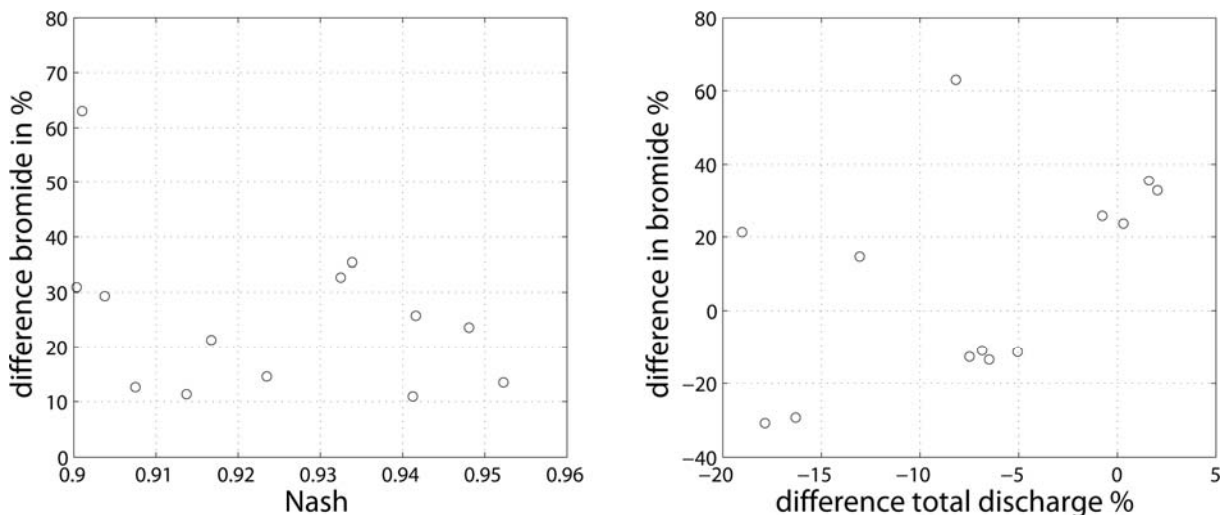
An alternative explanation for the differences between the modelled and observed IPU breakthrough is that the first flush of pesticides may be explained by facilitated transport, as suggested by Zehe and Flühler (2001a) in their experiment. The IPU concentrations of their experiment included both facilitated and dissolved transport. The facilitated transport behaviour has been as documented in several studies (de Jonge et al., 1998; de Jonge et al., 2004; Villholt et al., 2000). Facilitated transport may still active during the later stages of the experiment. This process cannot be captured with the proposed model. Overall, it can be stated that a simulation of pesticide transport, without having detailed local data on the adsorption characteristics in different subsurface compartments (e.g. Mallawatantri et al., 1996; Larsbo et al., 2009) and a much more complex description of the adsorption process, is largely an unsatisfying issue of trial-and-error, even when using data from the Footprint data base.

4.4.3 Equifinality of spatial hillslope structures

Several networks of worm burrows allow me to produce an integrated system response, i.e. dynamics of water flow and of accumulated bromide leaching, although the set of best model

structures can be boiled down to four (runs 1, 4, 9, and 10) by taking the water and the bromide mass balances into account. Also, McGuire et al. (2007) were able to reduce model uncertainty and increased parameter identifiability by the additional use of tracer data in the hillslope model used (Hill-vi, Weiler and McDonnell, 2004), compared to a single calibration on discharge data. Figure 4-8 shows the relative difference between simulated and observed cumulated bromide leaching plotted against the Nash-Sutcliffe efficiency (left panel) and against the water balance error (right panel). As there is no clear relationship between these quality criteria, all of them have to be evaluated to reject non behavioural model setups.

To further elaborate the similarities and differences of the four acceptable model setups (see Table 4-1) I state that all those assumed wet initial conditions for the entire model domain (chapter 3). This is consistent with available soil moisture data from 25 TDR (Zehe and Flüher, 2001a), which characterised top soil water content. This corroborates that detailed data on the initial soil moisture state reduces equifinality. All of the acceptable model setups are parameterised with the highest possible hydraulic conductivity for the tile drain (2.03×10^{-1} m/s) and an impermeable layer below the tile drain. The maximum water flow in macropores and the density of worm burrows per unit area show a clear interaction. Runs 1 and 4 are based on 30 worm burrows per m^2 and a lower maximum water flow of 7.9×10^{-6} m^3/s in macropores, while the runs 9 and 10 are parameterised with a reduced worm burrow density (10 per m^2) which is compensated by a higher maximum water flow of 1.33×10^{-5} m^3/s . The occurrence of saturated conditions below the tile drain showed no clear pattern between the different runs.



- Select those hillslope architectures as behavioural that reproduced tile drain discharge with a Nash-Sutcliffe efficiency larger than 0.9 and match the water balance within the error range (10%). Thus runs 7, 8, 11, and 13 would be rejected.
- Select from the behavioural hillslope architectures of the previous stage those that match dynamics of accumulated bromide leaching with a coefficient of determination larger than 0.9 and match the bromide mass balance within the error range (15%). Thus runs 2, 3, 5, 6, 8, 11, 12, and 13 would be rejected.

From this I conclude:

- The number of hillslope architectures that are behavioural with respect to reproducing tile drain discharge dynamics can be reduced by using orthogonal data sources such as tracer data (McGuire et al., 2007; Klaus et al., 2008) and analysing the mass balances.
- Generic knowledge about the origin of dominating structures is crucial to reproduce these structures in a simplified yet a sufficiently realistic manner and thus reduce equifinality in the spatial model setup to a minimum amount.

Nevertheless, in this case four behavioural hillslope architecture structures remain. This is consistent with findings of Comegna et al. (2001), who showed that a good accordance of observed and modelled hydrographs does not lead to an appropriate unique description of the solute transport mechanisms.

Probably we have to accept that a possible cause of equifinality is that part of the indeterminacy may be essentially system inherent, in the sense that several types of architectures of subsurface flow pathways may yield the same integral response in discharge and mass flows.

5 Linking the old water with the new water paradigm: macropore – soil matrix interaction during a series of irrigation experiments at a tile drained hillslope*

This chapter is the first part of this thesis dealing with experimental studies. The modelling parts showed that including structures in a hillslope model allows a successful modelling of water and solute transport. A main part of the experimental chapters is a series of three field scale (400 m²) irrigation experiments that were repeated at the same tile drained experimental site. This approach was chosen to allow for a step by step learning and improvement of the experiments. Such experimental studies are useful to increase the knowledge about the detailed processes related to preferential flow structures at the hillslope scale. This will contribute to a better understanding of the role of preferential flow structures in the transport of pesticides and nutrients or the water flow in the vadose zone. This understanding can also improve the modelling approaches in chapter 3 and chapter 4. Within this chapter the hydrological processes that generate the tile drain discharge at a cultivated field site during rainfall driven condition are investigated. A multi tracer approach is used together with soil moisture and discharge observations. The isotopic composition of soil water was measured before and after the experiment to investigate: a) the role of macropore-matrix interaction, b) the role of this process in the generation of tile drain discharge, and c) the role of soil water in the discharge, since “old water” often dominates event runoff at hillslopes. Then the results and process knowledge gained in this chapter are used to investigate pesticide transport in relation to the hydrological processes in chapter 6. This chapter starts with an introduction on the role of different end members in hillslope runoff and the detailed research questions. Then the field site and the methods are introduced (5.2). The results are presented in chapter 5.3, discussed in chapter 5.4. Finally conclusions are drawn in chapter 5.5.

*based on: Klaus, J., Zehe, E., Elsner, M., and Külls, C. Manuscript in preparation

5.1 Introduction

Hillslope and catchment scale runoff response often consists of a high fraction of pre-event water - also called “old water”. Kirchner et al. (2003) called this phenomenon the “rapid mobilization of old water paradox”. Several studies corroborate that pre-event water strongly contributes to runoff events at the catchment (Sklash and Farvolden, 1979; Buttle, 1994) and the hillslope scale (McDonnell, 1990; Burns et al., 2001). In contrast, Weiler et al. (1999) determined that pre-event fractions in surface and subsurface hillslope runoff were only 10% and 22.5%, respectively, at their study site. Different tracers have been proposed to separate the event hydrograph into different runoff components as for instance stable isotopes of the water molecule (e.g. Sklash and Farvolden, 1979; Lyon et al., 2008; Roa-Garcia and Weiler, 2010) as well as conservative solute tracers (Wels et al., 1991; Weiler et al., 1999; Hoeg et al., 2000).

On the other hand, many studies corroborate that preferential flow may have a strong influence of runoff processes at the hillslope (Smettem et al., 1991; Weiler and McDonnell, 2007) and the catchment scales (Blöschl and Zehe, 2005; Zehe et al., 2007) which is most important for contaminant transport (Flury et al., 1995; Šimůnek et al., 2003). Preferential flow is often explained by the fact that “new” event water and dissolved substances bypass the soil matrix and thus penetrate into large depths (Jarvis, 2007).

McDonnell (1990) explained the fraction of old water in hillslope runoff by fast vertical macropore transport of event water inducing old water to enter lateral preferential pathways. Based on the use of deuterium and chloride as natural tracers, Leaney et al. (1993) found that sampled throughflow water consisted mainly of rainfall water (>90%), that must have been transported via macropores bypassing the soil matrix. Vogel et al. (2008) found in a modelling study using a dual continuum approach and sampled oxygen-18 concentrations that 24% of 1192 mm annual precipitation exited the model domain as subsurface stormflow via preferential flow. Stumpp and Maloszweski (2010) used weekly oxygen-18 samples in a lysimeter study to model the fraction of preferential flow for different cropping periods. Using a lumped parameter approach and HYDRUS-1D, they found between 1.1% and 4.3% preferential flow for the lumped parameter approach and 1.1% and 20.5% for the HYDRUS-1D approach, respectively. Kumar et al. (1997) found between 10% and 20% preferential flow per year at a tile drained field site where the fractions were higher during intense precipitation events. In a similar study, Stone and Wilson (2006) used differences in surface water chloride concentrations and tile drain baseflow concentrations to separate tile drain discharge into a matrix and preferential flow component. Preferential flow was in total 11% and 51% for two events while it was 40% and 81% during peak flow. Those studies suggest that water flow through soils is not only driven by translatory flow, which assumes that water entering the soil as precipitation displaces the water present previously, pushing it deeper into the soil and eventually into the stream (Horton and Hawkins, 1965; Hewlett and Hibbert, 1967), but also by preferential flow. Stewart and McDonnell (1991) found, based on deuterium isotopes, that much of precipitation water bypassed the soil at hillslopes of the

Maimai catchment, while the bypass water consisted mainly of old water. Königer et al. (2010) used deuterated water to investigate flow processes in the unsaturated zone in a sprinkling experiment. They collected soil samples 12 and 35 days after irrigation and found a distinct change of deuterium background towards the concentration of applied water within one meter depth. Van der Hoven et al. (2002) investigated the effect of interaction between a fault and the surrounding micropores on the concentration of ^{18}O during precipitation and drying, and found a clear interaction between the preferential flow paths and the micropore space. Weiler and Naef (2003a) studied the role of preferential flow during the infiltration process and the interaction between those preferential flow paths and the soil matrix. By using a dye tracer and soil profiles they found that preferential flow was initiated at the soil surface or at partially saturated soil layers. Weiler and Flühler (2004) classified water flow through soils based on dye pattern, and could distinguish between different levels of macropore-matrix interaction. This interaction plays a crucial role in the water transported via macropores, as macropore flow depends on soil matrix infiltration capacity, interaction between macropores and matrix (Weiler, 2005) and connectivity of macropores (Tsuboyama et al., 1994).

Overall water flow through soils is driven and influenced by numerous processes such as flow in the soil matrix, preferential flow and macropore-matrix interaction. Additional studies have shown that the isotopic composition of event water is often dominated by “old water”. Different explanations are existing, like mobilisation of old water when surface infiltrated water percolate into the soil matrix at the end of the macropores (McDonnell, 1990), or pressure propagation in the system. Nevertheless, the existing concepts cannot fully explain the frequently observed high pre-event water fractions. The knowledge of these processes is of strong importance for performing better hydrological modelling, understanding long term transport behaviour of contaminants, and understanding the role of near surface structures in the mobilisation of soil water.

The overall goal of this study is thus to investigate the link between “new water” and the “old water” by developing a conceptual flow model that describes water paths and water sources at a tile drained field site. Such a conceptual model can improve the understanding of the transport of agrochemicals which is an important concern in agricultural landscapes. In particular I focus on the following questions:

- Which are the flow paths through the soil? Is it dominated by translatory or macropore flow, and how are these processes connected?
- Can I quantify the interaction between macropores and the soil matrix? How does this interaction help me to constrain a conceptual flow model of the study site?
- Various hillslope studies point out the relevance of pre-event water in discharge. Which part of the soil profiles is the primary source for this pre-event water?

My approach was to employ multiple tracers within a series field scale irrigation experiments to investigate flow processes through macropores, the interaction between macropores and the soil matrix, and the source of the discharging water at a tile drained field site (Weiler et al., 1999; Zehe and Flühler, 2001a; Lange et al., 2010). I regard the tile drained field site as a

large scale natural lysimeter, as proposed by Richard and Steenhuis (1988), and I used bromide, deuterium (^2H) and oxygen-18 (^{18}O) tracers together with hydrometric observations. Further, I investigated the change of soil water isotopic composition during the experiment and quantified this interaction based on a compartmental model approach.

5.2 Study site and Methods

5.2.1 Study site

The experiments were performed in the Weiherbach catchment that is described in detail in chapter 2.

Experimental site and determination of soil characteristics

The irrigation experiments were performed at a field site located parallel to the Weiherbach brook (49°08'08"N 8°44'42"O). This is a 20 × 20 m² plot, approximately 10 m from the stream banks. This field has been reused for agricultural purposes for the last eight years, before that it was fallow land. A single tile drain tube is located about 1-1.2 m below the surface, embedded in a gravel layer. The tile drain outlet, a plastic tube with a diameter of approx. 20 cm, enters the Weiherbach brook about 30 cm above the baseflow water level. The soil is a Colluvisol with a strong gleyic horizon starting at a depth between 40 and 70 cm below the surface, which fits well with observations of perennial flow from the tile drain.

Soil cores (100 cm³) were extracted at three different locations at five depths (between 7.5 cm and 60 cm, non-uniform between the different locations) to measure soil hydraulic conductivity (constant and falling head method) and porosity. The soil hydraulic conductivity showed stratification with decreasing hydraulic conductivity, decreasing porosity, and increasing bulk density with depth. The hydraulic conductivities were 5.3×10^{-8} m/s, 1.8×10^{-8} m/s, and 1×10^{-9} m/s at 50-60 cm depth, and between 1×10^{-4} m/s and 1×10^{-6} m/s in the upper 10 cm. The soil porosity decreased from approx. 0.5 to 0.4, and the bulk density increased from approx. 1.3 g/cm³ to 1.7 g/cm³. The measured values are consistent with published soil data of Delbrück (1997) and Schäfer (1999). Soil tillage of the experimental field has been annual conventional ploughing to a depth of about 25-30 cm. The experiments were performed before the annual soil tillage took place. Macropores generated by earthworms are the main factor of vertical preferential pathways in the Weiherbach catchment (Zehe and Flühler, 2001a; 2001b) and were counted at a horizontal soil profile in 10 cm depth after the experiments.

5.2.2 Experimental design of the study

Most experimental studies that perform irrigation experiments are singular events. The idea of this study was to perform a series of repeated irrigation experiments (three in total) with slightly changing experimental conditions. The series was performed to learn step by step and adjust the experimental design or underpin the gained knowledge within the next experiment. While this chapter focus on the relation between old and new water and the processes

generating the tile drain discharge, an additional focus was the related pesticide transport that is examined in the subsequent chapter (see chapter 6). The third experiment was mainly designed to investigate whether or how many pesticides can be remobilised from the soil and transported to the tile drain, and what are the dominating hydrological processes in this case.

5.2.3 Experimental setup

In the following I will explain the setup of the different experiments. Measurements of soil moisture and irrigation rate were improved after the first experiment. The tile drain was sealed by a plastic board with a triangular notch (opening angle was 25°). Water level in the tube was measured during the experiment by means of a pressure probe (PD-2, SOMMER) with a temporal resolution of 1 minute. After the experiment, the sampling rate was reduced to 10 minute intervals. Water levels were transformed into discharge using a rating curve that was determined by frequent discharge measurements with a bucket during the experiments; I estimate the accuracy at 0.02 l/s, which is determined by the accuracy of the pressure probe and the rating curve.

The irrigation was performed by a system of eight garden sprinklers (e.g. Wienhöfer et al., 2009) that were adjustable in range and received the same pressure to have the same sprinkling rate, this setup was the same during all experiments. Meteorological conditions for the weeks before the experiments were logged at a nearby met station. Before the 1st and the 2nd experiment the pesticides Flufenacet and Isoproturon were applied. This will be the focus of the subsequent chapter.

First experiment

The first experiment was performed on 16th September 2008. The irrigation rate was measured with 10 precipitation samplers with a support of 200 cm² and an opening 30 cm above ground. Irrigation was carried out in three blocks of 60 min, 80 min, and 60 min duration, with 30 min breaks between the blocks. In this experiment, a tracer solution (1500 l) containing 1600 g bromide and 2000 g brilliant blue was applied during the first irrigation block on the field site (minute 15 to minute 35). The irrigation water had a constant isotopic signature (¹⁸O=-8.1 ‰, ²H=-56.1‰).

The day before the experiment six plastic access tubes with a diameter of 27 mm were installed vertically into the soil. They ranged from the surface to 1 m depth, without disturbing the surrounding soil matrix. These access tubes were used to measure soil moisture with a “Profile Probe – PR2” (Delta-T Devices, Burwell, UK) at six different depths (10, 20, 30, 40, 60, and 100 cm) and at six locations. These measurements were not performed continuously but only in-between the irrigation blocks.

Shortly before, during and after the experiment, water samples were taken for several tasks. Before the experiment, background concentrations of bromide, brilliant blue, oxygen-18 and deuterium were measured in both the tile drain and the irrigation water. Irrigation water was pumped out of the nearby Weiherbach brook. During the experiment, the irrigation water was

sampled three times to check whether the isotope composition remained constant. Additionally, the solute breakthrough curves were sampled by taking manual water samples at the tile drain outlet. In the beginning samples were taken with a high temporal resolution of 5 minutes as Zehe and Flüßler (2001a) reported a very fast first solute breakthrough during their experiment that was carried out at a nearby field site. Later, the sampling rate was reduced. In total 51 water samples were collected during the experimental day; the last sample was taken two hours after the end of the experiment. Additionally, the falling limb of the hydrograph was sampled every eight hours for five days by an automatic sampler (ISCO). Six and seven days after the irrigation two additional samples were taken by hand.

Second experiment

This experiment was performed on the 15th September 2009. Compared to the first experiment I improved measurements of the irrigation rate and the soil moisture measurement. Irrigation rate was measured with 20 evenly distributed precipitation samplers with a support of 37.4 cm² and approx. 5 cm above ground. Irrigation occurred in three blocks, 35 min, 90 min, and 90 min, with breaks of 22 min and 30 min. Bromide (2400 g) was applied dissolved in 1500 l water with the first irrigation block (minute 13 to 35). The irrigation water had a constant isotopic signature during the experiment ($^{18}\text{O}=-8.35\text{‰}$, $^2\text{H}=-56.0\text{‰}$).

To measure soil moisture continuously six Theta Probes (Delta-T Devices, Burwell, UK) were installed in a vertical soil profile at the streamside boundary of the experimental plot at depths of 10 cm, 30 cm, and 50 cm, two probes at each depth. The moisture content was logged every five minutes with the DL6 (Delta-T Devices, Burwell, UK). Additional soil moisture was measured at 20 evenly distributed locations at the field site before the experiment, between the irrigation blocks and after the experiment with a Theta Probe. Also soil samples were taken with a hand auger. This was done to determine the soil water isotopic composition at three locations down to a depth of approx. 60 cm before and after the experiment. The three sampling locations for soil water isotopic composition followed a transect, from the lower boundary (near stream) to the upper boundary. Sampling holes were closed afterwards, and the samples after the experiment were taken approx. 50 cm away from the pre-experiment samples.

The background level of tracers was sampled in the tile drain outlet before the start of the experiment and collected a total of 25 water samples during the experiment at intervals of 15 minutes, the last two samples with intervals of 30 min, and three samples on the day after the experiment.

Third experiment

The third experiment was performed on the 5th October 2009. The irrigation rate was measured the same way as in the second experiment. Irrigation was performed in two 90 min blocks with a 30 min break between them. No artificial tracers were applied and the irrigation water had a constant isotopic composition ($^{18}\text{O}=-8.31\text{‰}$, $^2\text{H}=-56.1\text{‰}$). Unfortunately wild

boars destroyed the soil moisture equipment before this experiment, so it was only possible to measure surface moisture, before the experiment, between the irrigation blocks and after the experiment. Again, tile drain background was sampled, and then 21 samples were taken during the experiment in a 15 minute interval.

5.2.4 Analytics

Water samples

Bromide and isotopes were measured directly in filtered (450 nm) water samples. Bromide concentrations were determined by anion chromatography (ICS-1000 Dionex). Brilliant blue was analysed with a UV-Visible spectrophotometer (UV-1601 Shimadzu) using a wave length of 630 nm. The detection limit in both cases is 0.1 mg/l.

For hydrogen isotope analysis ($^2\text{H}/^1\text{H}$), water samples were reduced to molecular hydrogen in a uranium reactor, and the gas was subsequently introduced into the inlet of an isotope ratio mass spectrometer (Delta-S, Finnigan MAT, Germany) where it was measured against a hydrogen monitoring gas. For oxygen isotope analysis ($^{18}\text{O}/^{16}\text{O}$) water samples were degassed and equilibrated with CO_2 of known isotopic composition. The CO_2 was subsequently introduced into the dual inlet of an isotope ratio mass spectrometer (Delta-S, Finnigan MAT, Germany) and measured again relative to a CO_2 monitoring gas. In both cases, calibration was accomplished with three in-house standards that were calibrated against the international reference materials VSMOW, SLAP and GISP (IAEA, Vienna). Isotope values $\delta^2\text{H}$ and $\delta^{18}\text{O}$ were expressed in parts per thousand (‰) as:

$$\delta = \frac{R_{\text{Sample}} - R_{\text{St}}}{R_{\text{St}}} \quad \text{Equation 5-1}$$

where R_{Sample} is the respective $^2\text{H}/^1\text{H}$, or $^{18}\text{O}/^{16}\text{O}$ ratio, and R_{St} the Vienna-Standard Mean Ocean Water (absolute VSMOW ratio is $^2\text{H}/^1\text{H}=155.76\pm 0.05\times 10^{-6}$ and $^{18}\text{O}/^{16}\text{O}=2005.2\pm 0.45\times 10^{-6}$).

The $\delta^2\text{H}$ measurements of water samples have a precision of $\pm 1\text{‰}$, those of $\delta^{18}\text{O}$ have a precision of $\pm 0.1\text{‰}$.

Analysis of soil water isotopic composition

The isotopic composition of soil water was determined using cavity ring-down laser spectrometry of water vapour equilibrated with the liquid soil water phase. Soil samples have been sealed in two nested gas-tight bags and equilibrated in a dry nitrogen atmosphere for 24 hours under controlled temperature ($\pm 0.1\text{ °C}$) conditions until water-vapour phase equilibrium had been established. Based on Majoube (1971) the isotopic composition of soil water was derived from the isotopic composition of water vapour based on temperature dependent thermodynamic equilibrium fractionation. Allison et al. (1987) have demonstrated

that water-vapour saturation and isotope equilibrium in the unsaturated zone prevail even in dry desert soil. Hendry et al. (2008) have used the same equilibration principle for wet clay soil and could establish water isotope profiles in deep clay. Based on parallel equilibration experiments of soil samples wetted with known liquid water isotope standards the rapid establishment of water-vapour equilibration and also of the isotope equilibration within much less than 24 hours could be confirmed (Külls, 2011, personal communication). A mass balance of soil water compared to the total amount of vapour at saturation indicates that Rayleigh effects are far below analytical precision of 0.15-0.25 ‰ for $\delta^{18}\text{O}$ and of 1.0-1.5 ‰ for $\delta^2\text{H}$ V-SMOW and do not affect the results significantly. The measurement was done using Picarro cavity ring-down laser spectrometry (Iannone et al., 2010) for water isotopes based on principles of tunable diode laser spectrometry (Gianfrani et al., 2003; Kerstel and Gianfrani, 2008; Gupta et al., 2009). Precision of measurements compared to double inlet mass spectrometer analyses is lower for $\delta^{18}\text{O}$ (0.25 ‰) and comparable for $\delta^2\text{H}$ (1.0 ‰).

5.2.5 Determination of event water proportion in tile drain hydrograph

To determine the fraction of irrigation water contributing to tile drain discharge during the experiment I performed a hydrograph separation based on a mass balance approach (Sklash and Farvolden, 1979). To determine the fraction of the three components in this system, i.e. tile drain baseflow, stored soil water and irrigation water, two tracers would be needed. Although Lyon et al. (2009) showed a general difference in ^{18}O and ^2H , I could not perform a hydrograph separation between event water (irrigation) and pre-event water (baseflow and soil water) as the isotopic composition of soil water was not uniform (see chapter 5.3.5). Therefore I used bromide and assumed that all irrigation water will mix with the applied tracer solution. The pre-event water, i.e. soil and baseflow water, have a zero background for bromide. I calculated the event water concentrations for the hydrograph separations as a time variant value $C_e(t)$ as follows:

$$C_e(t) = \frac{M_{in}(t) - M_{out}(t)}{P(t)} \quad \text{Equation 5-2}$$

where t is the experimental time in min, $M_{in}(t)$ is the bromide mass (g) that was applied on the field plot until time t , $M_{out}(t)$ is the bromide mass (g) that has left the system via the tile drain until time t , and $P(t)$ is the total irrigation amount applied on the plot until time t (litres). The hydrograph separation was then performed following Sklash and Farvolden (1979):

$$Q(t) = Q_e(t) + Q_p(t) \quad \text{Equation 5-3}$$

where $Q(t)$ is the tile drain discharge at time t , $Q_e(t)$ is the amount of irrigation water in the discharge at time t , and $Q_p(t)$ is the amount of pre-event water in the tile drain discharge at time t .

$$C(t)Q(t) = C_e(t)Q_e(t) + C_p Q_p(t) \quad \text{Equation 5-4}$$

where $C(t)$ is the total bromide concentration (g/l) in the tile drain at time t , and C_p is the bromide concentration of the pre-event water, in this case a zero concentration.

Based on the Equation 5-2, Equation 5-3, and Equation 5-4 a hydrograph separation between event and pre-event water can be performed, when the concentration of each component is known. I did this with high temporal resolution, leading to a time series over duration of the hydrograph. Additionally, the total proportion of irrigation water during the hydrograph could be calculated, and this was done until minute 500 of the experiments. The hydrograph separation was done based on the measured tile drain response and the sampling during the event, and additionally I performed a hydrograph separation assuming no baseflow in the tile drain. As I did not apply bromide during the third experiment, and the bromide within the soil was not evenly distributed I did not perform a hydrograph separation for this experiment.

5.2.6 Determination of macropore-matrix interaction with isotopic data

To investigate the macropore-matrix interaction I used the measured soil water isotopic composition of the second experiment. I used compartmental mixing cell modelling, based on the theory of Woolhiser et al. (1982), Campana and Simpson (1984), and Adar et al. (1988), to determine this interaction. For recent applications and methods see Klaus et al. (2008). I set up different conceptual interaction models based on the measured soil water isotopic composition and calculated the macropore-matrix interaction by mixing of event and pre-event water within the soil compartments for the three sampled locations. The analysis is based on the following assumptions:

1. The measured pre-experiment soil water isotopic composition represents the average composition of the sampled soil matrix compartment.
2. The samples taken after the experiment denotes only the soil matrix isotopic composition as the macropores started to empty as the irrigation stopped. At the time of sampling (90-120 min after the experiment), the macropores were empty.

Two perceptual models of macropore-matrix interaction (Figure 5-1) were tested based on the isotopic data. The first model describes simple mixing of the pre-event matrix water with the irrigation water during the experiment, and the second model includes additional inflow from the soil compartment above. Calculations of the proportion between event and pre-event water were performed with ^{18}O and ^2H together. The first model is thus analogous to a two component hydrograph separation, with the difference that it is an over-determined system of linear equations. The second model is analogous to a three component hydrograph separation. Based on the following three equations:

$$x_1 + x_2 + x_3 = 1 \quad \text{Equation 5-5}$$

$$x_1 C_{DE} + x_2 C_{DU} + x_3 C_{DP} = C_{DF} \quad \text{Equation 5-6}$$

$$x_1 C_{OE} + x_2 C_{OU} + x_3 C_{OP} = C_{OF} \quad \text{Equation 5-7}$$

that denote for the water mass balance (Equation 5-5), the mass balance of deuterium (Equation 5-6), and the mass balance of oxygen-18 (Equation 5-7), the following matrix can be derived:

$$\begin{pmatrix} 1 & 1 & 1 \\ C_{DE}/C_{DF} & C_{DU}/C_{DF} & C_{DP}/C_{DF} \\ C_{OE}/C_{OF} & C_{OU}/C_{OF} & C_{OP}/C_{OF} \end{pmatrix} \begin{pmatrix} x_1 \\ x_2 \\ x_3 \end{pmatrix} = \begin{pmatrix} 1 \\ 1 \\ 1 \end{pmatrix} \quad \text{Equation 5-8}$$

where x_1 is the fraction of irrigation water, x_2 the fraction of water from the above soil compartment, and x_3 the fraction of water that was stored within a soil compartment before the experiment. C denotes the known isotopic composition while the subscripts D and O denote deuterium and oxygen-18, respectively. The subscripts E , U , P , and F denote event, upstream cell, pre-event, and final, i.e. the after event composition.

Since x_1 , x_2 , and x_3 are constrained between 0 and 1 in Equation 5-8, I had to use linear programming to solve the mixing problem. The error was minimized by a least squares procedure. The matrix (Equation 5-8) is solved for three inflow components.

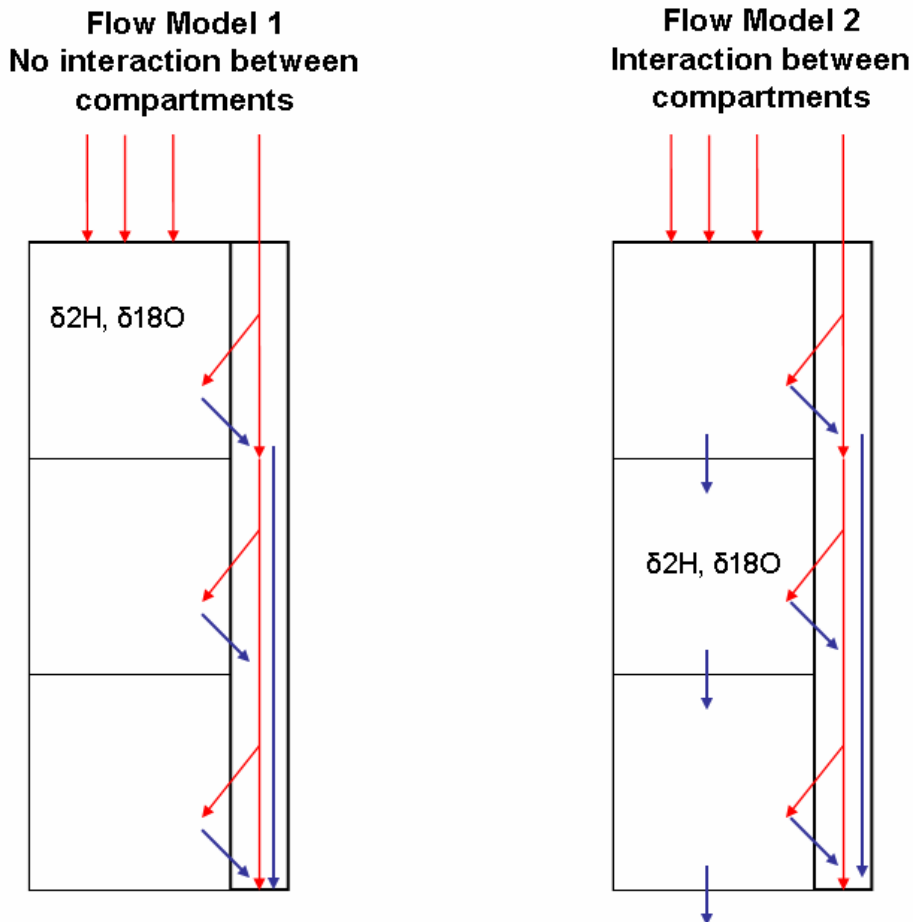


Figure 5-1: Perceptual flow models for interaction of macropores and soil matrix compartments. Red arrows denote for the irrigation water, blue arrows denote for soil water.

5.3 Results

5.3.1 Pre-experiment conditions

As there were no continuous on-site measurements of soil moisture I report the precipitation amount for 45 days and 10 days before the experiment (Table 5-1). The 45 day period for the third experiment is given without the irrigation sum of the second experiment. Also the Haude potential evaporation for the pre-experimental period is reported in Table 5-1. Air temperature and precipitation (tipping bucket) were measured at a nearby met-station (700 m distance). As the first two experiments both took place in mid-September the initial conditions are comparable. The first experiment took place after a much wetter summer with more than three times the precipitation of the second experiment. Additionally, the potential evaporation sum, on a 45 day basis, was lower for the first experiment. Thus, the first experiment was performed in wetter conditions than the second experiment.

Table 5-1: Pre-experiment conditions, 45-day and 10-day sum of pre-event precipitation (mm), and 45-day and 10-day potential evaporation.

	45-day precipitation mm	10-day precipitation mm	45-day potential evaporation mm	10-day potential evaporation mm
Experiment 1	137.0	10.9	102.8	15.3
Experiment 2	43.3	9.2	146.2	24.1
Experiment 3	30.1	0.0	109.2	19.5

The macropores per square meter were counted after experiments 1 and 2 to a 10 cm depth. Table 5-2 summarises the number of burrows per square meter. They are classified based on their diameter, burrows or channels with a diameter below 2 mm were not included.

Table 5-2: Number of macropores with specific diameter (d) per square meter, measured at two plots for each of the two first experiments.

Diameter	2-3 mm	3-5 mm	>5 mm	total
Plot 1, Experiment 1	68	20	0	88
Plot 2, Experiment 1	40	8	1	49
Plot 1, Experiment 2	65	21	2	88
Plot 2, Experiment 2	90	19	1	110

5.3.2 Spatial variability of irrigation rate

Based on the ten (1st experiment) and 20 (2nd and 3rd experiment) irrigation samplers, I evaluated the spatial correlation structure of the irrigation rates by calculating experimental variogram (Kitanidis, 1997) and fitting theoretical variogram functions. This geostatistical analysis revealed no correlation structure. Thus I used the mean value of all samplers as average irrigation rate, summarised in Table 5-3.

5.3.3 Hydrographs, tracer breakthrough curves, and soil moisture

The following results present the data of each experiment in a separate section, structured by hydrograph, tracer breakthrough, and the soil moisture data. The description of the results closes with a short summary of the main findings of each experiment.

Table 5-3: Summary of irrigation for each experiment, duration (D), amount (A) and intensity (Int) for every irrigation block. Standard deviation is given for the precipitation sums in brackets.

	Block 1			Block 2			Block 3			Total
	D (min)	A (mm)	Int (mm/h)	D (min)	A (mm)	Int (mm/h)	D (min)	A (mm)	Int (mm/h)	sum (mm)
Experiment 1	80	12.3 (8.7)	9.3	60	11.9 (9.7)	11.9	80	9.7 (5.4)	7.28	33.9 (22.2)
Experiment 2	35	5.3 (2.3)	9.1	90	17.6 (8.9)	11.7	90	18.2 (8.9)	12.1	41.1 (18.6)
Experiment 3	90	18.1 (9.9)	12.1	90	21.8 (11.6)	14.5	-	-	-	39.9 (18.9)

Experiment 1

Hydrograph behaviour

Flow in the tile drain averaged 0.11 l/s for the 30 min period before the experiment. The first irrigation block, with 12.3 mm in 80 min including the tracer solution, caused no measurable increase in discharge. During the following 30 min irrigation break, a small increase in tile drain discharge can be observed, but not clearly above uncertainty. During the second irrigation block (11.9 mm in 60 min), the tile drain discharge increased abruptly 140 min after the start of the experiment and the discharge peaked at 0.204 l/s 14 min after the end of the second irrigation block. After a short recession the discharge started to increase during the third irrigation block (9.7 mm in 80 min). The hydrograph peaked 8 min after end of irrigation at 0.373 l/s. The total irrigation amount was 33.9 mm. Table 5-3 summarises the irrigation blocks while Figure 5-2 (left column) presents the hydrograph and tracer data of the first experiment.

Tracer breakthrough curves

Isotopic background concentrations in the tile drain were -8.10‰ for $\delta^{18}\text{O}$ and -56.4‰ for $\delta^2\text{H}$. The field site was irrigated with water of only slightly different isotopic composition ($\delta^{18}\text{O}=-8.35‰$ and $\delta^2\text{H}=-58.5‰$). Figure 5-2, left column, centre row, shows the temporal variation of ^{18}O and ^2H in experiment 1.

During the first irrigation block and the break between block 1 and 2 (the first 110 min), the concentration of oxygen-18 fluctuated around the background value, with an average of -8.07‰. The moment the discharge increased the concentration of ^{18}O increased as well, and the dynamic was closely linked to discharge dynamics. The first peak in $\delta^{18}\text{O}$ (-7.31‰) occurred 19 minutes before the first discharge peak, while the second ($\delta^{18}\text{O}=-7.03‰$)

occurred 7 minutes after the second discharge peak; please keep in mind the sampling interval of 15 minutes.

Deuterium concentrations behaved similarly, although the concentration for the first 110 min were higher than the background (average: $\delta^2\text{H}=-54.7\text{‰}$). The first peak also occurred 19 min before the hydrograph peak ($\delta^2\text{H}=-46.5\text{‰}$) and the second peak ($\delta^2\text{H}=-45.4\text{‰}$) 8 min before the hydrograph peak.

Note that the isotope values in the irrigation water were lower ($\delta^{18}\text{O}=-8.35\text{‰}$, $\delta^2\text{H}=-58.5\text{‰}$) than the background values in the tile drain ($\delta^{18}\text{O}=-8.10\text{‰}$, $\delta^2\text{H}=-56.4\text{‰}$). Nevertheless, $\delta^{18}\text{O}$ and $\delta^2\text{H}$ values increased with increasing tile drain discharge. One day after the irrigation, $\delta^{18}\text{O}$ -concentrations were (within the measurement error) back at the background level, while the $\delta^2\text{H}$ was slightly greater than the background.

Bromide, which labelled the irrigation water, exceeded the background concentration within 65 minutes after irrigation began (50 min after tracer application). Bromide concentrations are strongly correlated with the hydrograph with a coefficient of determination of $R^2=0.87$ at the rising limb. Bromide showed a short plateau concentration around 0.7 mg/l during the first irrigation break and then followed the dynamic of the hydrograph, with two peaks at concentrations of 9.18 mg/l and 15.41 mg/l (280 min). The additional applied brilliant blue showed a similar behaviour with lower concentrations, due to sorption.

Soil moisture observations

The installation of the access tube, just the day before the experiment, limits the quality of the soil moisture data, since the contact between the plastic tube and the soil was limited. The absolute measured moisture values are too high, considering that maximum measured porosity was at 54% and that only in the loose topsoil. Before the experiment, soil moisture was stratified, with drier conditions in the upper 30 cm, and higher moisture at 60 cm and 100 cm depth. Soil moisture at 10 cm depth reached its maximum at four of six measuring location after the first irrigation block, and remained constant throughout the day. At the two other soil moisture stations maximum was reached after the second and third block, respectively. The soil moisture at 20 cm depth increased slightly until experimental minute 200, and then stayed constant or decreased.

Main findings in the first experiment

Based on the combination of the different tracer approaches I summarise the experimental results. An increase in tile drain discharge did not begin directly after the start of the irrigation, but during the second irrigation block, and was then strongly linked to the irrigation pattern. At times when no significant change in isotopic composition of tile drain discharge was measurable, I did neither observe bromide nor brilliant blue in the tile drain discharge. At the moment when discharge clearly increased, bromide, brilliant blue, $\delta^{18}\text{O}$, and $\delta^2\text{H}$ concentrations increased. The change in isotopic composition points to an activation of an additional water source, probably soil water.

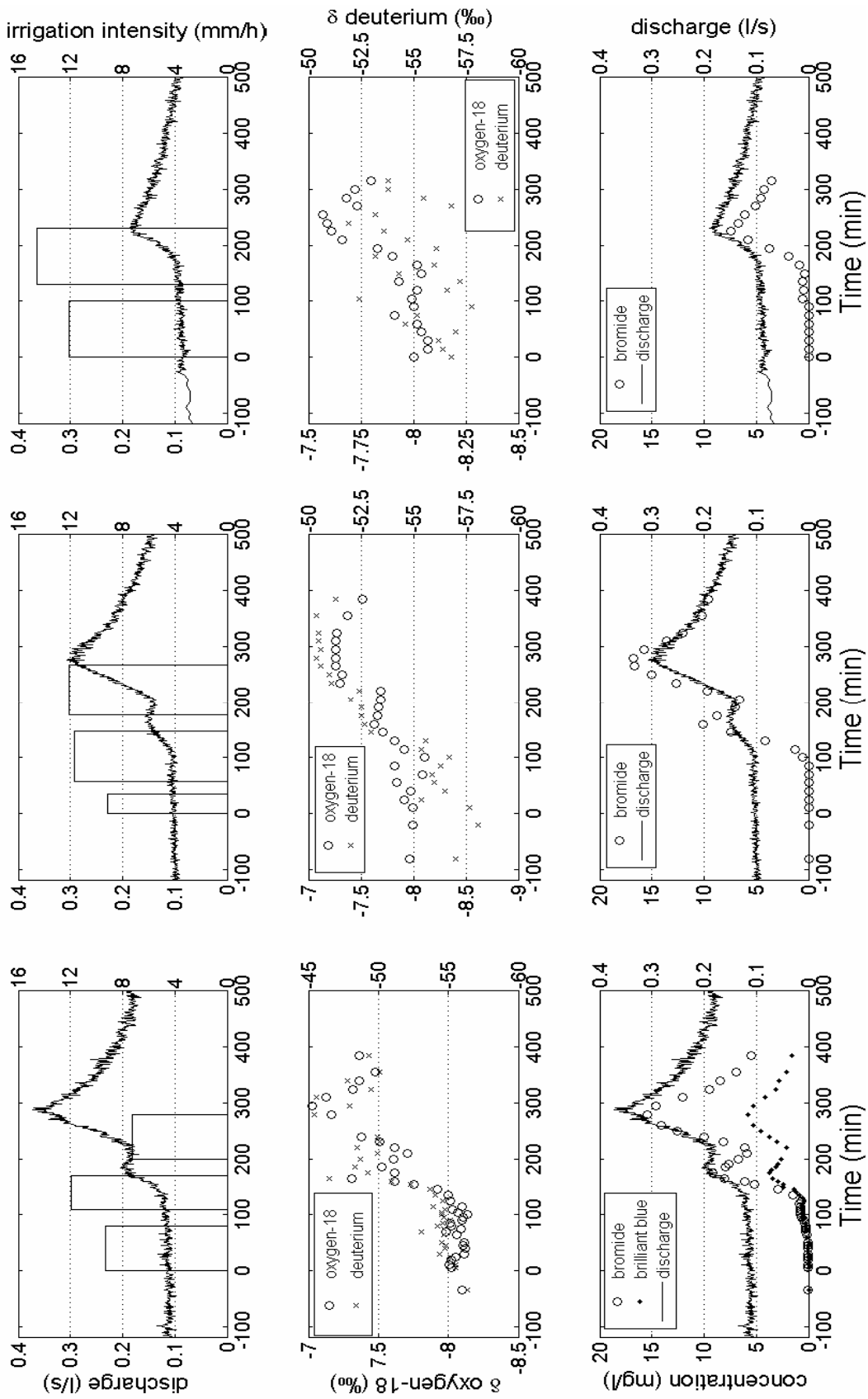


Figure 5-2: Summary of the experiments, left column is experiment 1 (highest pre-experiment precipitation), centre column experiment 2 (moderate pre-experiment precipitation), right column experiment 3 (lowest pre-experiment precipitation). Hydrographs, irrigation intensity, isotopic composition of tile drain water, bromide and brilliant blue concentrations are plotted.

Experiment 2

Hydrograph behaviour

The tile drain showed an average discharge of 0.101 l/s for the 30 min before the experiment. During the first irrigation block (5.3 mm in 35 min) the tile drain discharge showed no measurable response. A significant increase in discharge began after 105 minutes after onset of the experiment, leading to a double peaked hydrograph. The first peak (0.157 l/s) occurred 164 minutes after the experiment started and the second peak (0.306 l/s) at minute 276, 8 minutes after the end of irrigation. Figure 5-2 (centre column) shows the hydrograph and the irrigation blocks, while precipitation amount is given in Table 5-3. The total irrigation sum was 41.1 mm.

Tracer breakthrough curves

Background $\delta^{18}\text{O}$ and $\delta^2\text{H}$ values in the tile drain of were -7.98‰ and -57.5‰, respectively. The irrigation water had an isotopic composition of $\delta^{18}\text{O}=-8.3‰$ and $\delta^2\text{H}=-56‰$. Figure 5-2 (centre column, centre plot) presents the temporal variation of ^{18}O and ^2H in experiment 2.

The average $\delta^{18}\text{O}$ value during the first irrigation block was -8‰. Near the time of the first hydrograph peak water $\delta^{18}\text{O}$ was -7.63‰ and during the second peak the value was -7.26‰. The fluctuations in ^{18}O were more erratic during the second experiment than during the first experiment and in general were more erratic than those of deuterium. Deuterium (Figure 5-2, centre column, centre plot) showed nearly continuous increases and peaked 4 minutes after discharge at $\delta^2\text{H}=-50.4‰$. The $\delta^{18}\text{O}$ -values the day after the experiment were at background levels, as were those of deuterium.

Similar to the first experiment the isotopic signature of the tile drain discharge increased during the experiment relative to the irrigation and background water, indicating a significant contribution from an additional water source.

After 100 minutes, bromide concentrations exceeded the background value, which occurred slightly before the increase in discharge. Bromide concentrations are strongly correlated with the hydrograph with a coefficient of determination of 0.9 at the rising limb. Bromide concentration peaked at 10.1 mg/l (minute 160) and at 16.8 mg/l (minute 276), near the times of peak discharge. The concentration was decreasing slightly after the end of the irrigation. The day after the experiment (not shown in Figure 5-2), concentrations were still above background.

Soil moisture observation

Surface soil moisture, measured during the irrigation breaks at the precipitation samplers, shows mainly uniform behaviour. At the beginning measured surface soil moisture was between 18.5% and 35%, with an average of 28% and a standard deviation of 4%. Then soil moisture increased towards saturation reaching average values of 36.7% (standard deviation:

4.5%), 39.7% (4%), and 43.5% (5.1%) after the end of each irrigation block. Surface water ponding occurred at the end of the first irrigation block, and became widespread during the second irrigation block. Soil moisture as a function of depth was measured at the stream side boundary of the experimental plot. Those parts of the plot received less irrigation than average, and only minor ponding occurred at this location. Figure 5-3 summarises the moisture dynamics during the experiment. The most rapid and strongest changes in soil moisture were measured at 10 cm depth, soil moisture at greater depths showed only small changes, remaining unsaturated throughout the experiment.

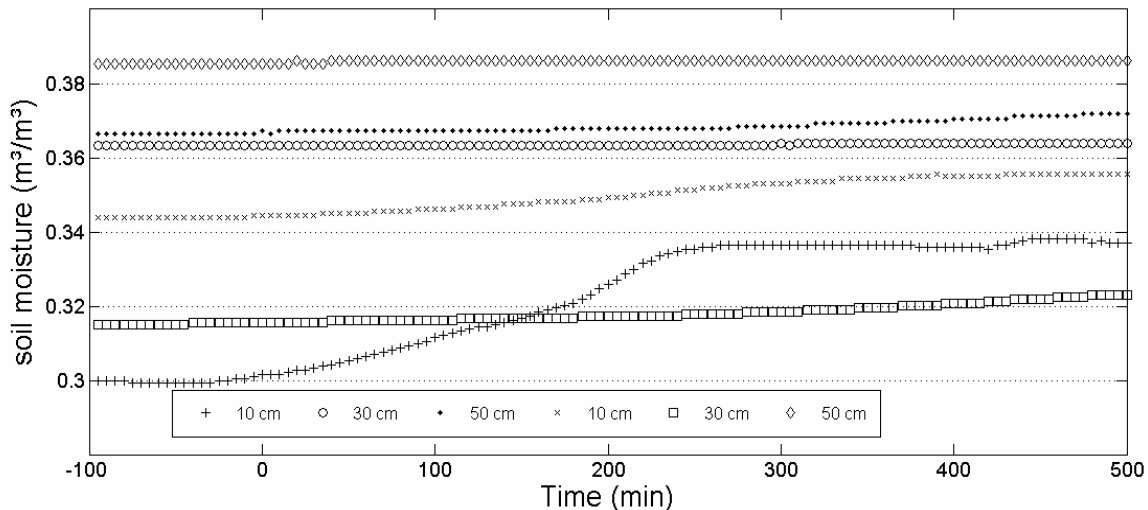


Figure 5-3: moisture dynamic during the second experiment, two theta probes for soil depths of 10 cm, 30 cm, and 50 cm, with a lateral distance of approximately 25 cm.

Main findings in the second experiment

Again tile drain discharge started to increase during the second irrigation block. It seems that a certain amount of cumulated irrigation is needed to activate subsurface water flows. After activation, the irrigation pattern and the hydrograph are again tightly linked. Isotope values increased until peak discharge was reached, becoming more distinct compared to tile drain background and irrigation water, thus an additional source of water contributed to tile drain discharge. Bromide concentrations slightly exceeded background values before discharge increased.

Experiment 3

Hydrograph behaviour

Pre-experiment water level and discharge were lowest for the third experiment (0.088 l/s) compared to the others (Figure 5-2, right column). Although discharge appeared to increase slightly during the first irrigation block (18.1 mm in 90 min); this change was within the range of accuracy. Approximately 180 min after the start of the irrigation, during the second irrigation block (21.8 mm in 90 min), discharge increased clearly and peaked 230 min after the start of the experiment (0.190 l/s). After the peak, discharge decreased and reached the pre-event level about 300 min later. The total irrigation amount (Table 5-3) was 39.9 mm.

Tracer breakthrough curve

During the first 180 min of the experiment, the measured ^{18}O was not significantly different than the background value of -8‰ . The ^{18}O -value in irrigation water (-8.31‰) was slightly less than the background value. With the increase in tile drain discharge $\delta^{18}\text{O}$ -values increased markedly. The peak concentration of $\delta^{18}\text{O}=-7.57\text{‰}$ was reached 255 min after the irrigation started.

There were no clear trends in the $\delta^2\text{H}$ values. The samples varied around a value of -55‰ with a maximum of -51.9‰ and a minimum of -57.8‰ and no clear temporal pattern. The trends in $\delta^{18}\text{O}$ values indicate an additional source of water that contributed to the tile drain discharge during the experiment, but this cannot be confirmed by the patterns in $\delta^2\text{H}$ values.

Background bromide concentrations in tile drain baseflow were below the detection limit, indicating no or very limited connectivity of the soils to the tile drain. Considerable amounts of bromide must have been stored in the soil from the previous experiment. During the irrigation no bromide was added to the system. Bromide was first detected (0.57 mg/l) 105 min after the irrigation began. Coincident with the increase of $\delta^{18}\text{O}$ -values, bromide concentrations also increased significantly and peaked 225 minutes after the experimental start at a value of 7.48 mg/l . The contribution of bromide indicates a contribution from soil water.

Soil moisture observation

Surface moisture, measured before the experiment and after the irrigation blocks, showed strong increases. Some measured locations showed no significant difference after the first and second irrigation block, indicating that saturation was reached after one irrigation block. Average surface soil moisture was 26.8% before the experiment, with a standard deviation of 5.3% , reached 42.8% after the first irrigation block ($\text{SD}=2.7\%$) and 44.9% after the second block ($\text{SD}=3.3\%$).

Main findings of the third experiment

In summary, bromide that was previously stored in the soil matrix, was remobilised during the experiment, and was exported by the tile drain. The time at which soil water began to contribute is clearer for bromide than for the isotopes. Nevertheless, the soils within the system showed no contribution to tile drain discharge at the beginning of the experiment, but the irrigation led to significant contributions of soil water.

5.3.4 Hydrograph separation to distinguish between irrigation water and pre-event water

In this section, the proportion of irrigation water in the tile drain hydrograph is evaluated. Figure 5-4 presents the results for the first two experiments. During the first experiment, the maximum proportion of irrigation/event water was 13.2% after 280 min, corresponding with the highest bromide concentrations. The proportion of event water follows the double peak shape of the hydrograph and the bromide concentrations. In total 4.95% of the tile drain discharge in the first 500 minutes of the experiment was irrigation water. Evaluating the

hydrograph only for the water that was mobilised within the experiment, the maximum proportion was 19.49% and the proportion of event water during both hydrograph peaks was similar.

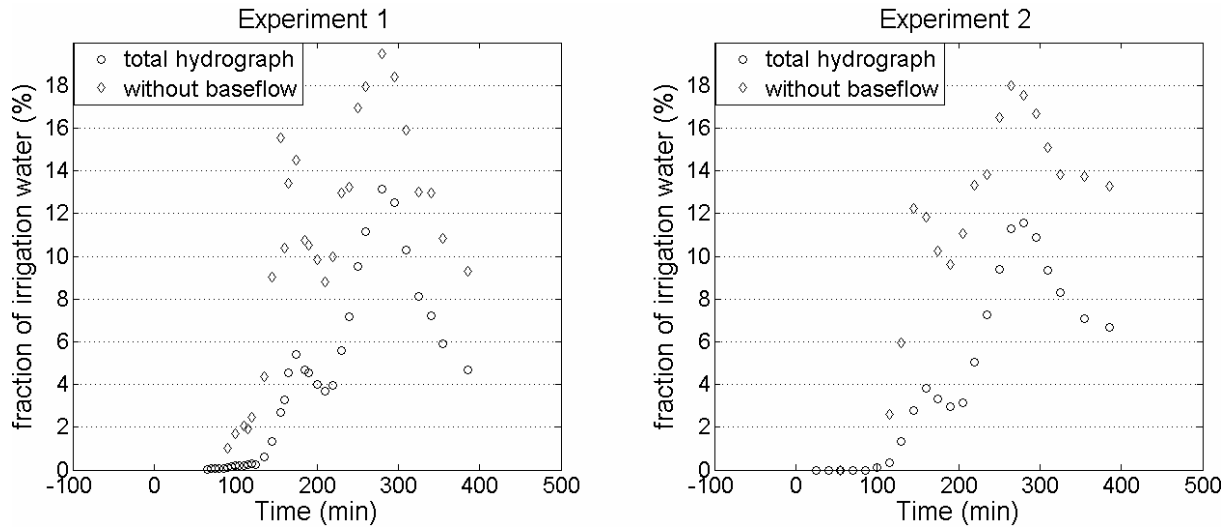


Figure 5-4: Hydrograph separation of the first (left) and second (right) experiment. Shown is the proportion of irrigation water at the tile drain discharge in the total measured discharge, and with baseflow subtracted.

The temporal pattern of event water fractions during the second experiment was similar to the corresponding one of the first experiment. The maximum proportions were slightly smaller with 11.57% (with baseflow) and 17.97% (without baseflow) compared to the first experiment, while the total proportion of event water was 6.15%, slightly higher. This latter observation resulted from the different shape of the declining hydrograph. In summary, the event water proportion showed high temporal variability during both experiments, and even when assuming no baseflow, the total event-water proportion never exceeded 20%. The pre-event water, as indicated by the isotope data, was mobilised soil water. At times when discharge was not significantly different from baseflow, I did not calculate the percentage of event water because since I would have to divide by very small numbers.

5.3.5 Isotopic composition of soil water

The isotopic composition of soil moisture was measured in a transect (before experiment 2), from the lower boundary (near stream) to the upper boundary. Sampling holes were closed afterwards, and the samples after the experiment were taken approx. 50 cm away from the pre-experiment samples.

Figure 5-5 presents the measured soil water isotopic composition for the sampling locations; the left column presents the oxygen-18 values and the right column the deuterium values. To repeat: the isotopic composition of irrigation water was $\delta^{18}\text{O}=-8.3\text{‰}$ and $\delta^2\text{H}=-56\text{‰}$. The pre-experiment isotopic composition of soil water showed a decrease in the δ -values for both isotopes with depth. This stratification is frequently observed in soil water studies (Barnes and Walker, 1989; Allison et al., 1993; Königer et al., 2010) and results from evaporation.

After the irrigation experiment, the isotopic composition of soil water moved towards the composition of the irrigation water. The stratification with depth was conserved, indicating mixing with existing soil water and not full replacement of soil water by irrigation water. Both isotopes, ^{18}O and ^2H , showed the same mixing process between soil water and irrigation water in the sampled soil profiles.

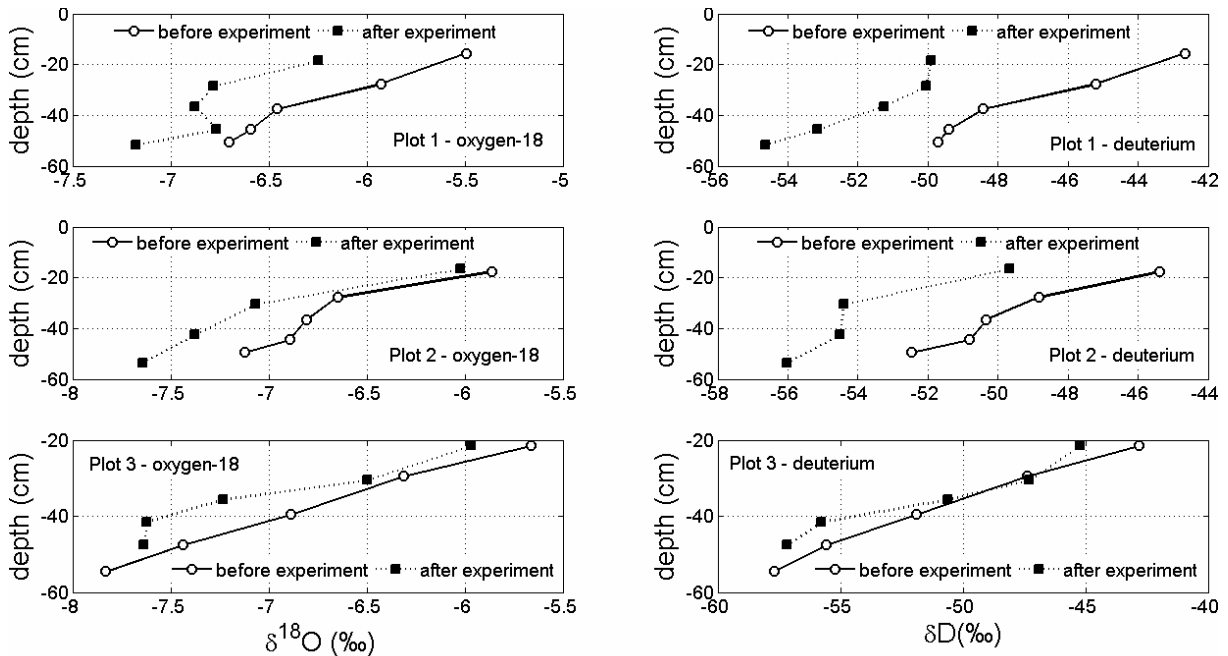


Figure 5-5: Measured isotopic composition of soil water, before (blue) and after (red) the second experiment at three sampling locations. Left column summarizes oxygen-18 (VSMOW in ‰) and the right column summarises deuterium (VSMOW in ‰).

5.3.6 Compartmental modelling

I performed compartmental mixing modelling to investigate the interaction between the macropore system and the soil matrix. So, what is the amount of water that entered the soil matrix compartment? I evaluated this interaction for every sampling location, to account for the spatial variability within the experimental plot that derived from variable soil structure.

Table 5-4 summarises the results of the compartmental modelling. The results based on two end members (pre-event soil matrix water and irrigation water) indicate a significant interaction between soil matrix and the irrigation water over the depth of the profile. For example, at sampling location 1, the matrix water after the experiment consisted of 9.95% to 34.06% irrigation water, depending on the depth. The results for location 2 and 3 are similar. Using water from the overlying soil compartment as an additional end member, led to somewhat different results. Mainly location 3 showed significant contributions of water from overlying soil layers while this is not pronounced for location 1 and 2.

With the applied linear programming, the sum of the individual errors of each mass balance equation (row in the matrix of Equation 5-8) is minimised. The mass balance error for each individual mass balance (water, ^{18}O and ^2H) showed a maximum deviation of -6.17%. In total

71.6% of the individual mass balance errors are below $\pm 2\%$. Approaches allowing water from compartment 2 to enter compartment 4 were not allowed during the modelling, as this would have led to an underdetermined linear equation system, and thus a non unique result.

Table 5-4: Results of the compartmental mixing modelling performed for every location, and for the two and three end member modelling. Soil depth is the centre depth of a soil compartment (cm), PESW is the proportion of pre-event soil matrix water in the soil compartment (%), IW is the proportion of irrigation water in the soil compartment (%), OC is the proportion of water from the overlying cell (%), Error WB the error in the water balance (%), Error ^2H the error in the mass balance of deuterium (%), and Error ^{18}O the error in the mass balance of oxygen-18 (%).

Location 1, two components							
Compartment	Soil depth (cm)	PESW	IW	OC	Error WB	Error ^2H	Error ^{18}O
1	-15.5	76.29	23.71	-	-2.10	6.17	-3.52
2	-27.5	65.94	34.06	-	-0.64	1.70	-1.02
3	-37.5	77.96	22.04	-	-0.82	1.87	-1.00
4	-45.5	90.05	9.95	-	-1.88	4.04	-1.93
5	-50.5	74.42	25.58	-	-1.77	3.99	-1.99
Location 1, three components							
2	-27.5	66.59	33.36	0.05	-0.79	1.70	-0.92
3	-37.5	77.45	22.54	0.01	-0.76	1.85	-1.08
4	-45.5	90.12	9.88	0.00	-1.89	4.04	-1.92
5	-50.5	0.01	29.89	70.10	-1.76	3.87	-1.89
Location 2, two components							
1	-17.5	89.17	10.83	-	-2.05	5.04	-2.63
2	-27.5	85.48	14.52	-	-1.89	4.85	-2.62
3	-36.5	72.76	27.24	-	-1.53	3.29	-1.61
4	-44.5	63.43	36.57	-	-1.24	2.59	-1.25
5	-49.5	67.85	32.15	-	-1.24	2.14	-0.84
Location 2, three components							
2	-27.5	85.56	14.44	0.00	-1.90	4.85	-2.61
3	-36.5	74.07	25.89	0.04	-1.66	3.30	-1.45
4	-44.5	63.27	36.72	0.00	-1.23	2.59	-1.27
5	-49.5	66.76	33.24	0.01	-1.16	2.15	-0.94
Location 3, two components							
1	-21.5	87.71	12.29	-	-0.43	1.28	-0.83
2	-29.5	94.26	5.74	-	0.54	-1.22	0.71
3	-39.5	59.34	40.66	-	-0.33	0.55	-0.21
4	-47.5	88.30	11.70	-	-1.30	1.43	-0.09
5	-54.5	100.00	0.00	-	0.18	2.02	-2.12
Location 3, three components							
2	-29.5	34.76	20.31	44.93	-0.01	-0.08	0.09
3	-39.5	34.52	48.65	16.83	-0.50	1.19	-0.65
4	-47.5	95.72	4.20	0.09	-1.63	1.18	0.51
5	-54.5	32.89	0.00	67.11	-1.81	2.56	-0.66

5.3.7 Backward determination of isotopic composition of soil water contributing to the hydrograph

The hydrograph separation approach can be solved in a backward approach to determine the isotopic signature of contributing soil water. Using Equation 5-3 and Equation 5-4 with the three components, namely irrigation water, soil water, and baseflow, I can determine the isotopic composition of soil water contributing to the hydrograph. The fraction of base flow contribution was calculated by the ratio of baseflow (assumed to be constant) to measured flow, and the fraction of soil water was calculated as residual.

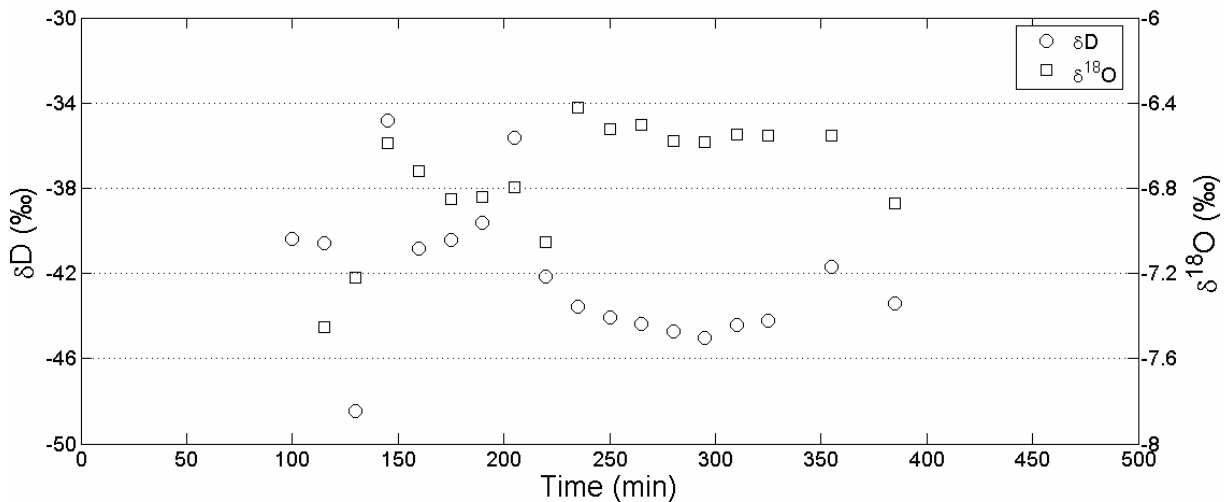


Figure 5-6: Results from the backward hydrograph separation. The isotope values denote the isotopic composition of the soil water contributing to the tile drain discharge during the hydrograph of the second experiment.

Figure 5-6 presents the isotopic composition of contributing soil water. Combined with Figure 5-5, I can infer on the soil layer that contributed water to the hydrograph. Unfortunately oxygen-18 and deuterium provide different results. The calculated soil water signature of $\delta^{18}\text{O}$ -values varies around -6.5‰ during the times of clear discharge increase while $\delta^2\text{H}$ -values are around -44‰ . So while ^{18}O would indicate a contribution of soil water from depths between 20 cm and 40 cm, deuterium results would indicate contributing soil layer at approx. 20 cm (or higher). Nevertheless, this calculation is very sensitive to a) measured discharge, b) calculated fraction of event water, and c) measured concentrations. For example, an assumed baseflow of 0.08 l/s compared to the measured 0.101 l/s would change the $\delta^2\text{H}$ -values around peakflow from -46‰ to -47‰ . Additionally, the spatial variation in isotopic composition of soil water might be higher than sampled by three profiles.

5.4 Discussion

5.4.1 Macropore-matrix interaction

The compartmental mixing model used to investigate the interaction between the soil matrix and the macropore domain showed a clear proportion of event water entering the soil matrix domain over a depth down to 60 cm. Only a small change in soil moisture at depths of 30 cm and 50 cm was observed. Please keep in mind that the soil moisture equipment was installed near location 1 and might not be representative for the total field plot.

The presence of a transient water table (after the experiment) at depths of 28 cm and 40 cm at sampling locations 1 and 2 indicates the assumption of empty macropores was probably violated at those locations in the lower compartments. Therefore, part of the irrigation water contribution to the lower soil depths was actually water that originated from macropores. Nevertheless, interaction of irrigation water with the soil matrix in the upper soil is evident. Macropore water entering the soil matrix has been observed in several experimental studies with dye tracers (Flury, 1996, Zehe and Flüher, 2001a; Weiler and Naef, 2003a, van Schaik et al., 2008).

The hydrograph separation with bromide and the isotopic composition of the hydrograph reveals large contributions of the soil water that exceeded 50% during the discharge peak. This is a clear sign of threshold behaviour (Tromp-van Meerveld and McDonnell, 2006a; 2006b; Zehe et al., 2007; Zehe and Sivapalan, 2009) in the interaction of macropore and matrix water. After crossing of this moisture threshold, the direction of the interaction changed. Below the threshold, macropores drained into the matrix, whereas the matrix began to drain into the macropore system after exceeding the threshold. This led to increased bromide concentrations in the tile drain and the isotopic composition then strongly deviated from that of baseflow and irrigation water. Such subsurface phenomena were previously observed and classified by Weiler and Naef (2003a) and Weiler and Flüher (2004). Additionally, this interaction may vary spatially as well as temporally; water leaves the soil matrix and enters the macropores in the upper soil, but may infiltrate from the macropores to the matrix at greater depths.

5.4.2 Vertical and lateral preferential flow

Patterns of variation in the isotopic composition of the soil provides insight to the role of macropores at this field site, and shows in a general way their role of wetting up and draining the soil depending on a threshold relationship. Macropore flow transports large amounts of water downwards in the profile. An additional question is: How is water transported vertically downward into the tile drain? And what is the dominating lateral flow mechanism? Shipitalo and Gibbs (2000) found that macropores up to a distance of 50 cm to a tile drain are directly connected to it.

If only a small area above the tile drain contributed, the total mass recovery of bromide (6.1%) and water (15%) (during experiment 2), could not be achieved. If bromide would not enter the soil matrix, a total recovery of 6.1% bromide would need a drained cross section of 1.2 m. In the tile drain modelling study of chapter 3 I showed that a hillslope contributing width of 2-3 meters is needed to fit the discharge of an irrigation experiment with a 2-dimensional hillslope model at a nearby tile drained hillslope. This would require lateral preferential transport in the system. Transport by pressure propagation can be neglected in this experiment, as most bromide arrived during the peak discharge and the upper soil layers also contributed during peak discharge, as corroborated by the isotope data. Although I observed a temporal water table at depths of 28 cm and 40 cm after the experiment at

locations 1 and 2, a shallow groundwater table is unlikely the reason for the lateral transport, as soil moisture measurements indicate no change of soil moisture in 50 cm depth, near location 1.

So, I find rapid transport of water and solutes that decreased within minutes after the irrigation ended, with a temporal water table at two of three locations after the experiment, but no significant increase in deep soil moisture. Thus, I suggest that a network of pores, decoupled from the soil matrix, caused lateral preferential transport. The interaction between the soil matrix and this pore system is less than the delivery of additional water, thus draining the mobilised soil water and the event water to the tile drain. A similar process was observed by van Schaik et al. (2008), who found lateral preferential flow in a hillslope pore network with a temporal water table, while the soil matrix remained largely unsaturated.

5.4.3 Capacity controlled threshold behaviour of subsurface flows

The flow system at this field site is dominated by the interaction between macropores and the soil matrix and the interplay between lateral and vertical preferential flow. The abrupt changes during the experiment in discharge and tracer concentration point to a threshold controlled process. Translatory flow (Hewlett and Hibbert, 1967) is not likely responsible for the vertical water transport, this became evident by the shapes of the isotope profiles in Figure 5-5. Translatory flow would lead to a downward movement of water with a distinct isotopic signature, while in this study a change towards the signature of irrigation water could be observed at every depth, similar to the frequent observed interaction of macropores and the soil matrix (e.g. Weiler and Naef, 2003a). This interaction depends on the system state and changes with time. At first water infiltrated from the macropores to the matrix with no tracer entering the tile drain, then some infiltrating water reached the drain. After a threshold was reached, soil matrix water began to enter the macropores leading to downward transport of pre-event water. A similar process was observed by McDonnell (1990) who found that water transported by vertical preferential flow paths induced old water to enter a lateral network of preferential flow.

In this study, lateral and vertical preferential flow networks are connected, as evidenced by the tracer data. A transient temporal water table in the pore network (van Schaik et al., 2008) developed during the experiment, and reached up to 28 cm below the surface at the end of the experiment. Water could then enter this network and rapidly enter the tile drain. Again, this whole process is driven by the threshold behaviour of the macropore-matrix interaction; this process provides a water supply that can saturate the pore network.

The studies of Tromp-van Meerveld and McDonnell (2006a) and Graham et al. (2010), showed the relevance of bedrock in the generation of subsurface stormflow, while the interaction of the macropores with the soil matrix drives the subsurface runoff generation in this study. The decreasing hydraulic conductivity with depth might favour this process. The pore system drains rapidly after the end of the experiment. Although discharge for experiments 1 and 2 was distinctly higher after the experiment than before, this water cannot

be attributed to the soil as evidenced by the isotope data, that represents base flow conditions during those times. So after the pore system was emptied, the connectivity of the soil to the tile drain was interrupted. At most only the deep soil layers contributed some water.

Figure 5-7 illustrates the different processes during the hydrograph. I classified the isotope samples and linked them to the hydrograph state. For experiments 1 and 2 it became evident that the isotopic composition was similar before and after the experiments. During the hydrograph, soil water contributed to the hydrograph, and led to different signatures during rise and fall of the hydrograph. Figure 5-7 gives an insight to the temporal development of source regions and source fractions. The threshold process can explain why water is transported through macropores but mainly consists of old water as found by Stewart and McDonnell (1991) in the Maimai catchment.

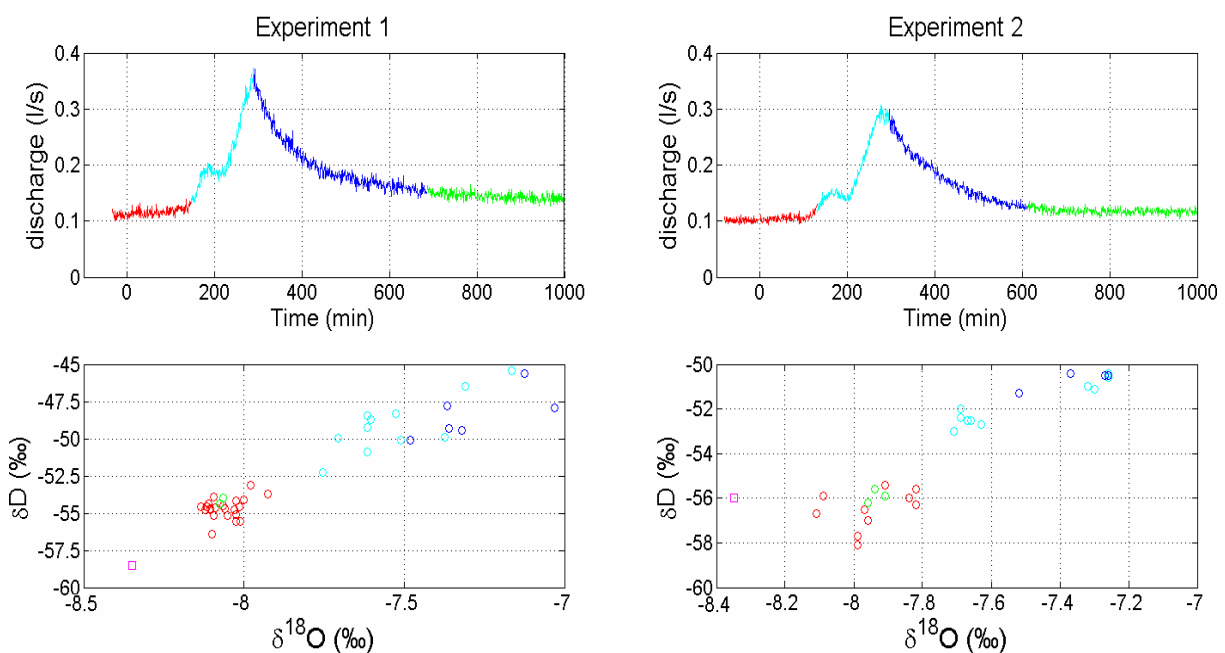


Figure 5-7: Correlation between hydrograph phases and isotopic composition of tile drain water. Left column are the results of the first experiment and the right column for the second experiment. Magenta denotes the isotopic composition of the irrigation water, light blue the isotopic composition of the rising hydrograph limb, dark blue the isotopic composition of the falling hydrograph limb, red the isotopic composition of baseflow conditions, and green the isotopic composition after the event.

5.4.4 Implications for hydrograph separation

Although I performed this experiment at the field/hillslope scale, the overall implications for isotope based hydrograph separations (Sklash and Farvolden, 1979) can be discussed, both at the hillslope and catchment scales. Much effort has been made to better describe the spatial and temporal variation of the isotopic composition of precipitation (Shanley et al., 2002; Lyon et al., 2008), a significant source of uncertainty in hydrograph separation. On the other hand, the sampled isotopic composition of baseflow is believed to represent the pre-event isotopic signature in a catchment. If I consider the field site as a catchment, and the tile drain as a stream, this assumption would fail totally. In this study, the difference between event and

baseflow water was distinctly less than the difference with stored soil water. During the event, after a certain threshold was exceeded, the soil water began to contribute to discharge.

Therefore, the spatial variability of soil water must be considered, as the connectivity to hydrological sources may increase during an event as a progressively greater soil volume contributes to subsurface runoff. Thus, a variable source soil volume approach is needed to describe pre-event water at catchments, analogous to the variable source area concept used to describe the catchment runoff process (Hewlett and Hibbert, 1967; Dunne and Black, 1970).

5.5 Conclusions

A threshold controlled runoff generation of the tile drain discharge was observed at the study site. Based on applied bromide tracer, rapid breakthrough was observed, nevertheless the proportions of irrigation water never exceeded 20% in the tile drain discharge. The discharge of irrigation water at peak flow was, however, nearly fourfold that of the baseflow in experiment 1. Measurable increases in discharge were reached at 18.2 mm, 14.6 mm and 30 mm total irrigation amount for the three experiments. The soil moisture reached a state where different soil layer began to drain via macropores, as evidenced by soil water isotope patterns, and a lateral macropore network was initiated. This study is limited by few soil moisture observations; a denser network of observations would allow greater spatial interpretation of the results.

Using soil isotopic sampling before and after the experiment allowed a quantification of macropore-matrix interaction and provided evidence that pre-event soil water from the upper soil layers contributed to discharge. This approach enhances understanding of hillslope processes based on detailed determination of active soil layers and the timing of their activation. Additionally, I can explain the contribution of old water to the tile drain discharge by threshold behaviour. Based on the different irrigation amounts that are needed to activate the system, I suggest a moisture driven threshold.

Finally, I return to the questions asked in the introduction:

- Water transport through soil is governed by macropore flow, yet this is not a new finding. Nevertheless, the water flow in the macropores is a mixture of event and pre-event water, with the latter dominant. The flow mechanism is driven by the interaction between the soil matrix and the macropore network.
- The measurement of soil water isotopic composition in combination with compartmental modelling provides insight to the magnitude of matrix-macropore interaction, indicating that up to 30% of soil water was derived from the irrigation.
- Within this study, based on soil water isotope measurement, hydrograph separation based on applied bromide and a backward hydrograph separation to determine the necessary isotopic signature of the soil water, I was able to locate the active soil layers that generated tile drain discharge. These were in the upper soil layers, to a depth of 40 cm; lower depths did not appear to contribute significantly to discharge.

In agricultural landscapes, detailed knowledge of flow processes will enable to develop a better, process-oriented prediction of water quality. In pesticide studies, the first flush effect that transports applied contaminants via preferential pathways to tile drain systems is well known. At this field site where a tile drained Colluvisol is located in the valley bottom, the upper soil layers contribute the most water during discharge events to the tile drain. This should lead to mobilisation of solutes and maybe even pesticides stored in these upper layers.

6 On the controlling factors of pesticide leaching within a series of three irrigation experiments – the role of preferential flow structures and threshold behaviour*

This chapter is the follow-up study of chapter 5. The hydrological processes that control and drive the generation of the tile drain discharge at the field site in the Weiherbach catchment are investigated in chapter 5. This chapter deals with the related pesticide transport at the same field site. The evaluation of pesticide transport was done within the same series of irrigation experiments and should enhance the understanding of the principal controlling factors for the often observed rapid breakthrough of pesticides at tile drained field sites when preferential flow paths are present. This transport often occurs without retardation compared to conservative tracers. The role of structures, how they interact with the soil matrix, and the role of the observed capacity threshold process (chapter 5) are addressed. It is also investigated how preferential flow paths favour long term leaching of pesticides and how particle bound transport contributes to pesticide leaching at this field site. Further, the approach of assessing the transport parameters of non-conservative solutes based on soil profiles is compared to integral transport behaviour of those solutes inferred from tile drain sampling. Two pesticides (Flufenacet and Isoproturon) are applied before the first two experiments, but not before the third one. A detailed soil sampling at a scale of $10 \times 10 \text{ cm}^2$ is used to observe solute transport in the soil together with temporally dense sampling of the concentration in the tile drain during the experiments. The transport parameters are calculated and the role of hydrological processes is evaluated by comparing the behaviour of the pesticides with the process knowledge gained in chapter 5. The chapter starts with an overview of pesticide leaching, the known related processes, and the research questions that are addressed in this study. Then the methods used are presented, the results are shown and discussed. Finally the conclusions are drawn.

*based on: Klaus, J., Zehe, E., Elsner, M., Palm, J., Schneider, D., Schröder, B., Steinbeiss, S., van Schaik, L., West, S. Manuscript in preparation.

6.1 Introduction

6.1.1 Tile drains and preferential transport

Tile drained systems regulate the moisture content of agricultural field sites and affect the hydrology of cultivated catchments (Schilling and Helmers, 2008; Li et al., 2010). Thus, they strongly influence the water quality of agriculturally used catchments (Algoazany et al., 2007; Schilling and Helmers, 2008). Tile drains bear significant risk for chemical leaching to surface water bodies (Vereecken, 2005). Especially in combination with preferential flow that is common in soils (Jarvis, 2007), tile drain systems have a significant impact on water quality of receiving water bodies. Preferential flow paths play a vital role in the transport of agrochemicals (Flury et al., 1995; Flury, 1996; Elliot et al., 2000; Šimůnek et al., 2003) and in the transport of anions (Flury et al., 1995; Villholth et al., 1998; Stone and Wilson, 2006). Preferential flow paths act as shortcuts for solute transport in the drains and subsequently into surface waters. Rapid flushing of tracer (Villholth et al., 1998; Lennartz et al., 1999; Köhne et al., 2006), nitrate (Mohanty et al., 1998), strongly adsorbing phosphates (Stamm et al. 1998; 2002) or pesticides (Kladivko et al., 1991; 2001; Czapar et al., 1992; Zehe and Flühler, 2001a) into surface waters was reported.

While preferential flow may lead to simultaneous early (e.g. within 30 min after application in Kung et al., 2000) appearance of reactive, i.e. non-conservative, and conservative solutes in the tile drain (Everts et al., 1989; Kung et al., 2000; Fortin et al., 2002), the total mass losses are usually driven by the sorption properties of the solutes, like K_{oc} – the organic carbon sorption constant (Kladivko et al., 1999). Different studies have shown the long term effect of tile drains on pesticide leaching (Gärdenäs et al., 2006; Rupp et al., 2006). Total amount of pesticide leached after application into surface waters were quantified (Donald et al., 1998; Gaynor et al., 2001; Leu et al., 2004) and annual losses range from 0.1% up to several percent (Flury, 1996). Kladivko et al. (1999) showed that long term pesticide leaching on a tile drain field site was event driven, the peak concentration of pesticide decreases with time since application, although exceptions occurred. Even small proportions of pesticides leaching to ground or surface water have a significant effect on the ecosystem or human health. On the one hand, small concentrations in surface water can harm the ecosystem, and on the other hand boundary values for drinking water might be exceeded in groundwater (cf. Jarvis, 2007).

6.1.2 Driving factors of pesticide leaching and transport

Various studies evaluated different factors of pesticide leaching: Aletto et al. (2010) gave a detailed report on the effect of tillage on pesticide leaching. The effect of soil moisture on pesticide leaching was investigated by Flury et al. (1995), who showed that movement of Atrazine was less pronounced in dry than wet soil. In line with these findings, Ng et al. (1995) showed that the loss of Atrazine and Metolachlor to surface waters is positively correlated to soil moisture. Kladivko et al. (1999) investigated the effect of tile drain spacing on long term pesticide leaching and showed that smaller spacing lead to higher pesticide losses into surface waters. Southwick et al. (1992) found, for one season, more Atrazine losses at a field site with wider tile drain spacing than at a site with smaller spacing.

Recently, McGrath et al. (2008) showed in a modelling study with 50000 realisations of precipitation events that the use of the retardation coefficient R as a measure of the mobility of resident solutes depends on the flow pathway considered. McGrath et al. (2008) also stated that the characterisation of fluxes in soils based on weakly sorbing resident tracers, may underestimate the potential for rapid transport of sorbing solutes under natural variations in rainfall. Yet different methods are applied to determine the transport parameter of solutes, e.g. soil column experiments (Young and Ball, 2000), soil profile excavation (Zehe and Flühler, 2001a), and solute breakthrough curves of tile drained field sites (Kung et al., 2000; Zehe and Flühler, 2001a) or springs (Wienhöfer et al., 2009). Different studies corroborate that pesticides, which were found to be rather immobile in laboratory columns, can be very mobile in field soils (Jury et al., 1986; Flury, 1996). The information of lab scale experiments are thus not transferable to field scale. This raises the question: Which method is appropriate to determine transport behaviour of reactive solutes in natural soils?

Mentioned previously, reactive and conservative tracers were found at the same time in tile drain discharge. Kung et al. (2000) found that bromide and rhodamine WT showed the same arrival and peak times when applied before an irrigation experiment. Kung et al. (2000) concluded that water dynamics of preferential flow paths dominated the initial phase of the contaminant transport, regardless of the retardation properties of contaminants. Various studies have shown the strong effect of precipitation characteristics on triggering preferential flow and contaminant leaching (Malone et al., 2004; McGrath et al., 2007; Nolan et al., 2008). Within a lysimeter study McGrath et al. (2010) showed that pesticide transport was a capacity-controlled threshold process dependent on the precipitation amount. McGrath et al. (2010) identified 19 mm precipitation as the threshold and found that 38% and 56% of the total transport of two used pesticides was attributed to rainfall events exceeding 19 mm. Only about 1% to 10% of total bromide mass was transported during those rain events. This reveals that transport of pesticides is strongly driven by high rainfall rates. In addition, McGrath et al. (2010) showed that the strongest pesticide leaching occurred about 208 days after the pesticide application, during a rainstorm.

Furthermore, particle bound transport is a major factor enhancing transport of pesticides or other strongly sorbing solutes (de Jonge et al., 1998; de Jonge et al., 2004). Villholt et al. (2000) found that 6% of total pesticide leaching of Prochloraz at a 5 m × 5 m field plot could be attributed to particle bound transport. De Jonge et al. (1998) found, for the same pesticide, between 2.5% and 13.1% particle bound transport in column experiments.

6.1.3 Summary, open research questions, and objectives

In summary, it is known that strongly reactive pesticides are transported intermittently through the unsaturated zone by preferential flow paths. There is almost no difference between reactive and conservative tracers in timing, only in absolute transported mass fraction, when transported in preferential flow paths during rainfall driven conditions. The transport of pesticides was found to be threshold (rainfall amount) dependent at lysimeter

scale. Pesticide mobilisation was observed to occur more than 200 days after application at lysimeters. Different studies showed the relevance of particle bound transport, and the problem of transferring transport characteristics between different scales.

Nevertheless, the understanding of the transport behaviour of adsorbing contaminants at the field scale remains incomplete:

- What are appropriate methods to assess dispersion and retardation behaviour of reactive solutes at the field scale in a representative manner?
- How preferential transport is initiated and what is the role of soil moisture and cumulative rainfall amount?
- How do matrix and macropore flow interactions affect field scale flow and transport at the event scale and in the long term?

The present study addresses these questions within a series of three irrigation experiments on a tile drain field site to investigate subsurface flow processes and their link to contaminant transport in the Weiherbach catchment. Within a related study (chapter 5), based on a multi tracer approach, it was shown that tile drain discharge largely consisted of pre-event water stemming from the soil matrix that enters the preferential pathways. Bromide concentrations were found to be strongly correlated to tile drain discharge. I was able to identify the approximate soil depth where soil water was mobilised. Lateral transport into the tile drain was attributed to a macropore network that became saturated during the course of the irrigation. This implies that hydrological connectivity between the tile drain, source areas of the pre-event water, and vertical preferential flow paths was established. Additionally, I found that onset of subsurface flow and tile drain event flow were a threshold processes controlled by water content and the related hydrological connectivity.

6.2 Study area and experimental methods

6.2.1 Study area

The study area is located in the cultivated Weiherbach catchment that is described in detail in chapter 2. The map in chapter 2 (Figure 2-1) presents the detailed location of the field plot. The field plot itself is described in detailed in chapter 5.2.1.

6.2.2 Experiment design

I preformed a series of three irrigation experiments with multiple tracers and two pesticides with a different K_{oc} , namely Flufenacet (K_{oc} of 202 ml/g) and Isoproturon (K_{oc} of 122 ml/g) (Footprint, 2006) at a tile drained field site located parallel to the Weiherbach brook (49°08'08"N 8°44'42"O). Isoproturon is in widespread use in the Weiherbach catchment and is regarded to be problematic in the catchment, since it is frequently observed in high concentrations in the brook. It is banned from tile drained field sites. Flufenacet is a successor of Isoproturon, with slightly stronger sorption behaviour. It is in frequent use in the Weiherbach catchment, and yet not many studies investigated its field scale behaviour. I want to shed light on the following questions:

- What are appropriate methods to assess the dispersion and retardation behaviour of reactive solutes at the field scale in a representative manner? How many soil profiles are needed for this and are the parameters derived from soil these profiles useful to characterise the leaching behaviour of the two pesticides into the tile drains?
- Does a thorough understanding of the flow process, in particular the role of preferential flow, the interaction between matrix and macropore flow, and about source areas of pre-event water help me to understand a) short term leaching of pesticides and especially the often enhanced mobility in preferential pathways and b) long term leaching behaviour with focus on remobilisation of pesticides that have been previously stored in the soil matrix?
- How important is particle bound transport in this case, especially for explaining the often reduced retardation of pesticides that leached into tile drains?

For this purpose I selected a $20 \times 20 \text{ m}^2$ field site, approximately 10 m from the stream banks. This field has been used for agricultural purposes for the last eight years before the experiment. Before that it was fallow land. A single tile drain tube is located about 1-1.2 m below the surface, embedded in a gravel layer. The tile drain outlet, a plastic tube with a diameter of approx. 20 cm, entered the Weiherbach brook about 30 cm above the baseflow water level. The soil is a Colluvisol with a strong gleyic horizon starting at a depth between 40 and 70 cm below the surface, which fits well with observations of perennial flow from the tile drain. The site is characterised in chapter 5.2.1 in more detail.

6.2.3 Experimental setup and data collection

In the following I will explain the setup of the different experiments. Tile drain water level and discharge, the irrigation rate, and the soil moisture were observed. Within chapter 5.3.1 the antecedent precipitation and temperature conditions of the experiments are summarised (see Table 5-1). The first experiment was performed under wetter initial conditions than the following two, and the third experiment showed the lowest antecedent precipitation.

Irrigation device and observations of cumulated irrigation

I performed the irrigation with a system of eight garden sprinklers (e.g. Wienhöfer et al., 2009) that were adjustable in range and receiving the same pressure to have the same sprinkling rate. This setup was the same during all experiments.

The first experiment was performed on 16th September 2008. The irrigation rate was measured with 10 precipitation samplers with a support of 200 cm² and the opening 30 cm above ground. Irrigation was carried out in three blocks of 60 min, 80 min, and 60 min duration, with a 30 min break between the blocks.

The second experiment was performed on the 15th September 2009. Compared to the first experiment I adjusted the measurement of the irrigation rate. Irrigation rate was measured with 20 evenly distributed precipitation samplers with a support of 37.4 cm² and approx. 5 cm

above ground. Irrigation occurred in three blocks, 35 min, 90 min, and 90 min, with breaks of 22 min and 30 min respectively.

The third experiment was performed on 5th October 2009. The irrigation rate was measured the same way as in the second experiment. Irrigation was performed in two 90 min blocks with a 30 min break between them. Table 5-3 summarises the time and rate of irrigation for all three experiments.

Application of tracers and pesticides

About 5 h before the first experiment the pesticides Isoproturon (IPU), 80 g in total, and Flufenacet (FLU), 20 g in total, were applied by the farmer using a tractor and a mounted spray bar on the experimental plot. Additionally a tracer solution (1500 l) containing 1600 g bromide was irrigated during the first irrigation block between minute 15 and minute 35, replacing the irrigation water. Again, 4 h before the second experiment, the farmer applied IPU (600 g) and FLU (40 g) the same way as in experiment 1 on the field plot. I applied 2400 g of bromide dissolved in 1500 l of water with the first irrigation block (minute 13 to 35). No additional tracers or pesticides were used in the third experiment, thus all of the out flowing solutes can be linked to the previous experiment.

Hydrological observations

The tile drain was sealed by a plastic board with a triangular notch (opening angle was 25°). Water level in the tube was measured by means of a PD-2 pressure probe (SOMMER, Koblach, Austria) with a temporal resolution of 1 minute during the experiment. After the experiment the sampling rate was reduced to 10 minute intervals. Water levels were transformed into discharge using a rating curve that was determined by frequent discharge measurements with a bucket during the experiments; I estimate the accuracy at 0.02 l/s, which is determined by the accuracy of the pressure probe and the rating curve. Soil moisture was observed for all three experiments, a detailed description of the observation and the results can be found in chapter 5.3.

Water sampling

In the first experiment I sampled with a high temporal resolution of 5 minutes at the beginning of the experiment, since Zehe and Flüßler (2001a) reported a very fast first solute breakthrough during their experiment that was carried out at a nearby field site. Later, the sampling rate was reduced. In total I collected 51 water samples during the experimental day; the last sample was taken two hours after the end of the experiment. Additionally, the falling limb of the hydrograph was sampled every eight hours for five days by an automatic sampler (ISCO). Six and seven days after the irrigation two additional samples were taken by hand.

This sampling procedure was adjusted for the second experiment. I sampled the background level of tracers in the tile drain outlet before the start of the experiment and collected a total of 25 water samples during the experiment at intervals of 15 minutes, the last two samples with intervals of 30 min, and three samples on the day after the experiment. The sampling during

the third experiment followed the sampling during the second experiment. Before the start of the third experiment the tile drain background was sampled. Then 21 samples were taken during the experiment every 15 minutes, but no samples were taken on the days after the experiment.

Soil sampling

Soil sampling was performed at five soil profiles, after the first experiment. One of them was excavated on day one, and two of them two days after the experiment. The remaining two were excavated seven days after the experiment. The five profiles are referred to in the following as P1, P2, P3, P4, and P5. Samples were taken on a 10 × 10 cm² grid by centring a 100 cm³ soil core in each grid cell. The depth of the sampling procedure was limited by the mechanical stability of the profile that was low in the gleyic horizon, thus P1 was sampled to a depth of 90 cm, P2 and P3 to a depth of 60 cm, and P4 and P5 to 80 cm depth. The soil samples were stored in a cool box for shipping (24-48 h) and then were stored frozen until extraction.

6.2.4 Analytics

Bromide and pesticide content of water samples

Bromide was measured directly in filtered (450 nm) water samples. Bromide concentrations were determined by anion chromatography (ICS-1000 DIONEX). The detection limit is 0.1 mg/l.

IPU and FLU were extracted from the water samples with SPE-Columns (StrataTM-X 33µm, Polymeric Sorbent, Phenomex[®]), where the dissolved pesticides adsorbed, and particles with possible adsorbed pesticides sedimented at the column surface. After drying the columns under nitrogen, the adsorbed solutes as well as the particle bound organic substances were extracted with 5 ml of methanol, in steps of 2.5 ml, 1.5 ml, and 1 ml. The solution was evaporated with nitrogen, and resolved for analysis. Concentrations were measured with an LC/MS-system (LC: Agilent Technologies 1200 Series, MS: Q-Trap LC-MS/MS, Applied Biosystems). Deuterated IPU served as internal standard.

To investigate the relevance of particle bounded pesticide transport, the water samples of the second experiment were split. One half was filtered with a 200 nm filter before the extraction procedure, while the other half was extracted unfiltered.

Bromide and pesticide content of soil samples

For bromide extraction, soil samples were dried at 105°C for 24 h. After homogenisation of the samples, particles exceeding 2 mm diameter were removed and 20 g of the dried soils were mixed with 50 ml of distilled water. This mixture was stirred for 30 min at 300 rotations per minute (rpm) and was sucked through a 450 nm filter. The solution was analysed with anion chromatography (ICS-1000, Dionex). For pesticide extraction, soil samples were sieved (2 mm) and air-dried for 24 hours. A small fraction of these samples was dried at 105°C for

24 h in the oven to determine its soil water content. From the remaining material the pesticides were extracted by adding water and acetonitril as well as magnesium sulphate, sodium chloride, and citrate salts as buffers. The mixture was shaken and centrifuged; the acetonitril phase was separated and went to analysis. Analysis was performed with a HPLC-MS/MS system (HPLC: Shimadzu, MS/MS: API 3000 Applied Biosystems). The procedure of pesticide extraction and analysis followed VDLUFA (2010).

6.2.5 Theory for travel time- and travel distance distributions

Transport behaviour of the soils was evaluated using the method of moments (Jury and Horton, 2004; Wienhöfer et al., 2009). From the soil profile a concentration distribution as a function of depth z , lateral position x at a fixed time, is obtained. Concentrations were averaged along the x direction and normalised by the tracer/pesticide mass recovered in the profile (m_t). In the case of a perfect mass recovery and a Dirac pulse as input signal, the normalised averaged concentration $h(z_i)$ is an estimator for the probability that tracer molecules travel into a depth increment $z_i-dz/2, z_i+dz/2$ in the travel time t .

$$h(z_i) = \frac{C_s(z_i)}{m_t} \quad \text{Equation 6-1}$$

where z_i is the depth in meters at the level i , $h(z_i)$ is the relative frequency in (m^{-3}), m_t is the total mass in the soil profile in kg, and C_s the average concentration at the soil depth z_i in kg/m^3 .

The first moment of the travel depth distribution is equal to the transport depth of the centre of mass:

$$\bar{Z} = \sum_i z_i h(z_i) V(z_i) \quad \text{Equation 6-2}$$

where \bar{Z} is the average transport distance in meters, and V the associated Volume to C in m^3 .

By dividing \bar{Z} by the total transport time, the average transport velocity is obtained. In the case of convective dispersive transport, i.e. well-mixed conditions, the variance of the travel depths ($var(z)$) increases linearly with travel time (t) (Jury and Roth, 1990). In this case, the dispersion coefficient (D) for the solute of interest in the investigated soil is equal to the variance divided by twice the travel time:

$$D = \frac{var(z)}{2t} \quad \text{Equation 6-3}$$

$$var(z) = \sum_i h(z_i) V(z_i) (z_i - \bar{Z})^2 \quad \text{Equation 6-4}$$

As the transport of reactive chemicals is retarded compared with conservative solutes, their transport velocity is smaller than for the conservative solute. The effective, average

retardation coefficient can be calculated as a fraction of the average travel velocities of conservative tracer and the reactive solute (Zehe and Flühler, 2001a):

$$R = \frac{v_c}{v_s} \quad \text{Equation 6-5}$$

where R is the dimensionless retardation coefficient, v_c is the transport velocity of the conservative solute in m/s, and v_s the transport velocity of the retarded solute in m/s.

6.3 Results

6.3.1 Bromide travel depth distribution

Table 6-1 and Table 6-2 are summarising the bromide recovery. Because maximum sampling depth was different between the profiles, Table 6-1 presents the data until the maximum sampling depth of each profile, while Table 6.2 presents data up to 60 cm depth, so support the comparability between the profiles. Please keep in mind that P4 and P5 were excavated seven days after the experiment. The recoveries were calculated assuming a profile width of 1 m.

Table 6-1: Transport parameters and recovery for the five soil profiles, based on the maximum sampling depth. D is the dispersion coefficient of bromide (m²/s), RIPU the retardation coefficient of IPU versus bromide, RFLU the retardation coefficient of FLU versus bromide, the recovery of IPU, FLU, and bromide is given.

Profile number	D (m ² /s)	RIPU	RFLU	Recovery IPU (mg)	Recovery FLU (mg)	Recovery bromide (g)
1	5.42×10^{-07}	1.95	2.69	82.05	11.4	5.46
2	7.44×10^{-08}	2.94	3.24	14.99	1.55	2.53
3	7.61×10^{-08}	1.35	1.97	7.85	0.33	3.77
4	4.39×10^{-08}	1.26	4.06	4.04	1.2	5.83
5	3.62×10^{-08}	1.5	4.6	3.49	1.56	7.83
Average	1.55×10^{-07}	1.80	3.31	22.48	3.21	5.08
Std.Dev.	2.17×10^{-07}	0.69	1.05	33.61	4.61	2.03

The recovered bromide mass based on the average recovery rates was 1938 g, and exceeded the applied mass by 338 g. The recovery at P4 and P5 is higher than for P1, P2 and P3. Obviously, bromide accumulated in P4 and P5. Considering the loss via the tile drain, and assuming no additional bromide losses, the average bromide recovery per profile (1 m width) should be 3.85 g. Based on the measured bromide concentrations, the average recovery per profile was 4.84 g, with a standard deviation of 2 g, so that P2 and P5 deviate more than one standard deviation from the average (Table 6-1).

Table 6-2: Transport parameters and recovery for the five soil profiles, based on the 60 cm sampling depth. DCB is the dispersion coefficient of bromide (m^2/s), RIPU the retardation coefficient of IPU versus bromide, RIPU the retardation coefficient of FLU versus bromide, the recovery of IPU, FLU, and bromide is given.

Profile number	DCB (m^2/s)	RIPU	RFLU	Recovery IPU (mg)	Recovery FLU (mg)	Recovery bromide (g)
1	1.34×10^{-07}	1.90	2.28	70.04	10.36	3.79
2	7.44×10^{-08}	2.94	3.28	14.99	1.55	2.53
3	7.61×10^{-08}	1.35	1.97	7.85	0.33	3.77
4	2.14×10^{-08}	1.23	4.09	3.52	1.16	4.78
5	2.29×10^{-08}	1.36	3.83	3.37	1.56	6.84
Average	6.58×10^{-07}	1.76	3.09	19.95	2.99	4.35
Std.Dev.	4.65×10^{-07}	0.72	0.93	28.39	4.15	1.60

Various reasons may explain the recovery exceeding 100%: a) spatial variability of soil structures, surface and subsurface redistribution of the solute, b) spatial variability of irrigation, and therefore spatial variability of bromide application, c) a reduced spatial extent of the irrigation (e.g. if the irrigation covered only 90% of the field plot, the concentrations in the profiles will increase by 10%), d) a bromide background at the detection limit of 0.1 mg/l (in the extracted solution) was used in the calculation of recovery, increasing the background to 0.2 mg/l will lower the recovered mass by more than 100 g for the field plot, and e) spatial variability of the bulk density, which cannot be considered on the small 10 cm \times 10 cm scale of soil sampling. In summary, none of the reasons alone can explain that bromide recovery exceeds 100%, but it is possible in combination of the different factors.

Normalised bromide concentrations are shown in Figure 6-1 and the corresponding 2-dimensional concentration patterns for each profile are provided in Figure 6-2. Comparing P1, P2, and P3 with P4 and P5, it becomes obvious that there was considerable ongoing bromide transport and lateral mixing in the soil in the days after the irrigation experiment. Please note that no natural precipitation was recorded during the observation period. The normalised concentration profiles (Figure 6-1) of the first days (P1-P3) are spotted patchy while the concentration patterns are much better mixed after one week (P4, P5). Nevertheless, most of the mass still remained in the upper 10 cm after seven days. It is interesting to note that in P1 and P3 bromide concentrations rise again in a depth greater than 50 cm, which corresponds to the gleyic horizon at the field plot. In P1 the mass fraction that travelled into a depth between 70 and 80 cm is almost identical to the mass fraction that travelled to a depth 10 and 20 cm. This accumulation of bromide in the lower part may be explained by a high proportion of macropores that end in this depth and by the decreasing saturated hydraulic conductivity with depth. Thus the transport of bromide was interrupted. Between the upper soil layer and the deep layer the interaction of soil matrix and the macropore system was low, thus the bromide concentration in this soil depths is low either. The high bromide concentrations found in the lowest grid cells of P1, P2, and P3 (Figure 6-2), are consistent with the observed bromide breakthrough into the tile drain (see chapter 6.3.3).

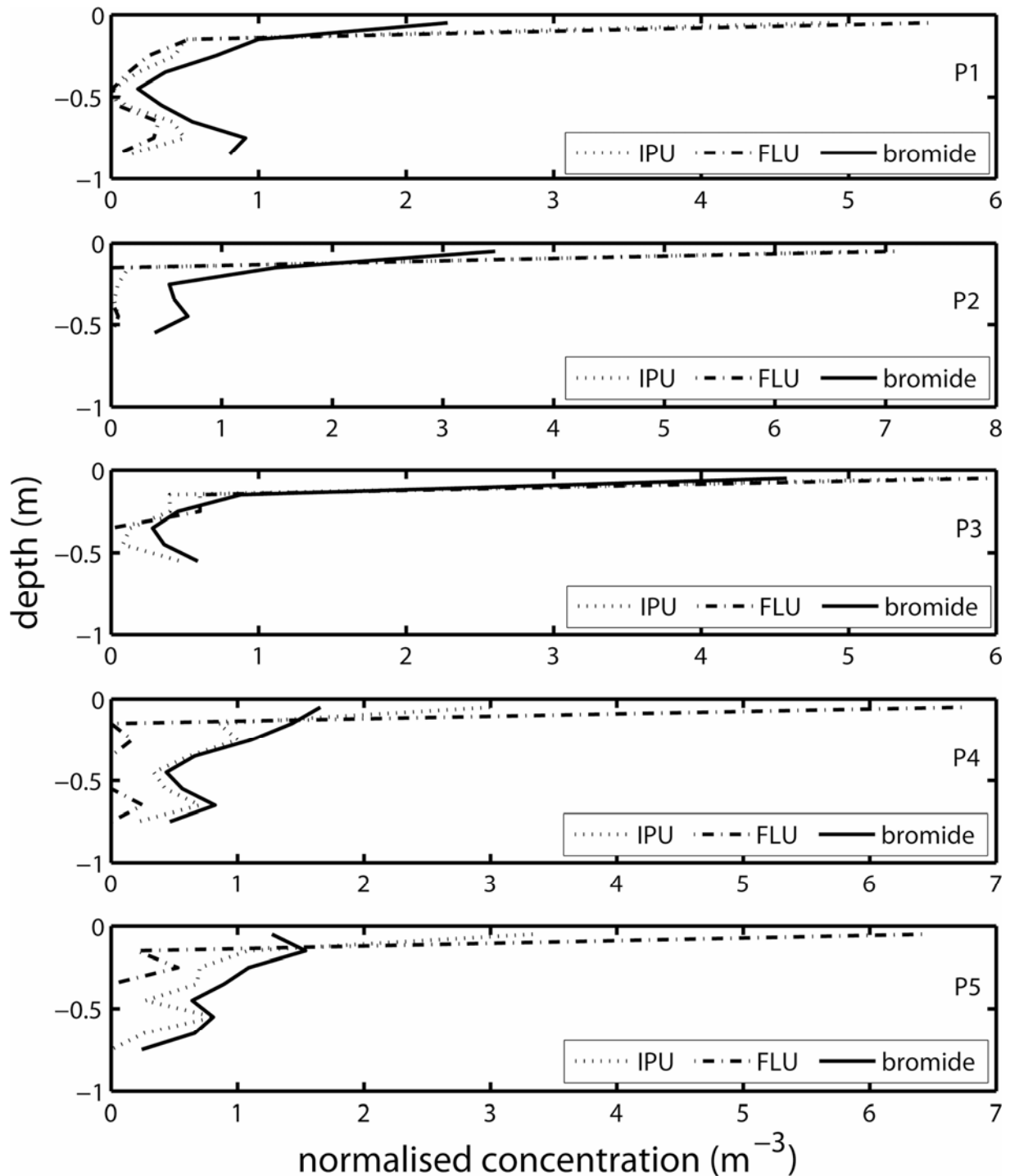


Figure 6-1: Normalised concentration profiles of each soil profile (P1, uppermost, P5 lowest one). P1 is one day old; P2 and P3, two days; P4 and P5, seven days. Bromide (solid), IPU (dotted), FLU (dashed-dotted).

The calculated dispersion coefficients of bromide are summarised in Table 6-1 and Table 6-2. Except for P1, the dispersion coefficients are within the same order of magnitude. This suggests that transport took place in similar flow paths. Additionally, the profiles sampled after 7 days (P4 and P5) have no distinctly different dispersion coefficient compared to the profiles sampled several days before. Comparing the results based on the sampling depth (total sampling depth, vs. 60 cm) the differences and similarities between the profiles remain unchanged.

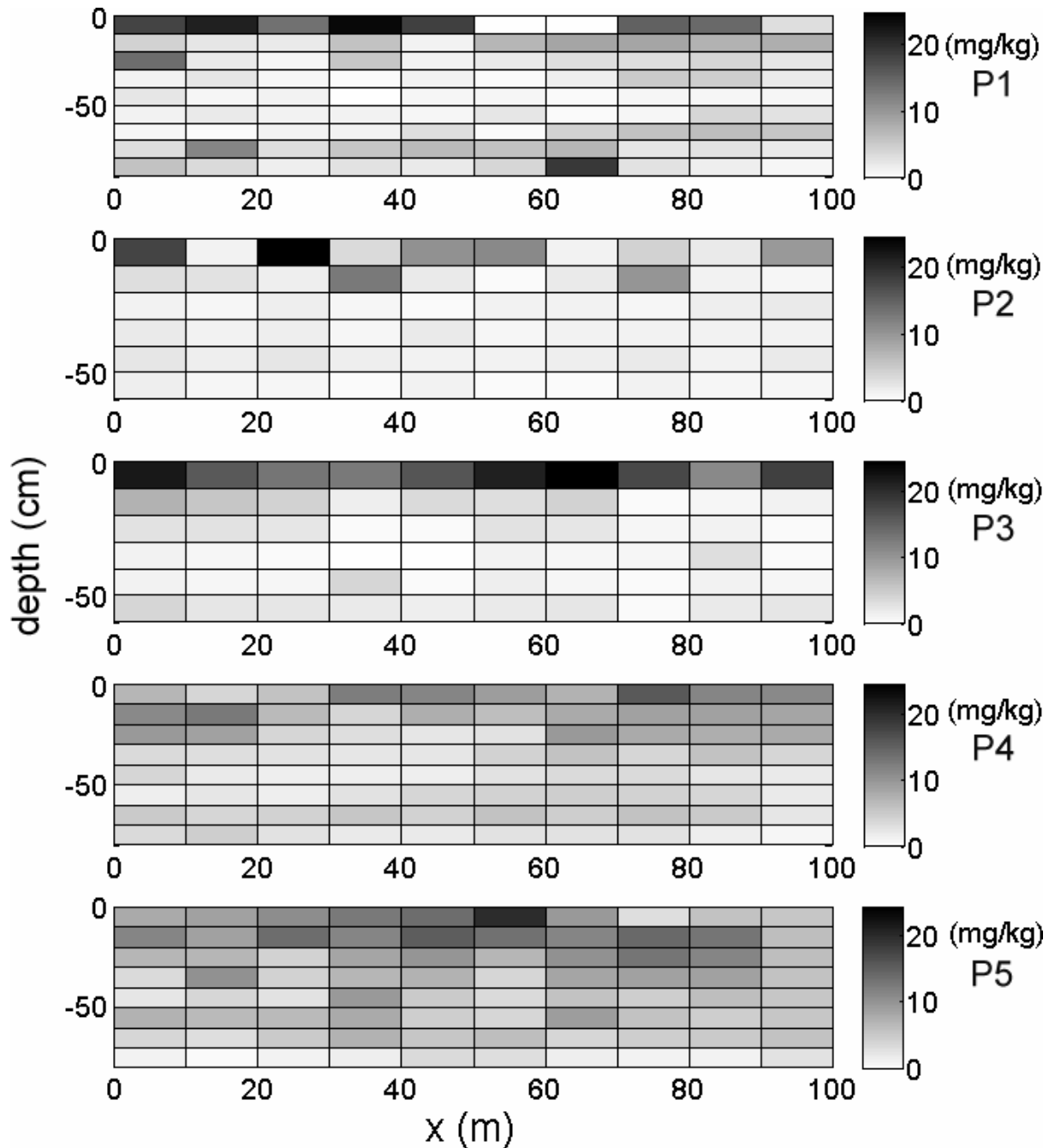


Figure 6-2: Bromide concentration in dry soil for the five soil profiles (mg/kg). P1 is the uppermost, P5 the lowest one.

6.3.2 Pesticide Transport in Soil

Recovery and depth transport

Table 6-1 and Table 6-2 list the mass of the recovered pesticides during the first experiment. The total recovery within the soil is 14 g for IPU (17.5%) and 1.8 g of FLU (9%), based on the averaged recovery rates of the P1, P2, and P3. Due to possible degradation, P4 and P5 were not used to calculate the average recovery. The total recovery is clearly below the applied mass of 80 g (IPU) and 20 g (FLU) (cf. chapter 6.4 for possible explanations). This total recovery of order 10 – 20 % is not consistent with the recovery in the tile drain (<0.1%, see chapter 6.3.3) nor with the recovery of bromide (>100%). The variability between the soil profiles is huge, and no correlation between the pesticide and the bromide recovery is found.

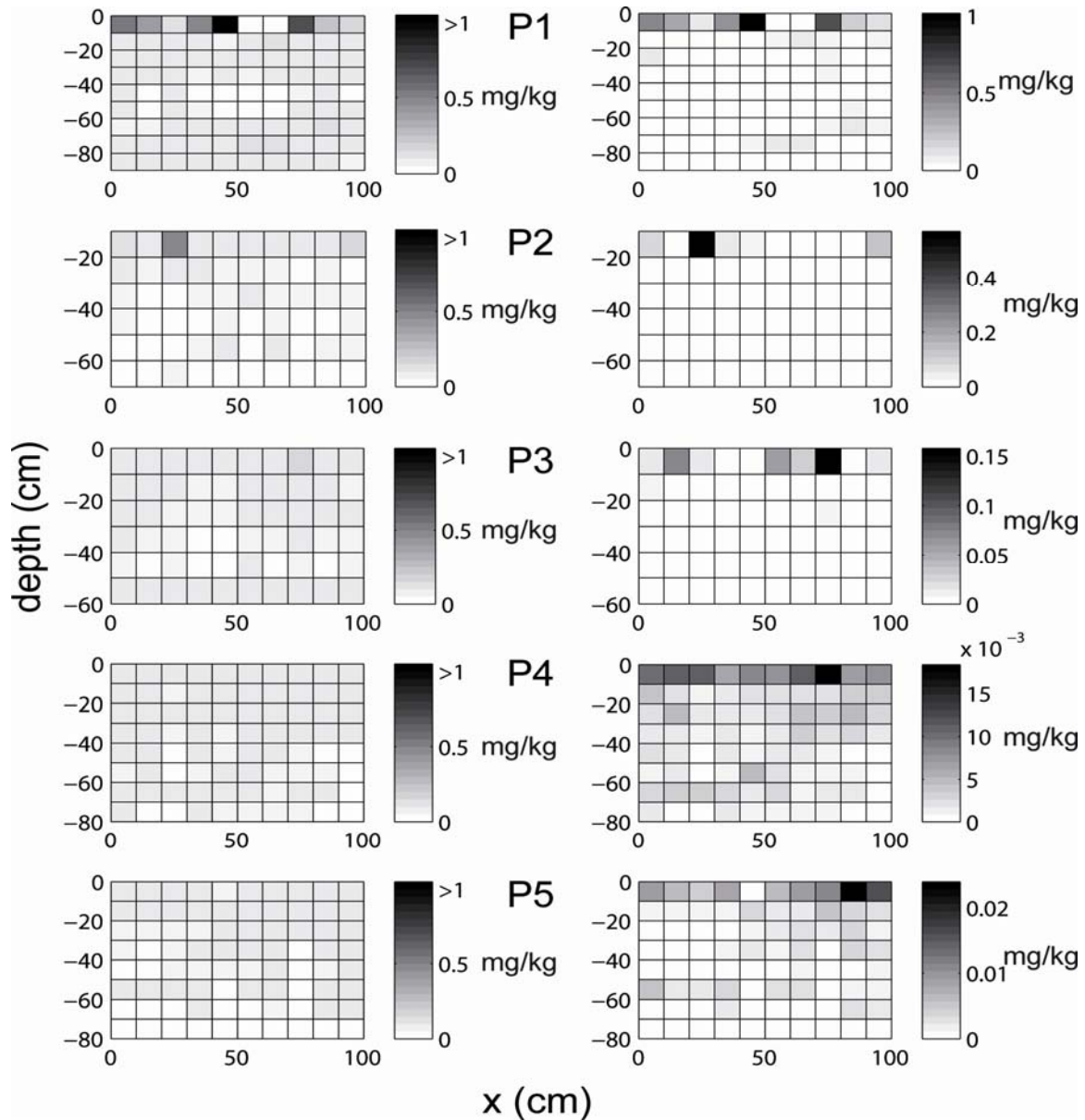


Figure 6-3: Isoproturon concentration profiles in two different grey scales (mg/kg dry soil); on the left side the concentrations are classified based on the maximum concentration in all profiles; on the right side the grey scale ends at the highest concentration for each profile.

Figure 6-1, Figure 6-3, and Figure 6-4 show that IPU and FLU have been transported into larger soil depths. IPU was found at a depth of up to 80 cm, while FLU was detectable in depths between 60 and 70 cm. Within P3, P4, and P5 IPU depth transport is more pronounced than FLU depth transport (Figure 6-1). Within P1 the shape of both pesticide concentration profiles is in very good accordance with the profile of the bromide concentrations. IPU and FLU normalised concentration profiles are similar in P1 and P2, with pronounced transport in P1 and weak transport in P2. The normalised concentrations however show a different normalised concentration profile in soil of profile P3. Although P4 and P5 are seven days old and pesticide concentrations are probably influenced by degradation, those give evidence about transport behaviour at the weekly scale. IPU and bromide concentration profiles converged one week after the experiment.

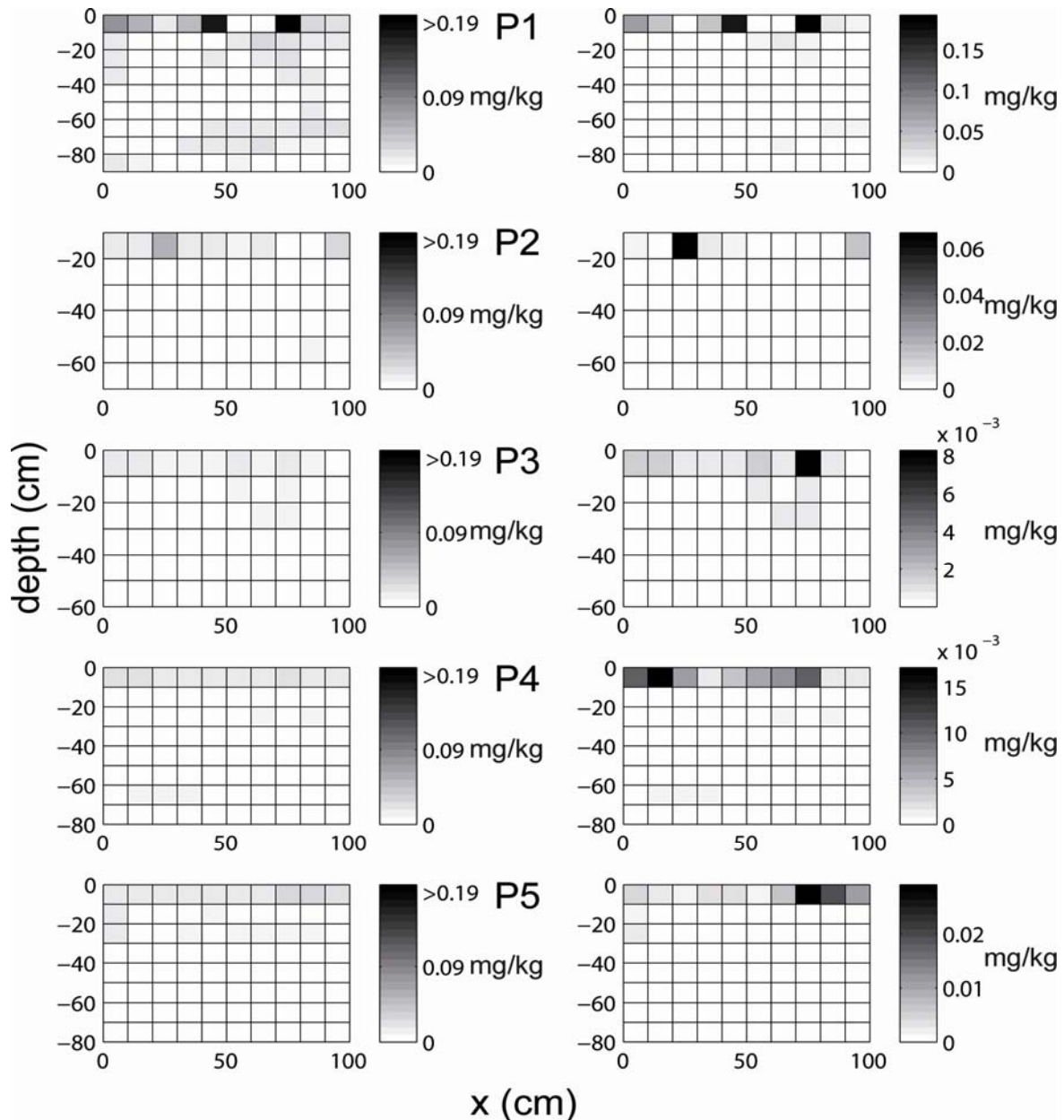


Figure 6-4: Flufenacet concentration profiles in two different grey scales (mg/kg dry soil); on the left side the concentrations are classified based on the maximum concentration in all profiles; on the right side the grey scale ends at the highest concentration for each profile.

Retardation compared to bromide

IPU with a K_{oc} of 122 ml/g and FLU with a K_{oc} of 202 ml/g (Footprint, 2006) are slightly different in terms of their sorption behaviour. This difference should influence the retardation coefficient compared to bromide. Table 6-1 presents the retardation coefficients based on the maximum sampling depth, while Table 6-2 presents the retardation coefficients based on 60 cm sampling depth. The retardation coefficients based on 60 cm depth are slightly less than those for the total sampling depth. The retardation and transport characteristics are clearly different between each soil profile, proving the influence of soil structure on the transport. The retardation coefficient of IPU compared to bromide is between 1.26 and 2.94 with a mean value of 1.8, while the retardation coefficients of FLU, as expected from the K_{oc} values, are higher with 1.97 to 4.6 and an average of 3.31. The proportion between the average

retardation coefficient of IPU and FLU in the soils of the field plot (0.6) is similar to the relation of the K_{oc} values (0.54).

Table 6-3 presents the impact of sampling depth on the retardation coefficient within one soil profile, P1 in this case. The retardation coefficient was calculated assuming that sampling was stopped in P1 at 10 cm, 20 cm, and so on. At 50 cm depth the retardation coefficient of IPU reached 10% deviation to the final value and remains rather constant, while the retardation coefficient of FLU changes from depth to depth until it reached the final value at 90 cm depth. Thus the retardation coefficient of pesticides is affected by sampling depth.

Table 6-3: Retardation coefficients of the pesticides compared to bromide in P1. For each depth only the mass above this depth was included in the calculations.

Depth (cm)	R_IPU (-)	R_FLU (-)
10	1.00	1.00
20	1.36	1.37
30	1.50	1.67
40	1.59	1.83
50	1.73	1.99
60	1.90	2.28
70	1.75	2.15
80	1.74	2.30
90	1.96	2.70

How many soil profiles are needed to describe transport variability?

Figure 6-5 presents data about the development of the retardation coefficients of IPU and FLU and the dispersion coefficient, when using P1 (based on 60 cm transport depth), the average of P1 and P2, the average of P1, P2, and P3, etc. Additionally, the variance is given with the error bars. Since neither the retardation coefficient nor the dispersion coefficient turn to a constant value after accounting for the average over five profiles, the variability of transport parameters on the field plot are not captured by these five profiles.

Summary on pesticide transport in the soil

The concentration patterns in Figure 6-3 and Figure 6-4 are strongly scattered, which suggests that the pesticides must be transported within preferential flow paths. While the concentrations are low in a depth of 40-60 cm, isolated patches with higher pesticide concentrations can be found in the deeper soil parts, where microbiological degradation might be low (Bolduan and Zehe, 2006). The retardation coefficients show a high spatial variability in the transport behaviour at the experimental site. Although IPU and FLU are clearly retarded compared to bromide, they reach a depth where they endanger the apparent shallow groundwater at this site and can leach into the tile drain, as found in chapter 6.3.3. The use of five soil profiles showed to be too little to describe the field scale transport variability.

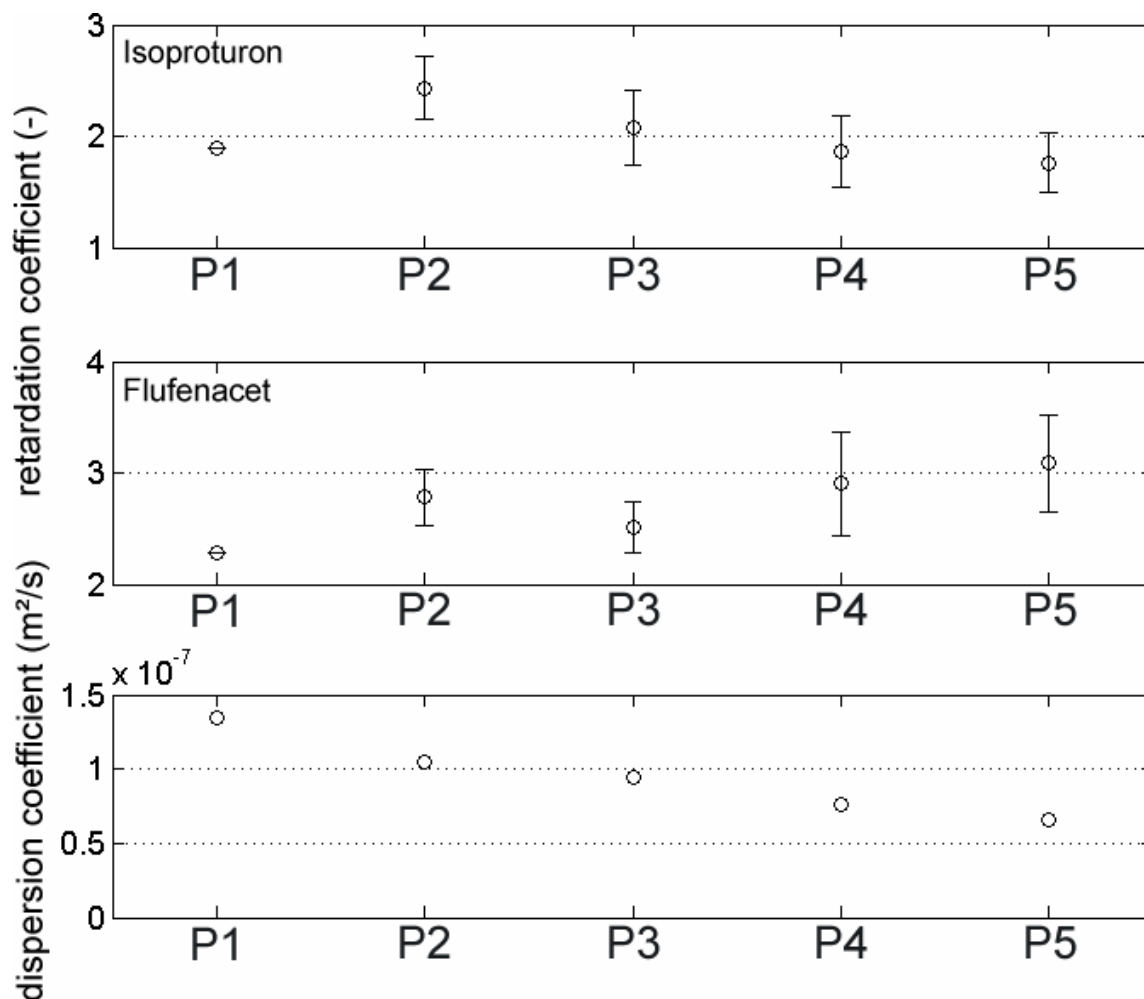


Figure 6-5: Average of the transport parameters based on the mean of one, two, three, four, and five soil profiles. The retardation coefficients of the pesticides Isoproturon and Flufenacet are presented in the upper two subplots, while the dispersion coefficient is presented in the lower subplot. The variance is given by the error bars.

6.3.3 Solute breakthrough and travel time distribution in the tile drain

Experiment 1

Bromide breakthrough

Figure 6-6 presents the bromide concentrations in tile drain discharge for the first experiment. Fifty minutes after tracer application bromide was detected for the first time in the tile drain. When neglecting the transport time in the tile drain, this corresponds to a travel velocity through the soil of 3.64×10^{-4} m/s, as the tile drain is located at 1.2 m depth. Bromide concentration increased continuously up to 0.85 mg/l at the beginning of the second irrigation block, then shortly decreased, to rise again to a peak value of 9.18 mg/l that occurs 175 min after irrigation onset. The first peak in tile drain discharge occurred 9 min later and at this time the concentrations were significantly lower (7.95 mg/l) and decreased further to a concentration minimum of 5.89 mg/l after 210 min. This concentration minimum is in near perfect coincidence with the local discharge minimum. The overall maximum bromide concentration of 15.41 mg/l occurs 280 minutes after the onset of the experiment, which is slightly earlier than the discharge peak.

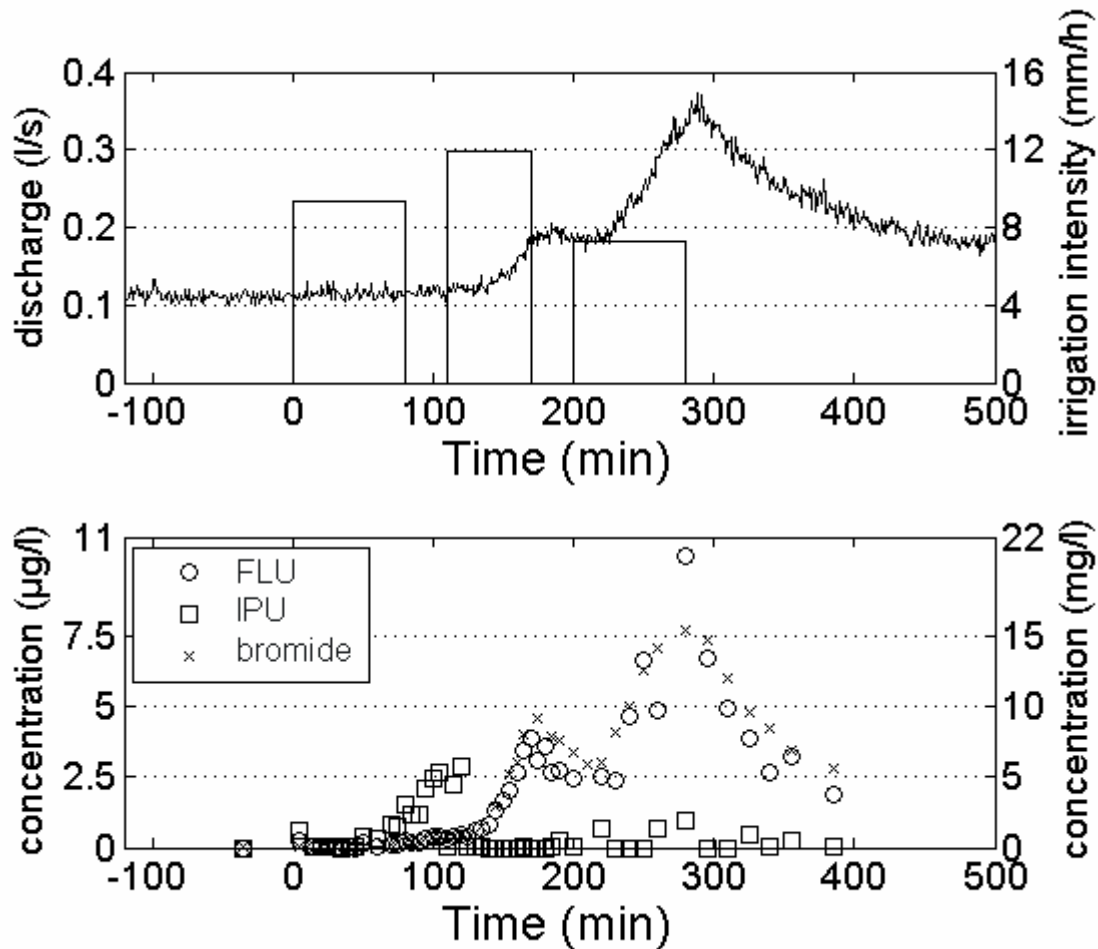


Figure 6-6: Breakthrough curve of bromide and the pesticides in the tile drain (lower panel) and the corresponding discharge and irrigation rate (upper panel) of the first experiment.

From the bromide samples of the days after the experiment only those of the first day after the experiment exhibited bromide concentrations above the detection limit. Bromide concentrations on the rising limb of the hydrograph are strongly correlated to discharge, with an $R^2=0.92$. The total mass recovery for bromide after one week of sampling was 59.03 g which corresponds to 3.69 % of the applied mass and 44.08 g (2.76 %) within 12 h after experimental start (Table 6-4).

Pesticide breakthrough

Water samples taken shortly after pesticide application and before the onset of irrigation showed no traces of the pesticides (Figure 6-6). After the onset of the irrigation, both pesticides were already detectable in the first water sample (taken 5 min after irrigation onset). Fifty minutes after irrigation onset the concentration for both pesticides started to increase almost continuously with time. While IPU concentrations peaked at a value of 2.91 µg/l after 120 min, FLU concentrations kept on rising. During the further course of the experiment, IPU concentrations dropped to nearly zero and recovered around the time of the first discharge peak. The second peak in IPU concentration (1 µg/l) coincided with the peaks in bromide and FLU concentration and the second discharge peak (Figure 6-6).

Table 6-4: Characteristics of the BTCs of the three experiments. For inter comparability, the calculations were performed on a 720 min period after the experiment started.

Recovery (mg)			
	Experiment 1	Experiment 2	Experiment 3
bromide	44083 (2.76%)	51810 (2.16%)	11625 (0.48%)
FLU	18.82 (0.09%)	3.23 (0.008%)	0.22 (<0.001%)
IPU	1.68 (0.002%)	0.01 (<0.001%)	0.15 (<0.001%)
center of mass (min)			
	Experiment 1	Experiment 2	Experiment 3
bromide	310.9	304.9	285.4
FLU	289.2	296.4	217.4
IPU	205.0	66.6	309.7
Retardation coefficient (-)			
	Experiment 1	Experiment 2	Experiment 3
FLU	0.93	0.97	0.76
IPU	0.66	0.22	1.08

FLU concentrations were strongly linearly correlated with bromide concentrations with an $R^2=0.9$, and peaked at a value of $10.31 \mu\text{g/l}$ (after 280 min). In contrast, I found no significant correlation between either the concentrations of the different pesticides or between IPU and bromide concentrations. Concentrations of the two pesticides in the days after the experiment showed no clear pattern, except that FLU concentrations remained larger than IPU concentrations. Mass recovery for IPU was very small, with 2.34 mg, which corresponds to 0.0029 % of the applied mass. Mass recovery of FLU was 24.82 mg (0.12 % of the applied mass). Both recoveries are based on all samples (seven days). To compare the transport behaviour of all three experiments, the 12 h recovery (RC_{12}) was calculated. RC_{12} was 1.68 mg (0.0021%) for IPU and 18.82 mg (0.09%) for FLU.

Experiment 2

Bromide breakthrough

After 100 minutes the first bromide sample exceeded the background, which is slightly before the increase of discharge (Figure 6-7). In this case, maximum transport velocity is 2.35×10^{-4} m/s and only 65% of the maximum flow velocity of the first experiment. Bromide concentrations show a strong correlation to the behaviour of the hydrograph. On the rising limb of the hydrograph the coefficient of determination of a linear regression between discharge and bromide concentrations is 0.9. Bromide concentration peaks at 10.1 mg/l (minute 160) and at 16.8 mg/l (minute 276), just around peak discharge time (164 min, 276 min). The concentration after the end of irrigation is slightly decreasing. The day after the experiment concentrations are still above detection limit.

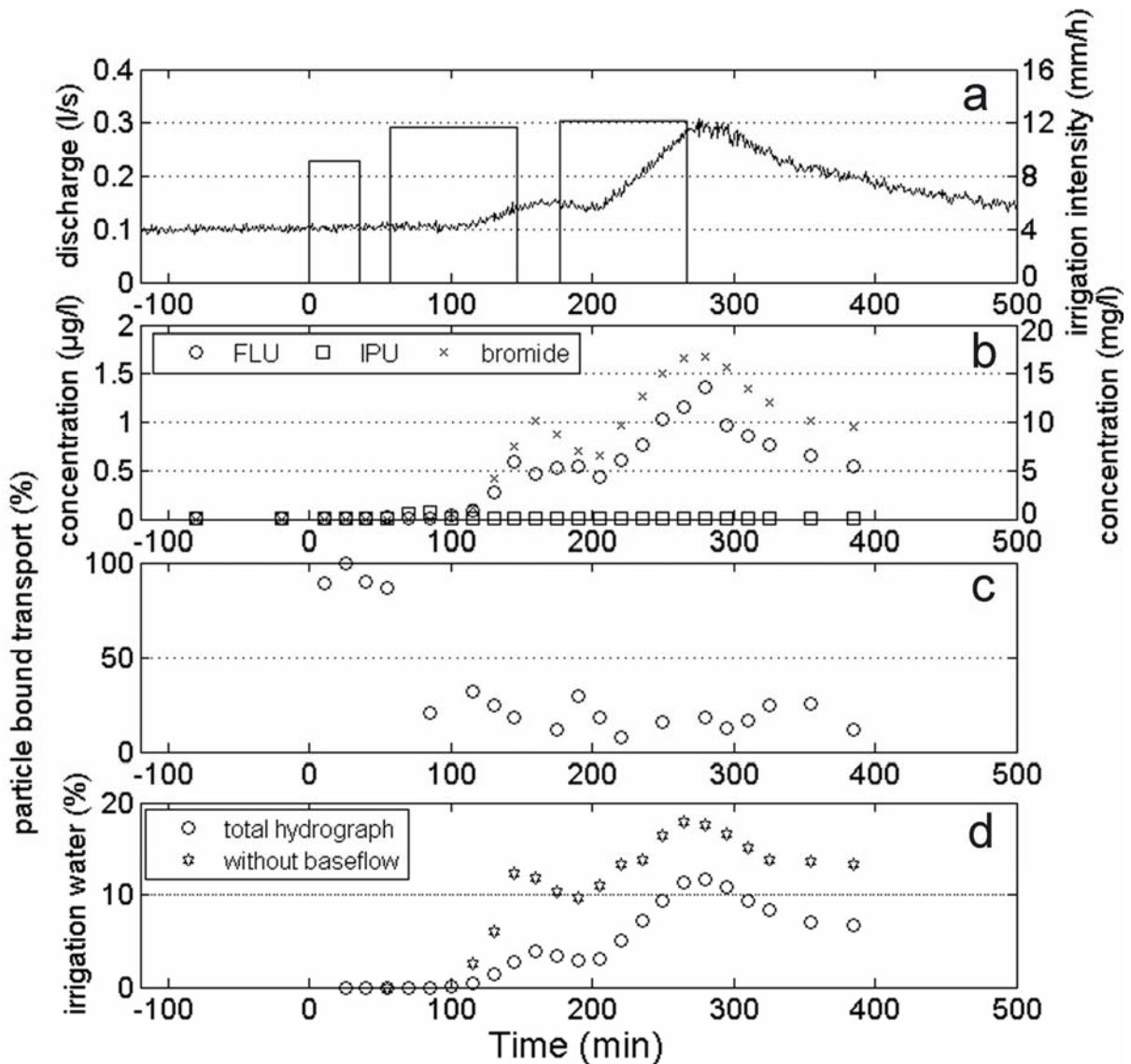


Figure 6-7: Tile drain reaction of the second experiment. a) discharge (l/s) and irrigation rate (mm/h), b) breakthrough curve of bromide and the pesticides in the tile drain, c) the proportion of particle bound FLU transport over the course of the experiment, d) and the proportion of event/irrigation water in the tile drain hydrograph.

During the second experiment no long term behaviour of solute transport was evaluated. Sampling stopped the day after the experiment. After 12 h a recovery of 51.81 g (2.16%) was achieved. Although irrigation and tracer application were similar in the first and second experiment, the first bromide occurrence was later and the total recovery was less in the second experiment compared to the first one.

Pesticide breakthrough

Figure 6-7 presents the breakthrough curve of the pesticides and bromide together with irrigation and the discharge. IPU concentrations were rather constant with a small peak 85 minutes after irrigation started, with $0.065 \mu\text{g/l}$. The IPU concentrations mainly remained below $0.01 \mu\text{g/l}$. This is surprisingly low, especially considering the higher application amount compared to the first experiment. Again, no correlation between IPU and bromide or of IPU and discharge was found. RC_{12} was $14.7 \mu\text{g}$ ($<0.00001\%$), see Table 6-4.

Again, FLU concentrations are distinctly exceeding the concentrations of IPU. FLU concentrations are constantly increasing, starting from about 100 minutes after the irrigation started. A first peak, with 0.59 $\mu\text{g/l}$ (145 min) and a main peak, with 1.36 $\mu\text{g/l}$ (280 min), were detected. The first smaller peak is 20 min before the first discharge peak, the second FLU peak falls around the main discharge peak that occurred 280 min after irrigation started. Again, FLU is strongly linearly positively correlated to bromide, the coefficient of determination R^2 is 0.97. In total 3.23 mg (0.008%) were exported via the tile drain, the RC_{12} is presented in Table 6-4.

Experiment 3

Bromide breakthrough

Background of bromide in the tile drain baseflow was below detection limit, indicating no or very limited connectivity of the soils to the tile drain. It has to be kept in mind, that 3 weeks before the experiment 2400 g of bromide were applied on the field plot, while only a few percent were exported during the second experiment, thus a large amount of bromide must have been stored in the soil. No additional bromide was added to the system during this irrigation experiment. Bromide was detected 105 min after irrigation start with 0.57 mg/l the first time and peaked 225 minutes after the experimental start with 7.48 mg/l, showing a strong and fast decrease afterwards (Figure 6-8). Again, the bromide concentrations are strongly positive correlated to discharge ($R^2=0.96$). In total 11.63 g of bromide were recovered within 12 h after the start of the irrigation, this is 0.48% of the bromide mass applied three weeks before in the second experiment (Table 6-4).

Pesticide breakthrough

No background concentrations of FLU and IPU were found in the tile drain prior the experiment, similar to the findings of bromide (see chapter 6.3.3). Figure 6-8 presents the breakthrough of the two pesticides during the third experiment. Both pesticides were detected above detection limit 105 minutes after irrigation start, coincident with the first occurrence of bromide. IPU showed a plateau concentration of around 0.06 $\mu\text{g/l}$ from minute 200 to the end of sampling. Within this experiment, IPU and bromide were correlated for the first time, with $R^2=0.84$. In this experiment IPU, behaves different compared to the experiments before. Surprisingly, RC_{12} was significantly higher compared to the second experiment that was performed three weeks before. The recovery was 0.15 mg (0.000024%), see Table 6-4.

FLU increased from the first occurrence to the peak at minute 210 (0.39 $\mu\text{g/l}$) and decreased from this moment onward. This peak might be an outlier, as it is exceeding every other sampled value by a factor of two. FLU is again linked to bromide, but less compared to the two experiments before. The coefficient of determination was 0.61, without considering the outlier, R^2 increases to 0.88, similar to IPU. During this experiment 0.22 mg (0.00055%) of FLU leached in the tile drain, see Table 6-4. Within the third experiment, three weeks after

the pesticide application, both pesticides could be remobilised from the soil and leached into the tile drain.

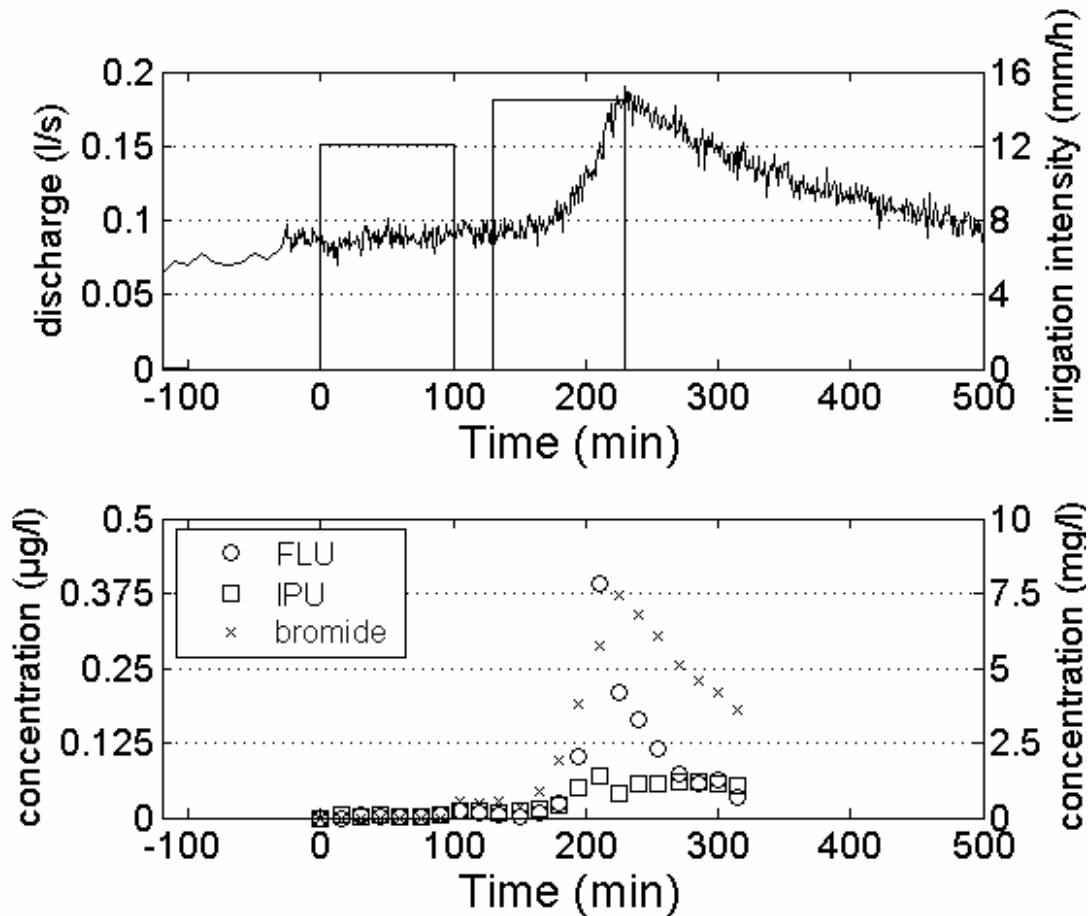


Figure 6-8: Breakthrough curve of bromide and the pesticides in the tile drain (lower panel) and the corresponding discharge and irrigation rate (upper panel) of the third experiment where no tracer were applied.

6.3.4 Effective retardation coefficients based on bromide and pesticide losses

Based on the recovery and the timing of the centre of mass, the retardation coefficients of the pesticides could be calculated for each experiment. The results are summarised in Table 6-4. IPU shows an irregular pattern of retardation coefficients. In the first and second experiment, IPU was transported faster than bromide (retardation coefficient: 0.65 and 0.22), while it is transported slower in the third experiment (retardation coefficient: 1.08). The pattern for FLU is more homogeneous, while the retardation coefficient is around 0.9 for the first two experiments it is with slightly smaller (0.76) for the third experiment. FLU is always transported faster than bromide, but with clearly smaller recoveries.

Figure 6-9 presents the temporal development of the retardation coefficient of FLU during the first experiment in the tile drain. The inner subplot presents the first six hours of the experiment, while the main plot presents the total sampling period (seven days). At the beginning of the experiment FLU is transported faster than bromide ($R < 0.5$). In the course of

the experiment the retardation coefficient is increasing towards 1, and remains around 0.9 from the day after the experiment to the end of sampling. Thus, FLU is transported slightly faster at the beginning of the experiment than bromide, with a mass fraction that is too small to affect the long term retardation coefficient. The transport after the experiment is not changing the retardation coefficient, as the mass transport is also too small.

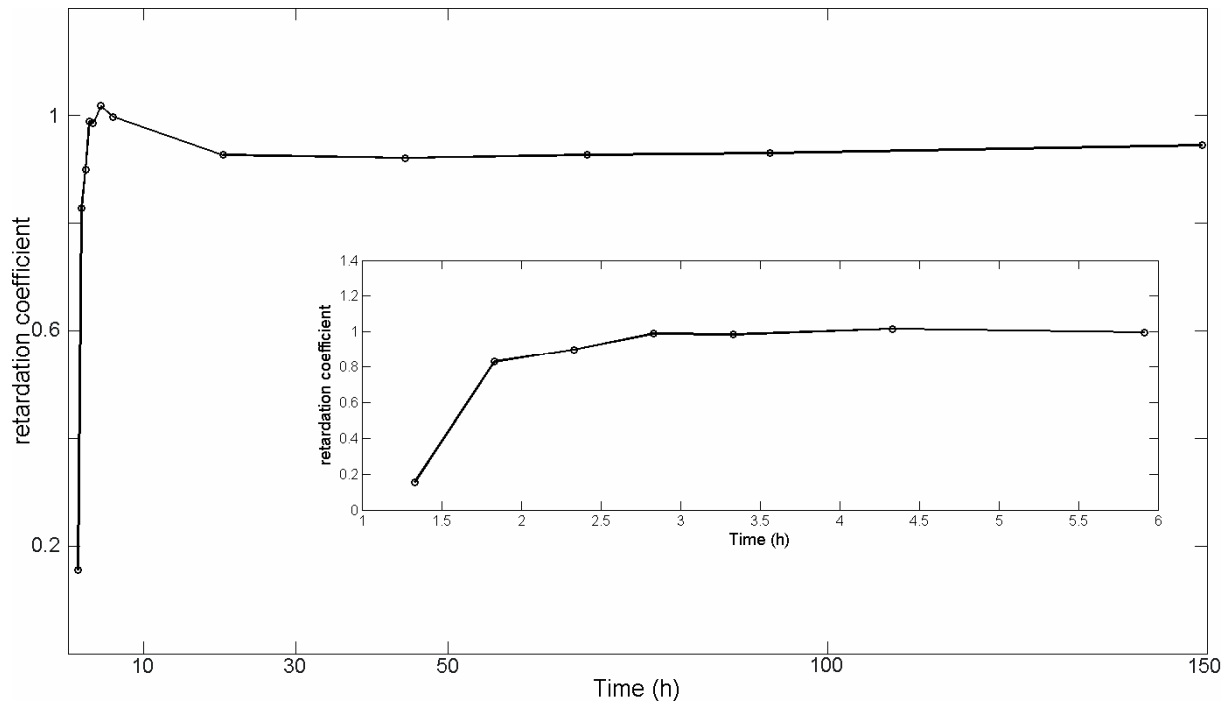


Figure 6-9: Temporal development of the retardation coefficient of FLU compared to bromide during the first experiment. The inside panel presents the initial phase (6 h) of the experiment.

6.3.5 Particle bound transport

Figure 6-7c presents the fraction of particle bound transport (<200nm) of FLU over the duration of the second experiment, Figure 6-7d presents the fraction of event water (see chapter 5.3.4). Following very high fractions of particle bound transport at the beginning of the experiment, the fraction of particle bound transport turns into a level of about 20% of the actual transported mass. The fraction of particle bound transport is neither correlated to the total FLU concentration, nor to the discharge. At the initial phase of the experiment particle bound transport seems to be the dominating process. Since the concentrations of FLU are very low during this phase, the difference between the particle bound and the total transport is very small, thus the finding may be erroneous. Nevertheless, particle bound transport (<200 nm) of FLU is a relevant process at this field site and accounts for about 20% of the total transported FLU mass. The concentrations of IPU were very small, so it was difficult to distinguish between particle bound transport and water transport, since the difference was often within the analytical error. Thus I do not present these results.

6.4 Discussion

6.4.1 Spatial variability of solute transport behaviour in the field soils

The excavation of different soil profiles on field scale showed a high variability within the soil profiles. The retardation coefficient of IPU and FLU, the recovery of bromide, IPU, and FLU, and the dispersion coefficient of bromide are highly spatially variable over the experimental plot. There is no correlation between the bromide recovery and the pesticide recovery. Nevertheless, the relation between IPU and FLU recovery is constant in the soil profiles P1, P2, and P3.

Both pesticides are applied in a homogenous way with the mounted spray bar, while bromide followed the non-uniform irrigation pattern (see chapter 5.3.2). Additional surface and subsurface redistribution by micro-topography (Weiler and Naef, 2003a) and lateral flow in the soil (Sinai and Dirksen, 2006) can lead to spatially variable recoveries. The very high recovery of the pesticides in P1 compared to the other soil profiles can be explained by the position of the soil profile. It is near the tile drain and near the boundary of the field plot. By the location near the drain, the moisture regime is more moderate than with more distance to the drain, leading to higher earthworm populations enhancing infiltration. Near the boundary of the field plot, the application rate of the pesticide has been higher than at other parts of the field plot, as the tractor remained there a moment longer during pesticide application. The variability of the dispersion coefficient is driven by variability of the preferential flow system. Starting with the transport parameters of one profile, and taking more and more profiles into account to calculate the average transport behaviour did not lead to stable transport parameters (see Figure 6-5). Thus, the study of the transport parameters in the five soil profiles, showed a) the limitation of the assessment of pesticide transport based on soil profiles, and b) that the variability at field scale can not be caught by five profiles.

6.4.2 No full pesticide recovery – degradation or unsatisfying sampling procedure?

An interesting issue in the pesticide recovery is that there is a huge gap between the applied pesticide amounts, the sum of tile drain exported pesticide, and pesticides recovered from the soil samples. In contrary, the bromide recovery exceeds the applied mass. A recovery exceeding 100% for bromide can be explained by the spatial variability of bromide concentrations in the field, redistribution, and sampling background. Thus five soil profiles were not able to cover the field scale variability of the distribution of a conservative solute. Nevertheless, the gap in pesticide recovery is too high to be explained by those reasons. Therefore the differences in the recovery of bromide and the recovery of the pesticides must be explainable by the differences in their chemical properties. At first, the degradation plays a role. The shortest DT-50-value (the time that is needed to degrade 50% of the mass) of IPU and FLU in literature is 7.2 days and 15 days respectively (Footprint, 2006). P4 and P5 are sampled seven days after the experiment, P1-P3 one and two days after the experiment. The samples were cooled until they were frozen 24-48 hrs after excavation. Assuming that micro-organisms had seven days to degrade both pesticides in the samples, the recovery should be

around 50% for IPU and 75% for FLU respectively. Thus degradation can only account for a part of the gap in recovery.

Due to their high K_{oc} compared to bromide, pesticide transport within the soil matrix is slow, they are retarded, and partly absorbed in the soil matrix. By the sampling scheme of centring a soil core with 5.3 cm diameter in each of the 10 cm on 10 cm grid cells, the upper 2.35 cm of a grid cell are not sampled. Thus it is possible that high proportions of the pesticides remained in the upper two centimeter of the soil, as found for FLU by Rouchaud et al. (2001), and are therefore missed by the sampling. A higher resolved soil sampling would be needed to account for an appropriate recovery of strongly non-conservative solutes. In summary, the low recovery of pesticides can be explained by degradation between the time point of pesticide application and the time point of freezing, and by limitations of the sampling scheme.

6.4.3 Profile information versus integral information

Kung et al. (2000) noted the problem of the right sampling protocol to assess pesticide leaching. They stated in their study that using a tile drained field site as a natural lysimeter (e.g. Richard and Steenhuis, 1988), as done within this work, is an improvement compared to collecting soil cores at various sampling locations once every day.

Within this study I assessed the travel distance distribution in the soil on a time scale that is linked to the time scale of significant solute transport (1 day, 2 days, and 7 days). The retardation coefficients of IPU in soil profiles were, on average, 1.8 (standard deviation: 0.7) which is in accordance with the study of Besien et al. (2000) and Zehe and Flühler (2001a). The former study compared bromide and IPU in unsaturated chalk columns and found a retardation of 1.23, while the later study found retardation coefficients between 0.7 and 2.3 in the soils of the Weiherbach catchment. FLU at the field site was much more mobile, as reported by Rouchaud et al. (2001). I found considerable leaching of FLU below 30 cm depth, even up to a depth of 80 cm, while Rouchaud et al. (2001) found no transport below 30 cm depth. The retardation coefficients determined by soil sampling are distinctly different to those determined by sampling the tile drain.

Compared to the collection of soil cores at various sampling locations, sampling a soil profile integrates more flow processes. The probability of observing preferential flow is higher. Nevertheless, recovery, retardation, and dispersion showed a high spatial variability at the study site. Thus the total extent of a single soil profile is much smaller than the representative elementary volume of the (macro-) porous medium at the field site. In summary, soil profiles based assessment of contaminant transport can only give a hint (by the depth transport) on pesticide leaching. They give no general information on the susceptibility of the soil and the pesticide for the timing of pesticide leaching or the amount of fast leaching pesticides to tile drains or shallow groundwater. The integral transport behaviour (tile drain) is different than the average behaviour of soil profiles.

6.4.4 Inconsistencies between FLU and IPU behaviour

Within the three irrigation experiments the behaviour of IPU was difficult to explain. Peak concentration and total recovery for FLU decreased between the second and third experiment, while this was not observed for IPU. Within the second experiment the application rates for both pesticides were higher than for the first experiment. Pesticide concentrations in the tile drain however are lower during the second experiment, while bromide concentrations are at least of a similar magnitude (Figure 6-6 and Figure 6-7). Especially the differences between the second and the third experiment lead to the suggestion that significant degradation took place in the sample bottles, although they were stored at 4°C in the dark. The higher IPU concentrations during the third experiment compared to the second experiment leads me to suggest that degradation in the stored sampling bottles was present. In addition, within the three weeks between the field experiments this degradation was faster in the sampling bottles than degradation in the field during the same time, explaining the differences in IPU. This has to be kept in mind at least when discussing the link between the hydrological behaviour and the transport of IPU and FLU.

6.4.5 Soil water flows driving pesticide transport

So far it is known that reactive solutes can be transported without retardation compared to conservative solutes in preferential flow paths (Everts et al., 1989; Kung et al., 2000), at least during the initial transport phase (Kung et al., 2000). Contrary to different breakthrough studies (Kung et al., 2000; Zehe and Flühler, 2001a), this work shows that bromide and FLU concentrations are not only transported fast, but that they are very strong correlated to the discharge (on the rising limb of the hydrograph), with R^2 exceeding 0.9 (see chapter 6.3.3), while IPU is not linked neither to discharge, nor to bromide concentrations.

The hydrograph separation within chapter 5.3.4 revealed the significant contribution of pre-event water from the soil matrix in the tile drain discharge. The maximum fraction of irrigation water (event water) was around 20% during peak discharge, the remaining 80% was pre-event water stored previously in the soil. Based on analysing isotopic composition of soil water (chapter 5.3.5), I found that fractions of irrigation water in soil samples reached up to 40% and were mainly between 10% and 30%. The observation of the discharge revealed a threshold like behaviour at the study site that is not driven by the actual precipitation amount, but by the actual connectivity and moisture at the field plot. The amount of transport and discharge was correlated to the antecedent precipitation and thus antecedent soil moisture of the field plot, underlining the role of the soil moisture at this field site at event scale (cf. Flury et al., 1995). Such behaviour is common threshold behaviour in hydrological systems (Zehe and Sivapalan, 2009). Precipitation controlled threshold behaviour was recently reported to account for significant pesticide leaching events in lysimeters (McGrath et al., 2010). My observations show that surface applied pesticides move slowly within the upper few centimeter of the soil with beginning irrigation and are additionally transported in a small mass fraction by the preferential flow paths during the initial phase of the rain (concluded based on the fast breakthrough in the first experiment). The solutes can enter the soil matrix over various depths by the interaction between the preferential flow paths and the soil matrix.

As long this threshold is not exceeded, there is no hydrological connectivity of the soil to the tile drain, and soil pores with large diameters are not active with high water tensions (Jarvis, 2007). If this saturation threshold is crossed a connectivity of the macropore system and the tile drain is established, similar to the observation for hillslopes (Lehmann et al., 2007). Additionally, the pesticides are directly transported to the tile drain or deeper soil layers by the preferential flow paths. The stored soil water is entering the macropores, mobilising the stored pesticides. Furthermore, the soil water that enters the macropores reduced the potential for the pesticide transported in the macropores to reach the adsorption places at the macropore coating or in the soil matrix. These processes are explaining the strong correlation between FLU and discharge, not the behaviour of IPU (see discussion on inconsistency in chapter 6.4.4). Overall, these processes enhance the risk of remobilisation of pesticides stored in the upper soil, especially when considering that the soil water stems from the upper soil (see chapter 5.3.7). This remobilisation of pesticides was showed in the third experiment, and is in accordance with the studies of Kladviko et al. (1999) and McGrath et al. (2010). Both found significant pesticide transport for more than the first rain event after application. This process can be explained by the role of “old water” in the total discharge. In the study of McGrath et al. (2010) the event that was responsible for the highest amount of pesticide leaching occurred more than 200 days after pesticide application, showing the relevance of long term pesticide storage.

About 20% of particle bound transport was observed for FLU. This fraction stayed constant throughout the experiment. While particle bound transport contributes a relevant amount to the total leached mass, it has no significant effect on the timing of the FLU occurrence and the development of the retardation coefficient. While Zehe and Flühler (2001a) suggested that particle bound transport is the major reason for the very fast occurrence of the peak concentration in the tile drain on an experimental plot in the same catchment, the data of this experiment does not support this assumption. Nevertheless there might be a fast transport of particle bound FLU in the initial phase, but the absolute difference between particle bound and total transport was too small and uncertain to prove that.

In summary, the observations within this study showed that the pesticide transport driven by water dynamics does not per se exist as observed by Kung et al. (2000), but that a hydrological threshold controls pesticide transport and leaching at this field site. While (McGrath et al., 2010) showed that pesticide leaching is linked to hydrological threshold behaviour at lysimeter scale, I was now able to reveal a similar process at field scale. This threshold controls both the initial transport during the first rain event after pesticide application and the remobilisation of stored pesticides, at least at this study site.

6.5 Conclusion

Using the results from chapter 5 and combining the observed pesticide transport with detailed understanding of hydrological processes at the field plot enhanced the understanding of pesticide transport. While particle bound pesticide transport and rapid pesticide transport in

preferential flow paths occurred, the dominating process leading to pesticide transport, leaching, and remobilisation is a threshold controlled hydrological behaviour at the field site. This process supplies soil water to discharge, enables connectivity within the preferential flow network, and limits the accessibility to the adsorption places. This has not only consequences for the first leaching event, but also on remobilisation of pesticides, as soil water contributes to tile drain discharge when this threshold is crossed.

I used two different sampling protocols to determine the transport behaviour of conservative and reactive solutes, soil profiles and tile drain sampling, and compared their value. With five soil profiles it was not possible to capture the overall field scale variability of the transport parameter in the soil (recovery, retardation, and dispersion). The pesticide recovery was additionally limited by the soil core sampling procedure and degradation processes.

The total extent of a single soil profile is much smaller than the representative elementary volume of the (macro-)porous medium at the field site and only presents the solute mass distribution at the time of sampling and does not sample quickly transported mass fractions. In contrary, the sampling in the tile drain revealed the fraction of solutes that travelled with high speed through the soil profile, which is corresponding to the fast part of a transit time distribution (McGuire and McDonnell, 2006). Thus different parts of the transit time distribution of solutes are sampled when the two sampling protocols are used. With the tile drain, the fraction of pesticides with a very short transit time are described, while the soil profiles provide long term insight into the remaining solutes within the system, thus the residence time. Yet we have to develop new ideas to bring both information together, as a long term sampling of pesticides in high temporal resolution is financially very demanding. Nevertheless, confirming the process of threshold controlled pesticide transport on field scale, additional to the known process on lysimeter scale (McGrath et al., 2010), will enable to better risk assessment of pesticide leaching, controlled by hydrological processes.

Finally I can conclude, referring to the research questions (6.1.3):

- Transport behaviour derived from soil profiles clearly differs from the retardation observed in the tile drain discharge, representing different parts of the transit and residence time distribution. The soil profiles represent different processes than the tile drain; an approach combining them might replace long term tile drain sampling. With an approach that used five soil profiles to assess the field scale transport behaviour, I was not able to determine the average transport behaviour at the field site distinctly. Although the value of soil profiles to determine the susceptibility of soils for short term leaching is limited, the depth transport of both pesticides to the maximum sampling depth might allow a suggestion of leaching susceptibility.
- I identified that a soil moisture controlled threshold process (see also chapter 5) controlled the time point of clear discharge increase. The fast transport of reactive solutes without retardation and the remobilisation could be attributed to this threshold. Thus, understanding of the detailed preferential flow processes clearly enhances the

understanding of pesticide leaching on event and long term scale and can further improve risk assessment and modelling approaches.

- Particle bound transport at this field site is responsible for about 20% of total transport. This proportion in total transport is relatively constant throughout the experiment, therefore the particle bound transport process cannot fully account for the reduced pesticide retardation, but contributes a relevant part to the total leached mass.

7 Linking macroporosity with the population of *Lumbricus terrestris* L. - a first attempt to obtain observable structure information for model parameterisation

In the introduction to this thesis the need of a model approach that links the representation of preferential flow in models more explicitly to experimental data and to observable structures was suggested (see chapter 1.4). This might improve modelling of preferential flow processes and lead to a better representation of water and solute transit times and thus might allow better hydrological modelling in the sense of Seibert and McDonnell (2002). They suggested that it is better to be “less right for the right reason” and having a better process representation in a model than being “right for the wrong reason” in modelling. This chapter presents the mapping of such observable structures – the vertically oriented macropores of the Weiherbach catchment. Further it is investigated whether it is possible to infer such information on a larger scale by data about the abundance of the deep burrowing earthworm *Lumbricus terrestris* L. If successful, this would allow catchment scale maps of macroporosity when combined with a population model of earthworms. These maps could be used to improve spatial information of process based hydrological models. The sampling was performed at different seasons. The correlation between density of macropores to the number and biomass of *Lumbricus terrestris* L. was investigated. This chapter starts with a short introduction of factors influencing macroporosity and first studies that link earthworm data to the susceptibility of soils to preferential flow. Then the methods and the field campaign are introduced. The results are presented and then discussed, before conclusions are drawn.

7.1 Introduction

Catchment scale description of the occurrence of preferential flow paths is a challenging task. The degree of potential preferential flow occurrence depends on soil-structure and biological and human influence on soil structure, thus leading to site specific preferential flow patterns. Bouma (1990) summarised different soil properties influencing preferential flow in soils: surface relief, surface texture, and water repellency. Additional non soil related factors like soil tillage (e.g. Andreini and Steenhuis, 1990), precipitation characteristics (e.g. Bouma, 1990), and soil moisture (e.g. Bouma, 1990) affect the occurrence of preferential flow. Temporal or seasonal variability of preferential flow can be induced by soil tillage, swelling and shrinking processes, and biological activity. A further overview of the several processes influencing potential and actually occurring preferential flow is made in chapter 1.1. While different processes like soil tillage (Andreini and Steenhuis, 1990) and surface erosion can destroy or seal preferential flow paths, those flow paths were found to be temporally stable for decades in deeper soil layers, evidenced by a study based on radionuclides (VandenBygaart et al., 1998; Hagedorn and Bundt, 2002). The earthworm *Lumbricus terrestris* L. is an important factor in the formation of preferential flow paths in the Weiherbach catchment. The susceptibility of the soils to preferential flow was found to be dependent on the slope position of the soil (Zehe and Flühler, 2001b).

The role of preferential flow was described earlier. In summary, preferential flow plays an important role in the hydrological behaviour of hillslopes (e.g. Weiler and McDonnell, 2007) and catchments (e.g. Zehe and Blöschl, 2004), and have a significant impact on solute transport (e.g. Flury, 1996). Various models were developed to account for preferential flow over different scales (see chapter 1.3 for a summary and relevant literature).

Within chapter 3 I parameterised the model CATFLOW with additional information on the density of preferential flow paths and successfully modelled water and solute transport of a tile drained field site. The parameterisation of a catchment scale model with information about the spatial and temporal variability of preferential flow paths might clearly improve the model performance. Yet, it is still challenging to parameterise hillslope models, or even catchment models with such information, since they are difficult to access. Thus an approach is needed that can predict the occurrence of preferential flow pattern by easily obtainable information. Within chapter 6 I showed that the average field scale transport parameters of solutes could not be covered by five soil profiles. An idea is to access such information on field scale by biological information that allows inferring to average transport behaviour. Jarvis et al. (2009) investigated if the susceptibility of soils to macropore flow could be predicted by different soil parameters. They concluded that macropore flow can be predicted to a sufficient degree based on easily obtainable soil information and site specific information. Lindhal et al. (2009) was able to predict the abundance of *Lumbricus terrestris* L. based on soil information. Such information is also taken into account by the approach of Jarvis et al. (2009). The most important influence on the abundance of *Lumbricus terrestris* L. were

“perennial land use, no-till arable cropping, organic additions (i.e., manure), and medium-textured soil” (Lindahl et al., 2009).

This thesis was carried out within the BIOPORE project (see chapter 2.3), a hydro-ecological research project, that aims to develop a species distribution model for *Lumbricus terrestris* L. that can predict spatial and temporal earthworm abundance. Based on such a model the occurrence of preferential flow on hillslope to catchment scale should be predicted based on the link between plot scale earthworm abundance and the corresponding macroporosity. Such information of macroporosity could also be used to parameterise the hillslope module of CATFLOW (see chapter 3.2.1).

Within this chapter I made an initial attempt to link information of the population of earthworms to the pattern of macropores, which may be seen as potential preferential flow paths. The working hypothesis supplying the foundation of this chapter is: “Information about the number of *Lumbricus terrestris* L. individuals and their biomass can be used as an indicator for macroporosity and thereby improve predictions of the occurrence of preferential flow”. Thus I performed a field study in the Weiherbach catchment at different locations to study the correlation between macropores and *Lumbricus terrestris* L.

7.2 Methodology

To account for the temporal variability of a) the population dynamics of *Lumbricus terrestris* L. and b) of soil structures acting as preferential flow paths I used two different seasons for the field observations. The data was collected in April and the following October. The field sites were chosen to account for different agricultural crops and soil types to the field sites. I avoided sampling field sites that were tilled shortly before the sampling. Figure 7-1 presents the sampling locations for the field observation within the Weiherbach catchment. Six locations were sampled in April and five locations were sampled in October. At every field plot the abundance and biomass of *Lumbricus terrestris* L. was determined. By application of a mustard solution on a 0.5 m × 0.5 m subplot at the sampling location the earthworms were extracted (e.g. Chan and Munro, 2001). Additionally the upper five centimeters were excavated and searched for earthworms. The number and weight of *Lumbricus terrestris* L. individuals was determined. In a next step horizontal soil profiles of 1 m × 1 m were excavated including the subplot of the worm extraction in three different depths: 10 cm, 30 cm, and 50 cm. Within chapter 1.2 different suggestions on how to determine preferential flow and preferential flow paths are summarised. I followed an approach to directly map the macropore system by counting and measuring the properties of individual preferential flow paths as suggested by Munyanski et al. (1994) and Zehe and Flühler (2001a). At every soil profile I counted the number of macropores and classified them depending on their diameter. The following classes were used: 2 to <4 mm, 4 to <6 mm, 6 to <8 mm, 8 to <10 mm, and ≥10 mm. Then the length of each worm burrow was measured with a bicycle gear cable. Based on the data gained, the correlation between the number of macropores/worm burrows (for each diameter class) and the earthworm data is investigated. I did this by a linear regression analysis and calculated the coefficient of determination R^2 (e.g. Montgomery and

Runger, 2006). Additionally, I determined the cumulative distribution function (cdf) of the pore lengths within each soil profile. Lengths between 0 and <10 cm are not included.

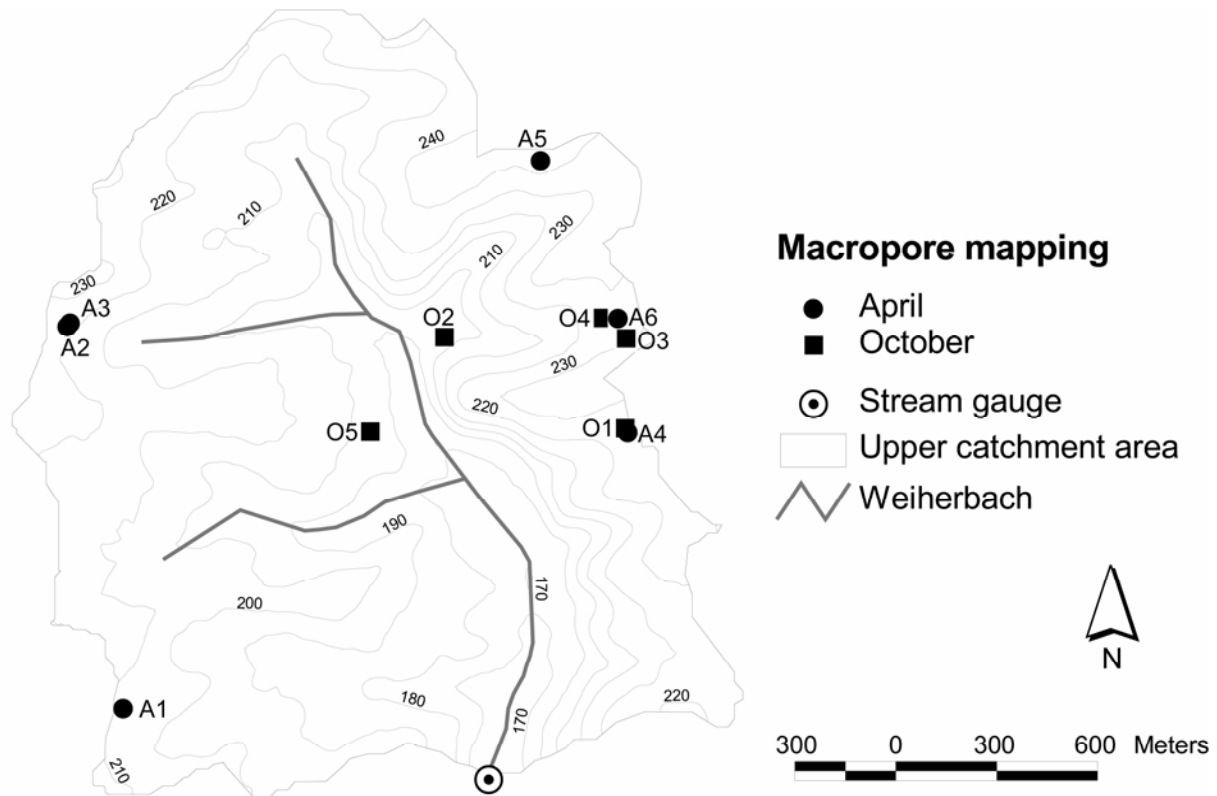


Figure 7-1: Sampling locations of the macropore mapping in the upper part of the Weiherbach catchment. April (circle) and October (square) are distinguished.

7.3 Results

The most basic information is the absolute number of macropores/worm burrows per location and depth. Table 7-1 summarises the number of macropores with a diameter ≥ 4 mm at each location. The role of smaller macropores with a diameter between 2 mm and 4 mm was more pronounced in a depth of 10 cm than in the deeper soil. Their fraction in the 10 cm depth was between 11.5% and 82.5%, while it was between 6% and 56.1% in 50 cm depth. There is no clear difference of the macropore densities between samples of the different seasons. The mean macropore density ($d \geq 4$ mm) increases over depth: 60.5 m^{-2} (April) and 79 m^{-2} (October) at 10 cm depth, 125.7 m^{-2} and 127.4 m^{-2} at 30 cm depth, and 150.8 m^{-2} and 216.4 m^{-2} at 50 cm depth.

Within the correlation analysis I differentiated between the April and October samples. Figure 7-2 presents the number of macropores/worm burrows for each diameter class (for each profile depth) versus the number of *Lumbricus terrestris* L. and Figure 7-3 presents the number of burrows/macropores versus the biomass, both for April. Figure 7-4 and Figure 7-5 present the data sampled in October. For a clear arrangement I plotted only regression lines with a $R^2 \geq 0.5$. Table 7-2 and Table 7-3 present the data from the correlation analysis for April and October, respectively. There is a clear difference between both observation periods. There are five $R^2 \geq 0.5$ for the upper 10 cm and three $R^2 \geq 0.5$ for a depth of 30 cm in April, while

there is only one $R^2 \geq 0.5$ for those soil depths in the October observation period. On the contrary, there are more $R^2 \geq 0.5$ for deeper soils horizons in October (4) than in April (1). Burrow diameter exceeding 10 mm were rare on the sampling locations, hence the correlation data for them has to be taken with care. Table 7-4 combines the data of the diameter classes of 4 mm and more, that can mainly be associated with burrows of *Lumbricus terrestris* L., differentiate between April and October. The differences in the correlation becomes more pronounced, while the April data suggest a strong correlation of either the number of *Lumbricus terrestris* L. or their biomass for soil depth of 10 cm and 30 cm, the October data suggest only a correlation between the number of burrows in 50 cm depth and the number of worms. The differences in the April data and October data are clear, thus a combination of both data sets to calculate an annual correlation between the input parameter does not make sense.

Table 7-1: Number of macropores/worm burrows with a diameter ≥ 4 mm per square meter. Classified by sampling season and soil profile depth.

	April: 10 cm depth	April: 30 cm depth	April: 50 cm depth	Oct: 10 cm depth	Oct: 30 cm depth	Oct: 50 cm depth
A/O1	66	142	112	64	195	260
A/O2	75	118	114	24	48	98
A/O3	123	198	129	90	114	214
A/O4	55	218	249	84	137	336
A/O5	24	41	123	133	143	174
A6	20	37	178	-	-	-
Mean	60.5	125.7	150.8	79.0	127.4	216.4
St.Dev.	37.8	76.3	53.8	39.7	53.4	89.5

Table 7-2: The coefficients of determination for April measuring the correlation between the number of worm burrows (based on the diameter class) and the number of *Lumbricus terrestris* L. or the biomass of *Lumbricus terrestris* L., respectively. $R^2 \geq 0.5$ are bold. NB: number of worm burrows/macropores, WI: number of *Lumbricus terrestris* L. individuals, BM: biomass of *Lumbricus terrestris* L. individuals.

April 09	R ² : NB-WI 10cm	R ² : NB-BM 10cm	R ² : NB-WI 30cm	R ² : NB-BM 30cm	R ² : NB-WI 50cm	R ² : NB-BM 50cm
2-4 mm	0.49	0.55	0.07	0.03	0.30	0.32
4-6 mm	0.49	0.85	0.40	0.63	0.60	0.48
6-8 mm	0.97	0.76	0.54	0.33	0.06	<0.01
8-10 mm	0.82	0.44	0.71	0.41	0.13	0.07
10 mm+	0.07	<0.01	0.07	<0.01	0.13	0.20

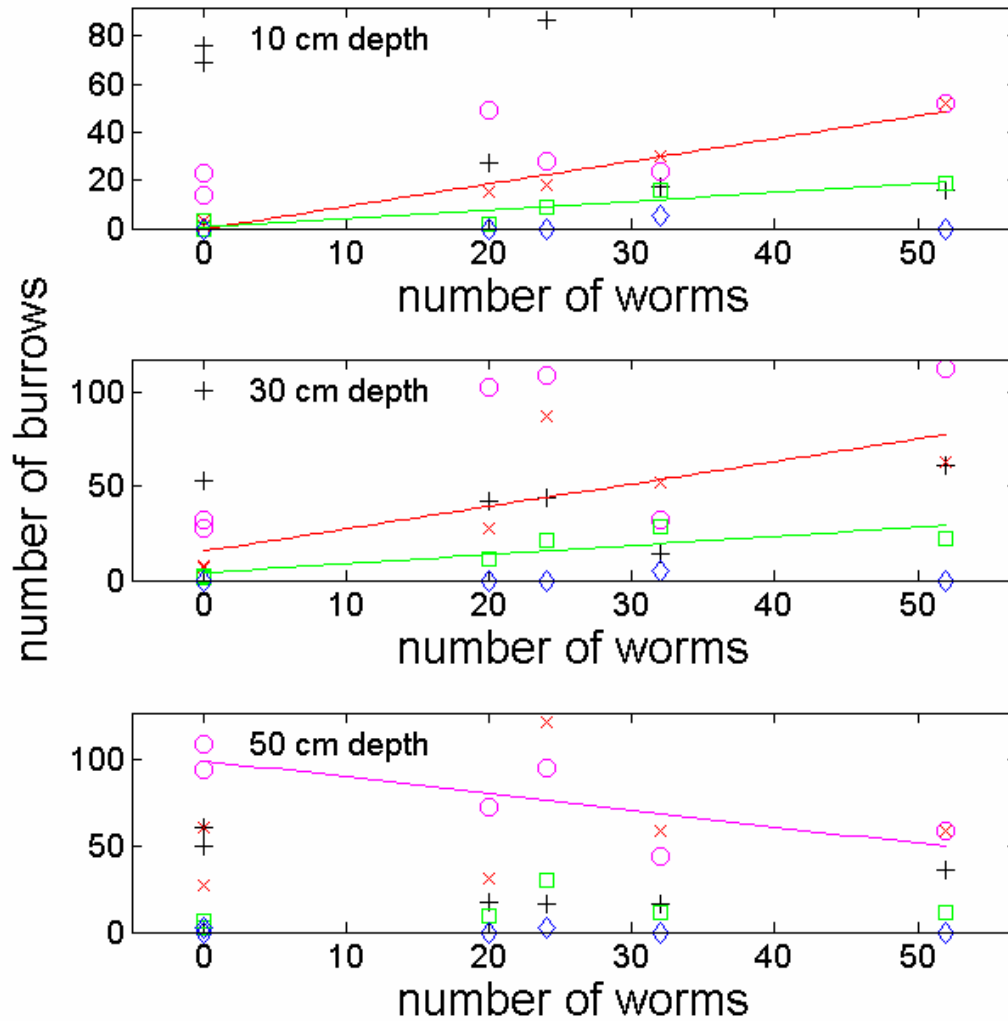


Figure 7-2: The number of macropores/worm burrows plotted versus the number of *Lumbricus terrestris* L. per m², based on the data sampled in April. Each subplot presents one of the evaluated soil depths (10 cm, 30 cm, and 50 cm). The regression line between the parameters is plotted for $R^2 \geq 0.5$. The colours present a distinct burrow diameter, black: 2-4 mm, magenta: 4-6 mm, red: 6-8 mm, green: 8-10 mm, and blue: ≥ 10 mm.

The cdf of the macropore length are presented in the Figure 7-6 (April) and Figure 7-7 (October). While the details are different between the soil profiles, some features generally apply. Plots with a higher macropore density have a wider cdf. The reason is that the probability to sample deeper burrows increases with the number of total burrows per square meter. The cdf for the soil profiles in 10 cm depth are often narrow, thus they rarely include long pores, at least measured long pores. Comparing the cdf of the different depths within one sampling location shows that the cdf are often similar between different soil depths.

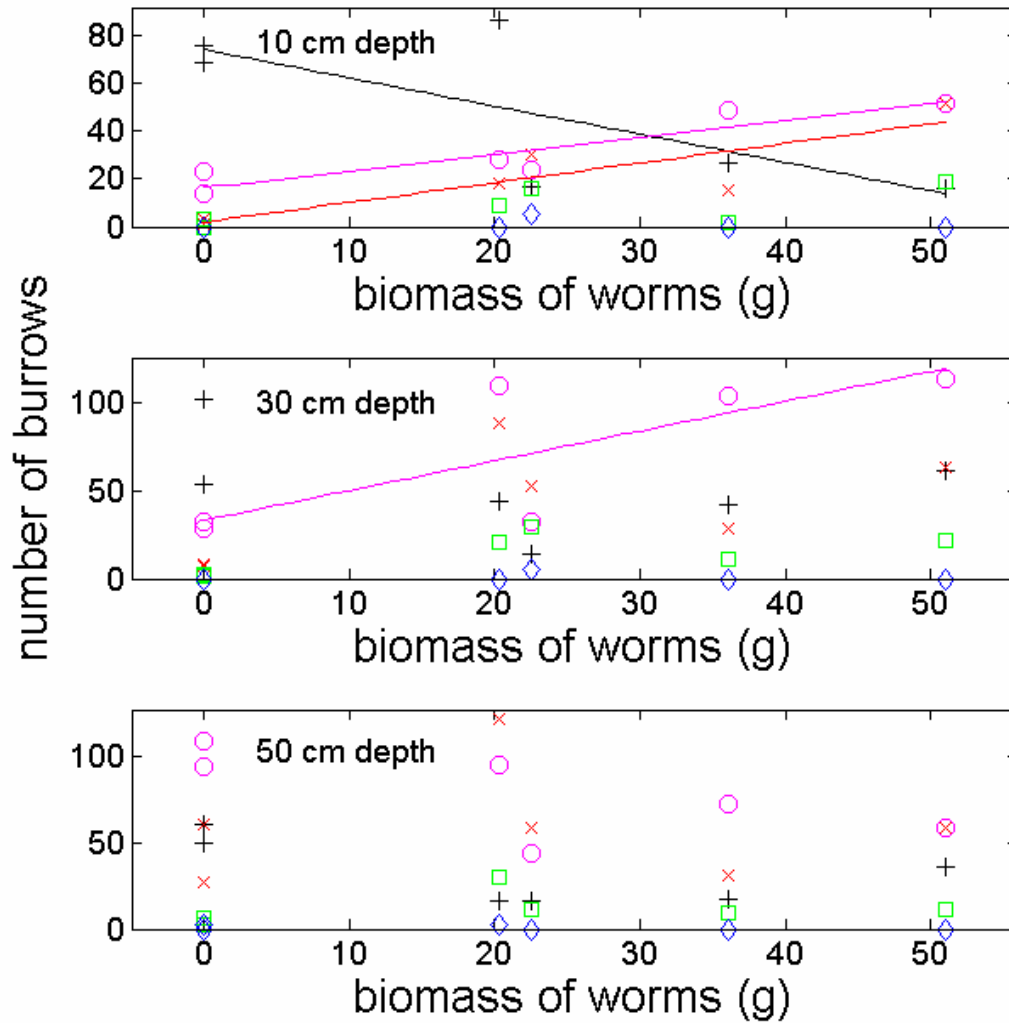


Figure 7-3: The number of macropores/worm burrows plotted versus the biomass of *Lumbricus terrestris* L. in g per m², based on the data sampled in April. Each subplot presents one of the evaluated soil depths (10 cm, 30 cm, 50 cm). The regression line between the parameters is plotted for R²≥0.5. The colours present a distinct burrow diameter, black: 2-4 mm, magenta: 4-6 mm, red: 6-8 mm, green: 8-10 mm, and blue: ≥10 mm.

Table 7-3: The coefficients of determination for October measuring the correlation between the number of worm burrows (based on the diameter class) and the number of *Lumbricus terrestris* L. or the biomass of *Lumbricus terrestris* L., respectively. R²≥0.5 are bold. NB: number of worm burrows/macropores, WI: number of *Lumbricus terrestris* L. individuals, BM: biomass of *Lumbricus terrestris* L. individuals

Oct. 09	R ² : NB-WI 10cm	R ² : NB-BM 10cm	R ² : NB-WI 30cm	R ² : NB-BM 30cm	R ² : NB-WI 50cm	R ² : NB-BM 50cm
2-4 mm	0.05	0.32	0.22	0.67	0.18	0.77
4-6 mm	0.20	0.03	0.04	0.19	0.93	0.09
6-8 mm	0.02	0.32	0.12	0.18	0.56	0.60
8-10 mm	<0.01	0.03	0.05	0.04	<0.01	<0.01
10 mm+	-	-	0	0.11	0	0.11

Table 7-4: The coefficients of determination between the number of worm burrows (diameter ≥ 4 mm) and the number of *Lumbricus terrestris* L. or their biomass, respectively. $R^2 \geq 0.5$ are bold. NB: number of worm burrows/macropores, WI: number of *Lumbricus terrestris* L. individuals, BM: biomass of *Lumbricus terrestris* L. individuals.

	R²: NB-WI 10cm	R²: NB-BM 10cm	R²: NB-WI 30cm	R²: NB-BM 30cm	R²: NB-WI 50cm	R²: NB-BM 50cm
April	0.95	0.87	0.64	0.61	0.02	0.06
Oct.	0.13	<0.01	0.24	0.18	0.92	0.28

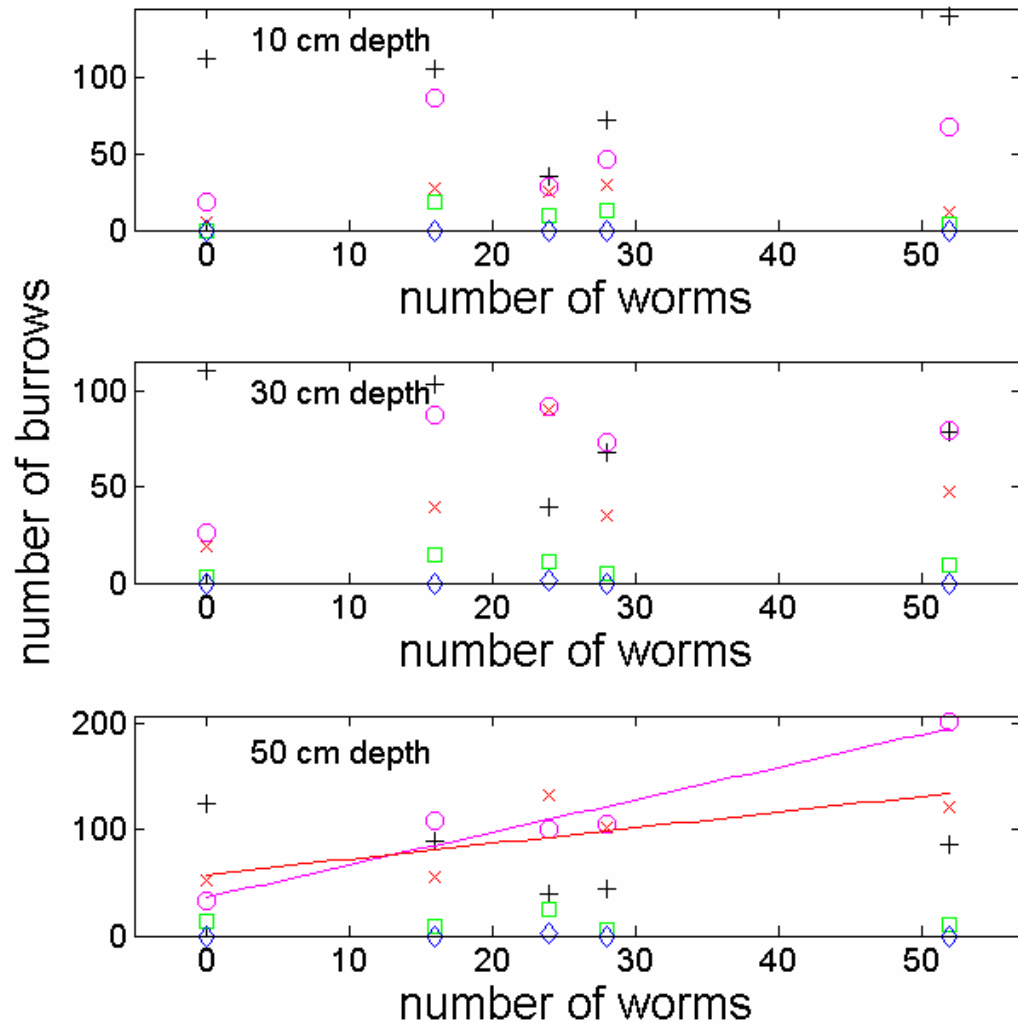


Figure 7-4: The number of macropores/worm burrows plotted versus the number of worms per m^2 , based on the data sampled in October. Each subplot presents one of the evaluated soil depths (10 cm, 30 cm, and 50 cm). The regression line between the parameters is plotted for $R^2 \geq 0.5$. The colours present a distinct burrow diameter, black: 2-4 mm, magenta: 4-6 mm, red: 6-8 mm, green: 8-10 mm, and blue: ≥ 10 mm.

7.4 Discussion

7.4.1 The pore system – burrow density and depth distribution

With an average worm burrow density (diameter ≥ 2 mm) of $109 m^{-2}$ in April and $172 m^{-2}$ in October the results are similar to the findings of Zehe (1999) and Zehe and Flüher (2001a). They found a burrow density of between $100 m^{-2}$ and $225 m^{-2}$ in the Weiherbach catchment (diameter ≥ 2 mm), while Weiler and Naef (2003a) found a burrow density between $228 m^{-2}$

and 623 m⁻² based on a diameter ≥ 1 mm and at different grassland sites. This study and the studies of Zehe (1999) and Zehe and Flühler (2001a) were performed at cultivated field sites. Considering that tillage strongly affects the number of macropores (e.g. Andreini and Steenhuis, 1990) the difference between grassland and cultivated land is reasonable. While the difference between April and October is within statistical variations, the clear increase of macropore density with depth is apparent (Table 7-1). This pattern is induced by the long term stability of macropores that was found for worm burrows by VandenBygaert et al. (1998) and Hagedorn and Bundt (2002). The parts of macropores located below the zone of soil tillage can persist several decades, while the parts of the macropores in the upper soil can be destroyed by tillage or closed by sedimentation of eroded material that enters the macropores. This fact complicates the approach to link *Lumbricus terrestris* L. population and the burrow system, as a long term population history must then be included, considering that a high variance of earthworm population between consecutive years was found by Butt et al. (1999).

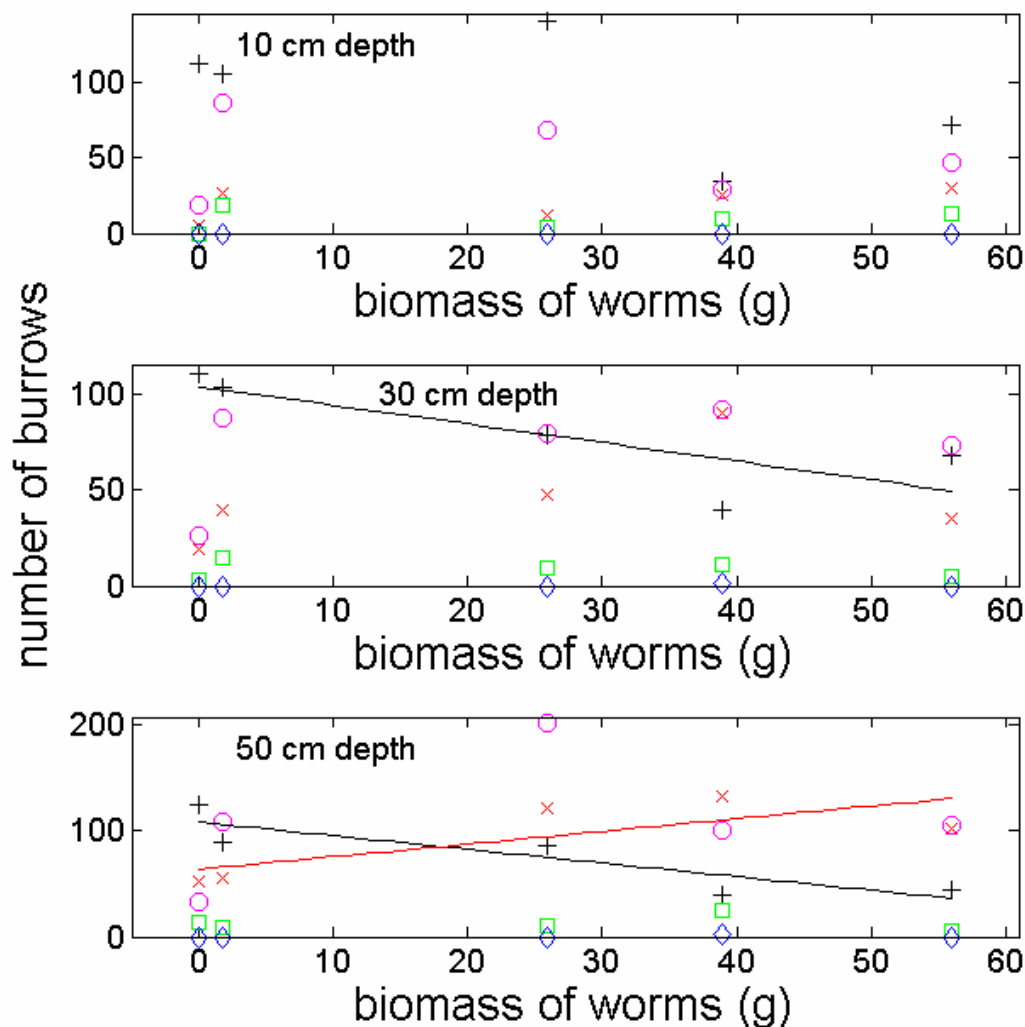


Figure 7-5: The number of macropores/worm burrows plotted versus the biomass of *Lumbricus terrestris* L. in g per m², based on the data sampled in October. Each subplot presents one of the evaluated soil depths (10 cm, 30 cm, and 50 cm). The regression line between the parameters is plotted for R² ≥ 0.5. The colours present a distinct burrow diameter, black: 2-4 mm, magenta: 4-6 mm, red: 6-8 mm, green: 8-10 mm, and blue: ≥10 mm.

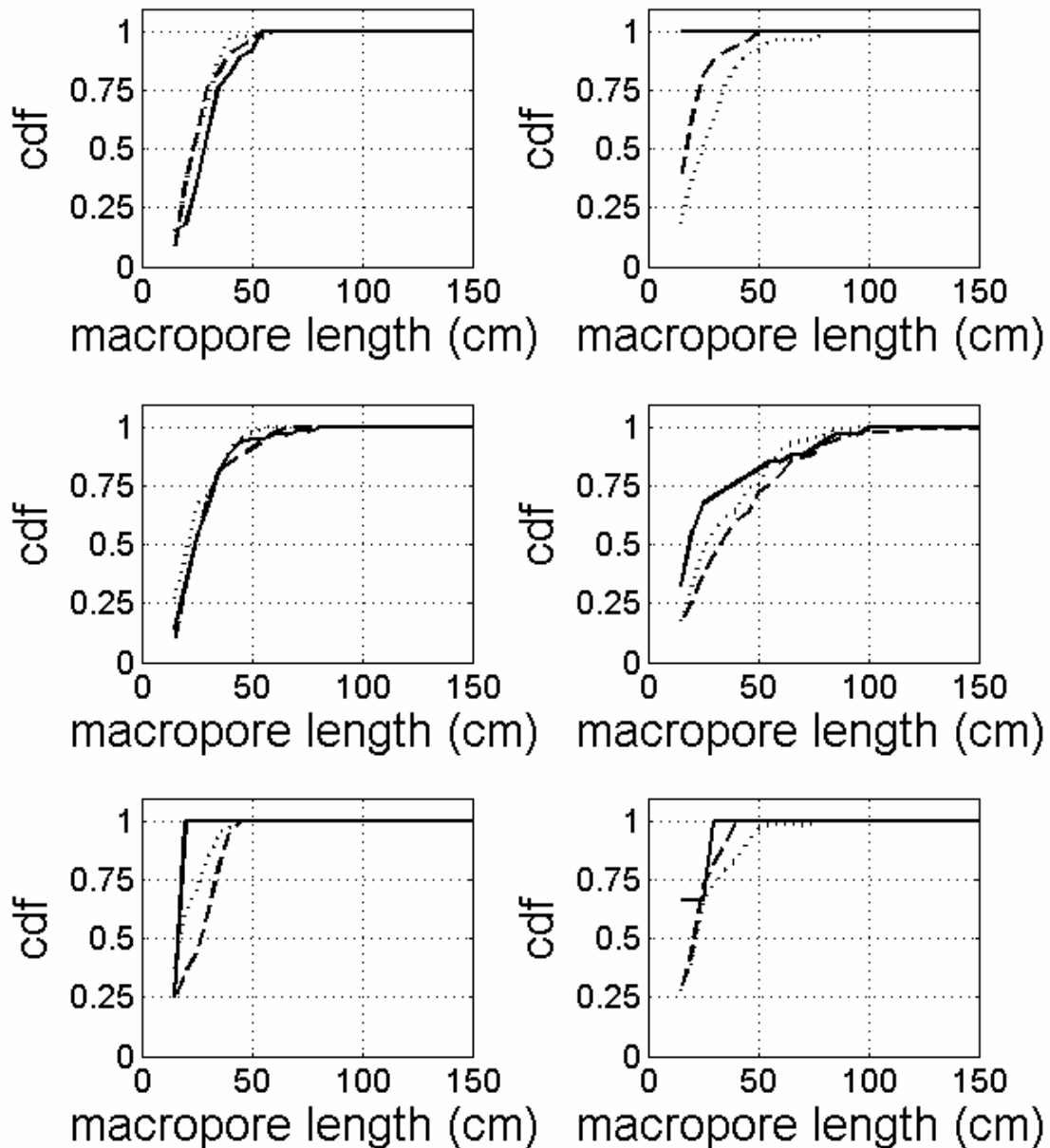


Figure 7-6: Cumulative density function of the macropore lengths measured at 10 cm depth (solid line), 30 cm depth (dashed line) and 50 cm depth (dotted line), April data

Comparing the cdf of Figure 7-6 and Figure 7-7, it becomes evident that the cdfs of different depths are often similar. This implies that the measured pore system in 10 cm is not consistent with the pore system at 30 cm or 50 cm depth, or there is a limitation in the measurement procedure. Measuring the pore length at the 10 cm depth profile frequently led to lengths less than 10 cm. Within the upper soil layers the tortuosity of the pore system is higher as there is a population of endogeic earthworms and juvenile anecic earthworms that build complex lateral burrow systems in the upper soil layers (Tugel et al., 2000). The change from vertical to a lateral orientation and the tortuosity might limit the use of the gear cable to follow the burrow system as it might get stuck. Additionally, the similarity of the cdfs may show that the cable gear is not reliable exceeding a specified burrow length, since the probability of getting stuck will increase with burrow length. Within this study the maximum observed burrow length was 110 cm, located at the soil horizon in 30 cm depth. The burrows of *Lumbricus*

terrestris L. can lead down to several meters, Edwards and Bohlen (1996) reported a burrow length of 240 cm. Thus the integration of this data into the approach that generates preferential flow structures in chapter 3.2.2 is difficult.

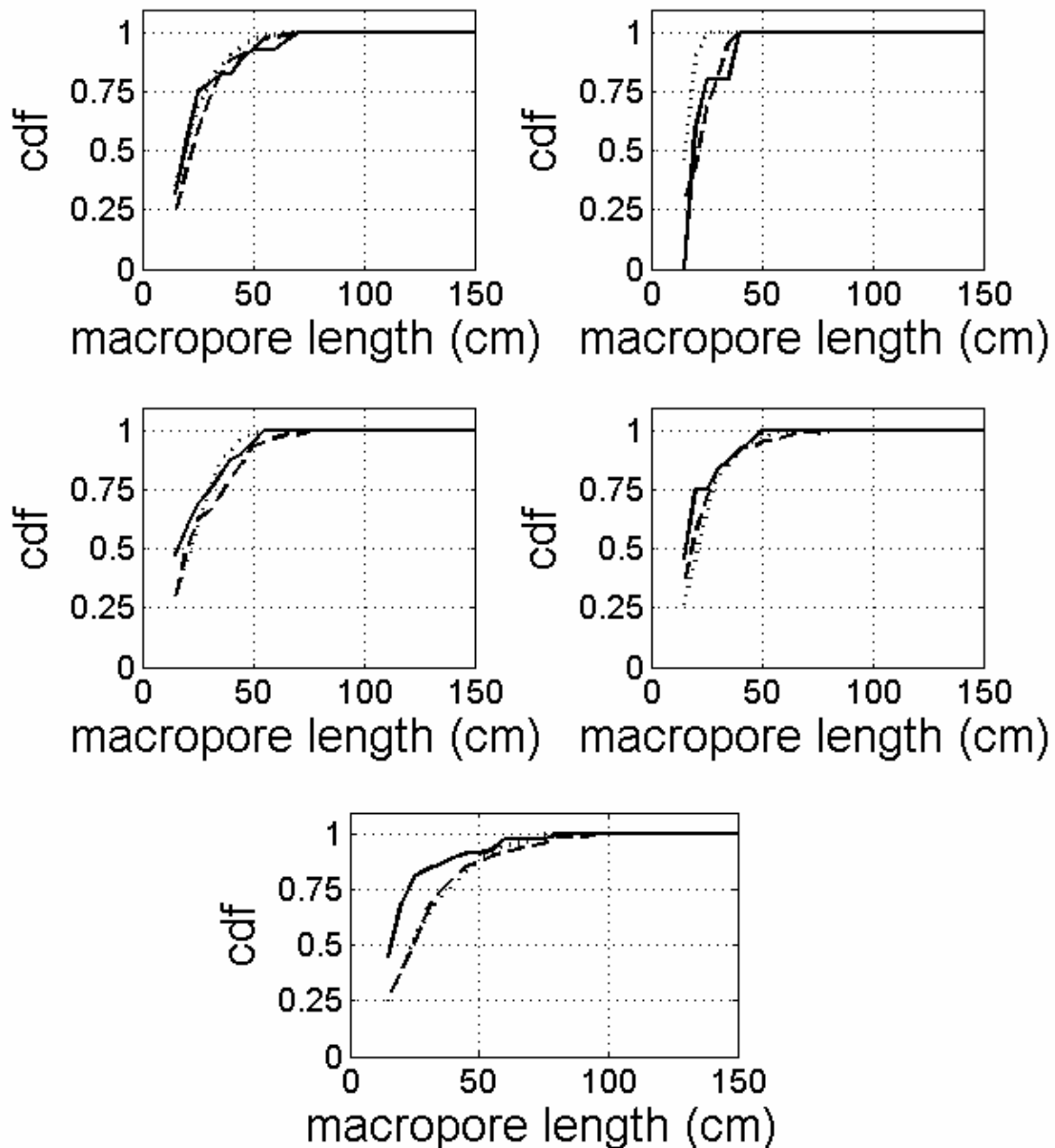


Figure 7-7: Cumulative density function of the macropore lengths measured at 10 cm depth (solid line), 30 cm depth (dashed line) and 50 cm depth (dotted line), October data.

7.4.2 The value and limitations of the correlation analysis

Especially the correlation analyses of macropores with a diameter ≥ 4 mm revealed a strong correlation (up to $R^2 > 0.9$) between the information of the *Lumbricus terrestris* L. population and the number of pores, for 10 cm and 30 cm sampling depth in the April data, but not for the data in October. I suggest that the earthworms might be withdrawn to deeper soil during October, or that the influence of last the surface treatment still had an effect. Using the number of *Lumbricus terrestris* L. or its biomass as the predictor variable reveals a difference between these (e.g. Table 7-1). The results of the correlation analysis suggest a difference in

the strength of the correlation between the parameters of the *Lumbricus terrestris* L. population and the density of the macropore system when comparing the data from April to the data of October. Additionally, the correlation is often poor. Therefore the macropore system has to be characterised by additional parameters, also suggested by Jarvis et al. (2009) and Lindahl et al. (2009). The temporal variability of the earthworm population (Butt et al., 1999) is not the only explaining variable. Additional factors that likely influence the pattern of the burrow system are linked to the cultivation of the field site, like soil tillage and the field crop. The goal within the correlation analysis was to directly link the population information to the macropore system in order to gain an annual pattern of potential preferential flow paths based on the annual and seasonal variability of the earthworm population that can be used to parameterise hydrological models with direct observables. To include more predictor variables, like soil type, tillage, slope location, type of field crop, or even the long term data of those factors, a larger amount of samples is needed (e.g. Jarvis et al., 2009) than gathered within this study. Based on more samples, an appropriate range of additional predictor variables could be covered to better explain the macropore pattern. I would thus suggest investigating the link of the population information to the burrow system primarily on grassland sites, as there is no soil tillage and no (short term) change in vegetation that will reduce the number of samples. Based on such knowledge, the study can then be extended to cultivated land, with several more factors influencing the macropore pattern.

7.5 Conclusion

To come back to the working hypothesis I suggested in the introduction (see chapter 7.1), I can conclude that there is a correlation between the number of individuals and their biomass to the occurrence of preferential flow paths, but this correlation is not very reliable. Using this information as the sole predictor variable is not sufficient to successfully predict the number of macropores. Thus more information, especially about cultivation, is needed to improve the correlation analysis. That leads to the need of more sampling locations to cover the different parameter ranges. Nevertheless, the investigation of the population dynamics of *Lumbricus terrestris* L. is a promising approach that might allow the prediction of the spatial variability in preferential flow paths within a catchment. This could be used in a further step to parameterise hydrological models.

8 A first glimpse to another catchment: different physical catchment properties – different preferential flow pattern

8.1 Introduction

The results of the studies in the Weiherbach catchment showed the relevance of vertical preferential flow structures in the transport of water and solutes at the hillslope scale, while e.g. Zehe and Blöschl (2004) additionally showed their importance on catchment scale runoff generation. The role of preferential flow on water and solute transport strongly depends on the physical properties of a catchment. Thus a second catchment with an important amount of preferential flow paths was observed in the BIOPORE project. This chapter give a first glimpse to this second research catchment – the Göberlein catchment. Contrary to the Weiherbach, this catchment is not dominated by bio-geomorphologic structures but by swelling and shrinking of soils. Below the catchment properties are presented, an impression of the first observations is given as well as an evaluation of the results, which is done in a qualitative way. Finally the proposed next steps in the research are outlined.

8.2 Catchment description

8.2.1 Location

The Göberlein catchment is located in northern Bavaria, Germany in the Hassberge-region, approx. 50 km from the city Würzburg and 30 km from Bamberg. The entire catchment has an area of 0.73 km² and is gauged at the outlet by a Thomson weir. The highest point is 350.5 m.a.s.l. and the lowest 277.5 m.a.s.l. (Figure 8-1).

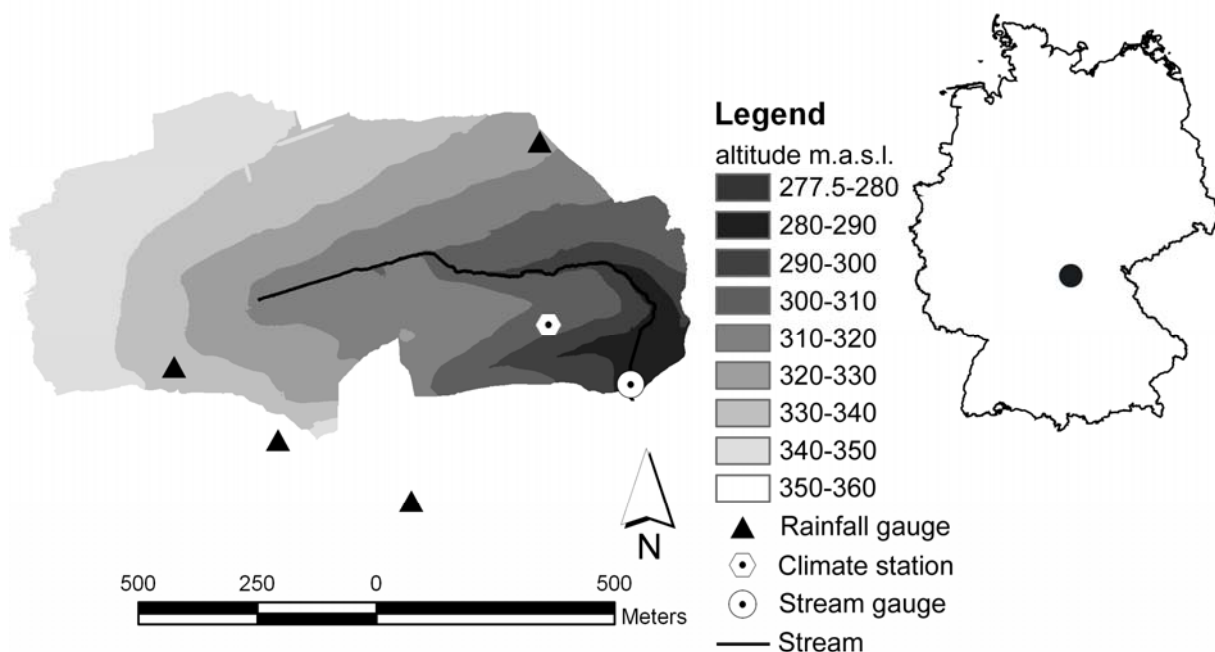


Figure 8-1: The Göberlein catchment

8.2.2 Geology and geomorphology

The underlying geology is dominated by gypsum-keuper (Gipskeuper), mainly claystone with stone-marl (Steinmergel) and layers of gypsum from the Germanic Trias. The surface morphology is strongly dominated by the rural replotting in the 1970s, when the field boundaries were changed and the stream and the road system were rearranged. While the stream flows in a natural bed in the lower catchment, it is forced parallel to the road and field boundaries in the upper catchment. In parts the stream flows directly at the bedrock.

8.2.3 Soils and soil structure

The soils within the catchment are often shallow, especially at the hilltops, with only 20-30 cm soil depth above the (weathered) bedrock. At the hillfoots they can reach up to 70 cm thickness and can be occasion exceeding 100 cm thickness in the stream valley. The catchment soils are dominated by sandy loams and loamy sands, with some rare silt and clay soils. The organic contents throughout the catchment are around 5% but can reach up to 10%. However, all soils contain significant proportions of clay particles, between 10% and 35%. In the valley bottom Colluvisols are present. The high clay content throughout the catchment leads to a strong swelling and shrinking behaviour which creates deep soil cracks down to the bedrock. These structures act as fast vertical preferential flow paths (Figure 8-2).

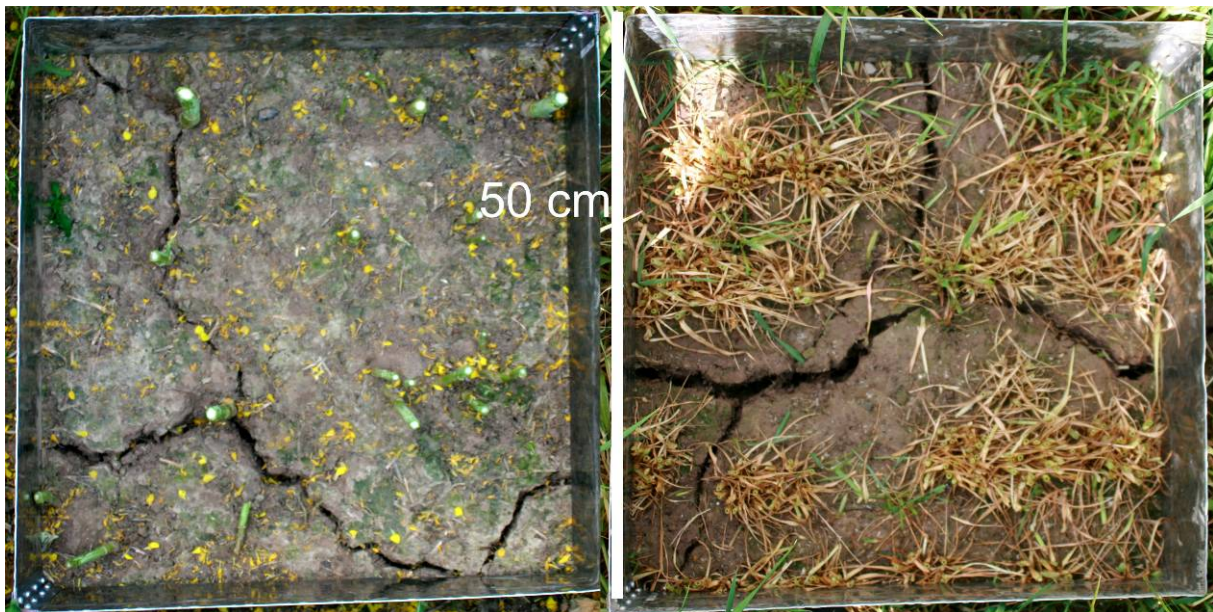


Figure 8-2: Extend of soil cracks on 50 cm × 50 cm field plots in the catchment.

8.2.4 Landuse

The Göberlein catchment is dominated by intense cultivation. About 94% are arable land, 3% is grassland, and about 3% is forested. The area of paved roads is less than 1%. The soil is usually treated with a reduce depth tillage down to 10 cm.

8.2.5 Hydro-meteorological network

Several observation devices are installed in the basin. One climate station measuring air temperature, air humidity, solar radiation, air pressure, wind velocity and direction, and precipitation was installed. This was accompanied by the installation of four Davies precipitation samplers distributed in or near the catchment (Figure 8-1). In addition, a Thomson weir was installed and the rating curve was determined by frequent discharge measurements. Since the discharge events are usually of only short duration, discharge measurements during high flow are rare. This probably leads to an overestimation of discharge during high flow events. Erosion is an important factor in the Göberlein catchment leading to sedimentation at the weir, increasing rating curve errors.

8.3 First observations

The first field observation pointed out the importance of soil cracking forming vertical preferential flow paths in the catchment. Contrary to the Weiherbach catchment, where the soils are on the top of an up to 15 m thick loess layer, the soils of the Göberlein catchment are shallow (<1 m) and located above bedrock (claystone). The formation of soil cracks is mainly driven by climate and soil type: long dry periods will lead to cracking, while wet periods reduce the amount of cracks or will close them (see chapter 1.1.2 for literature on soil cracking).

Thus I postulate following working hypotheses:

- The soil cracks will lead to significant depth infiltration at soil profile scale, and will therefore influence the transport of solutes, especially, pesticides in the soil, and solutes on catchment scale
- The formation of soil cracks is strongly influencing the runoff behaviour of the catchment.

The field work followed these hypotheses, investigating the plot scale solute transport, and linking the plot scale preferential flow structures to the catchment scale runoff behaviour.

8.3.1 Climate and Hydrology

The climate station supplied data since the end of 2008. The total precipitation was 498.6 mm in 2009 and 581.6 mm in 2010. The precipitation behaviour was similar between the years, only the summer months (July-September) showed a distinct difference with 114 mm (2009) to 280 mm (2010). Since the gauge was constructed in March 2009, only one year of completed discharge data exists. In 2010 the total runoff was 250.4 mm, which is 43.5% of annual precipitation. The discharge data is presented by Figure 8-3 together with the daily precipitation sum. Comparing the pattern of both some reveals the following:

- Snowmelt events lead to several strong runoff events, labelled with 1, including the highest peak flow in the observation period
- During dry catchment states precipitation events do not cause strong flood events, see labelled with 2.

- In summer 2010 a series of several days with high precipitation continuously wetted the catchment. The height of the discharge events increased from precipitation event to precipitation event, labelled with 3.

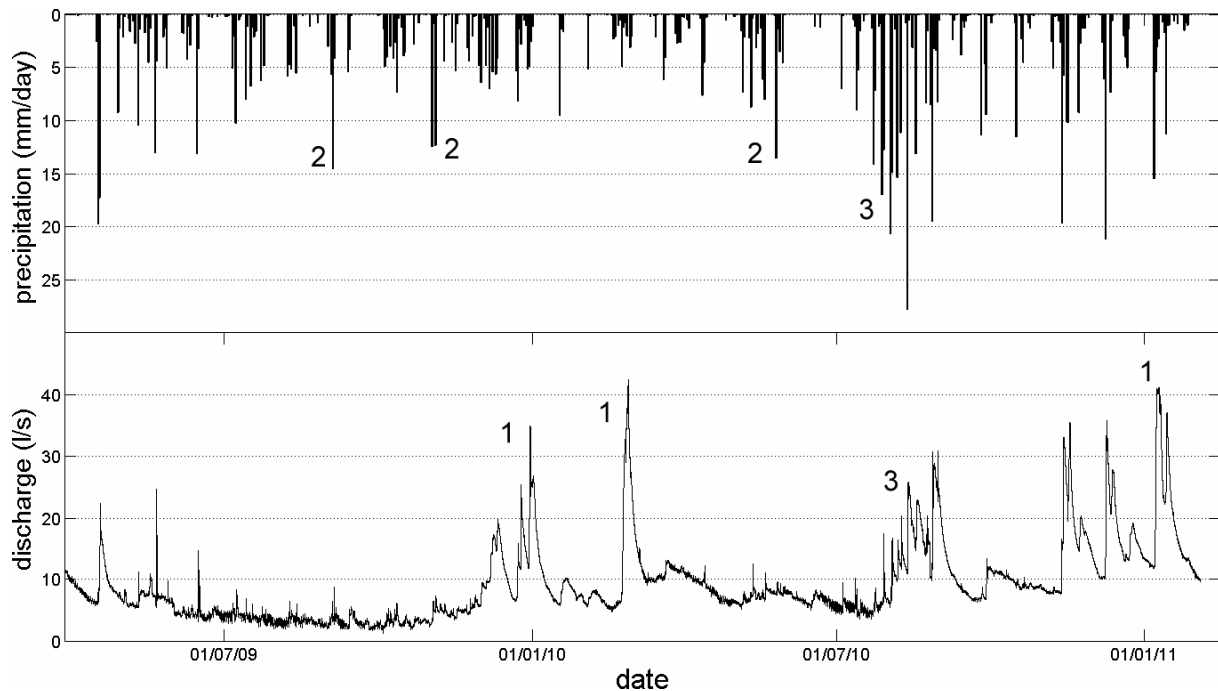


Figure 8-3: daily precipitation (upper panel) and discharge (lower panel) in the Göberlein catchment. Number 1 labels snow melt events, 2 labels precipitation events during dry catchment state, and 3 labels the wetting up of the catchment after a dry period.

8.3.2 Plot scale irrigation experiments and preferential flow

The effect of the cracking soils in the catchment was investigated by a series of plot scale irrigation experiments. I chose two experimental seasons: June 2009, the beginning of the dry summer season, and April 2010, at the end of winter season. Discharge, as integral measurement of catchment state, was smaller for June 2009 (<0.1 mm/day) than for April 2010 (0.4 mm/day).

I performed the irrigation experiments at three different sites within each experimental phase. At each site two neighbouring 1 m² subplots were irrigated with 43 mm and 23 mm precipitation in one hour, and 4 g/l of the tracer brilliant blue were included in the irrigation water. Soil moisture was observed during the experiments, with five (or six) Theta Probes in a depth of 10 cm (3 devices) and 25-30 cm (2-3 devices). Soil cores (100 cm³) were excavated in depths of 10 cm and 25-30 cm to determine saturated hydraulic conductivity, bulk density, and porosity. The land use, depth to bedrock, and soil types were different for each irrigation site. Figure 8-4 presents two different vertical soil profiles dyed with brilliant blue. The irrigation experiments revealed the following observations:

- Under dry catchment conditions the soil cracks allow the infiltration of the total irrigation amount

- Cultivation practice can significantly reduce the infiltration leading to surface runoff
- The soil cracks are able to transport the water directly down to the bedrock
- Under dry catchment conditions the exchange between the soil cracks and the surrounding soil matrix is low, indicated by only small extend of dyed soil at the boundary of soil matrix and soil cracks (Figure 8-4).

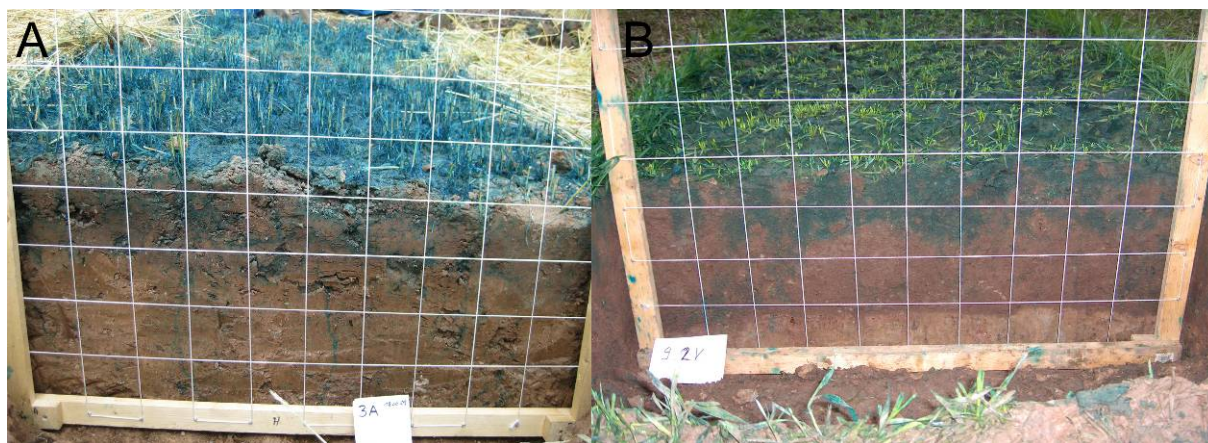


Figure 8-4: Different infiltration pattern in the Göberlein catchment. A: irrigation on a field site cultivated with crop during dry catchment state. B: irrigation on a field site cultivated with crop during moist catchment state.

8.3.3 Conceptual understanding of rainfall runoff behaviour and the role of preferential flow

The catchment is strongly controlled by the moisture state. During dry catchment conditions (compare the low flow period of 2009 in Figure 8-3) strong precipitation events were not followed by strong discharge events, as preferential flow structures, in this case soil cracks, lead to a rapid infiltration in the soil. The dry soil matrix has the capacity to store the water and only a small proportion becomes runoff. During wetter catchment conditions the infiltration capacity of the soils is lower. The wet shallow soils lead to saturation excess surface runoff and the reduce infiltration capacity might favour hortonian overland flow. Additional the high saturation lead to a smaller amounts of water that can enter the soil matrix from the preferential flow paths, initiating water flow at hillslope scale. The detailed processes are yet not investigated. In summary I suggest the catchment is controlled by a soil moisture threshold that allows soil cracking enhancing infiltration and a soil moisture threshold that allows saturation overland flow and enables connectivity of the hillslopes to the stream channels.

8.4 Further research steps

The qualitative catchment description will be transferred to a quantitative description when a long enough discharge time series is available, and based on this series the precipitation runoff behaviour will be analysed. The focus will be on the difference between the wet and dry season, therefore an analysis of event based runoff coefficients (Blume et al., 2007) will be carried out. Most important will be the detailed analysis of the plot scale irrigation

experiments to get a better understanding of the several factors controlling the infiltration in the catchment, which must be linked to the soil moisture observations provided by a recently installed station.

9 Synthesis

9.1 Summary of achievements

This thesis is focused on the role of bio-geomorphic structures in hydrology. A modelling study was performed to investigate the effect of spatially explicit representation of those structures. In addition, a systematic research was conducted on the role of those structures in the mobilisation of old water and the rapid non-retarded transport of pesticides during a series of irrigation experiments. This led to several scientific achievements which are summarised in respect to the general objectives presented in chapter 1.4.2.

9.1.1 How to represent structures in a hillslope model?

Preferential flow is frequently conceptualised in a functional way or based on e.g. dual permeability approaches. The required information to parameterise these approaches is mainly based on assumption or calibration. The idea within this thesis was to represent structures favouring preferential flow in an explicit way based on observable information. Preferential flow structures – in this case vertical earthworm burrows – were included in an explicit way in a hillslope model (CATFLOW). This was done considering their nature, namely as connected explicit flow path with high hydraulic conductivity and low retention properties. The approach first simulates the occurrence of a burrow and follows extending the burrow in depth by simulating the digging of an earthworm (see chapter 3). Both steps of the simulation are based on data collected in previous campaigns (Zehe and Flüher, 2001a), such as macropore surface density, the length distribution, and hydraulic conductivity of the burrows. The occurrence of a burrow is simulated with a Poisson process, which uses real surface density of worm burrows data. An agent based approach extends the burrows to depth. The generated structure network was similar to structures observed in the field (see Figure3-2). This data driven generation of preferential flow structures is a new contribution to the conceptualisation and parameterisation of hillslope models, since it allows the generation of a macropore network based on observable information.

9.1.2 How feasible is the explicit representation of structure to reproduce water and solute transport?

The feasibility of the explicit representation of the vertical preferential flow paths was tested in a 2-dimensional physically based model. Within an irrigation experiment at a tile drain field site discharge and bromide breakthrough were observed (Zehe and Flüher, 2001a). Modelling was performed using different parameter sets that described the preferential flow network and the initial conditions. A scaling parameter has to be introduced to scale the width of the modelled hillslope, since the model represents a 3-dimensional reality with a 2-dimensional environment. Not the total width if the irrigated field was drained by the tile drain. In total 67 of 432 model setups could successfully reproduce event discharge in the tile drain ($NS \geq 0.75$), 13 of those setups yielded a $NS \geq 0.9$, and were considered as very good runs (see chapter 3). While hydrological models often perform well in respect to discharge, the behaviour of solutes is often poorly covered unless additional calibration parameters are

introduced. In this thesis the discharge runs with a $NS \geq 0.9$ were used and allowed modelling bromide transport without any further calibration or adjustment of the introduced scaling parameter (see chapter 3.2.4). At least four of these runs allowed successful modelling of the total bromide transport. The temporal dynamics were not captured well during the first 100 min of the experiment, but were thereafter reproduced satisfactorily. This, and the fact that the magnitude of the concentration was also registered, shows that the introduced scaling factor (from two dimensions to three dimensions) is a physically reasonable assumption. Overall a linear regression between the modelled and measured cumulative output showed a slope of nearly one (in the best case 0.957). Modelling of (conservative) solute transport and discharge with explicit representation of preferential flow paths was successful without any further calibration of solute transport. This clearly shows the advantage of such an approach to bring together water and solute transit times at hillslopes, at least on event scale.

9.1.3 Parameter identifiability and equifinality

Different realisations of the macropore network were created based on existing data. The key parameters were varied based on the existing data range and data supplied by literature (chapter 3.2.3). Several of those model setups reproduced the observed tile drain discharge well, 13 runs yielded a $NS \geq 0.9$. Even at the well investigated field site used in the modelling study considerable equifinality occurred when the key parameters were varied within the range of measurements and values supplied by literature. Introducing criteria of model rejection as suggested by Beven (2010) and using the results of the transport modelling as additional information (chapter 4.4.3), it was possible to reduce the number behavioural model setups from 432 to four. Nevertheless, several model setups can reproduce both, discharge and cumulated bromide transport without compromising either field knowledge or the available data base. Thus predicative uncertainty due to equifinality is an issue in 2-dimensional physically based models. The important scientific achievement about parameter identifiability and equifinality in this thesis is that an additional independent data source (solute transport modelling) can reduce the system inherent equifinality. But the study also showed that we have to accept that several parameter sets can reproduce the same integral system response, and thus equifinality can not be reduced to zero.

9.1.4 Explicit structures to perform better contaminant modelling

Modelling pesticide transport at the hillslope scale remains challenging. Although discharge and bromide modelling was successful, a reproduction of the pesticide transport failed (see chapter 4.3.3). Both approaches used, namely heterogeneous (differentiate between macropore and soil matrix) and homogeneous parameterisation of the adsorption parameters could not model the temporal behaviour of the pesticide Isoproturon. Nevertheless, the overall amount of transported mass could be reproduced, as long as the transport in the soil macropores was modelled without any retardation.

9.1.5 On the value of repeatable field experiments to enhance process understanding

Most hydrological field studies are singular experiments. In this thesis the approach was to conduct a series of similar experiments at the same study site. Being a natural setting the initial conditions were different, thus the results of the experiments with respect to discharge and total solute transport were different as well. It was possible to show the importance of antecedent precipitation on bromide and pesticide transport in a tile drained field site. The basic idea behind the experimental approach was to gain process insight by consecutive experiments. The approach of performing an experiment, examining the results, improving the experimental setup, and performing the next experiments showed to be an efficient way of learning. Only by a series of experiment the detailed processes could be identified step by step (i.e. the role of pre-event soil water, the macropore-matrix interaction, and the pesticide transport). With this thesis the importance of performing hydrological experiments not in a singular way, but as a sequence of experiments, is shown. This allows a step by step learning of the underlying processes.

9.1.6 The role of macropore – matrix interaction on the ratio of “new” and “old” water in the hydrograph

A multi tracer approach that labelled the irrigation water with bromide and measured the isotopic composition of soil water, irrigation water, and discharging water was used. Based on this approach a high proportion of pre-event water was found in the tile drain event discharge, although the preferential flow paths are directly connected to the tile drain (chapter 5). The use of compartmental mixing cell modelling showed to be a valuable tool to determine the interaction between the soil macropores and the soil matrix. It not only showed that the mixing of irrigation water with the pre-event soil water took place over the entire depth of the soil profile, but also that the interaction is a spatially variable. The interaction of the soil matrix with a macropore system was previously confirmed by dye tracer (e.g. Weiler and Flühler, 2004). Together with the tracer composition of the tile drain hydrograph the temporal variability of this process was shown, since increase in discharge was accompanied by contribution of soil water. This process was driven by a reversal of the macropore-matrix interaction controlled by threshold behaviour. At first water left the macropores and infiltrated in the matrix. After crossing a moisture threshold the water from the soil matrix entered the macropores. Finally, it was possible to determine the depth of the soil layers that mainly contributed to the tile drain discharge. Thus a clear progress in process hydrology was achieved by identifying that the macropore-matrix interaction during rainfall driven conditions is a key process that governs the rapid mobilisation of “old” water and thus explains the high proportion of pre-event water in the tile drain hydrograph. The value of pre-event and after-event soil isotopic composition to study hydrological processes was shown (chapter 5).

9.1.7 The role of bio-geomorphic structures in rapid pesticide transport and remobilisation of stored pesticides

The transport of two surface applied pesticides is strongly driven by the mechanism of tile drain runoff generation. Previous studies showed that reactive solutes can be transported with no retardation compared to conservative solutes (e.g. Kung et al., 2000) and that a precipitation threshold was an important factor of pesticide leaching at lysimeters (McGrath et al., 2010). In this thesis results of a series of irrigation experiments showed that the transport of pesticides was correlated to the transport of bromide ($R^2 > 0.9$). Most of the pesticide transport occurred when the direction of macropore-matrix interaction was from the matrix to the macropores. Through this process the surface applied pesticides are directly transported in the preferential flow structures and can only reach adsorption spaces in a limited way. The third experiment showed that bio-geomorphic structures favour the long term leaching and remobilisation of stored pesticides, since the stored pesticides can enter the macropores from the soil matrix. Particle bound pesticide transport contributes about 20% of the total transport of the pesticide Flufenacet independent from the hydrological processes. Thus the experiments enhanced the understanding of processes that lead to pesticide transport. Bio-geomorphic structures together with a threshold controlled reversal of the macropore-matrix interaction drive the rapid transport without retardation and the remobilisation of stored water. The latter is a process that is crucial for long term leaching.

9.1.8 Mapping macropore structures to obtain observables for model parameterisation

Methods to achieve information on the occurrence and distribution of preferential flow networks on hillslope or catchment scale are limited. Nevertheless such information is very useful to parameterise hydrological models or to assess processes related to preferential flow. To gain such information, the preferential flow structures were determined by macropore mapping and sampling the number and biomass of the earthworm *Lumbricus terrestris* L. The correlation between this information was determined by linear regression for the two different sampling periods in April and October. While the data suggested a clear correlation of earthworm data and the number of preferential flow paths for the sampling period in April, there was only a slight or even no correlation in October (see chapter 7.3). The link between the macropore network at 10 cm, 30 cm, and 50 cm depth was not obvious when comparing the cumulative density functions, thus the evaluation of the depth distribution was limited. Nevertheless this study was a first attempt to infer information for model parameterisation at plot scale by biological information. Such a link would allow inferring catchment scale pattern of structures favouring preferential flow by the catchment scale earthworm distribution, which could be determined by an ecological population model.

9.2 Discussion and outlook

Each of the chapter of this thesis included a detailed discussion on the results of the individual chapter with its detailed research questions. The aim of this synthesis chapter is to link the different modelling and experimental studies, discussing points that could not be included in

the chapters that are organised in paper form, as well as the role of structure in models and field experiments, and the possibility of combining these points.

9.2.1 Including structures in the hillslope model – limitations in the generation, representation, and parameterisation

Limitations by spatial model resolution

Not many hydrological models represent hydrological structures in an explicit way. Vogel et al. (2006) used explicit structure at plot scale, while Nieber and Sidle (2010) represented soil pipes in an explicit way in a 3-dimensional hillslope model. In this thesis I could show that an approach that represents structures in an explicit way in a hillslope model allowed a successful reproduction of both tile drain event discharge and cumulated bromide transport (chapter 3 and chapter 4). Representing these structures in an explicit way is limited in several ways: The spatial resolution in the model, expressed by grid cells with approx. 30 cm × 2 cm, is distinctly larger than the maximum observed burrow diameter. The macroporous structures in the model are parameterised by the maximum possible water flow (volume per time), which is an observable input parameter. If this water volume passes a 30 cm wide macropore (in the model), compared to a 1 cm or 2 cm wide macropore (in reality), the maximum flow velocity will be reduced. This limits the feasibility of the model to reproduce fast transport velocities. Additionally, this maximum flow volume is uniformly applied for all generated macroporous structures in the model. This underestimates the field scale variability of the flow processes. Further, the fact that endogeic earthworms form a complex lateral burrow system in the upper soil layers (Tugel et al., 2000) is not considered in the generation of the macropore network. The applied approach (chapter 3.2.2) mainly focuses on large macropores with high conductivity that reaches nearly vertically into deeper soil layers and neglects the role of smaller and short macropores. While the water is also transported by small macropores that might end in 10 cm depth, the model concentrates the water flow to macropores that reach continuously in the deep soil. This leads to less moist upper soil layers, with all related hydrological consequences. Nevertheless the approach clearly improved modelling the hillslope response.

Zehe et al. (2010a) used CATFLOW in a thermodynamic modelling study and represented a hillslope in a very fine lateral grid size of 2 cm resulting in computation times of up to 200 hrs. Such calculation times are simply too long for most modelling approaches. As a way out, the grid size could be arranged in a variable way, such that cells including a macropore are in accordance with the diameter of macroporous structures while the grid cells can be larger in lateral extent when they contain no macropores. Such an approach may allow a representation of both, the flow volume and the flow velocity in the macropores more precisely, without extreme calculation times.

Richards based macropore flow and macropore-matrix interaction

In the modelling part of this work, the water flow in the structures and the interaction between the macropores and the soil matrix is solved based on the Richards equation. This is similar to

other studies that explicitly represent structures in the model (Vogel et al., 2006; Nieber and Sidle, 2010) or solve both domains in a dual permeability model based on the Richards equation (Gerke and van Genuchten, 1993). Since the Richards equation is invariably accompanied by a set of constitutive relations characterising the unsaturated soil hydraulic properties, in many cases following Mualem (1976) and van Genuchten (1980), these parameters have to be describe. All of the cited studies, and also this thesis, used different Mualem-van Genuchten parameter to describe the flow in the macropores. The parameterisation used in this thesis is similar to the one of Gerke and van Genuchten (1993). This brings up some open research questions that should that should be considered when dealing with further application of such an explicit approach as the effect of different Mualem-van Genuchten parameters to characterize the macropores should be studied in more detail. Nevertheless, several different parameter sets in the different studies lead to successful modelling of the role of macropores. Although the exact parameterisation is unclear, the approach of using the explicit representation together with a Richards based numerical solution offers a clear advantage to other representation of preferential flow. Since the interaction between the soil matrix and the macropores is self organising based on the network of structures and the state variables of each grid cell, no further assumptions have to be made.

Alternatives in parameterisation of model structures based on observables

Within chapter 7 an attempt was made to collect the necessary information to parameterise the approach that generates the macropore system for the modelling studies. This data is easily observable, although requires a lot of field work. The problem with this data is that, as discussed above, the model does only represent the network of the deep macropores with high hydraulic conductivities and not the numerous small or short macropores. Including these in the hillslope module of CATFLOW (see chapter 3.2) is not yet possible in an explicit way, when using a reasonable spatial grid size. In addition, it is known that not all pores conduct water under rainfall driven conditions (Beven and Germann, 1982), this strongly depends on the initiation of macropore flow at the surface or within the soil (Weiler, 2005). It remains unclear how this variability could be addressed in the model. A next step can be that the parameterisation of the model is carried out by the use of the resulting pattern of preferential flow inferred from dye tracer experiments, similar to van Schaik et al. (2010). However, this will be limited by the field scale variability of transport parameters In chapter 6.3 I showed that even five soil profiles were not able to capture the variance in the transport parameters at a 400 m² field site.

9.2.2 Better process representation in hydrological models – but how far we have to go?

Seibert and McDonnell (2002) concluded in their paper about experimentalist and modeller dialogue that it is better to have a less good overall model fit, if different soft data is represented in a better way. Thus models should be better “less right for the right reason” than “right for the wrong reason” (Seibert and McDonnell, 2002). In a series of papers (Köhne and Gerke, 2005; Haws et al., 2005; Köhne et al., 2006; Gerke et al., 2007) one- and two-

dimensional single and double domain approaches were tested whether they can predict water flows and tracer transport at field/hillslope scale. In summary, it was shown that even the double permeability approach had deficiencies to reproduce both water flows and corresponding tracer BTC at the same time in systems where preferential flow played an important role. Using an explicit representation of structures that act as preferential flow paths in a model a better process representation was achieved. Following the same approach in this thesis allowed successful modelling of both, tile drain discharge and conservative solute transport at event scale (chapter 3 and 4). This shows that a more realistic representation of structures leads to a more realistic process representation and thus improves the capability of the model to deal with more than discharge modelling. The question if the approach is feasible to deal with long term modelling remains open and should be aimed in a further step.

Internal process representation and reduction of equifinality

The used model approach was able to produce a soil moisture pattern that can be deemed to be rather realistic, when compared with the field studies (e.g. De Lannoy et al., 2006; Penna et al., 2009). At this point, better soil moisture observation could clearly improve the ability to test the feasibility of the model approach to reproduce not only the integral response of water and solutes but also internal processes such as soil moisture distribution, of course limited by the grid size. Zehe et al. (2010b) were able to show field scale variability with a network of TDR probes. Such detailed experimental data is needed to further constrain the used model approach. Since additional independent information can reduce equifinality and increase parameter identifiability (McGuire et al, 2007; and the results of the modelling study in chapter 4), a successful modelling of internal processes will also reduce equifinality and further increase parameter identifiability. A progress in observation techniques to observe 3-dimensional state variables like soil moisture, matrix potential, and solute concentration will thus be very valuable. More data that can be used in model validation will help to develop models that perform right for the right reason. If the parameterisation is based on observables this will then lead to a reduced equifinality.

Field data to improve the process representation

I was able to gain detailed process understanding in water and solute transport mechanisms at one field site in the Weiherbach catchment (chapter 5 and chapter 6). Is such detailed information useful to be included in hydrological modelling? And is it possible to include these processes in a model without getting lost in details? Modelling preferential flow often assumes that water enters the preferential flow paths and directly bypasses the soil with some degree of interaction. On the contrary, the field experiments performed in this work showed that there is complex spatial and temporal variable interaction between the macropores and the surrounding soil matrix. This process strongly influenced the composition of event and pre-event water in the hydrograph. This interaction is a very small scale process that is crucial for solute transport. Nevertheless, including such a process in a hillslope model will not be easy. The process of interaction between the macropores and the soil matrix is very limited in scale and highly variable over the depth of the soil profile. In addition, a threshold process reversed the direction of interaction during irrigation. Including a process with a spatial

extend clearly smaller than the model grid size, is a challenging task, but the experimental data suggest that it is urgently needed due to the strong relevance to the proportion between event and pre-event water in the hydrograph.

9.2.3 Modelling reactive transport – how useful are structures?

Limited modelling of reactive transport

The experimental data showed the strong link between the hydrological behaviour and the transport of reactive solutes at the study site. A clear part of the pesticides was not able to reach the adsorption places (at the macropore coating or the soil matrix) since water entered the macropores from the soil matrix. This was consistent with the modelling study (chapter 4.3.3) based on the experiment of Zehe and Flüher (2001a). When no retardation occurred in the macropores the model performed as its best, accordingly with the results of different field studies (e.g. Kladvko et al., 1991; Kung et al., 2000). Nevertheless, the model was not able to capture the behaviour of the Isoproturon concentrations, but at least it was possible to determine the amount of leached pesticide mass depending on the parameterisation of the Freundlich isotherme (see chapter 4.3.3).

Using a heterogeneous parameterisation of the sorption parameters as suggested e.g. by Ray et al. (2004), did not lead to an improvement in modelling Isoproturon. This means that a much better parameterisation of the transport and Freundlich parameters is needed to describe the detailed behaviour of reactive solutes appropriately. The sorption behaviour will be spatially highly variable due to soil characteristics and porosity. Additional sorption of reactive solutes depends on flow velocity (Perillo et al., 1998). Thus every grid cell must have a distinct parameterisation that can account for soil type, pore size distribution, and accessibility to the adsorption places. As a prerequisite the modelling of water flow must supply a flow velocity distribution for each grid cell to account for the velocity dependent retardation. In addition, the process of macropore-matrix interaction and particle bound transport must be represented in a detailed way. E.g. Jarvis et al. (1999) included particle transport in the model MACRO. Such detailed data is usually not accessible on field scale and the necessary details are not represented by available models. This complex modelling might only be possible for the core scale, where both, the state and the structure of a soil core can be observed by scanning techniques (see 1.2.1).

Depth distribution of connective structures for pesticide risk assessment

Fortunately we do not need to know the exact highly resolved temporal concentration pattern of a leaching contaminant for a useful risk assessment. What we need in order to assess this risk is the amount of the reactive solute that leaches into surface waters or groundwater bodies before it is degraded. Bolduan and Zehe (2006) showed that the degradation of pesticides is low in distinct soil locations where the microbiological activity is low. Since McGrath et al. (2010) and the experiments in chapter 6 showed that stored pesticides can easily be remobilised under rainfall driven conditions in combination with preferential flow, it is also important to know the amount of pesticides that are stored at depths where degradation is low.

Thus a simplified approach of reactive solute transport can be used for risk assessment based on the estimation of travel depths. The approach of representing preferential flow paths as explicit connective structures allows to determine the amount of pesticide that is transported into depths where it can enter tile drains, shallow groundwater, or soils with low degradation potential. Modelling the depth distribution of solutes, controlled by the depth distribution of the generated macropore network, allows a simplified risk assessment of the amount of the contaminant that is transported to a critical depth before it is finally degraded. Thus a consequent next step would be the modelling of such long term leaching to critical depths correlated to solute degradation times, to determine the risk of pesticide application at a macroporous soil above shallow groundwater among others. Modelling the leaching depths in combination with different precipitation, initial conditions, and macropore networks may allow to develop a transfer function based risk assessment.

9.3 Conclusion

The main objectives of this work were introduced in chapter 1.4.2. These were addressed in the subsequent chapters. While I summarised the achievements of this thesis in detail in chapter 9.1, this is a short conclusion referring to the main objectives. The results from the Göberlein catchment are not included in the subsequent final conclusions. The Göberlein catchment showed the strong relevance of a different type of preferential flow paths, from plot scale infiltration to catchment scale runoff generation. The swelling and shrinking of the soils follows different climatic and physical influences than the bio-geomorphic structures in the Weiherbach catchment. I finally conclude:

- It is possible to include bio-geomorphic structures in a hillslope model in an explicit way, based on observable parameters (chapter 3).
- These observables can be gained by field experiments; however the direct use to parameterisation shows some limitations (chapter 7).
- This approach allows successful modelling of event discharge and event based conservative solute transport on hillslope scale (without further calibration of the solute transport), and is able to reproduce internal hillslope processes (chapter 3 and chapter 4).
- The associated equifinality can be reduced by an additional data source (solute modelling), but is still present (chapter 4).
- Preferential flow structures in combination with a threshold controlled reversal of the direction of macropore-matrix interaction explain the high proportion of pre-event water at the studied tile drained field site in the Weiherbach catchment (chapter 5)
- This threshold behaviour additionally controls short term pesticide leaching, since it limits the access to the adsorption places (chapter 6) and
- favours long term pesticide leaching by a remobilisation of stored soil water and stored pesticides (chapter 6).

References

- Abbasi, F., Šimůnek, J., Feyen, J., Van Genuchten, M.T. and Shouse, P.J., 2003. Simultaneous inverse estimation of soil hydraulic and solute transport parameters from transient field experiments: Homogeneous soil. *Trans. A.S.A.E.*, 46(4): 1085-1095.
- Ackermann, M., 1998. Hydrogeologische Systemanalyse und Grundwasserhaushalt des Weiherbach-Einzugsgebietes. PhD Thesis, AGK-Schriftenreihe, 56. University of Karlsruhe.
- Adar, E.M., Neuman, S.P. and Woolhiser, D.A., 1988. Estimation of spatial recharge distribution using environmental isotopes and hydrochemical data, I. Mathematical model and application to synthetic data. *Journal of Hydrology*, 97(3-4): 251-277.
- Ahuja, L.R. and Hebson, C., 1992. Root Zone Water Quality Model, USDA, ARS, Fort Collins, CO.
- Algoazany, A.S., Kalita, P.K., Czapar, G.F. and Mitchell, J.K., 2007. Phosphorus transport through subsurface drainage and surface runoff from a flat watershed in east central Illinois, USA. *Journal of Environmental Quality*, 36(3): 681-693.
- Allaire, S.E., Gupta, S.C., Nieber, J. and Moncrief, J.F., 2002. Role of macropore continuity and tortuosity on solute transport in soils: 1. Effects of initial and boundary conditions. *Journal of Contaminant Hydrology*, 58(3-4): 299-321.
- Allaire, S.E., Gupta, S.C., Nieber, J. and Moncrief, J.F., 2002. Role of macropore continuity and tortuosity on solute transport in soils: 2. Interactions with model assumptions for macropore description. *Journal of Contaminant Hydrology*, 58(3-4): 283-298.
- Allaire, S.E., Roulier, S. and Cessna, A.J., 2009. Quantifying preferential flow in soils: A review of different techniques. *Journal of Hydrology*, 378(1-2): 179-204.
- Alletto, L., Coquet, Y., Benoit, P., Heddadj, D. and Barriuso, E., 2010. Tillage management effects on pesticide fate in soils. A review. *Agronomy for Sustainable Development*, 30(2): 367-400.
- Allison, G.B., Colin-Kaczala, C., Filly, A. and Fontes, J.C., 1987. Measurement of isotopic equilibrium between water, water vapour and soil CO₂ in arid zone soils. *Journal of Hydrology*, 95(1-2): 131-141.
- Anderson, A.E., Weiler, M., Alila, Y. and Hudson, R.O., 2009. Subsurface flow velocities in a hillslope with lateral preferential flow. *Water Resources Research*, 45.
- Andreini, M.S. and Steenhuis, T.S., 1990. Preferential paths of flow under conventional and conservation tillage. *Geoderma*, 46(1-3): 85-102.
- Bardossy, A., 2007. Calibration of hydrological model parameters for ungauged catchments. *Hydrology Earth System Sciences*, 11(2): 703-710.
- Barnes, C.J. and Walker, G.R., 1989. The distribution of deuterium and oxygen-18 during unsteady evaporation from a dry soil. *Journal of Hydrology*, 112(1-2): 55-67.
- Bear, J., 1972. *Dynamics of fluids in porous media*. American Elsevier, New York, 764 pp.
- Bergström, L. and Jarvis, N.J., 1993. Leaching of dichloroprop, bentazon, and Cl⁻ in undisturbed field lysimeters of different agricultural soils. *Weed Science*, 41: 251-261.
- Besien, T.J., Williams, R.J. and Johnson, A.C., 2000. The transport and behaviour of isotopuron in unsaturated chalk cores. *Journal of Contaminant Hydrology*, 43(2): 91-110.
- Beudert, G., 1997. Gewässerbelastung und Stoffaustrag von befestigten Flächen in einem kleinen, ländlichen Einzugsgebiet. PhD Thesis, Schriftenreihe Institut für Siedlungswasserwirtschaft, Band 80. University of Karlsruhe.
- Beudert, G. and Hahn, H.H., 2008. Bilanzierung des Stoffaustrags aus dem Einzugsgebiet unter besonderer Berücksichtigung des Abtrags von befestigten Flächen. In: E. Plate

- and E. Zehe (Editors), *Hydrologie und Stoffdynamik kleiner Einzugsgebiete: Prozesse und Modelle*. Schweizerbart'sche Verlagsbuchhandlung (Nägele u. Obermiller), Stuttgart, pp. 160-181.
- Beven, K., 1993. Prophecy, reality and uncertainty in distributed hydrological modelling. *Advances in Water Resources*, 16(1): 41-51.
- Beven, K., 1996. Equifinality and uncertainty in geomorphological modelling. In: B.L. Rhoads and C.E. Thorn (Editors), *The Scientific Nature of Geomorphology*. Wiley, Chichester, pp. 289-313.
- Beven, K., 2001a. How far can we go in distributed hydrological modelling? *Hydrology Earth System Sciences*, 5(1): 1-12.
- Beven, K., 2001b. On hypothesis testing in hydrology. *Hydrological Processes*, 15(9): 1655-1657.
- Beven, K., 2002. Towards an alternative blueprint for a physically based digitally simulated hydrologic response modelling system. *Hydrological Processes*, 16(2): 189-206.
- Beven, K., 2006. A manifesto for the equifinality thesis. *Journal of Hydrology*, 320(1-2): 18-36.
- Beven, K., 2010. Preferential flows and travel time distributions: Defining adequate hypothesis tests for hydrological process models. *Hydrological Processes*, 24(12): 1537-1547.
- Beven, K. and Clarke, R., 1986. On the variation of infiltration into a homogenous soil matrix containing a population of macropores. *Water Resources Research*, 22(3): 383-388.
- Beven, K. and Freer, J., 2001. Equifinality, data assimilation, and uncertainty estimation in mechanistic modelling of complex environmental systems using the GLUE methodology. *Journal of Hydrology*, 249(1-4): 11-29.
- Beven, K. and Germann, P., 1982. Macropores and water flow in soils. *Water Resources Research*, 18(5): 1311-1325.
- Binley, A. and Beven, K., 2003. Vadose zone flow model uncertainty as conditioned on geophysical data. *Ground Water*, 41(2): 119-127.
- Blake, G., Schlichting, E. and Zimmermann, U., 1973. Water recharge in a soil with shrinkage cracks. *Soil Science Society of America Journal*, 37(5): 669-672.
- Blöschl, G. and Zehe, E., 2005. On hydrological predictability. *Hydrological Processes*, 19(19): 3923-3929.
- Blume, T., Zehe, E. and Bronstert, A., 2007. Rainfall runoff response, event-based runoff coefficients and hydrograph separation. *Hydrological Sciences Journal*, 52(5): 843-862.
- Blume, T., Zehe, E. and Bronstert, A., 2009. Use of soil moisture dynamics and patterns at different spatio-temporal scales for the investigation of subsurface flow processes. *Hydrology Earth System Sciences*, 13(7): 1215-1233.
- Boivin, A., Šimůnek, J., Schiavon, M. and van Genuchten, M.T., 2006. Comparison of pesticide transport processes in three tile-drained field soils using HYDRUS-2D. *Vadose Zone Journal*, 5(3): 838-849.
- Bolduan, R. and Zehe, E., 2006. Mikrobieller Abbau des Herbizids Isoproturon in Bioporen und der Bodenmatrix - Eine Feldstudie. *Journal of Plant Nutrition Soil Science*, 169: 87-94.
- Boll, J., Steenhuis, T.S. and Selker, J.S., 1992. Fiberglass Wicks for sampling of water and solutes in the Vadose Zone. *Soil Science Society of America Journal*, 56(3): 701-707.
- Bouma, J., 1990. Using morphometric expressions for macropores to improve soil physical analyses of field soils. *Geoderma*, 46(1-3): 3-11.
- Bouma, J. and Dekker, L.W., 1978. A case study on infiltration into dry clay soil I. Morphological observations. *Geoderma*, 20(1): 27-40.

- Bouma, J., Jongerius, A., Boersma, O., Jager, A. and Schoonderbeek, D., 1977. The function of different types of macropores during saturated flow through four swelling soil horizons. *Soil Science Society of America Journal*, 41(5): 945-950.
- Braudeau, E., Costantini, J.M., Bellier, G. and Colleuille, H., 1999. New device and method for soil shrinkage curve measurement and characterization. *Soil Science Society of America Journal*, 63(3): 525-535.
- Bronstert, A. and Plate, E.J., 1997. Modelling of runoff generation and soil moisture dynamics for hillslopes and micro-catchments. *Journal of Hydrology*, 198(1-4): 177-195.
- Bronswijk, J.J.B., 1988. Modeling of water balance, cracking and subsidence of clay soils. *Journal of Hydrology*, 97(3-4): 199-212.
- Burns, D.A., McDonnell, J.J., Hooper, R.P., Peters, N.E., Freer, J.E., Kendall, C. and Beven, K., 2001. Quantifying contributions to storm runoff through end-member mixing analysis and hydrologic measurements at the Panola Mountain Research Watershed (Georgia, USA). *Hydrological Processes*, 15(10): 1903-1924.
- Butt, K., Shipitalo, M., Bohlen, P., Edwards, W.M. and Parmelee, R., 1999. Long-term trends in earthworm populations of cropped experimental watersheds in Ohio, USA. *Pedobiologica*, 43: 713-719.
- Buttle, J.M., 1994. Isotope hydrograph separations and rapid delivery of pre-event water from drainage basins. *Progress in Physical Geography*, 18(1): 16-41.
- Buttle, J.M. and McDonald, D.J., 2002. Coupled vertical and lateral preferential flow on a forested slope. *Water Resources Research*, 38(5): 1060.
- Campana, M.E. and Simpson, E.S., 1984. Groundwater residence times and recharge rates using a discrete-state compartment model and ^{14}C data. *Journal of Hydrology*, 72(1-2): 171-185.
- Celia, M., Bouloutas, E. and Zarba, R., 1990. A General mass-conservative numerical solution for the unsaturated flow equation. *Water Resources Research*, 26(7): 1483-1496.
- Cey, E.E. and Rudolph, D.L., 2009. Field study of macropore flow processes using tension infiltration of a dye tracer in partially saturated soils. *Hydrological Processes*, 23(12): 1768-1779.
- Chan, K.-Y. and Munro, K., 2001. Evaluating mustard extracts for earthworm sampling. *Pedobiologica*, 45(3): 272-278.
- Chertkov, V.Y., 2000. Modeling the pore structure and shrinkage curve of soil clay matrix. *Geoderma*, 95(3-4): 215-246.
- Chertkov, V.Y., 2004. A physically based model for the water retention curve of clay pastes. *Journal of Hydrology*, 286(1-4): 203-226.
- Christiansen, S.J., Thorsen, M., Clausen, T., Hansen, S. and Refsgaard, C.J., 2004. Modelling of macropore flow and transport processes at catchment scale. *Journal of Hydrology*, 299(1-2): 136-158.
- Clothier, B.E., Green, S.R. and Deurer, M., 2008. Preferential flow and transport in soil: progress and prognosis. *European Journal of Soil Science*, 59: 2-13.
- Comegna, V., Coppola, A. and Sommella, A., 2001. Effectiveness of equilibrium and physical non-equilibrium approaches for interpreting solute transport through undisturbed soil columns. *Journal of Contaminant Hydrology*, 50(1-2): 121-138.
- Coppola, A., Comegna, V., Basile, A., Lamaddalena, N. and Severino, G., 2009. Darcian preferential water flow and solute transport through bimodal porous systems: Experiments and modelling. *Journal of Contaminant Hydrology*, 104(1-4): 74-83.
- Czapar, G.F., Horton, R. and Fawcett, R.S., 1992. Herbicide and tracer movement in soil columns containing an artificial macropore. *Journal of Environmental Quality*, 21(1): 110-115.

- de Jonge, H., Jacobsen, O.H., de Jonge, L.W. and Moldrup, P., 1998. Particle-facilitated transport of prochloraz in undisturbed sandy loam soil columns. *Journal of Environmental Quality*, 27(6): 1495-1503.
- de Jonge, L.W., Moldrup, P., Rubaek, G.H., Schelde, K. and Djurhuus, J., 2004. Particle leaching and particle-facilitated transport of phosphorus at field scale. *Vadose Zone Journal*, 3(2): 462-470.
- De Lannoy, G.J.M., Verhoest, N.E.C., Houser, P.R., Gish, T.J. and Van Meirvenne, M., 2006. Spatial and temporal characteristics of soil moisture in an intensively monitored agricultural field (OPE3). *Journal of Hydrology*, 331(3-4): 719-730.
- de Rooij, G.H., 2000. Modeling fingered flow of water in soils owing to wetting front instability: A review. *Journal of Hydrology*, 231-232: 277-294.
- de Rooij, G.H. and Stagnitti, F., 2000. Spatial variability of solute leaching. *Soil Science Society of America Journal*, 64(2): 499-504.
- Delbrück, M., 1997. Großflächiges Bromid-Tracerexperiment zur räumlichen und zeitlichen Variabilität des Wassertransports an einem Lößhang. PhD Thesis, Ruprecht-Karls-University of Heidelberg, Heidelberg, Germany.
- Delbrück, M., 2008. Tracer-Untersuchungen auf der Hangskale zur Regionalisierung der Sickerwasserbewegung. In: E. Plate and E. Zehe (Editors), *Hydrologie und Stoffdynamik kleiner Einzugsgebiete: Prozesse und Modelle*. Schweizerbart'sche Verlagsbuchhandlung (Nägele u. Obermiller), Stuttgart, pp. 199-211.
- Deurer, M. and Clothier, B.E., 2005. Unraveling microscale flow and geometry: NMRI and X-ray tomography. In: J. Alvarez-Benedi and R. Munoz-Carpena (Editors), *Soil-Water-Solute Process Characterization – An Integrated Approach*. CRC Press, Boca Raton, FL, USA, pp. 253-288.
- Doerr, S.H., Shakesby, R.A., Dekker, L.W. and Ritsema, C.J., 2006. Occurrence, prediction and hydrological effects of water repellency amongst major soil and land-use types in a humid temperate climate. *European Journal of Soil Science*, 57(5): 741-754.
- Donald, W.W., Hjelmfelt, A.T. and Alberts, E.E., 1998. Herbicide distribution and variability across Goodwater Creek watershed in north central Missouri. *Journal of Environmental Quality*, 27(5): 999-1009.
- Dooge, J.C.I., 1986. Looking for hydrologic laws. *Water Resources Research*, 22(9S): 46-58.
- Dunne, T. and Black, R., 1970. Partial area contributions to storm runoff in a small New England watershed. *Water Resources Research*, 6(5): 1296-1311.
- Durner, W., 1994. Hydraulic conductivity estimation for soils with heterogeneous pore structure. *Water Resources Research*, 30(2): 211-223.
- Durner, W., Priesack, E., Vogel, H.J. and Zurmühl, T., 1999. Determination of parameters for flexible hydraulic functions by inverse modeling. In: M.T. van Genuchten, F.J. Leij and L. Wu (Editors), *Characterization and measurement of the hydraulic properties of unsaturated porous media*. University of California, Riverside, CA, pp. 817-829.
- Edwards, C.A. and Bohlen, P.J., 1996. *Biology and ecology of earthworms* Chapman & Hall, London, UK.
- Edwards, W.M., Norton, L.D. and Redmond, C.E., 1988. Characterizing macropores that affect infiltration into nontilled soil. *Soil Science Society of America Journal*, 52(2): 483-487.
- Edwards, W.M., Shipitalo, M.J., Owens, L.B. and Norton, L.D., 1989. Water and nitrate movement in earthworm burrows within long-term no-till cornfields. *Journal of Soil and Water Conservation*, 44(3): 240-243.
- Eitel, B., 1989. Morphogenese im südlichen Kraichgau unter besonderer Berücksichtigung tertiärer und pleistozäner Decksedimente. *Stuttgarter geographische Studien*, Stuttgart, 111 pp.

- Elliott, J.A., Cessna, A.J., Nicholaichuk, W. and Tollefson, L.C., 2000. Leaching rates and preferential flow of selected herbicides through tilled and untilled soil. *Journal of Environmental Quality*, 29(5): 1650-1656.
- Everts, C.J., Kanwar, R.S., Alexander, E.C. and Alexander, S.C., 1989. Comparison of tracer mobilities under laboratory and field conditions. *Journal of Environmental Quality*, 18(4): 491-498.
- Footprint, 2006. The FOOTPRINT pesticide properties DataBase. Database collated by the University of Hertfordshire as part of the EU-funded FOOTPRINT project (FP6-SSP-022704). <http://www.eu-footprint.org/ppdb.html>.
- Flury, M., 1996. Experimental evidence of transport of pesticides through field soils-a review. *Journal of Environmental Quality*, 25(1): 25-45.
- Flury, M., Flühler, H., Jury, W.A. and Leuenberger, J., 1994. Susceptibility of soils to preferential flow of water: A field study. *Water Resources Research*, 30(7): 1945-1954.
- Flury, M., Leuenberger, J., Studer, B. and Flühler, H., 1995. Transport of anions and herbicides in a loamy and a sandy field soil. *Water Resources Research*, 31(4): 823-835.
- Fortin, J., Jury, W.A. and Anderson, M.A., 1998. Dissolution of trapped nonaqueous phase liquids in sand columns. *Journal of Environmental Quality*, 27(1): 38-45.
- Freer, J., Beven, K. and Ambrose, B., 1996. Bayesian estimation of uncertainty in runoff prediction and the value of data: An application of the GLUE approach. *Water Resources Research*, 32(7): 2161-2173.
- Gärdenäs, A.I., Šimůnek, J., Jarvis, N. and van Genuchten, M.T., 2006. Two-dimensional modelling of preferential water flow and pesticide transport from a tile-drained field. *Journal of Hydrology*, 329(3-4): 647-660.
- Gaynor, J.D., Tan, C.S., Drury, C.F., Ng, H.Y.F., Welacky, T.W. and van Wesenbeeck, I. J., 2001. Tillage, intercrop, and controlled drainage - subirrigation influence atrazine, metribuzin, and metolachlor loss. *Journal of Environmental Quality*, 30(2): 561-572.
- Gerke, H.H., 2006. Preferential flow descriptions for structured soils. *Journal of Plant Nutrition and Soil Science*, 169(3): 382-400.
- Gerke, H.H., Dusek, J., Vogel, T. and Kohne, J.M., 2007. Two-dimensional dual-permeability analyses of a bromide tracer experiment on a tile-drained field. *Vadose Zone Journal*, 6(3): 651-667.
- Gerke, H.H. and Köhne, M.J., 2004. Dual-permeability modeling of preferential bromide leaching from a tile-drained glacial till agricultural field. *Journal of Hydrology*, 289(1-4): 239-257.
- Gerke, H.H. and van Genuchten, M.T., 1993. A dual-porosity model for simulating the preferential movement of water and solutes in structured porous media. *Water Resources Research*, 29(2): 305-319.
- Gerlinger, K., 1997. Erosionsprozesse auf Lössböden: Experimente und Modellierung. Mitteilung Inst. Wasserbau und Kulturrechnik der Universität Karlsruhe, 194.
- Gerlinger, K., 2008. Untersuchung der räumlichen und zeitlichen Variabilität der Erosionsneigung von Böden als Grundlage eines Erosionsmodel. In: E. Plate and E. Zehe (Editors), *Hydrologie und Stoffdynamik kleiner Einzugsgebiete: Prozesse und Modelle*. Schweizerbart'sche Verlagsbuchhandlung (Nägele u. Obermiller), Stuttgart, pp. 235-250.
- Germann, P., 1990. Macropores and hydrological hillslope processes. In: T.P. Anderson and T.P. Burt (Editors), *Process studies in hillslope hydrology*. John Wiley & Sons, Chichester, UK, pp. 327-363.
- Germann, P. and Beven, K., 1985. Kinematic wave approximation to infiltration into soils with sorbing macropores. *Water Resources Research*, 21(7): 990-996.

- Germann, P., Helbling, A. and Vadilonga, T., 2007. Rivulet approach to rates of preferential infiltration. *Vadose Zone Journal*, 6(2): 207-220.
- Germann, P.F., 1987. The three modes of water flow through a vertical pipe. *Soil Science*, 144(2): 153-154.
- Germann, P.F. and Di Pietro, L., 1999. Scales and dimensions of momentum dissipation during preferential flow in soils. *Water Resources Research*, 35(5): 1443-1454.
- Gerold, G., 1992. Prognosemodell für die Gewässerbelastung durch Stofftransport in einem kleinen ländlichen Einzugsgebiet, Schlussbericht zur ersten Phase des MBFT-Verbundprojektes, Institut für Hydrologie und Wasserwirtschaft der Universität Karlsruhe.
- Gianfrani, L., Gagliardi, G., van Burgel, M. and Kerstel, E., 2003. Isotope analysis of water by means of near infrared dual-wavelength diode laser spectroscopy. *Optics Express*, 11(13): 1566-1576.
- Gish, T.J., Dulaney, W. P., Kung, K.J.S., Daughtry, C.S.T., Doolittle, J.A. and Miller, P. T., 2002. Evaluating use of ground-penetrating radar for identifying subsurface flow pathways. *Soil Science Society of America Journal*, 66(5): 1620-1629.
- Gish, T.J., Kung, K.J.S., Perry, D.C., Posner, J., Bubenzer, G., Helling, C.S., Kladvko, E.J. and Steenhuis, T.S., 2004. Impact of preferential flow at varying irrigation rates by quantifying mass fluxes. *Journal of Environmental Quality*, 33(3): 1033-1040.
- Graham, C.B., Woods, R.A. and McDonnell, J.J., 2010. Hillslope threshold response to rainfall: (1) A field based forensic approach. *Journal of Hydrology*, 393(1-2): 65-76.
- Greco, R., 2002. Preferential flow in macroporous swelling soil with internal catchment: Model development and applications. *Journal of Hydrology*, 269(3-4): 150-168.
- Grevers, M.C.J. and Jong. E.D., 1990. The characterization of soil macroporosity of clay soil under then grasses using image analysis. *Canadian Journal of Soil Science*, 70(1): 93-103.
- Grossmann, J. and Udluft, P., 1991. The extraction of soil water by the suction-cup method: A review. *Journal of Soil Science*, 42(1): 83-93.
- Gupta, P., Noone, D., Galewsky, J., Sweeney, C. and Vaughn, B.H., 2009. A new laser-based, field-deployable analyzer for laboratory-class stable isotope measurements in water. *Geochimica et Cosmochimica Acta*, 73(13): A480-A480.
- Hagedorn, F. and Bundt, M., 2002. The age of preferential flow paths. *Geoderma*, 108(1-2): 119-132.
- Hahn, H.H. and Beudert, G., 1997. Schlussbericht des BMBF-Verbundprojektes: Prognosemodell für die Gewässerbelastung durch Stofftransport aus kleinen ländlichen Einzugsgebieten – Weiherbachprojekt. Teilprojekt 8: Stofftransport und Bilanzierung von Nährstoffen. Untersuchung des Stoffaustrages unter besonderer Berücksichtigung der Abspülung von befestigten landwirtschaftlichen Flächen, Institut für Siedlungswasserwirtschaft der Universität Karlsruhe.
- Haws, N.W., Rao, P.S.C., Šimůnek, J. and Poyer, I.C., 2005. Single-porosity and dual-porosity modeling of water flow and solute transport in subsurface-drained fields using effective field-scale parameters. *Journal of Hydrology*, 313(3-4): 257-273.
- Hendrickx, J.M.H., Dekker, L.W. and Boersma, O.H., 1993. Unstable wetting fronts in water-repellent field soils. *Journal of Environmental Quality*, 22(1): 109-118.
- Hendrickx, J.M.H. and Flury, M., 2001. Uniform and preferential flow mechanisms in the vadose zone. In: National Research Council, Conceptual models of flow and transport in the fractured vadose zone. National Academy Press, Washington, DC, pp. 149-187.
- Hendriks, R.F.A., Oostindie, K. and Hamminga, P., 1999. Simulation of bromide tracer and nitrogen transport in a cracked clay soil with the FLOCR/ANIMO model combination. *Journal of Hydrology*, 215(1-4): 94-115.

- Hendry, M.J., Wassenaar, L.I. and Lis, G.P., 2008. Stable isotope composition of gaseous and dissolved oxygen in the subsurface. *Geochimica et Cosmochimica Acta*, 72(12): A367-A367.
- Hewlett, J.D. and Hibbert, A.R., 1967. Factors affecting the response of small watersheds to precipitation in humid areas. In: W.E. Sopper and H.W. Lull (Editors), *Forest Hydrology*. Pergamon Press, New York, pp. 275-290.
- Hill, D.E. and Parlange, J.Y., 1972. Wetting front instability in layered soils. *Soil Science Society America Proceedings*, 36: 697-702.
- Hoeg, S., Uhlenbrook, S. and Leibundgut, C., 2000. Hydrograph separation in a mountainous catchment — combining hydrochemical and isotopic tracers. *Hydrological Processes*, 14(7): 1199-1216.
- Hopmans, J.W., Cislerova, M. and Vogel, T., 1994. X-ray tomography of soil properties. In: S.H. Ande and J.W. Hopmans (Editors), *Tomography of Soil-Water-Root Processes*. ASA, SSSA, Madison, WI, USA, pp. 17-28.
- Hopp, L. and McDonnell, J.J., 2009. Connectivity at the hillslope scale: Identifying interactions between storm size, bedrock permeability, slope angle and soil depth. *Journal of Hydrology*, 376(3-4): 378-391.
- Horn, R., Taubner, H., Wuttke, M. and Baumgartl, T., 1994. Soil physical properties related to soil structure. *Soil and Tillage Research*, 30(2-4): 187-216.
- Horton, J.H. and Hawkins, R.H., 1965. Flow path of rain from the soil surface to the water table. *Soil Science*, 100: 377-383.
- Iannone, R.Q., Romanini, D., Cattani, O., Meijer, H.A.J. and Kerstel, E.R.T., 2010. Water isotope ratio ($\delta^2\text{H}$ and $\delta^{18}\text{O}$) measurements in atmospheric moisture using an optical feedback cavity enhanced absorption laser spectrometer. *Journal of Geophysical Research*, 115(D10): D10111.
- Jardine, P.M., Wilson, G.V. and Luxmoore, R.J., 1990. Unsaturated solute transport through a forest soil during rain storm events. *Geoderma*, 46(1-3): 103-118.
- Jarvis, N., 1994. The MACRO model (version 3.1): technical description and sample simulations, Reports and Dissertations 19. Swedish University of Agricultural Science, Department Soil Science, Uppsala, 51 pp.
- Jarvis, N.J., 2007. A review of non-equilibrium water flow and solute transport in soil macropores: Principles, controlling factors and consequences for water quality. *European Journal of Soil Science*, 58(3): 523-546.
- Jarvis, N.J., 2009. Near-saturated hydraulic properties of macroporous soils. *Vadose Zone Journal*, 7(4): 1302-1310.
- Jarvis, N.J., Hollis, J.M., Nicholls, P.H., Mayr, T. and Evans, S.P., 1997. MACRO--DB: A decision-support tool for assessing pesticide fate and mobility in soils. *Environmental Modelling & Software*, 12(2-3): 251-265.
- Jarvis, N.J., Leeds-Harrison, P.B. and Dosser, J.M., 1987. The use of tension infiltrometers to assess routes and rates of infiltration in a clay soil. *Journal of Soil Science*, 38(4): 633-640.
- Jarvis, N.J., Moeys, J., Hollis, J.M., Reichenberger, S., Lindahl, A.M.L. and Dubus, I.G., 2009. A conceptual model of soil susceptibility to macropore flow. *Vadose Zone Journal*, 8(4): 902-910.
- Jarvis, N.J., Villholth, K.G. and Ulén, B., 1999. Modelling particle mobilization and leaching in macroporous soil. *European Journal of Soil Science*, 50(4): 621-632.
- Jarvis, N.J., Zavattaro, L., Rajkai, K., Reynolds, W.D., Olsen, P.A., McGechan, M., Mecke, M., Mohanty, B., Leeds-Harrison, P.B. and Jacques, D., 2002. Indirect estimation of near-saturated hydraulic conductivity from readily available soil information. *Geoderma*, 108(1-2): 1-17.

- Jones, J.A.A., 1997. Pipeflow contributing areas and runoff response. *Hydrological Processes*, 11(1): 35-41.
- Jones, J.A.A., 2010. Soil piping and catchment response. *Hydrological Processes*, 24(12): 1548-1566.
- Jones, J.A.A. and Connelly, L.J., 2002. A semi-distributed simulation model for natural pipeflow. *Journal of Hydrology*, 262(1-4): 28-49.
- Ju, S.H. and Kung, K.J.S., 1997. Impact of funnel flow on contaminant transport in sandy soils: Numerical simulation. *Soil Science Society of America Journal*, 61(2): 409-415.
- Jury, W., Elabd, H. and Resketo, M., 1986. Field study of napropamide movement through unsaturated soil. *Water Resources Research*, 22(5): 749-755.
- Jury, W.A. and Flühler, H., 1992. Transport of chemicals through soil: Mechanisms, models, and field applications, *Advances in Agronomy*. Academic Press, pp. 141-201.
- Jury, W.A. and Horton, R., 2004. *Soil Physics*. John Wiley & Sons, Inc., Hoboken, NJ, USA.
- Jury, W.A. and Roth, K., 1990. *Transfer functions and solute transport through soils: Theory and applications*. Birkhäuser, Basel.
- Kasteel, R., Pütz, T. and Vereecken, H., 2007. An experimental and numerical study on flow and transport in a field soil using zero-tension lysimeters and suction plates. *European Journal of Soil Science*, 58(3): 632-645.
- Kasteel, R., Vogel, H.J. and Roth, K., 2002. Effect of non-linear adsorption on the transport behaviour of Brilliant Blue in a field soil. *European Journal of Soil Science*, 53(2): 231-240.
- Kerstel, E. and Gianfrani, L., 2008. Advances in laser-based isotope ratio measurements: Selected applications. *Applied Physics B: Lasers and Optics*, 92(3): 439-449.
- Kim, D.J., Angulo Jaramillo, R., Vauclin, M., Feyen, J. and Choi, S.I., 1999. Modeling of soil deformation and water flow in a swelling soil. *Geoderma*, 92(3-4): 217-238.
- Kirchner, J.W., 2003. A double paradox in catchment hydrology and geochemistry. *Hydrological Processes*, 17(4): 871-874.
- Kitanidis, P.K., 1997. *Introduction to Geostatistics: Applications in hydrogeology*. Cambridge University Press, Cambridge, UK, 271 pp.
- Kladivko, E.J., Brown, L.C. and Baker, J.L., 2001. Pesticide transport to subsurface tile drains in humid regions of North America. *Critical Reviews in Environmental Science and Technology*, 31(1): 1 - 62.
- Kladivko, E.J., Grochulska, J., Turco, R.F., Van Scoyoc, G.E. and Eigel, J.D., 1999. Pesticide and nitrate transport into subsurface tile drains of different spacings. *Journal of Environmental Quality*, 28(3): 997-1004.
- Kladivko, E.J., Van Scoyoc, G.E., Monke, E.J., Oates, K.M. and Pask, W., 1991. Pesticide and nutrient movement into subsurface tile drains on a silt loam soil in Indiana. *Journal of Environmental Quality*, 20(1): 264-270.
- Klaus, J., Külls, C. and Dahan, O., 2008. Evaluating the recharge mechanism of the Lower Kuiseb Dune area using mixing cell modeling and residence time data. *Journal of Hydrology*, 358(3-4): 304-316.
- Klaus, J. and Zehe, E., 2010. Modelling rapid flow response of a tile-drained field site using a 2D physically based model: Assessment of 'equifinal' model setups. *Hydrological Processes*, 24(12): 1595-1609.
- Köhne, J.M., 2005. Mini suction cups and water-extraction effects on preferential solute transport. *Vadose Zone Journal*, 4(3): 866-880.
- Köhne, J.M. and Gerke, H.H., 2005. Spatial and temporal dynamics of preferential bromide movement towards a tile drain. *Vadose Zone Journal*, 4(1): 79-88.
- Köhne, J.M., Köhne, S. and Šimůnek, J., 2006. Multi-process herbicide transport in structured soil columns: Experiments and model analysis. *Journal of Contaminant Hydrology*, 85(1-2): 1-32.

- Köhne, J.M., Köhne, S. and Šimůnek, J., 2009a. A review of model applications for structured soils: a) Water flow and tracer transport. *Journal of Contaminant Hydrology*, 104(1-4): 4-35.
- Köhne, J.M., Köhne, S. and Šimůnek, J., 2009b. A review of model applications for structured soils: b) Pesticide transport. *Journal of Contaminant Hydrology*, 104(1-4): 36-60.
- Köhne, S., Lennartz, B., Köhne, J.M. and Simunek, J., 2006. Bromide transport at a tile-drained field site: Experiment, and one- and two-dimensional equilibrium and non-equilibrium numerical modeling. *Journal of Hydrology*, 321(1-4): 390-408.
- Kolle, O. and Fiedler, F., 2008. Messung der Energie- und Feuchtebilanz der Bodenoberfläche. In: E. Plate and E. Zehe (Editors), *Hydrologie und Stoffdynamik kleiner Einzugsgebiete: Prozesse und Modelle*. Schweizerbart'sche Verlagsbuchhandlung (Nägele u. Obermiller), Stuttgart, pp. 137-160.
- Königer, P., Leibundgut, C., Link, T. and Marshall, J.D., 2010. Stable isotopes applied as water tracers in column and field studies. *Organic Geochemistry*, 41(1): 31-40.
- Külls, C., 2011. personal communication.
- Kumar, A., Kanwar, R.S. and Hallberg, G.R., 1997. Separating preferential and matrix flows using subsurface tile flow data. *Journal of Environmental Science and Health . Part A: Environmental Science and Engineering and Toxicology*, 32(6): 1711 - 1729.
- Kung, K.J.S., 1990a. Preferential flow in a sandy vadose zone: 1. Field observation. *Geoderma*, 46(1-3): 51-58.
- Kung, K.J.S., 1990b. Preferential flow in a sandy vadose zone: 2. Mechanism and implications. *Geoderma*, 46(1-3): 59-71.
- Kung, K.J.S. and Donohue, S.V., 1991. Improved solute-sampling protocol in a sandy vadose zone using ground-penetrating radar. *Soil Science Society of America Journal*, 55(6): 1543-1545.
- Kung, K.J.S., Steenhuis, T. S., Kladvik, E. J., Gish, T. J., Bubenzer, G. and Helling, C. S., 2000. Impact of preferential flow on the transport of adsorbing and non-adsorbing tracers. *Soil Science Society of America Journal*, 64(4): 1290-1296.
- Lange, J., Arbel, Y., Grodek, T. and Greenbaum, N., 2010. Water percolation process studies in a Mediterranean karst area. *Hydrological Processes*, 24(13): 1866-1879.
- Larsbo, M. and Jarvis, N., 2005. Simulating solute transport in a structured field soil. *Journal of Environmental Quality*, 34(2): 621-634.
- Larsbo, M. and Jarvis, N., 2006. Information content of measurements from tracer microlysimeter experiments designed for parameter identification in dual-permeability models. *Journal of Hydrology*, 325(1-4): 273-287.
- Larsbo, M., Stenström, J., Etana, A., Börjesson, E. and Jarvis, N.J., 2009. Herbicide sorption, degradation, and leaching in three Swedish soils under long-term conventional and reduced tillage. *Soil and Tillage Research*, 105(2): 200-208.
- Lawes, J.B., Gilbert, J.H. and Warington, R., 1882. On the amount and composition of the rain and drainage waters collected at Rothamsted. William Clowes & Sons, London.
- Leaney, F.W., Smettem, K.R.J. and Chittleborough, D.J., 1993. Estimating the contribution of preferential flow to subsurface runoff from a hillslope using deuterium and chloride. *Journal of Hydrology*, 147(1-4): 83-103.
- Legout, A., Legout, C., Nys, C. and Dambrine, E., 2009. Preferential flow and slow convective chloride transport through the soil of a forested landscape (Fougères, France). *Geoderma*, 151(3-4): 179-190.
- Lehmann, P., Hinz, C., McGrath, G., Tromp-van Meerveld, H.J. and McDonnell, J.J., 2007. Rainfall threshold for hillslope outflow: An emergent property of flow pathway connectivity. *Hydrology Earth System Sciences*, 11(2): 1047-1063.

- Lennartz, B., Michaelsen, J., Widmoser, P. and Wichtmann, W., 1999. Time variance analysis of preferential solute movement at a tile-drained field site. *Soil Science Society of America Journal*, 63(1): 39-47.
- Leu, C., Singer, H., Stamm, C., Müller, S.R. and Schwarzenbach, R.P., 2004. Variability of herbicide losses from 13 fields to surface water within a small catchment after a controlled herbicide application. *Environmental Science & Technology*, 38(14): 3835-3841.
- Li, H., Sivapalan, M., Tian, F. and Liu, D., 2010. Water and nutrient balances in a large tile-drained agricultural catchment: A distributed modeling study. *Hydrology Earth System Sciences*, 14(11): 2259-2275.
- Lindahl, A.M.L., Dubus, I.G. and Jarvis, N.J., 2009. Site classification to predict the abundance of the deep-burrowing earthworm *Lumbricus terrestris* L. *Vadose Zone Journal*, 8(4): 911-915.
- Lindenmaier, F., Buck, W. and Plate, E., 2008. Charakterisierung des Untersuchungsgebietes. In: E. Plate and E. Zehe (Editors), *Hydrologie und Stoffdynamik kleiner Einzugsgebiete: Prozesse und Modelle*. Schweizerbart'sche Verlagsbuchhandlung (Nägele u. Obermiller), Stuttgart, pp. 81-100.
- Lindenmaier, F., Zehe, E., Dittfurth, A. and Ihringer, J., 2005. Process identification at a slow-moving landslide in the Vorarlberg Alps. *Hydrological Processes*, 19: 1635-1651.
- Logsdon, S.D., 1995. Flow mechanisms through continuous and buried macropores. *Soil Science*, 160(4): 237-242.
- Lorenz, G., 1992. Stickstoffdynamik in Catenen einer erosionsgeprägten Lößlandschaft. *Hohenheimer Bodenkundliche Hefte*, Nr.1. Universität Hohenheim.
- Ludwig, R., Gerke, H.H. and Wendroth, O., 1999. Describing water flow in macroporous field soils using the modified macro model. *Journal of Hydrology*, 215(1-4): 135-152.
- Lyon, S.W., Desilets, S.L.E. and Troch, P.A., 2008. Characterizing the response of a catchment to an extreme rainfall event using hydrometric and isotopic data. *Water Resources Research*, 44(6): W06413.
- Lyon, S.W., Desilets, S.L.E. and Troch, P.A., 2009. A tale of two isotopes: Differences in hydrograph separation for a runoff event when using δD versus $\delta^{18}O$. *Hydrological Processes*, 23(14): 2095-2101.
- Majoube, M., 1971. Fractionnement en oxygène-18 et en deuterium entre l'eau et sa vapeur. *Journal De Chimie Physique*, 197: 1423-1436.
- Mallawatantri, A.P., McConkey, B.G. and Mulla, D.J., 1996. Characterization of pesticide sorption and degradation in macropore linings and soil horizons of Thatuna silt loam. *Journal of Environmental Quality*, 25(2): 227-235.
- Malone, R.W., Weatherington-Rice, J., Shipitalo, M.J., Fausey, N., Ma, L., Ahuja, L.R., Don Wauchope, R. and Ma, Q., 2004. Herbicide leaching as affected by macropore flow and within-storm rainfall intensity variation: A RZWQM simulation. *Pest Management Science*, 60(3): 277-285.
- Maurer, T., 1997. Physikalisch begründete, zeitkontinuierliche Modellierung des Wassertransports in kleinen ländlichen Einzugsgebieten. PhD Thesis. *Mitteilungen Inst. f. Hydrologie u. Wasserwirtschaft*, 61. University of Karlsruhe, 252 pp.
- McDonnell, J., 1990. A rationale for old water discharge through macropores in a steep, humid catchment. *Water Resources Research*, 26(11): 2821-2832.
- McDonnell, J.J., McGuire, K., Aggarwal, P., Beven, K. J., Biondi, D., Destouni, G., Dunn, S., James, A., Kirchner, J., Kraft, P., Lyon, S., Maloszewski, P., Newman, B., Pfister, L., Rinaldo, A., Rodhe, A., Sayama, T., Seibert, J., Solomon, K., Soulsby, C., Stewart, M., Tetzlaff, D., Tobin, C., Troch, P., Weiler, M., Western, A., Wörman, A. and Wrede, S., 2010. How old is streamwater? Open questions in catchment transit time

- conceptualization, modelling and analysis. *Hydrological Processes*, 24(12): 1745-1754.
- McDonnell, J.J., Sivapalan, M., Vaché, K., Dunn, S., Grant, G., Haggerty, R., Hinz, C., Hooper, R., Kirchner, J., Roderick, M.L., Selker, J. and Weiler, M., 2007. Moving beyond heterogeneity and process complexity: A new vision for watershed hydrology. *Water Resour. Res.*, 43(7): W07301.
- McGarry, D. and Malafant, K.W.J., 1987. The analysis of volume change in unconfined units of soil. *Soil Science Society of America Journal*, 51(2): 290-297.
- McGrath, G.S., Hinz, C. and Sivapalan, M., 2007. Temporal dynamics of hydrological threshold events. *Hydrology Earth System Sciences*, 11(2): 923-938.
- McGrath, G.S., Hinz, C. and Sivapalan, M., 2008. Modelling the impact of within-storm variability of rainfall on the loading of solutes to preferential flow pathways. *European Journal of Soil Science*, 59(1): 24-33.
- McGrath, G.S., Hinz, C., Sivapalan, M., Dressel, J., Pütz, T. and Vereecken, H., 2010. Identifying a rainfall event threshold triggering herbicide leaching by preferential flow. *Water Resources Research*, 46(2): W02513.
- McGuire, K.J. and McDonnell, J.J., 2006. A review and evaluation of catchment transit time modeling. *Journal of Hydrology*, 330(3-4): 543-563.
- McGuire, K.J., Weiler, M. and McDonnell, J.J., 2007. Integrating tracer experiments with modeling to assess runoff processes and water transit times. *Advances in Water Resources*, 30(4): 824-837.
- McIntosh, J., McDonnell, J.J. and Peters, N.E., 1999. Tracer and hydrometric study of preferential flow in large undisturbed soil cores from the Georgia Piedmont, USA. *Hydrological Processes*, 13(2): 139-155.
- McIntyre, N.R. and Wheeler, H.S., 2004. Calibration of an in-river phosphorus model: Prior evaluation of data needs and model uncertainty. *Journal of Hydrology*, 290(1-2): 100-116.
- Merz, B. and Bardossy, A., 1998. Effects of spatial variability on the rainfall runoff process in a small loess catchment. *Journal of Hydrology*, 212-213: 304-317.
- Merz, B. and Plate, E.J., 1997. An analysis of the effects of spatial variability of soil and soil moisture on runoff. *Water Resources Research*, 33(12): 2909-2922.
- Mohanty, B.P., Bowman, R.S., Hendrickx, J.M.H., Šimůnek, J. and van Genuchten, M.T., 1998. Preferential transport of nitrate to a tile drain in an intermittent-flood-irrigated field: Model development and experimental evaluation. *Water Resources Research*, 34(5): 1061-1076.
- Mohanty, B.P., Bowman, R.S., Hendrickx, J.M.H. and van Genuchten, M.T., 1997. New piecewise-continuous hydraulic functions for modeling preferential flow in an intermittent-flood-irrigated field. *Water Resources Research*, 33(9): 2049-2063.
- Montgomery, D.C. and Runger, G.C., 2006. *Applied statistics and probability for engineers*. Wiley.
- Moore, E.C.S., 1898. *Sanitary Engineering*. B.T. Batsford, London.
- Mori, Y., Iwama, K., Maruyama, T. and Mitsuno, T., 1999. Discriminating the influence of soil texture and management-induced changes in macropore flow using soft X-rays. *Soil Science*, 164(7): 467-482.
- Mualem, Y., 1976. A new model for predicting the hydraulic conductivity of unsaturated porous media. *Water Resources Research*, 12(3): 513-522.
- Mulungu, D.M.M., Ichikawa, Y. and Shiiba, M., 2005. A physically based distributed subsurface-surface flow dynamics model for forested mountainous catchments. *Hydrological Processes*, 19(20): 3999-4022.

- Munyankusi, E., Gupta, S.C., Moncrief, J.F. and Berry, E.C., 1994. Earthworm macropores and preferential transport in a long-term manure applied typic hapludalf. *Journal of Environmental Quality*, 23(4): 773-784.
- Nash, J.E. and Sutcliffe, J.V., 1970. River flow forecasting through conceptual models part I - A discussion of principles. *Journal of Hydrology*, 10(3): 282-290.
- Ng, H.Y.F., Gaynor, J.D., Tan, C.S. and Drury, C.F., 1995. Dissipation and loss of atrazine and metolachlor in surface and subsurface drain water: A case study. *Water Research*, 29(10): 2309-2317.
- Nieber, J.L. and Sidle, R.C., 2010. How do disconnected macropores in sloping soils facilitate preferential flow? *Hydrological Processes*, 24(12): 1582-1594.
- Nolan, B.T., Dubus, I.G., Surdyk, N., Fowler, H.J., Burton, A., Hollis, J.M., Reichenberger, S. and Jarvis, N.J., 2008. Identification of key climatic factors regulating the transport of pesticides in leaching and to tile drains. *Pest Management Science*, 64(9): 933-944.
- Or, D., 2008. Scaling of capillary, gravity and viscous forces affecting flow morphology in unsaturated porous media. *Advances in Water Resources*, 31(9): 1129-1136.
- Page, T., Beven, K.J., Freer, J. and Neal, C., 2007. Modelling the chloride signal at Plynlimon, Wales, using a modified dynamic TOPMODEL incorporating conservative chemical mixing (with uncertainty). *Hydrological Processes*, 21(3): 292-307.
- Panday, S. and Huyakorn, P.S., 2004. A fully coupled physically-based spatially-distributed model for evaluating surface/subsurface flow. *Advances in Water Resources*, 27(4): 361-382.
- Pang, L., Close, M.E., Watt, J.P.C. and Vincent, K.W., 2000. Simulation of picloram, atrazine, and simazine leaching through two New Zealand soils and into groundwater using HYDRUS-2D. *Journal of Contaminant Hydrology*, 44(1): 19-46.
- Peng, X. and Horn, R., 2005. Modeling soil shrinkage curve across a wide range of soil types. *Soil Science Society of America Journal*, 69(3): 584-592.
- Penna, D., Borga, M., Norbiato, D. and Dalla Fontana, G., 2009. Hillslope scale soil moisture variability in a steep alpine terrain. *Journal of Hydrology*, 364(3-4): 311-327.
- Perillo, C.A., Gupta, S.C., Nater, E.A. and Moncrief, J.F., 1998. Flow velocity effects on the retardation of FD&C Blue no. 1 food dye in soil. *Soil Science Society of America Journal*, 62(1): 39-45.
- Perillo, C.A., Gupta, S.C., Nater, E.A. and Moncrief, J.F., 1999. Prevalence and initiation of preferential flow paths in a sandy loam with argillic horizon. *Geoderma*, 89(3-4): 307-331.
- Perret, J., Prasher, S.O., Kantzas, A., Hamilton, K. and Langford, C., 2000. Preferential solute flow in intact soil columns measured by SPECT scanning. *Soil Science Society of America Journal*, 64(2): 469-477.
- Perret, J.S., Prasher, S.O. and Kacimov, A.R., 2003. Mass fractal dimension of soil macropores using computed tomography: From the box-counting to the cube-counting algorithm. *European Journal of Soil Science*, 54(3): 569-579.
- Philip, J.R., 1975. Stability analysis of infiltration. *Soil Science Society America Proceedings*, 39: 1042-1049.
- Plate, E. and Zehe, E., 2008. *Hydrologie und Stoffdynamik kleiner Einzugsgebiete: Prozesse und Modelle*. Schweizerbart'sche Verlagsbuchhandlung (Nägele u. Obermiller), Stuttgart, 366 pp.
- Pryce, O., 2010. Development of environmental tracers for phosphorus and sediments. PhD Thesis, Lancaster University, Lancaster, UK.
- Raats, P.A.C., 1973. Unstable wetting fronts in uniform and nonuniform soils. *Soil Science Society America Proceedings*, 37: 681-685.

- Ray, C., Vogel, T. and Dusek, J., 2004. Modeling depth-variant and domain-specific sorption and biodegradation in dual-permeability media. *Journal of Contaminant Hydrology*, 70(1-2): 63-87.
- Richard, T.L. and Steenhuis, T.S., 1988. Tile drain sampling of preferential flow on a field scale. *Journal of Contaminant Hydrology*, 3(2-4): 307-325.
- Ritsema, C.J. and Dekker, L.W., 1995. Distribution flow: A general process in the top layer of water repellent soils. *Water Resources Research*, 31(5): 1187-1200.
- Ritsema, C.J. and Dekker, L.W., 1996. Influence of sampling strategy on detecting preferential flow paths in water-repellent sand. *Journal of Hydrology*, 177(1-2): 33-45.
- Roa-Garcia, M.C. and Weiler, M., 2010. Integrated response and transit time distributions of watersheds by combining hydrograph separation and long-term transit time modeling. *Hydrology Earth System Sciences*, 14(8): 1537-1549.
- Ross, P.J. and Smettem, K.R.J., 2000. A simple treatment of physical nonequilibrium water flow in soils. *Soil Science Society of America Journal*, 64(6): 1926-1930.
- Roth, K. and Hammel, K., 1996. Transport of conservative chemical through an unsaturated two-dimensional Miller-similar medium with steady state flow. *Water Resources Research*, 32(6): 1653-1663.
- Rouchaud, J., Neus, O., Eelen, H. and Bulcke, R., 2001. Persistence, mobility, and adsorption of the herbicide flufenacet in the soil of winter wheat crops. *Bulletin of Environmental Contamination and Toxicology*, 67(4): 609-616.
- Rupp, D.E., Peachey, R.E., Warren, K.L. and Selker, J.S., 2006. Diuron in surface runoff and tile drainage from two grass-seed fields. *Journal of Environmental Quality*, 35(1): 303-311.
- Sander, T. and Gerke, H.H., 2009. Modelling field-data of preferential flow in paddy soil induced by earthworm burrows. *Journal of Contaminant Hydrology*, 104(1-4): 126-136.
- Schäfer, D., 1999. Bodenhydraulische Eigenschaften eines Kleineinzugsgebiets - Vergleich und Bewertung unterschiedlicher Verfahren. PhD Thesis, University of Karlsruhe, Karlsruhe, Germany.
- Schäfer, D. and Montenegro, H., 2008. Ermittlung bodenhydraulischer Parameter für Böden des Weiherbachgebiets. In: E. Plate and E. Zehe (Editors), *Hydrologie und Stoffdynamik kleiner Einzugsgebiete: Prozesse und Modelle*. Schweizerbart'sche Verlagsbuchhandlung (Nägele u. Obermiller), Stuttgart, pp. 111-130.
- Scherer, U., 2008. Prozessbasierte Modellierung der Bodenerosion in einer Lösslandschaft. PhD Thesis. Schriftenreihe SWW Karlsruhe 129, 261 pp.
- Scherer, U. and Gerlinger, K., 2008. Simulation von Erosion und Sedimentation auf der Ereignisskala. In: E. Plate and E. Zehe (Editors), *Hydrologie und Stoffdynamik kleiner Einzugsgebiete: Prozesse und Modelle*. Schweizerbart'sche Verlagsbuchhandlung (Nägele u. Obermiller), Stuttgart, pp. 271-280.
- Schilling, K.E. and Helters, M., 2008. Effects of subsurface drainage tiles on streamflow in Iowa agricultural watersheds: Exploratory hydrograph analysis. *Hydrological Processes*, 22(23): 4497-4506.
- Schulz, K., Beven, K. and Huwe, B., 1999. Equifinality and the problem of robust calibration in nitrogen budget simulations. *Soil Science Society of America Journal*, 63(6): 1934-1941.
- Schulz, K., Seppelt, R., Zehe, E., Vogel, H.J. and Attinger, S., 2006. Importance of spatial structures in advancing hydrological sciences. *Water Resources Research*, 42(3): W03S03.
- Schwarzbach, M., 1988. *Das Klima der Vorzeit: Eine Einführung in die Paläoklimatologie*. Enke, Stuttgart, 380 pp.

- Schwärzel, K. and Punzel, J., 2007. Hood infiltrometer - a new type of tension infiltrometer. *Soil Science Society of America Journal*, 71(5): 1438-1447.
- Seibert, J. and McDonnell, J.J., 2002. On the dialog between experimentalist and modeler in catchment hydrology: Use of soft data for multicriteria model calibration. *Water Resources Research*, 38(11): 1241.
- Selker, J.S., Steenhuis, T.S. and Parlange, J.-Y., 1996. An engineering approach to fingered vadose pollutant transport. *Geoderma*, 70(2-4): 197-206.
- Selker, J.S., Steenhuis, T.S. and Parlange, J.Y., 1992. Wetting front instability in homogeneous sandy soils under continuous infiltration. *Soil Science Society of America Journal*, 56(5): 1346-1350.
- Shanley, J.B., Kendall, C., Smith, T.E., Wolock, D.M. and McDonnell, J.J., 2002. Controls on old and new water contributions to stream flow at some nested catchments in Vermont, USA. *Hydrological Processes*, 16(3): 589-609.
- Shipitalo, M. and Butt, K., 1999. Occupancy and geometrical properties of *Lumbricus terrestris* L. burrows affecting infiltration. *Pedobiologica*, 43: 782-794.
- Shipitalo, M.J. and Gibbs, F., 2000. Potential of earthworm burrows to transmit injected animal wastes to tile drains. *Soil Science Society of America Journal*, 64(6): 2103-2109.
- Sidle, R.C., Noguchi, S., Tsuboyama, Y. and Laursen, K., 2001. A conceptual model of preferential flow systems in forested hillslopes: Evidence of self-organization. *Hydrological Processes*, 15(10): 1675-1692.
- Šimůnek, J., Jarvis, N.J., van Genuchten, M.T. and Gärdenäs, A., 2003. Review and comparison of models for describing non-equilibrium and preferential flow and transport in the vadose zone. *Journal of Hydrology*, 272: 14-35.
- Šimůnek, J., Sejna, M. and van Genuchten, M.T., 1999. The HYDRUS-2D software package for simulating two-dimensional movement of water, heat, and multiple solutes in variably saturated media, Version 2.0, IGWMC - TPS - 53, International Ground Water Modeling Center, Colorado School of Mines, Golden, CO.
- Šimůnek, J. and van Genuchten, M.T., 2008. Modeling nonequilibrium flow and transport processes using HYDRUS. *Vadose Zone Journal*, 7(2): 782-797.
- Šimůnek, J., Wendroth, O., Wypler, N. and van Genuchten, M.T., 2001. Non-equilibrium water flow characterized by means of upward infiltration experiments. *European Journal of Soil Science*, 52(1): 13-24.
- Sinai, G. and Dirksen, C., 2006. Experimental evidence of lateral flow in unsaturated homogeneous isotropic sloping soil due to rainfall. *Water Resources Research*, 42(12): W12402.
- Sklash, M.G. and Farvolden, R.N., 1979. The role of groundwater in storm runoff. *Journal of Hydrology*, 43(1-4): 45-65.
- Smettem, K.R.J., Chittleborough, D.J., Richards, B.G. and Leaney, F.W., 1991. The influence of macropores on runoff generation from a hillslope soil with a contrasting textural class. *Journal of Hydrology*, 122(1-4): 235-251.
- Southwick, L.M., Willis, G.H. and Selim, H.M., 1992. Leaching of atrazine from sugarcane in southern Louisiana. *Journal of Agricultural and Food Chemistry*, 40(7): 1264-1268.
- Stamm, C., Flüher, H., Gächter, R., Leuenberger, J. and Wunderli, H., 1998. Preferential transport of phosphorus in drained grassland soils. *Journal of Environmental Quality*, 27(3): 515-522.
- Stamm, C., Sermet, R., Leuenberger, J., Wunderli, H., Wydler, H., Flüher, H., Gehre, M., 2002. Multiple tracing of fast solute transport in a drained grassland soil. *Geoderma*, 109(3-4): 245-268.
- Stewart, M.K. and McDonnell, J.J., 1991. Modeling base flow soil water residence times from deuterium concentrations. *Water Resources Research*, 27(10): 2681-2693.

- Stone, W.W. and Wilson, J.T., 2006. Preferential flow estimates to an agricultural tile drain with implications for glyphosate transport. *Journal of Environmental Quality*, 35(5): 1825-1835.
- Stump, C. and Maloszewski, P., 2010. Quantification of preferential flow and flow heterogeneities in an unsaturated soil planted with different crops using the environmental isotope $\delta^{18}\text{O}$. *Journal of Hydrology*, 394(3-4): 407-415.
- Topp, G.C., Davis, J.L. and Annan, A.P., 1980. Electromagnetic determination of soil water content: Measurements in coaxial transmission lines. *Water Resources Research*, 16(3): 574-582.
- Trojan, M.D. and Linden, D.R., 1992. Microrelief and rainfall effects on water and solute movement in earthworm burrows. *Soil Sci. Soc. Am. J.*, 56(3): 727-733.
- Tromp-van Meerveld, H.J. and McDonnell, J.J., 2006a. Threshold relations in subsurface stormflow: 1. A 147-storm analysis of the Panola hillslope. *Water Resources Research*, 42(2): W02410.
- Tromp-van Meerveld, H.J. and McDonnell, J.J., 2006b. Threshold relations in subsurface stormflow: 2. The fill and spill hypothesis. *Water Resources Research*, 42(2): W02411.
- Tsuboyama, Y., Sidle, R.C., Noguchi, S. and Hosoda, I., 1994. Flow and solute transport through the soil matrix and macropores of a hillslope segment. *Water Resources Research*, 30(4): 879-890.
- Tsutsumi, D., Sidle, R.C. and Kosugi, K.I., 2005. Development of a simple lateral preferential flow model with steady state application in hillslope soils. *Water Resources Research*, 41(12): W12420.
- Tugel, A., Lewandowski, A. and Happe-vonArb, D., 2000. *Soil Biology Primer*. Rev. edition. Soil and Water Conservation Society., Ankeny, Iowa.
- Uchida, T., Asano, Y., Onda, Y. and Miyata, S., 2005. Are headwaters just the sum of hillslopes? *Hydrological Processes*, 19(16): 3251-3261.
- Uchida, T., Kosugi, K.I. and Mizuyama, T., 2001. Effects of pipeflow on hydrological process and its relation to landslide: A review of pipeflow studies in forested headwater catchments. *Hydrological Processes*, 15(11): 2151-2174.
- Vaché, K.B. and McDonnell, J.J., 2006. A process-based rejectionist framework for evaluating catchment runoff model structure. *Water Resources Research*, 42(2): W02409.
- Van der Hoven, S.J., Solomon, D.K. and Moline, G.R., 2002. Numerical simulation of unsaturated flow along preferential pathways: Implications for the use of mass balance calculations for isotope storm hydrograph separation. *Journal of Hydrology*, 268(1-4): 214-233.
- van Genuchten, M.T., 1980. A closed-form equation for predicting the hydraulic conductivity of unsaturated soils. *Soil Science Society of America Journal*, 44(5): 892-898.
- van Schaik, N.L.M.B., 2010. The role of macropore flow from plot to catchment scale. *Netherlands Geographical Studies*, 390, PhD Thesis, 174 pp.
- van Schaik, N.L.M.B., Hendriks, R.F.A. and van Dam, J.C., 2010. Parameterization of macropore flow using dye-tracer infiltration patterns in the SWAP Model. *Vadose Zone Journal*, 9(1): 95-106.
- van Schaik, N.L.M.B., Schnabel, S. and Jetten, V.G., 2008. The influence of preferential flow on hillslope hydrology in a semi-arid watershed (in the Spanish Dehesas). *Hydrological Processes*, 22(18): 3844-3855.
- VandenBygaart, A.J., Protz, R., Tomlin, A.D. and Miller, J.J., 1998. ^{137}Cs as an indicator of earthworm activity in soils. *Applied Soil Ecology*, 9(1-3): 167-173.

- VDLUFA, 2010. Amtliche Sammlung von Untersuchungsverfahren § 64 LFGB, 2007; Methode L 00.00-115 (QuEChERS), adapted to the matrix soil by VDLUFA; submitted for VDLUFA Method-Book, volume VII.
- Vereecken, H., 2005. Mobility and leaching of glyphosate: A review. *Pest Management Science*, 61(12): 1139-1151.
- Villholth, K.G., Jarvis, N.J., Jacobsen, O.H. and de Jonge, H., 2000. Field investigations and modeling of particle-facilitated pesticide transport in macroporous Soil. *Journal of Environmental Quality*, 29(4): 1298-1309.
- Villholth, K.G., Jensen, K.H. and Fredericia, J., 1998. Flow and transport processes in a macroporous subsurface-drained glacial till soil I: Field investigations. *Journal of Hydrology*, 207(1-2): 98-120.
- Vogel, H.J., Cousin, I., Ippisch, O. and Bastian, P., 2006. The dominant role of structure for solute transport in soil: Experimental evidence and modelling of structure and transport in a field experiment. *Hydrology Earth System Sciences*, 10(4): 495-506.
- Vogel, T., Gerke, H.H., Zhang, R. and Van Genuchten, M.T., 2000. Modeling flow and transport in a two-dimensional dual-permeability system with spatially variable hydraulic properties. *Journal of Hydrology*, 238(1-2): 78-89.
- Vogel, T., Sanda, M., Dusek, J., Dohnal, M. and Votrubova, J., 2008. Using oxygen-18 to study the role of preferential flow in the formation of hillslope runoff. *Vadose Zone Journal*, 9(2): 252-259.
- Votrubová, J., Císlerová, M., Gao Amin, M.H. and Hall, L.D., 2003. Recurrent ponded infiltration into structured soil: A magnetic resonance imaging study. *Water Resources Research*, 39(12): 1371.
- Wang, Z., Tuli, A. and Jury, W.A., 2003. Unstable flow during redistribution in homogeneous soil. *Vadose Zone Journal*, 2(1): 52-60.
- Weihermüller, L., Kasteel, R., Vanderborght, J., Putz, T. and Vereecken, H., 2005. Soil water extraction with a suction cup: Results of numerical simulations. *Vadose Zone Journal*, 4(4): 899-907.
- Weiler, M., 2001. Mechanisms controlling macropore flow during infiltration. PhD Thesis, ETH Zürich, 172 pp.
- Weiler, M., 2005. An infiltration model based on flow variability in macropores: Development, sensitivity analysis and applications. *Journal of Hydrology*, 310: 294-315.
- Weiler, M. and Flühler, H., 2004. Inferring flow types from dye patterns in macroporous soils. *Geoderma*, 120(1-2): 137-153.
- Weiler, M. and McDonnell, J., 2004. Virtual experiments: A new approach for improving process conceptualization in hillslope hydrology. *Journal of Hydrology*, 285: 3-18.
- Weiler, M. and McDonnell, J.J., 2007. Conceptualizing lateral preferential flow and flow networks and simulating the effects on gauged and ungauged hillslopes. *Water Resources Research*, 43(3): W03403.
- Weiler, M. and Naef, F., 2003a. An experimental tracer study of the role of macropores in infiltration in grassland soils. *Hydrological Processes*, 17: 477-493.
- Weiler, M. and Naef, F., 2003b. Simulating surface and subsurface initiation of macropore flow. *Journal of Hydrology*, 273: 139-154.
- Weiler, M., Scherrer, S., Naef, F. and Burlando, P., 1999. Hydrograph separation of runoff components based on measuring hydraulic state variables, tracer experiments and weighting methods. *IAHS Publications*, 258: 249-255.
- Wells, R.R., DiCarlo, D.A., Steenhuis, T.S., Parlange, J.Y., Römkens, M.J.M. and Prasad, S.N., 2003. Infiltration and surface geometry features of a swelling soil following successive simulated rainstorms. *Soil Science Society of America Journal*, 67(5): 1344-1351.

- Wels, C., Cornett, R.J. and Lazerte, B.D., 1991. Hydrograph separation: A comparison of geochemical and isotopic tracers. *Journal of Hydrology*, 122(1-4): 253-274.
- Western, A.W., Blöschl, G. and Grayson, R.B., 1998. Geostatistical characterisation of soil moisture patterns in the Tarrawarra catchment. *Journal of Hydrology*, 205(1-2): 20-37.
- Western, A.W. and Grayson, R.B., 1998. The Tarrawarra data set: Soil moisture patterns, soil characteristics, and hydrological flux measurements. *Water Resources Research*, 34(10): 2765-2768.
- Wienhöfer, J., Germer, K., Lindenmaier, F., Färber, A. and Zehe, E., 2009. Applied tracers for the observation of subsurface stormflow at the hillslope scale. *Hydrology Earth System Sciences*, 13(7): 1145-1161.
- Wildenschild, D., Vaz, C.M.P., Rivers, M.L., Rikard, D. and Christensen, B.S.B., 2002. Using X-ray computed tomography in hydrology: Systems, resolutions, and limitations. *Journal of Hydrology*, 267(3-4): 285-297.
- Woolhiser, D.A., Gardner, H.R. and Olsen, S.R., 1982. Estimation of multiple inflows to a stream reach using water chemistry data. *Transaction ASAE*, 25(3): 616-626.
- Young, D.F. and Ball, W.P., 2000. Column experimental design requirements for estimating model parameters from temporal moments under nonequilibrium conditions. *Advances in Water Resources*, 23(5): 449-460.
- Zak, S.K. and Beven, K.J., 1999. Equifinality, sensitivity and predictive uncertainty in the estimation of critical loads. *The Science of The Total Environment*, 236(1-3): 191-214.
- Zehe, E., 1999. Stofftransport in der ungesättigten Bodenzone auf verschiedenen Skalen. PhD Thesis. Mitteilungen des Instituts für Hydrologie und Wasserwirtschaft der Universität Karlsruhe (TH), Karlsruhe, 227 pp.
- Zehe, E., Becker, R., Bardossy, A. and Plate, E.J., 2005. Uncertainty of simulated catchment runoff response in the presence of threshold processes: Role of initial soil moisture and precipitation. *Journal of Hydrology*, 315: 183-202.
- Zehe, E. and Blöschl, G., 2004. Predictability of hydrologic response at the plot and catchment scales: Role of initial conditions. *Water Resources Research*, 40(W10202).
- Zehe, E., Blume, T. and Blöschl, G., 2010a. The principle of 'maximum energy dissipation': A novel thermodynamic perspective on rapid water flow in connected soil structures. *Philosophical Transactions of the Royal Society B: Biological Sciences*, 365(1545): 1377-1386.
- Zehe, E., Elsenbeer, H., Lindenmaier, F., Schulz, K. and Blöschl, G., 2007. Patterns of predictability in hydrological threshold systems. *Water Resources Research*, 43(7): W07434.
- Zehe, E. and Flühler, H., 2001a. Preferential transport of isotopuron at a plot scale and a field scale tile-drained site. *Journal of Hydrology*, 247: 100-115.
- Zehe, E. and Flühler, H., 2001b. Slope scale variation of flow patterns in soil profiles. *Journal of Hydrology*, 247: 116-132.
- Zehe, E., Graeff, T., Morgner, M., Bauer, A. and Bronstert, A., 2010b. Plot and field scale soil moisture dynamics and subsurface wetness control on runoff generation in a headwater in the Ore Mountains. *Hydrology Earth System Sciences*, 14(6): 873-889.
- Zehe, E., Lee, H. and Sivapalan, M., 2006. Dynamical process upscaling for deriving catchment scale state variables and constitutive relations for meso-scale process models. *Hydrology Earth System Sciences*, 10(6): 981-996.
- Zehe, E., Maurer, T., Ihringer, J. and Plate, E.J., 2001. Modeling water flow and mass transport in a loess catchment. *Physics and Chemistry of the Earth*, 26(7-8): 487-507.
- Zehe, E. and Sivapalan, M., 2009. Threshold behaviour in hydrological systems as (human) geo-ecosystems: manifestations, controls, implications. *Hydrology Earth System Sciences*, 13(7): 1273-1297.

- Zhang, D., Beven, K. and Mermoud, A., 2006. A comparison of non-linear least square and GLUE for model calibration and uncertainty estimation for pesticide transport in soils. *Advances in Water Resources*, 29(12): 1924-1933.
- Zhang, G.P., Savenije, H.H.G., Fenicia, F. and Pfister, L., 2006. Modelling subsurface storm flow with the Representative Elementary Watershed (REW) approach: application to the Alzette River Basin. *Hydrology Earth System Sciences*, 10(6): 937-955.
- Zhao, P., Shao, M. and Melegy, A., 2010. Soil water distribution and movement in layered Soils of a dam farmland. *Water Resources Management*, 24(14): 3871-3883.
- Zhu, Q. and Lin, H.S., 2009. Simulation and validation of concentrated subsurface lateral flow paths in an agricultural landscape. *Hydrology Earth System Sciences*, 13(8): 1503-1518.
- Zurmühl, T. and Durner, W., 1996. Modeling transient water and solute transport in a biporous soil. *Water Resources Research*, 32(4): 819-829